

University of Alberta

**Immobilization of Homogeneous Asymmetric
Hydrogenation Catalysts by Alternating ROMP Assembly**

by

Corbin Kurt Ralph 

A thesis submitted to the Faculty of Graduate Studies and Research in partial
fulfillment of the requirements for the degree of Doctor of Philosophy

Department of Chemistry

Edmonton, Alberta
Fall 2007



Library and
Archives Canada

Bibliothèque et
Archives Canada

Published Heritage
Branch

Direction du
Patrimoine de l'édition

395 Wellington Street
Ottawa ON K1A 0N4
Canada

395, rue Wellington
Ottawa ON K1A 0N4
Canada

Your file *Votre référence*
ISBN: 978-0-494-33048-7
Our file *Notre référence*
ISBN: 978-0-494-33048-7

NOTICE:

The author has granted a non-exclusive license allowing Library and Archives Canada to reproduce, publish, archive, preserve, conserve, communicate to the public by telecommunication or on the Internet, loan, distribute and sell theses worldwide, for commercial or non-commercial purposes, in microform, paper, electronic and/or any other formats.

The author retains copyright ownership and moral rights in this thesis. Neither the thesis nor substantial extracts from it may be printed or otherwise reproduced without the author's permission.

AVIS:

L'auteur a accordé une licence non exclusive permettant à la Bibliothèque et Archives Canada de reproduire, publier, archiver, sauvegarder, conserver, transmettre au public par télécommunication ou par l'Internet, prêter, distribuer et vendre des thèses partout dans le monde, à des fins commerciales ou autres, sur support microforme, papier, électronique et/ou autres formats.

L'auteur conserve la propriété du droit d'auteur et des droits moraux qui protègent cette thèse. Ni la thèse ni des extraits substantiels de celle-ci ne doivent être imprimés ou autrement reproduits sans son autorisation.

In compliance with the Canadian Privacy Act some supporting forms may have been removed from this thesis.

Conformément à la loi canadienne sur la protection de la vie privée, quelques formulaires secondaires ont été enlevés de cette thèse.

While these forms may be included in the document page count, their removal does not represent any loss of content from the thesis.

Bien que ces formulaires aient inclus dans la pagination, il n'y aura aucun contenu manquant.


Canada

Abstract

It is highly desirable to develop heterogeneous asymmetric catalysts that can be readily removed from the reaction media in order to ease purification and to allow reuse of the catalyst. One approach is the use of insoluble polymer-supported catalysts to facilitate simple catalyst recovery and reuse. Most polymeric chiral hydrogenation catalysts are made by first polymerizing a chiral phosphine ligand, or to graft the phosphine to a polymer support. The critical step then becomes metallating the resulting polymeric ligand to produce active catalytic sites. The extent of metallation and site isolation of the active centers on these insoluble polymers are among the major problems associated with the above methods. This dissertation describes the development of an alternating ring-opening metathesis polymerization (ROMP) with chiral diphosphine/diamine – Ru systems as monomers to prepare highly reusable polymeric asymmetric hydrogenation catalysts.

The alternating ROMP methodology was developed using *trans*- $\text{RuCl}_2((R,R)\text{-Norphos})\text{Py}_2$ (I) as a monomer, with cyclooctene (COE) as a spacer monomer, and with $\text{RuCl}_2(\text{CHPh})(\text{PCy}_3)_2$ (II) as the ROMP catalyst. Employing COE as a spacer monomer provided effective site isolation of the active centers along the polymer backbone. Further the Py ligands in the diphosphine catalyst were displaced with (*R,R*)-dpen to produce the polymeric catalyst, *trans*- $[\text{RuCl}_2((R,R)\text{-Norphos})((R,R)\text{-dpen})]_x[\text{COE}]_y$ (III). The polymeric catalyst III was deposited onto BaSO_4 to produce a heterogeneous catalyst that was reused 10x

for the hydrogenation of 1'-acetonaphthone with a higher enantiomeric excess (*ee*) than with the monomer catalyst (85% vs 48% *ee*).

To demonstrate the versatility of the alternating ROMP methodology, the first ROMP-active BINAP monomer was prepared by incorporating the norbornyl group at the 5,5'-position of the naphthalene units of BINAP to give (*R*)-5,5'-dinorimido-BINAP (**IV**). The catalyst monomer *trans*-RuCl₂((*R*)-5,5'-dinorimido-BINAP)(Py)₂ (**V**) was prepared by replacing the norbornadiene ligand in the compound *trans*-RuCl₂(NBD)Py₂ (**VI**) with **IV**. The alternating ROMP assembly of **V** and COE using **II** as catalyst resulted in an extended, three-dimensional catalyst-organic framework. The catalyst-organic framework was converted to contain Noyori-type active sites that were recycled for an unprecedented 25 times at low catalyst loading without loss of enantioselectivity, activity, and without detectable Ru leaching.

Acknowledgements

To my supervisor Steve, I would like to thank you for providing me with innovative and challenging research projects to work on during my graduate studies. I am grateful for our countless discussions on every aspect of my research, even when it seemed we were thinking too hard or as Robin infamously stated during his 502 “overdoing it”. To the Bergens’ group (past and present), each have contributed in their own way in helping me complete this task. I often found motivation through our discussions and frustrations along the way. Thanks for listening and keep up the good work!

I am grateful for the expertise and experience of the support staff in the NMR Laboratory, Spectral & Analytical Laboratory, X-ray Structure Determination Laboratory, Electronics & Machine Shops, Glassblowing Shop and Purchasing. A special thanks to Mark Miskolzie and Glen Bigam for always going the extra mile, especially during the atropisomer “rotamer” business.

I am so thankful for my loving and supportive family who made this journey possible. Your prayers and encouragement helped me throughout the duration of my graduate studies. Bill and Donna, thanks for being in my corner. You guys are awesome! Dad, thanks for always encouraging me to keep my chin up and reminding me that each step is one step closer to completion. Mom, thanks for telling me how to eat an elephant. Our conversations, especially during the writing process, were amazing and I will always remember Jeremiah

29:11. To Bryant & Valerie (Jaiken, Hannah), Deanna & Bart (JuJu, Daniel), Chad, and Karla (Jon), a special thanks to each of you.

To my wife Krista, wow, we're here. It is not possible to express my thanks to you for all the love and support you have given. You have been amazing through this whole process. Thanks for all those long walks and bike rides, listening to me discuss how I'm going to write the next section or what experiment to do next. Thank you for reading and editing my entire dissertation and never asking when this will be finished. I love you and I'm back, let's start the next chapter...

Jeremiah 29:11 – “For I know the plans I have for you,” declares the Lord, “plans to prosper you and not to harm you, plans to give you hope and a future.”

Table of Contents

Chapter 1

Introduction

General definitions.....	1
Asymmetric catalysis and the need to immobilize.....	1
Benefits of immobilization and methods used.....	3
Polymer-supported catalysts in asymmetric hydrogenation.....	5
Pioneering work by Kagan and Stille.....	6
Polymer-supported BINAP systems and applications.....	13
Grafting to polystyrene.....	14
Copolymerization of functionalized BINAP monomers.....	21
Research objectives.....	28
References.....	30

Chapter 2

Reusable polymeric asymmetric hydrogenation catalyst made by ring-opening metathesis polymerization

Introduction.....	36
Reasons for immobilizing homogeneous catalysts.....	36
Rational design of more efficient and reusable systems.....	37
ROMP as an immobilization technique.....	38
Essential features of ROMP.....	39
Select examples of functionalized polymers prepared by ROMP.....	43

Objectives	45
Results and Discussion	46
Synthesis of <i>trans</i> -RuCl ₂ (Py) ₂ ((<i>R,R</i>)-Norphos) (41)	46
ROMP of monomer 41	49
Alternating ROMP of 41 and COE.....	50
NMR investigation of the alternating ROMP process.....	54
Generation of <i>trans</i> -[RuCl ₂ ((<i>R,R</i>)-Norphos)((<i>R,R</i>)-dpen)] _x [COE] _y (46)	62
Preparation of a reusable alternating polymer catalyst	64
BaSO ₄ as support	66
Use of the supported alternating polymer catalyst 47	68
Conclusion	72
Experimental.....	73
General procedures and methods.....	73
Reactions and syntheses	74
References	87

Chapter 3

Synthesis of a ROMP active BINAP monomer

Introduction	95
Reasons to adapt the alternating ROMP methodology to BINAP.....	95
Previous methods to functionalize BINAP	96
Incorporation of norbornene groups onto the BINAP framework.....	100
Results and Discussion	101

Functionalization at the 6,6'-positions	101
Attempted Diels-Alder reaction	102
Functionalization at the 5,5'-positions	104
Improved synthesis of (<i>R</i>)-5,5'-diamino-BINAP (54)	105
Reaction of 54 with acryloyl chloride	109
Synthesis of (<i>R</i>)-5,5'-dinorimido-BINAP (55)	109
Mixture of three NMR distinct, diastereomeric atropisomers	111
NMR evidence	115
Isolation of a single C ₂ -dissymmetric diastereomer.....	118
Intpretation of the ¹ H NMR data	120
Variable temperature NMR study on the interconversion process of the diastereomeric atropisomers	123
Conclusion	124
Experimental	125
General procedures and methods	125
Reactions and syntheses	126
References	148

Chapter 4

A highly reusable catalyst for enantioselective ketone hydrogenation.

Catalyst-organic frameworks by alternating ROMP assembly

Introduction	151
Metal-organic frameworks	151

Results and Discussion	155
Section A: Preparation of metal containing monomers for ROMP	155
Synthesis of <i>trans</i> -RuCl ₂ ((<i>R</i>)-5,5'-dinorimido-BINAP)(Py) ₂ (57).....	155
Influence of the metal center on the interconversion process.....	157
Section B: Immobilization of the homogeneous catalyst 57 by the alternating ROMP methodology.....	165
Judicial choice of Grubbs metathesis catalysts	165
Alternating ROMP assembly of <i>trans</i> -RuCl ₂ ((<i>R</i>)-5,5'-dinorimido-BINAP)(Py) ₂ (57) and COE.....	167
NMR investigations on the alternating ROMP of 57 and COE ...	170
Nature of the extended, three-dimensional alternating catalyst-organic framework.....	177
Preparation of Noyori's catalyst within the polymeric framework and supported on BaSO ₄	179
Section C: Preliminary investigations of the supported alternating catalyst-organic framework towards asymmetric hydrogenations	181
Initial hydrogenations.....	181
Optimized reaction conditions.....	184
Section D: Reusability and versatility of the supported catalyst-organic frameworks	188
Reusability	188
Rate of reaction for runs 5 through 29	195
Ruthenium leaching from the catalyst framework	197

Versatility of the alternating catalyst-organic framework.....	199
Conclusion	201
Experimental.....	202
General procedures and methods.....	202
Reactions and syntheses	204
References	217

Chapter 5

Concluding Remarks

Alternating ROMP methodology.....	221
ROMP active BINAP monomer	222
Highly reusable catalyst-organic frameworks.....	223
Future research directions.....	225
References	226

List of Tables

Chapter 1

No Tables

Chapter 2

Table 2-1. Enantioselective hydrogenation of 1'-acetonaphthone with 47	81
Table 2-2. Crystallographic experimental details for 41	84
Table 2-3. Selected interatomic distances (Å) for 41	86
Table 2-4. Selected interatomic angles (deg) for 41	86

Chapter 3

Table 3-1. Rh(I)-catalyzed asymmetric hydrogenation of functionalized olefins	98
Table 3-2. Crystallographic experimental details for 49	138
Table 3-3. Selected interatomic distances (Å) for 49	140
Table 3-4. Selected interatomic angles (deg) for 49	140
Table 3-5. Crystallographic experimental details for 52	141
Table 3-6. Selected interatomic distances (Å) for 52	143
Table 3-7. Selected interatomic angles (deg) for 52	143
Table 3-8. Crystallographic experimental details for 54	144
Table 3-9. Selected interatomic distances (Å) for 54	146
Table 3-10. Selected interatomic angles (deg) for 54	147

Chapter 4

Table 4-1. Heterogeneous hydrogenation of 1'-acetonaphthone using **65'** 182

Table 4-2. Hydrogenation of **25** using **65'** with a swelling co-solvent 184

Table 4-3. Recycling of catalyst framework **65'** for hydrogenation of **25** 191

Table 4-4. Asymmetric hydrogenation of aromatic ketones..... 200

Table 4-5. Ba-(L)-tartrate supported catalyst for asymmetric hydrogenations
..... 201

Chapter 5

No Tables

List of Figures

Chapter 1

- Figure 1-1.** Various $[\text{RuCl}_2((R)\text{-BINAP})((R,R)\text{-diamine})]$ complexes 18
- Figure 1-2.** MeO-PEG-supported BINAP 25

Chapter 2

- Figure 2-1.** Commercially available catalysts for ROMP 39
- Figure 2-2.** Perspective view of **41** showing the atom labeling scheme..... 48
- Figure 2-3.** In situ ^1H NMR spectra of the alternating ROMP of **41** and COE.
..... 56
- Figure 2-4.** Plot of the consumption of COE and **41** vs time for the alternating ROMP of COE and **41** in a 2.72:1 ratio using **37** as catalyst 58
- Figure 2-5.** ^{31}P NMR spectra of the alternating ROMP of **41** and COE with **37**..... 61
- Figure 2-6.** ^{31}P NMR spectra of the alternating polymer **45** before and after treatment with (R,R) -dpen to give **46**..... 63
- Figure 2-7.** Conversion(%) and ee vs. runs for hydrogenation of 1'-acetonaphthone catalyzed by **47** 70

Chapter 3

- Figure 3-1.** Perspective view of **49** showing the atom labeling scheme 103
- Figure 3-2.** Perspective view of **52** showing the atom labeling scheme 107
- Figure 3-3.** Perspective view of **54** showing the atom labeling scheme 108

Figure 3-4. ^{31}P NMR (162MHz, CDCl_3) of 55	111
Figure 3-5. Three diastereomeric atropisomers of 55	112
Figure 3-6. Effect of <i>ortho</i> substituents on twist angle	114
Figure 3-7. ^{31}P NMR of 55	116
Figure 3-8. ^{31}P – ^{31}P COSY of 57	117
Figure 3-9. ^{31}P NMR of 56 at room temperature a) 0 min b) after 10-15 min c) after 2 h.....	119
Figure 3-10. ^1H NMR of 56 a) at -20°C b) at room temperature 10 min c) of 55 at room temperature	121
Figure 3-11. Variable Temperature ^{31}P NMR of 55	124

Chapter 4

Figure 4-1. ^{31}P NMR spectra (at room temperature in CD_2Cl_2) of (a) 55 recorded at 202 MHz and (b) 57 recorded at 161.8 MHz.....	158
Figure 4-2. ^{31}P NMR (at 161.8 MHz in CD_2Cl_2) of the metallation of 55b (a) after 24 h (b) after 7 days	160
Figure 4-3. ^{31}P NMR (at 161.8 MHz in CD_2Cl_2) of 59 (a) at RT and (b) at - 40°C	162
Figure 4-4. ^{31}P NMR spectra (at 161.8 MHz in CD_2Cl_2) of 60	165
Figure 4-5. Comparison of ^1H NMR spectra of the alternating ROMP of 57 and COE (1:4) with catalyst 37	172
Figure 4-6. Comparison of the ^{31}P NMR spectra of the alternating ROMP of 57 and COE (1:4) with catalyst 37	176

Figure 4-7. ^{31}P NMR spectra (161.8 MHz in CD_2Cl_2) of the alternating polymer framework **64** before and after treatment with (R,R)-dpen resulting in **65**..... 180

Figure 4-8. Plot of yield (%) and *ee* vs the number of recycles for asymmetric hydrogenation of 1'-acetonaphthone catalyzed by **65'** 190

Figure 4-9. Pictures of the stainless steel hydrogenation bomb after the recycling experiment. (a) The solid catalyst was coated around the bomb walls away from the reaction solution, (b) and on the bomb lid. (c) Supported catalyst remaining after reaction mixture was removed.....194

Chapter 5

No Figures

List of Schemes

Chapter 1

Scheme 1-1. Polymer-supported Wilkinson's catalyst.....	6
Scheme 1-2. Kagan's polymer-supported DIOP	7
Scheme 1-3. Immobilized DIOP ligand	9
Scheme 1-4. Immobilized DIOP ligand with chiral alcohol groups	10
Scheme 1-5. Immobilized BPPM ligand	12
Scheme 1-6. Functionalization and grafting of BINAP to polystyrene	14
Scheme 1-7. Synthesis of carbapenem antibiotics.....	15
Scheme 1-8. Asymmetric isomerization and Takasago (-)-menthol synthesis.	17
Scheme 1-9. Practical asymmetric synthesis of PDE-IV inhibitor.....	19
Scheme 1-10. Synthesis of polymer-supported catalyst 24	20
Scheme 1-11. Lemaire's functionalization of BINAP and synthesis of polyureas	22
Scheme 1-12. Chan's preparation of a soluble polymer-supported BINAP ligand	24
Scheme 1-13. Pu's sterically regular polymer BINAP ligand	26

Chapter 2

Scheme 2-1. Mechanism of Ring-Opening Metathesis Polymerization.....	41
Scheme 2-2. Polymeric palladium catalyst prepared by ROMP	44
Scheme 2-3. Synthesis of A/B/C triblock copolymer	45

Scheme 2-4. Alternating ROMP of **41** and COE using catalysts **37** or **38**.... 51

Chapter 3

Scheme 3-1. Synthesis of (<i>R</i>)-5,5'-diamino-BINAP	99
Scheme 3-2. Bayston's route for derivatizing BINAP	99
Scheme 3-3. Strategies for incorporating norbornene groups onto BINAP.	100
Scheme 3-4. Functionalization of BINAP at the 6,6'-positions	101
Scheme 3-5. Attempted Diels-Alder reaction	104
Scheme 3-6. Nitration route to (<i>R</i>)-5,5'-diamino-BINAP (54).....	105

Chapter 4

Scheme 4-1. Self-supported Noyori's catalyst for hydrogenation.....	152
Scheme 4-2. Metal-organic catalyst for asymmetric hydrogenation	153
Scheme 4-3. Alternating ROMP assembly of 57 and COE	169
Scheme 4-4. Rate of Polymer Growth.....	175
Scheme 4-5. Schematic representation of the extended, three-dimensional catalyst-organic framework 64	178
Scheme 4-6. Proposed mechanism for trans-RuCl ₂ -(diphosphine)(diamine).	187

Chapter 5

No Schemes

List of Equations

Chapter 1

equation 1 - 1: enantiomeric excess (<i>ee</i> %)	1
equation 1 - 2: Hydrogenation of MAC acid	9
equation 1 - 3: Hydrogenation of α -acetamidoacrylic acid	11
equation 1 - 4: Hydrogenation of methyl acetoacetate	16
equation 1 - 5: Hydrogenation of 1'-acetonaphthone	20
equation 1 - 6: Synthesis of naproxen	24

Chapter 2

equation 2 – 1: Reaction of 39 and 40	47
equation 2 – 2: Reaction of 41 and (<i>R,R</i>)-dpen	49
equation 2 – 3: Reaction of 45 and (<i>R,R</i>)-dpen	63
equation 2 – 4: Hydrogenation of 1'-acetonaphthone	69

Chapter 3

equation 3 – 1: Reaction of 54 and acryloyl chloride	109
equation 3 – 2: Reaction of 54 and dicarboxylic anhydride	110
equation 3 – 3: Effect of <i>ortho</i> -substituted aryl groups	114

Chapter 4

equation 4 – 1: Reaction of 55 and 40	155
--	-----

equation 4 – 2: Reaction of 64 and (<i>R,R</i>)-dpen	179
equation 4 – 3: Hydrogenation of 25	181
equation 4 – 4: Reaction of 64 and (<i>R</i>)-daipen.....	199

Chapter 5

No equations

List of Abbreviations

AIBN	2,2'-azobisisobutyronitrile
Å	angstrom
atm	atmosphere(s)
β-Dex	β-cyclodextrin
BINAP	(<i>R</i>)- or (<i>S</i>)-2,2'-bis(diphenylphosphino)-1,1'-binaphthyl
BPPM	(2 <i>S</i> ,4 <i>S</i>)- or (2 <i>R</i> ,4 <i>R</i>)-4-diphenylphosphino-2-diphenylphosphinomethyl-1-(<i>N</i> - <i>t</i> -butoxy)pyrrolidine
^t Bu	<i>tert</i> -butyl
COE	cyclooctene
COSY	correlation spectroscopy
Daipen	(<i>R</i>)- or (<i>S</i>)-1,1-di-4-anisyl-2-isopropyl-1,2-ethylenediamine
DCP	dicyclopentadiene
DIC	diisopropylcarbodiimide
DIOP	(2 <i>R</i> ,3 <i>R</i>)- or (2 <i>S</i> ,3 <i>S</i>)- <i>O</i> -isopropylidene-2,3-dihydroxy-1,4-bis(diphenylphosphino)butane
DMA	<i>N,N'</i> -dimethylacetamide
DMF	<i>N,N'</i> -dimethylformamide
DMSO	dimethyl sulfoxide
Dpen	(<i>R,R</i>)- or (<i>S,S</i>)-1,2-diphenylethylenediamine
dppe	1,2-bis(diphenylphosphino)ethane
ee	enantiomeric excess
equiv	equivalent(s)

GC	gas chromatography
GTA	γ -cyclodextrin
h	hour(s)
HOBt	hydroxybenzotriazole
Hz	hertz
MAC	methyl α -acetamidocinnamate
MeOH	menthol
min	minute(s)
mm	millimeter(s)
mmol	millimol(s)
mL	milliliter
MOF	metal-organic framework
NBD	norbornadiene
NMR	nuclear magnetic resonance
Norphos	(2 <i>S</i> ,3 <i>S</i>)- or (2 <i>R</i> ,3 <i>R</i>)-2,3-bis(diphenylphosphino)bicyclo[2.2.1]hept-5-ene
PCy ₃	tricyclohexylphosphine
PEG	polyethyleneglycol
Ph	phenyl
PS-CH ₂ NH ₂	amino polystyrene
psi	pounds per square inch
Py	pyridine
<i>i</i> Pr	<i>iso</i> -propyl

ROMP	ring-opening metathesis polymerization
rt	room temperature
THF	tetrahydrofuran
TON	turnover number
TOF	turnover frequency

Chapter 1

Introduction

The demand for optically pure compounds has steadily risen over the past 10-15 years,¹ primarily for use in the pharmaceutical,² agrochemical,³ flavor and fragrance industries.⁴ According to a survey from the market research firm Frost & Sullivan, the worldwide sales of single enantiomer compounds is projected to grow annually by 11.4% over the next few years to \$14.94 billion (USD) by the end of 2009.⁵ Among the various methods used to prepare enantiopure compounds, asymmetric catalysis is the most attractive from an atom-economy point of view and it has the most potential for general asymmetric synthesis.^{1,6} Asymmetric catalysis deals with the enantioselective conversion of a prochiral compound to a chiral product with the help of a chiral catalyst. The most important advantage of asymmetric catalysis is the feature of chiral multiplication whereby the chiral information from a catalyst is transferred to produce large quantities of optically pure compounds. The efficiency of chiral multiplication is expressed in terms of enantiomer excess (*ee*), turnover number (TON), and turnover frequency (TOF). Where *ee* is a measure of how much more of one enantiomer is present than the other (equation 1 - 1), TON is the number of product molecules produced per molecule of catalyst and TOF is the TON per unit time.

$$ee \% = \frac{\text{major enantiomer} - \text{minor enantiomer}}{\text{major enantiomer} + \text{minor enantiomer}} \times 100 \quad (1 - 1)$$

Asymmetric catalysis is one of the most important developments in modern chemistry. Further, the 2001 Chemistry Nobel Prize was awarded to W. S. Knowles and R. Noyori for enantioselective hydrogenation and K. B. Sharpless for enantioselective oxidation catalysis.^{7,8} Among the numerous chemical transformations developed using asymmetric catalysts, the most utilized systems are those for the hydrogenation of C=C, C=O and C=N functionalities. Here, the most versatile and effective catalysts in terms of selectivity and activity are homogeneous diphosphine complexes of rhodium, ruthenium, and iridium.⁹ In fact, asymmetric hydrogenation has become a core technology in the industry sector, representing more than half of all catalytic enantioselective processes currently operating on a commercial scale.¹⁰ However, with fewer than 20 full-scale asymmetric catalytic processes being practiced on a commercial scale, this number is lower than one might expect given the huge amount of attention devoted to this subject.¹¹ For example, a literature search using asymmetric catalysis as the key word provided nearly 21,000 hits in the last 15 years with more than half of these occurring in the last 5 years.¹²

The low number of industrial applications of asymmetric catalysis is partly due to problems associated with separation and reuse of expensive homogeneous chiral catalysts. Specifically, due to the risk of product contamination from heavy metals used in catalysis, regulatory authorities demand a low limit (<10 ppm) for residual metal impurities, and therefore time-consuming cleaning operations are required in the work-up stage.¹³ In addition,

the transition metals employed in asymmetric catalysis are expensive and usually decompose during the clean-up process, preventing recycling. For example, considering a process that uses 1 mol % Ru, a batch reaction of 2000 mol of substrate will consume 2 kg (20 mol) of ruthenium metal. With this year's average price for ruthenium metal ~\$21 (USD) per gram this translates into \$42,000 for a single production batch.¹⁴ Furthermore, the chiral ligands typically used can cost from \$5000 to > \$20,000 per kg for industrial scale. Hence, due to the cost associated with the use of metal/ligand complexes and the high purity requirements, a great deal of research has been devoted to immobilizing homogeneous chiral catalysts in an effort to develop more cost-effective, sustainable commercial processes for the production of chiral chemicals.^{15,16}

The idea behind immobilization of homogenous catalysts is to combine the advantages of heterogeneous and homogeneous catalysis. Specifically, heterogeneous catalysts offer easy separation from the product stream, improved handling, and repeated recycling potential. In contrast, homogeneous catalysts tend to give higher catalytic efficiencies and usually are well-defined at the molecular level which provides high levels of mechanistic insight of the reaction parameters to enable fine-tuning of the catalysts. Furthermore, immobilization of homogeneous catalysts allows for continuous processes, which would be a major step forward in terms of productivity for the production of chiral compounds.¹⁷ Thus, an ideal immobilized catalyst is one that offers minimum metal leaching into the product stream, can be recovered by simple procedures

such as filtration, and can be recycled with constant activity and selectivity which are at least as good as or better than those of the homogeneous analogue.

Numerous approaches for the immobilization of homogeneous catalysts have been developed over the past three decades with varying degrees of success.^{16,18} These include covalent or non-covalent attachment of the chiral ligand, the metal center, and or less frequently the performed metal complex onto a support (e.g., inorganic solids or organic polymers). Covalent attachment is by far the most often employed strategy and is achieved by grafting homogeneous systems to a functionalized support or by copolymerization of suitably functionalized ligands with co-monomers. Non-covalent methods involve entrapment, adsorption, and ion exchange techniques. These are less frequently employed because of problems related to the appropriate pore size, poor stability, and limited adaptability, respectively. Another immobilization technique that has emerged as an important alternative is the use of biphasic systems for catalysis. This concept is based on the premise that the transition metal catalyst is soluble in one phase (e.g., aqueous phase, fluorous phase, supercritical CO₂ or ionic liquids) and the substrates/products are retained in a separate phase.¹⁹ In principle, the reaction takes place at the interface between the two phases allowing for simple work-up procedures for the isolation of products and catalyst. As an example, Jessop and coworkers used a fluorous biphasic system for the hydrogenation of styrene to ethylbenzene.²⁰ In this case, a fluorinated version of Wilkinson's catalyst was induced to dissolve in the organic phase (cyclohexane) under 40-60 bar of CO₂. After the reaction was complete, the pressure was

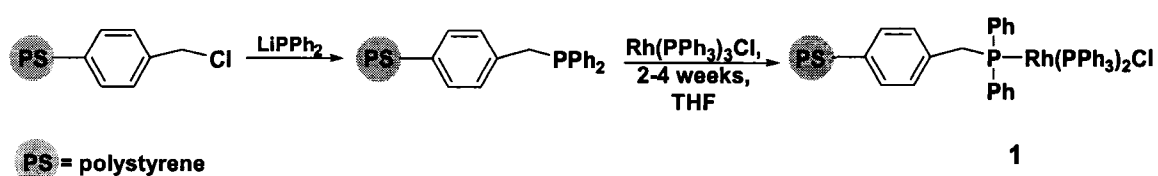
released and the catalyst precipitated quantitatively from the organic phase. A fluorosilica gel was used to capture the catalyst and they found that the same batch of catalyst could be reused up to five times. More recently, Jessop's group has used liquid poly(ethylene glycol) and supercritical CO₂ as solvents for catalytic reductions.²¹

Despite the numerous techniques developed, most examples of immobilized catalysts tend to display lower activities and enantioselectivities as compared to those observed for their homogeneous counterparts. However, a comprehensive discussion on the immobilization methods mentioned above is well outside the scope of this work. The focus of this research deals primarily with the use of polymer-supported asymmetric hydrogenation catalysts. Thus, previous examples of polymer-supported catalysts employed in asymmetric hydrogenation reactions are presented. Emphasis is placed on the synthetic routes taken to prepare the polymer-supported catalysts while presenting the pros and cons associated with each method to direct towards a rational design of more efficient immobilized systems. As well, the polymer-supported systems are assessed based on their catalytic performance as compared to the corresponding homogeneous system, the level of reusability achieved and the degree of metal leaching.

The early approaches for polymer-supported catalysts were inspired by Merrifield's methodology for solid-phase peptide synthesis using cross-linked polystyrene as a support.²² In 1971, Grubbs et al. reported the first example of a polymer-supported catalyst for hydrogenation, whereby the equivalent of

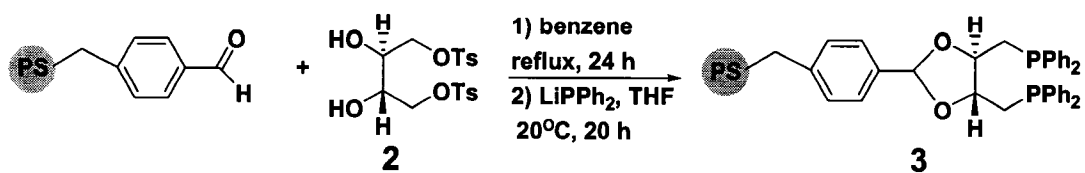
Wilkinson's catalyst, $\text{Rh}(\text{PPh}_3)_3\text{Cl}$, was attached to a polymer-support derived from Merrifield resin.²³ In this work, chloromethylated polystyrene (Merrifield resin), cross-linked with 2% divinylbenzene (DVB), was derivatized to incorporate diphenylphosphinomethyl groups, followed by treatment with excess tris(triphenylphosphine)rhodium(I) chloride for 2-4 weeks in THF to give the immobilized version of Wilkinson's catalyst (**1**, Scheme 1-1). Although the preparation of **1** was sluggish and not at all practical, it did show activities comparable to those seen in solution for the hydrogenation of a series of alkenes. Furthermore, the supported catalyst **1** was recovered by filtration and reused ten times with only a small variation in activity. Grubbs' work was an important first step, which demonstrated that covalent attachment of homogeneous catalysts to organic polymers was a viable immobilization technique and merited attention.

Scheme 1-1. Polymer-supported Wilkinson's catalyst.



As an extension to Grubbs' work, Kagan et al. reported the first immobilized chiral enantioselective catalyst based on their chiral diphosphine ligand DIOP (2,3-O-isopropylidene-2,3-dihydroxy-1,4-bis(diphenylphosphino)-butane) for the asymmetric hydrogenation of alkenes.²⁴ Here, diol **2** was attached to polystyrene-supported benzaldehyde and treated with lithium diphenylphosphide to give the polymer-supported DIOP ligand (**3**, Scheme 1-2).

Scheme 1-2. Kagan's polymer-supported DIOP.

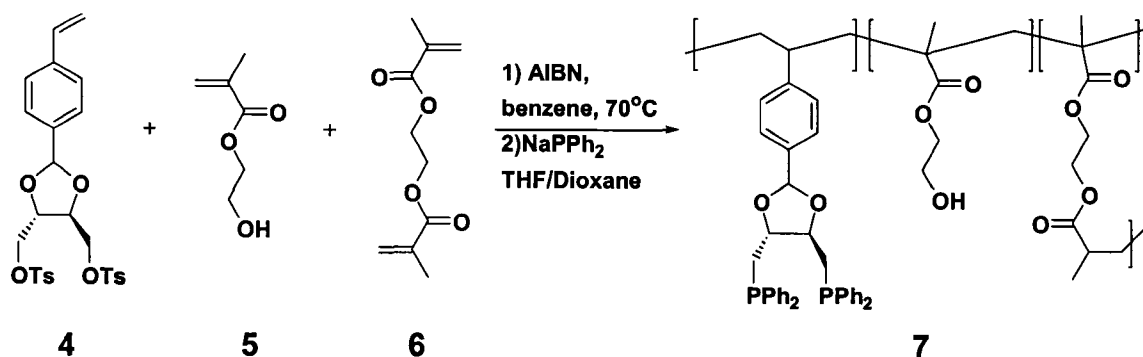


3 was treated with $[\text{RhCl}(\text{C}_2\text{H}_4)_2]_2$ in benzene at room temperature (rt) to generate the active hydrogenation catalyst. The resulting immobilized Rh-DIOP catalyst was used for the asymmetric hydrogenation of simple olefins but showed a much poorer performance than the soluble counterparts. For example, ethylstyrene was hydrogenated quantitatively in 12 h in only 1.5% ee, whereas the soluble catalyst gave 15% ee with complete conversion in under 5 h. Also, α -acetamidocinnamic acid could not be hydrogenated using the immobilized Rh-DIOP catalyst, whereas the homogeneous catalyst gave very good results for this reaction. Kagan concluded that the cause of the low activity was a result of poor compatibility between the reaction solvent and the polymer support. Specifically, the solvent of choice for the hydrogenation of dehydroamino acids is typically a polar alcohol solvent such as ethanol. However, in this case the polymer support was found to contract in ethanol, thereby restricting access of the substrate to the active catalytic sites. This was an early illustration of the problems of matrix diffusion and solvent dependence on the activity of polymer-supported catalysts and these are characteristic features of immobilized catalysts that continue to cause problems in this field. Often the solvent used to gain optimal activity in the homogeneous phase actually prevents catalysis in the heterogeneous phase and finding a compatible solvent with the polymer support

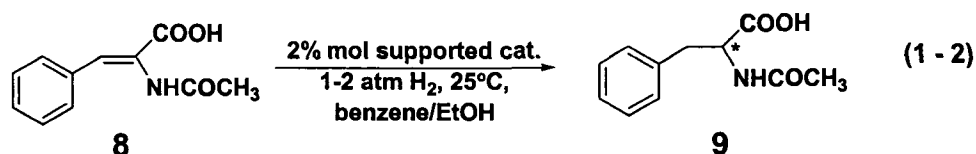
while maintaining high activities and selectivities is a necessary, time-consuming process. Thus, immobilized systems that operate under the same conditions as the homogeneous counterparts are more desirable since they allow for more direct correlations between the homogeneous and the heterogenized systems and provide faster development times.

In an effort to address the issue of solvent dependence, Stille and co-workers focused on incorporating functional groups into the polymer matrix that would allow the polymer to swell in polar solvents to promote access to the active sites. Rather than attachment to Merrifield resin, insoluble polymer-supported catalysts were prepared through copolymerization of suitably functionalized styrene and vinyl monomers. In the first example, an insoluble DIOP-like ligand was prepared by free radical copolymerization of the ditosylate styrene monomer **4**, hydroxyethyl methacrylate **5** and cross-linker ethylene dimethacrylate **6** using AIBN as initiator (Scheme 1-3).²⁵ Subsequent treatment with sodium diphenylphosphide gave the cross-linked phosphinated polymer ligand **7**. The substitution reaction of the tosylate groups was carried out after polymerization to avoid unwanted anionic polymerization, however, only half of the tosyl sites were substituted with phosphines to give a ligand loading of approximately 10 mol %. As well, to ensure the isolation of active sites in the polymer backbone, a low concentration of **4** was maintained in the monomer feed ratio, and this further contributed to a lower ligand loading. The polymer-supported ligand **7** was reacted in situ with 25% of the theoretical amount of $[\text{RhCl}(\text{C}_2\text{H}_4)_2]_2$ in a benzene/ethanol solvent mixture for 36 h to generate the active catalytic sites

Scheme 1-3. Immobilized DIOP ligand.



within the polymer matrix. In this case, benzene acts as a swelling solvent. The authors stated that an excess of phosphine sites were maintained to limit the possibility of monophosphine sites containing Rh and to ensure that any phosphine sites that may have been oxidized during handling would not coordinate to Rh. It is noted that no characterization of the metallated polymers was reported. The catalytic activity of the immobilized Rh-DIOP catalyst was tested in the hydrogenation of α -acetamidocinnamic acid (**8**, MAC acid) in a benzene/ethanol solvent mixture, at 25°C with 1-2 atm of H₂ and a substrate/catalyst (S/C) ratio of 50 (equation 1 - 2). Under these conditions the immobilized catalyst gave **9** in 100% yield in 5 h and 86% ee as compared to

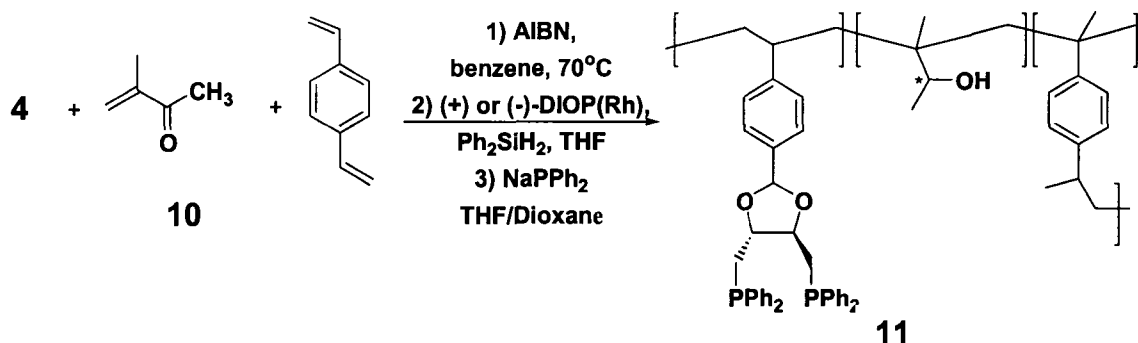


100% yield in 1 h and 81% ee for the homogeneous Rh-DIOP catalyst. The slower rate of reaction obtained with the polymer-supported catalyst is a result of poor diffusion of the substrate into the polymer. Moreover, the polymer-

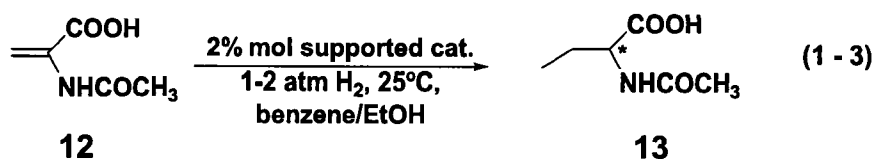
supported catalyst performed poorly upon repeated reuse as a result of polymer degradation by hydrolysis of the ether groups in the polymer backbone.

In a related study, Stille incorporated chiral pendant alcohol groups within the polymer backbone to examine the role between the polymer support and the catalytic sites.²⁶ The polymer-supported ligand **11** was prepared by copolymerization of methyl vinyl ketone **10** with **4** in a 9:1 ratio by radical initiation in the presence of 2 mol % of DVB (Scheme 1-4). Next, *R* or *S* pendant alcohol groups were generated by enantioselective hydrosilylation with the homogeneous (+)- or (-)-DIOP-Rh catalyst in THF, followed by phosphination to give **11**. To evaluate the effect of the chiral pendant alcohol group, the supported

Scheme 1-4. Immobilized DIOP ligand with chiral alcohol groups.



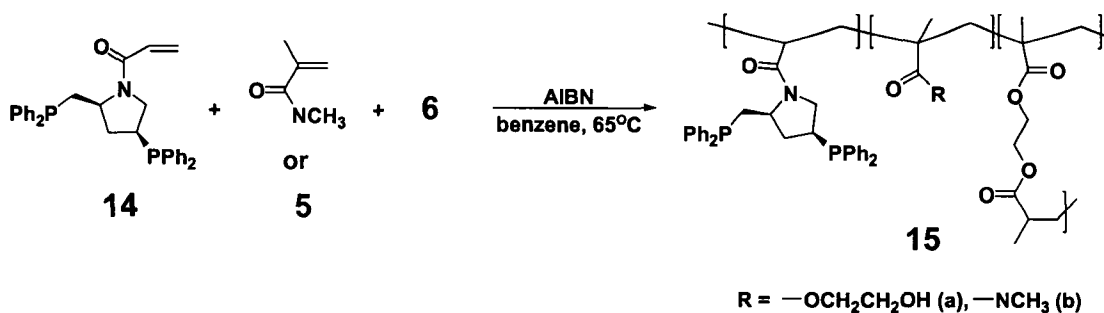
catalysts were generated in situ by reacting **11** with [RhCl(C₂H₄)₂]₂ in a 8:1 ratio in a benzene/ethanol solvent mixture for 24 h and used in the asymmetric hydrogenation of α -acetamidoacrylic acid **12** (equation 1 - 3). For the hydrogenation of **12** carried out at 1 atm of H₂, 25 °C with a S/C = 100 in a



benzene/ethanol solvent mixture, the supported catalyst (with *R*-alcohol) gave **13** in 75% ee, slightly higher than the soluble Rh-DIOP catalyst (70% ee). Switching the solvent system to THF, the homogeneous catalyst resulted in only 7% ee, whereas the supported catalyst gave **13** in 40% ee and was reused three times. In addition, a 15% difference in optical yields was observed by simply changing the chirality of the pendant alcohol (40% ee for *R* vs 24% ee for *S*). In this work, Stille showed that interactions between the polymer support and the catalytic sites do occur and that such interactions can be tuned to give improved enantioselectivities.

Stille also prepared insoluble polymers based on the BPPM (2,3-bis-(diphenylphosphino)-*N*-phenylmaleimide) ligand through radical copolymerization of monomer **14** with **5** or *N,N*-dimethacrylamide and using **6** as a cross-linking agent (Scheme 1-5).²⁷ The polymer-supported ligands **15a** and **15b** were metallated in situ using [Rh(COD)Cl]₂ as the precursor with a ligand/metal ratio of 0.5. Again, in this study interactions between the polymer backbone and the active sites were observed to have an effect on catalyst performance. The hydrogenation of MAC acid (**8**) was carried out at 20°C with a hydrogen pressure of 55 bar in ethanol and a S/C ratio of 50, in the presence of 6 mol % of triethylamine. For the supported catalyst containing the pendant alcohol groups 91% ee was obtained, whereas the supported catalyst containing the pendant

Scheme 1-5. Immobilized BPPM ligand.



amide groups occurred with 64% ee. The drop in selectivity was linked to the ability of the amide functionality to compete with phosphine sites during the metallation step resulting in non-chiral catalytic sites. Another interesting observation was made by comparison with results obtained by Achiwa where a similar polymer catalyst gave only 23% ee for the hydrogenation of **8**.²⁸ The only difference in ligand preparation of these two supported catalysts was the absence of a cross-linking agent in Achiwa's case. This is an important observation that illustrates the benefit of a cross-linker to impart rigidity to the polymer matrix as it shows that a more rigid polymer structure provides more stable catalytic sites and better site isolation.

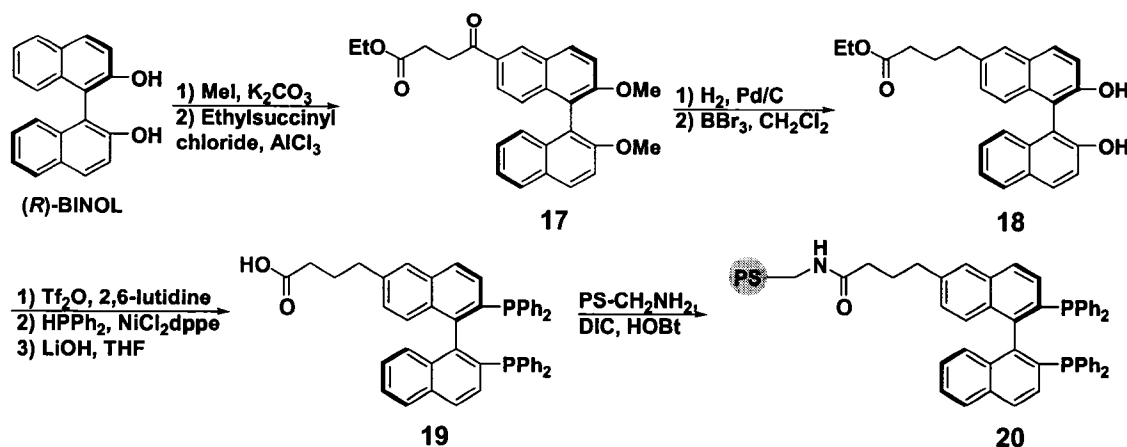
Although the pioneering work by Kagan and Stille is not useful from a practical standpoint in terms of catalytic performance, their efforts provide key insight into the problems associated with the immobilization of homogeneous catalysts onto polymer supports and ways to address these shortcomings. For example, solvent compatibility issues and poor accessibility to the active sites due to matrix diffusion problems can be addressed by the copolymerization method of suitably functionalized monomers and the use of swelling co-solvents.

As well, it has been shown that functionality incorporated in the polymer backbone has an influence on catalyst performance and can be fine-tuned to enhance selectivities. The main limitations with the pioneering work deal with poor metallation procedures, low ligand loading on the polymer support, lack of control over site distribution, poorer catalytic activity compared to the homogeneous counterparts and limited reusability.

More recent strategies used to prepare polymer-supported catalysts for asymmetric hydrogenation have dealt with the immobilization of BINAP due to its success as a chiral ligand. BINAP is one of the most effective and versatile ligands for asymmetric catalysis, and has been successfully applied to a variety of asymmetric catalyzed transformations leading to the synthesis of many biologically important compounds, both in academia and industry.²⁹ Particularly, Rh- and Ru-BINAP catalysts have been very well-developed for the asymmetric hydrogenation of a variety of prochiral substrates such as ketones, olefins and more recently imines.³⁰ As such, the remaining examples presented in this review deal with techniques used to prepare polymer-supported BINAP catalysts. As well, applicable commercial applications and synthetic processes of biologically important molecules that utilize BINAP are also presented to underline the potential of immobilizing BINAP-based systems.

The first polymer-supported BINAP hydrogenation catalyst was reported in 1998 by Bayston et al. and followed the more traditional approach of grafting a suitably functionalized BINAP monomer to a commercially available polystyrene resin (Scheme 1-6).³¹ Here, the carboxylic acid-functionalized BINAP ligand **19**

Scheme 1-6. Functionalization and grafting of BINAP to polystyrene.

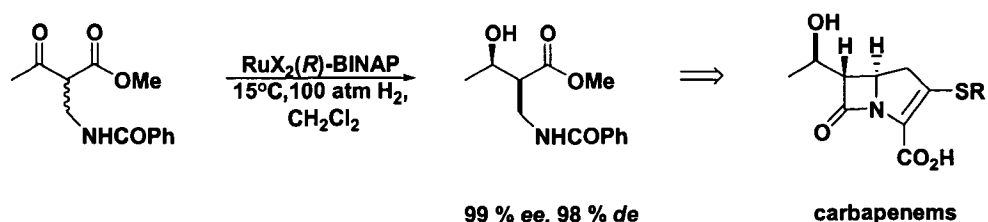


was prepared by Friedel-Crafts acylation of optically pure BINOL protected as ethers to form **17**. Selective reduction of the ketone group, followed by removal of the methyl esters using BBr_3 gave **18** and after conversion to the ditriflate species, the phosphine groups were introduced by routine BINAP synthesis involving a nickel-mediated double phosphination with HPPH_2 .³² The resulting mono-substituted BINAP ligand **19** was coupled to commercially available aminomethylated polystyrene resin (cross-linked with 1% DVB) through condensation between the carboxylic acid functionality on **19** and the available amino groups on the polymer to give **20**. It is noted that not all available amino groups were ligated since of the 0.21 mmol of NH_2/g of aminopolystyrene, a ligand loading of 0.18 mmol/g was achieved. It is also interesting that Bayston chose a mono-substituted BINAP derivative rather than a di-substituted derivative in order to gain maximum flexibility and mobility of the active centers and to prevent cross-linking of the polymer matrix. This approach contradicts the previous work by Stille where an increase in rigidity in the polymer backbone was

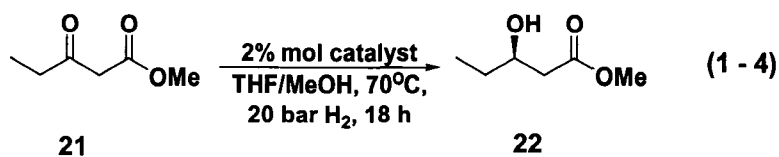
desired in order to provide better site isolation and contribute to the overall stability of the supported catalyst.

Bayston prepared an active hydrogenation catalyst by reacting **20** with $\text{Ru}(\text{COD})(\text{methallyl})_2$ and HBr in acetone to generate what is believed to be $[\text{Ru}(\mathbf{20})\text{Br}_2]$.³³ It is noted that no characterization of the metallated polymers was reported. Such halogen-containing complexes as $\text{RuX}_2(\text{BINAP})$ ($\text{X} = \text{Cl}, \text{Br}$) were originally developed by Noyori et al. and are efficient catalysts for the asymmetric hydrogenation of functionalized ketones.³⁴ This catalyst system is very well established and has been applied to the synthesis of a large variety of pharmaceutically important chiral molecules.³⁵ For example, Takasago International Co. has utilized this technology as a key step in the manufacture of carbapenem antibiotics (120 tons/year) as shown in Scheme 1-7.³⁶ Hence, the immobilization of this catalyst system could have an immediate impact on already established industrial processes.

Scheme 1-7. Synthesis of carbapenem antibiotics.



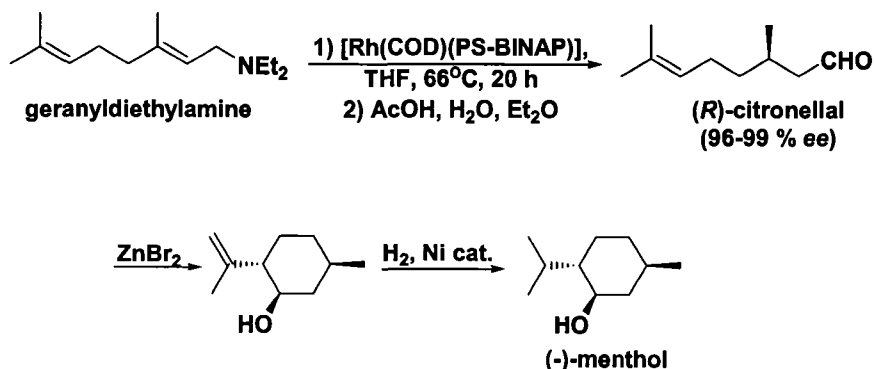
The utility of Bayston's supported catalyst for the asymmetric hydrogenation of functionalized ketones was tested using methyl acetoacetate **21** as a test substrate (equation 1 - 4).⁹ The hydrogenation using the supported



catalyst (10 bar H₂ with a S/C = 50, 70°C, THF/MeOH, 18 h) occurred with 97% ee (100% yield) as compared to 99% ee (100% yield) obtained with the homogeneous BINAP-Ru catalysts (20 bar H₂, S/C = 50, 40°C, CH₂Cl₂, 16h). In this case, a swelling co-solvent (THF) was employed in order to obtain rates comparable to the homogeneous catalyst. The polymer-supported catalyst was recovered by filtration and reused by subjecting the catalyst to the same hydrogenation conditions. However, a loss in activity and selectivity was observed upon repeated reuse with the 3rd run requiring 36 h to give 82% yield and 90% ee. More importantly, metal leaching was reported to be less than 1 mol % of the total amount of ruthenium used in the reaction.

The commercial availability of Bayston's polystyrene-BINAP ligand **20** has resulted in other examples where it has been employed for heterogeneous asymmetric catalysis. For example, Chapuis and co-workers at Firmenich treated **20** with [Rh(COD)₂]CF₃SO₃ to generate the supported catalyst [Rh(**20**)(COD)]⁺ (**23**) and then tested in the asymmetric isomerization of geranyldiethylamine to (*R*)-citronellal (Scheme 1-8).³⁷ This asymmetric isomerization reaction represents the first commercial application of BINAP and is used by Takasago for the industrial synthesis of (-)-menthol (1000 tons/year).³⁸ An interesting feature of the industrial process is that the ability to recycle the homogeneous BINAP-Rh^I catalyst is what made this process commercially

Scheme 1-8. Asymmetric isomerization and Takasago (-)-menthol synthesis.

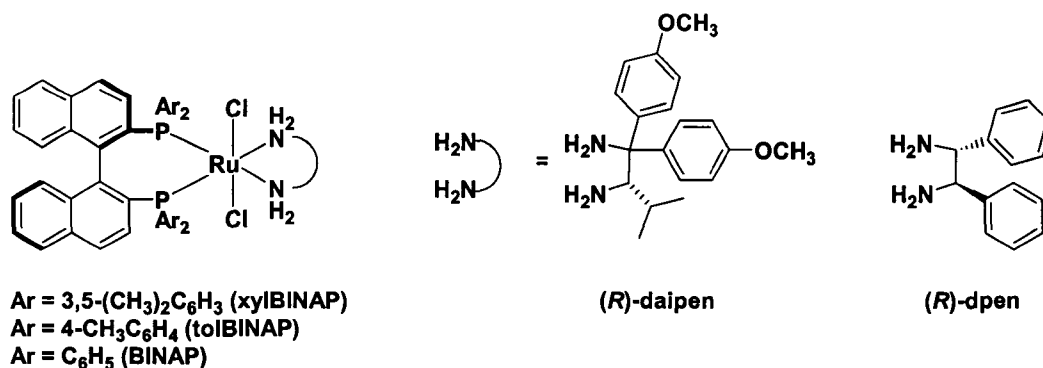


viable. In this case, the active catalyst is recovered after removal of the product by distillation. Typically, recovery of transition metal catalysts by distillation only works if the product is volatile since most homogeneous catalysts are thermally sensitive and decompose at elevated temperatures or reduced pressures.³⁹ Thus, an immobilized catalyst system would have a broader scope and would also avoid the extra distillation step required to obtain clean products, providing a faster turn-around time between runs.

Chapuis employed the immobilized catalyst **23** in THF at 66°C with a S/C ratio of 400 and (*R*)-citronellal was obtained with 100% yield and 99% ee. In addition, the supported catalyst was recovered by filtration and reused 37 times to give a total TON greater than 14,000. Although the level of reusability and selectivity were exceptional, the activity of the polymer-supported system is far inferior to the homogeneous catalyst. For example, in the industrial process, the homogeneous catalyst operates at a S/C ratio of 8000 (80-100°C, THF) to give (*R*)-citronellal in 99% ee and can be reused more than 50 times.

Another BINAP-based catalyst system that has received a lot of attention towards immobilization is Noyori's *trans*-RuCl₂(BINAP)(diamine) system.^{8,40,41} This catalyst system consists of *trans*-RuCl₂(diphosphine)(diamine) plus base in alcohol solvents and serves as one of the most outstanding reactions in asymmetric catalysis for the hydrogenation of simple ketones in very high TON's, TOF's and ee's. This catalyst system allows for the preferential reduction of carbonyls over pre-existing carbon-carbon multiple bonds and since both the diphosphine and diamine ligands are chiral, the reactivity and selectivity are fine-tuned by changing the sterics and electronic properties of the auxiliaries. Some possible catalyst precursors that have been prepared by different combinations of diphosphines and diamines are shown in Figure 1-1.

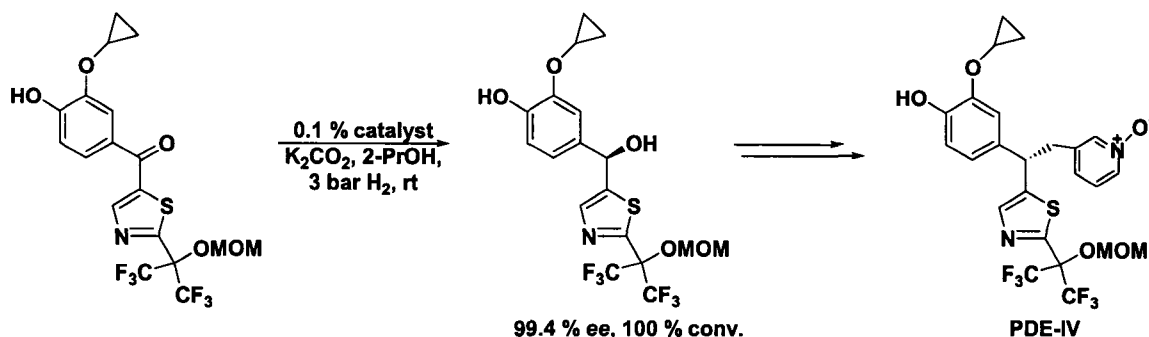
Figure 1-1. Various [RuCl₂((*R*)-BINAP)((*R,R*)-diamine)] complexes.



The use of appropriate chiral diphosphines and diamines allows for the asymmetric hydrogenation of a wide range of ketones and this technology has been applied to the synthesis of various biologically important chiral compounds.⁴² As a recent example, Chen et al. (Merck) employed *trans*-

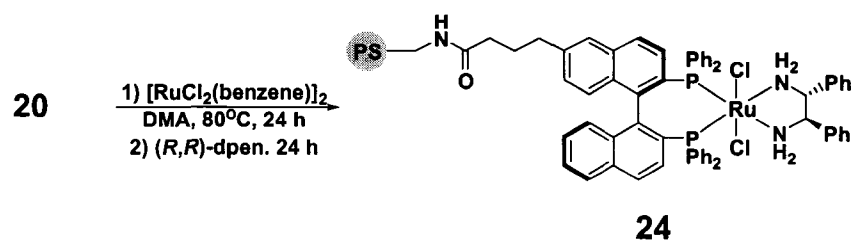
$\text{RuCl}_2((R)\text{-xyIBINAP})((R)\text{-daipen})$ in the key step for the synthesis of phosphodiesterase-IV (PDE-IV) inhibitor, a potential therapeutic agent for treatment of asthma (Scheme 1-9).⁴³ This example is a good demonstration of the functional group tolerance of the Ru-(diphosphine)(diamine) catalyst system and the authors stated that a S/C ratio of 1000 makes this process viable. Hence, due to its industrial potential numerous attempts have been made to immobilize Noyori's Ru-(diphosphine)(diamine) catalyst system.

Scheme 1-9. Practical asymmetric synthesis of PDE-IV inhibitor.

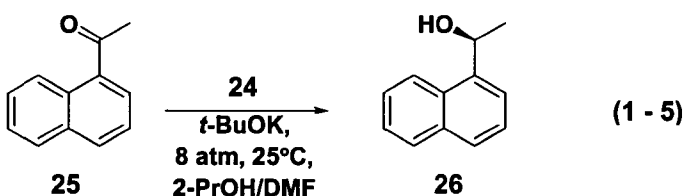


As an example, Noyori treated Bayston's polystyrene-BINAP ligand **20** (0.133 mmol) with $[\text{RuCl}_2(\eta^6\text{-benzene})]_2$ (0.206 mmol) in *N,N*-dimethylacetamide (DMA) at 80°C for 24 h followed by treatment with (*R,R*)-dpen (0.667 mmol) for another 24 h to give the polystyrene-supported catalyst **24** (Scheme 1-10).⁴⁴ The metallation step was not clean and ^{31}P NMR analysis showed that the polymer resin consisted of 81% of the desired diphosphine/diamine complex along with a mixture of unreacted ligand and some unknown compound. Despite the mixture of products, the polymer resin was used for the asymmetric hydrogenation of

Scheme 1-10. Synthesis of polymer-supported catalyst **24**.



various aromatic ketones. For the hydrogenation of 1'-acetonaphthone **25** (8 atm of H₂, 25°C, *i*-PrOH/DMF, S/C = 2470) with 2 mol % of *t*-BuOK an ee of 98% was obtained that is comparable to 97% ee for the homogeneous catalyst (equation 1 - 5). The heterogenized catalyst gave a TOF = 390 h⁻¹, however, no rate data were obtained for the homogeneous system under these conditions. More importantly, the heterogenized catalyst was recovered by filtration and reused in 14 experiments with a total TON of 33,000. However, while the product ee remained high (97-98%), the activity decreased rapidly after the 9th run, with the reaction time extended to 84 h for complete conversion in the 10th run as compared to 20 h for the 2nd run.

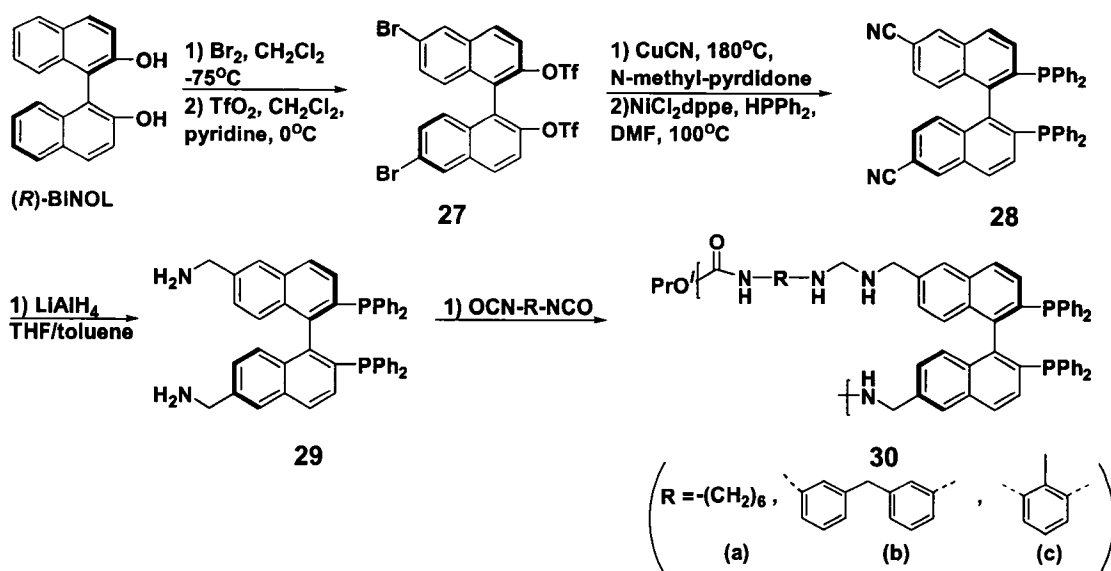


The main drawback with this supported catalyst system is the common matrix diffusion issues and the incompatibility of the polystyrene resin with 2-propanol, the solvent of choice for these reactions. Hence, the reactions were

carried out in a 2-propanol/DMF (1/1) solvent mixture, where DMF acts as a swelling co-solvent to provide better access to the catalytic sites in order to conserve the TOF. The need for a swelling co-solvent limits the applicability of the supported catalyst for large scale operation and for minimal environmental impact, toxic solvents such as DMF should be avoided. Thus, due to the poor compatibility of the reaction solvent used for the hydrogenation reaction, polystyrene supports are less frequently employed as an immobilization vehicle. Instead, the copolymerization method introduced by Stille has been more often used for the immobilization of BINAP and the remaining examples presented are prepared this way. The copolymerization methodology also offers the advantage to fine-tune the polymer backbone and to incorporate active sites throughout the polymer chain rather than just at the terminals of the polymer support.

Lemaire and co-workers incorporated BINAP into the polymer backbone by copolymerization of a suitably bis-functionalized BINAP monomer with diisocyanates, as shown in Scheme 1-11.⁴⁵ In this procedure optically pure BINOL was brominated at the 6,6'-positions, followed by triflation to give the protected dibromo-BINOL species **27**. Substitution of the two bromo groups with two cyano groups and introduction of the two diphenylphosphino moieties by standard phosphination procedures gave 6,6'-dicyano-BINAP **28**.³² Reduction of the cyano groups using lithium aluminum hydride resulted in 6,6'-diaminomethyl-BINAP **29**, with an overall yield of 21%. Finally, insoluble polymers were obtained from the polycondensation of **29** with the diisocyanates to generate the polyureas **30a-c**. The incorporation of the polyurea functionality in the polymer

Scheme 1-11. Lemaire's functionalization of BINAP and synthesis of polyureas.



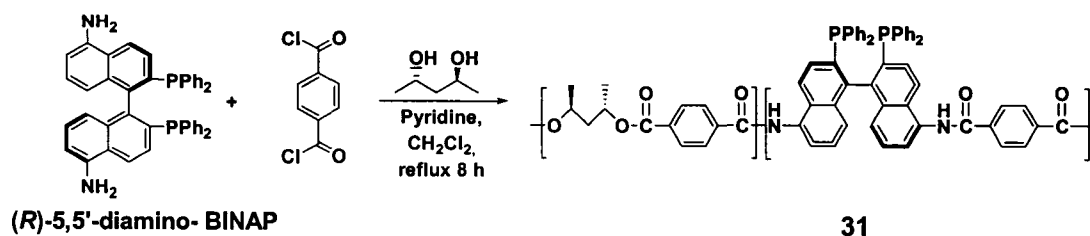
backbone was designed to allow for better solubility/swellability properties in methanol, the solvent of choice for hydrogenations of β -ketoesters. Active catalysts were prepared in situ by reacting the polyureas with $\text{Ru}(\text{COD})(\text{methallyl})_2$ and HBr in acetone and tested in the hydrogenation of methyl acetoacetate **21** (40 atm of H_2 , 50°C , S/C = 1000, MeOH). No characterization data were reported for any of the metallated polymers. The most effective catalyst system was **30c**, which gave 100% yield and 99% ee, the same as those obtained with the (*R*)-BINAP ligand in the homogeneous phase. In addition, the rigid polymer catalyst system based on **30c** could be recovered by centrifugation/filtration and reused three times without loss of selectivity or activity. With **30b** good results were obtained in the first run (97% yield, 99% ee), but for the second run a significant drop in yield from 97% to 53% occurred. With the more flexible polymer system **30a**, 52% yield and 88% ee was obtained

but this could not be reused. No rate comparisons were made between the polymer-supported catalyst and the homogeneous catalyst.

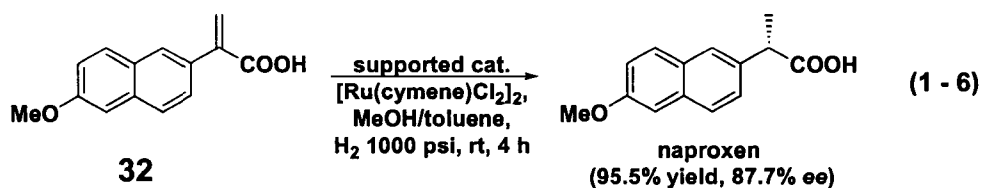
Lemaire's work clearly shows that rigidity plays a significant role and that the more rigid spacer linker gave better results in terms of catalyst performance and reusability. This is strong evidence that supports the idea that a less flexible polymer is more likely to maintain a stable catalyst conformation in the polymer. However, too much rigidity can have a negative impact by restricting the accessibility of the active sites. For example, when **30c** was cross-linked with 30% triisocyanatotoluene, a significant decrease in activity and selectivity (35% yield, 9% ee) was observed. Hence, the degree of rigidity is an important parameter and a balance between stable catalyst conformations and site accessibility must be considered. The polyureas prepared by Lemaire were also used for hydrogenation of aryl-ketones with modest results.⁴⁶

In an attempt to further address the matrix diffusion problems associated with most polymer-supported systems, Chan et al. prepared the first soluble polymer-supported BINAP catalyst which resulted in better activity than the monomeric catalyst while retaining the high enantioselectivity.⁴⁷ The concept was based on a "one phase catalysis and two phase separation" whereby catalysis takes place in the homogeneous phase and recovery is achieved by a precipitation and filtration method. In this work, a soluble polyester-supported BINAP ligand **31** was synthesized by the polycondensation of (*R*)-5,5'-diamino-BINAP, terephthaloyl chloride and (2*S*,4*S*)-pentanediol in the presence triethylamine in methylene chloride (Scheme 1-12). The synthesis of the (*R*)-5,5'-

Scheme 1-12. Chan's preparation of a soluble polymer-supported BINAP ligand.



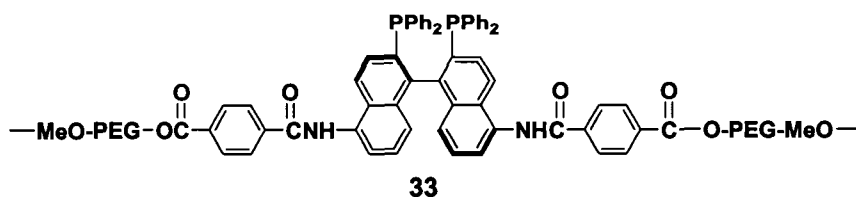
diamino-BINAP is not covered here since it is discussed in more detail in Chapter 3. The active catalyst was generated in situ by mixing **31** with $[\text{RuCl}_2(\text{cymene})]_2$ toluene, THF, CH_2Cl_2 , but recovered by precipitation in methanol. The soluble nature allowed for detailed characterization by standard solution NMR spectroscopy. The supported catalyst was tested in the asymmetric hydrogenation of 2-(6'-methoxy-2'-naphthyl)acrylic acid (**32**) to naproxen (equation 1 - 6). This reaction represents another important application of BINAP chemistry, where BINAP-based catalysts have been used for the synthesis of the anti-inflammatory drug, naproxen, which is obtained in 97% ee.⁴⁸ Under the conditions reported in equation 1 - 6, the polyester-supported catalyst (S/C = 200) gave naproxen in 87.7% ee and 95.5% yield with a TOF = 47.8 h⁻¹. Under identical conditions, the homogeneous BINAP catalyst occurred in 56.5% yield and 88.7% ee with a much lower TOF = 28.3 h⁻¹. Furthermore, the supported catalyst was quantitatively precipitated by the addition of methanol (7-fold excess), recovered by filtration and reused for 10 cycles without loss of activity



and selectivity. Metal leaching experiments showed that less than 16 ppb of Ru content was present in the product stream, representing greater than 99.9% catalyst recovery. The main limitation with Chan's soluble polymer-supported catalyst is that the recovery process is slow and the requirement of a large excess of a precipitating solvent makes the process cumbersome for batch type reactors.

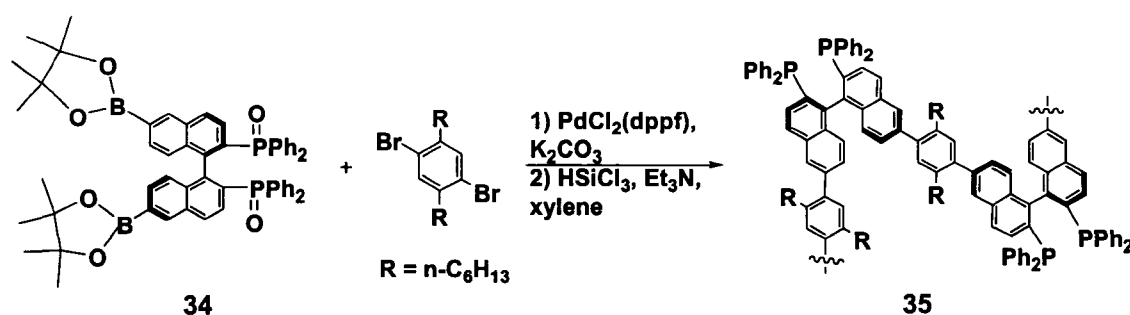
As an extension to this work Chan et al. prepared a more rigid polymer-supported BINAP system by using polyethylene glycol monomethylether (MeO-PEG-OH) as co-support (Figure 1-2).⁴⁹ The MeO-PEG supported BINAP ligand **33** was prepared by condensation of (*R*)-5,5'-diamino-BINAP with terephthaloyl chloride and MeO-PEG-OH. Apart from the increase in rigidity, the presence of poly(ethylene glycol) improved the solubility of the polymeric system in methanol, allowing for the hydrogenation of 2-arylacrylic acids to be done under more favorable conditions. The active catalyst was prepared as described above and the hydrogenation of **32** (MeOH, 100 psi of H₂, rt, S/C = 200) occurred with 91.2% ee and 100% yield in 2 h (TOF = 100 h⁻¹). The supported catalyst was recovered by the precipitation/filtration method and reused three times without loss of activity or selectivity.

Figure 1-2. MeO-PEG-supported BINAP.



Another soluble polymer containing BINAP in the main chain was described by Pu et al.⁵⁰ In this work a rigid and sterically regular polymeric structure **35** was prepared via multiple palladium catalyzed Suzuki coupling of 1,4-dibromo-2,5-dialkylbenzene with a chiral BINAP-boronic ester, followed by reduction of the phosphinoxy groups with trichlorosilane (Scheme 1-13).⁵⁰ The BINAP monomer **34** was synthesized in eight steps starting from optically pure BINOL and due to the long synthetic procedure it is not covered in this Chapter.⁵¹ The polymer-supported ligand **35** was used to prepare rhodium(I) and ruthenium(II) based systems for the asymmetric hydrogenation of dehydroamino acids derivatives and ketones, respectively. The supported catalyst systems are soluble in common organic solvents such as THF, toluene and CH₂Cl₂, but are insoluble in methanol and are recovered by the precipitation/filtration method described by Chan. ³¹P NMR analysis showed that well-ordered polymer structures were obtained.

Scheme 1-13. Pu's sterically regular polymer BINAP ligand.



The supported Rh-based catalyst was prepared in situ by reacting **35** with [Rh(COD)₂]₂BF₄ in a 1.1/1 ratio in THF. The hydrogenation of (Z)-methyl α-

(benzamido)cinnamate (30 psi of H₂, rt, THF, S/C = 50) occurred with 99% yield and 75% ee comparable to 99% yield and 76% ee obtained with the (*R*)-BINAP ligand in the homogeneous phase. In this case, the supported catalyst was only used one time before a significant drop in activity and selectivity was observed. The supported Ru-based catalyst was prepared by treatment of **35** with [RuCl₂(C₆H₆)₂] in DMF followed by addition of (*R,R*)-dpen to generate the BINAP/dpen-Ru active site within the polymer structure. Using the supported catalyst, 1'-acetonaphthone was hydrogenated (200 psi, rt, 2-PrOH, 20 mol % base, 66 h) in near 100% yield with 92% ee. These results are not comparable to those obtained with the homogeneous BINAP catalyst which typically operates at S/C = 1000 with complete conversion in 20 h and 98% ee.⁴¹ The supported system showed poor reusability and after one run 89% ee was observed. No data was provided for metal leaching of these polymer-supported catalysts. In Pu's case, the polymer-supported catalysts were carefully designed to provide a high density of active sites in a well-defined rigid structure to maintain both the steric and electronic properties of the monomeric catalyst. However, the results obtained show that despite all these factors the supported catalysts were not as efficient as the homogeneous catalysts.

As illustrated in this review there are a number of drawbacks associated with polymer-supported catalysts that need to be addressed before they can become a viable option for industry. For example, the procedures used to prepare these polymer-supported catalysts are far from trivial, and often the final immobilized catalyst suffers from low ligand loading, incomplete metallation and

ill-defined catalytic sites. Furthermore, since lengthy functionalization procedures substantially increase catalyst cost, it is imperative that a much higher level of reusability is achieved than has been demonstrated. As well, the catalytic performance of polymer-supported catalysts can be influenced by the nature of the polymer support, especially in terms of catalyst durability and enantioselectivity, and therefore the role of the polymer backbone must be considered. It is also beneficial that the polymer-supported catalysts perform well under homogenous conditions since subtle changes to the reaction conditions can influence catalyst performance. The work reviewed above also shows that in some cases an increase in activity and selectivity is observed. However, in most cases the polymer-supported catalysts suffer from lower catalytic efficiencies than those of the homogeneous system and therefore the immediate benefit of recovery and reuse of the expensive catalyst has not been realized. Hence, there is a need for more efficient polymer-supported catalysts that can operate under homogeneous conditions with high levels of reusability while maintaining constant activities and selectivities, as good as or better than the homogeneous counterparts, and without metal leaching.

The primary goal of this research was to develop new procedures for the synthesis of polymer-supported catalysts in an effort to address the limitations discussed above. In this way, an alternating ring-opening metathesis polymerization (ROMP) methodology was developed for the reproducible synthesis of well-ordered, highly efficient and reusable polymeric asymmetric hydrogenation catalysts. To extend our knowledge of the factors governing the

alternating polymerization sequence and to better predict the polymer structure, detailed in situ NMR studies were performed. Due to the success of this methodology another major goal was to show the adaptability and versatility of this new immobilization technique. In this way, a novel ROMP-active BINAP monomer was synthesized and the alternating ROMP methodology was employed to assemble catalyst-organic frameworks. These insoluble frameworks were used as ketone hydrogenation catalysts that showed an extraordinary level of reusability without losses in activity and selectivity, and without detectable metal leaching. The work presented in this thesis is a major step forward for the development of sustainable asymmetric catalyzed processes that could help bridge the gap between potential and application.

References

- (1) Marino, S. T.; Stachurska-Buczek, D.; Huggins, D. A.; Krywult, B. M.; Sheehan, C. S.; Nguyen, T.; Choi, N.; Parsons, J. G.; Griffiths, P. G.; James, I. W.; Bray, A. M.; White, J. M.; Boyce, R. S. *Molecules* **2004**, *9*, 405-426.
- (2) Farina, V.; Reeves, J. T.; Senanayake, C. H.; Song, J. H. J. *Chem. Rev.* **2006**, *106*, 2734-2793.
- (3) Tombo Ramos, G. M.; Blaser, H. U. *Pesticide Chemistry and Bioscience*; Royal Society of Chemistry: (Eds.: Brooks, G. T., Roberts, T. R.), 1999.
- (4) Noyori, R. *Chem. Tech* **1992**, *22*, 360-367.
- (5) Rouhi, A. M. *Chem. Eng. News* **2004**, *82*, 47-62.
- (6) Trost, B. M. *Angew. Chem. Int. Ed. Engl.* **1995**, 259-281.
- (7) Knowles, W. S. *Angew. Chem. Int. Ed.* **2002**, *41*, 1999-2007. ()
Sharpless, K. B. *Angew. Chem. Int. Ed.* **2002**, *41*, 2024-2032.
- (8) Noyori, R. *Angew. Chem. Int. Ed.* **2002**, *41*, 2008-2022.
- (9) Blaser, H. U.; Malan, C.; Pugin, B.; Spindler, F.; Steiner, H.; Studer, M. *Adv. Synth. Catal.* **2003**, *345*, 103-151.
- (10) Blaser, H. U. *Chem. Commun.* **2003**, 293-296.
- (11) Federsel, H. J. *Nat. Rev. Drug Discovery* **2005**, *4*, 685-697.
- (12) SciFinder, June 26, 2007.
- (13) Garrett, C. E.; Prasad, K. *Adv. Synth. Catal.* **2004**, 889-900.
- (14) <http://www.engelhard.com/eibprices/DPCharts.aspx>.

- (15) (a) *Chiral Catalyst Immobilization and Recycling*; Wiley-VCH: (Eds.: D. E. De Vos, I. F. J. Vankelecom, P. A. Jacobs), **2000**. (b) Song, C. E. *Annu. Rep. Prog. Chem., Sect. C, Phys. Chem.* **2005**, *101*, 143.
- (16) (a) Clapham, B.; Reger, T. S.; Janda, K. D. *Tetrahedron* **2001**, *57*, 4637-4662. (b) Dioos, B. M. L.; Vankelecom, I. F. J.; Jacobs, P. A. *Adv. Synth. Catal.* **2006**, *348*, 1413-1446. (c) End, N.; Schoning, K. U. *Immobilized Catalysts Topics In Current Chemistry* **2004**, *242*, 241-271. (d) Fan, Q. H.; Li, Y. M.; Chan, A. S. C. *Chem. Rev.* **2002**, *102*, 3385-3465. (e) Leadbeater, N. E. *Curr. Med. Chem.* **2002**, *9*, 2147-2171. (f) Leadbeater, N. E.; Marco, M. *Chem. Rev.* **2002**, *102*, 3217-3273.
- (17) Chen, B.; Dingerdissen, U.; Krauter, J. G. E.; Rotgerink, H.; Mobus, K.; Ostgard, D. J.; Panster, P.; Riermeier, T. H.; Seebald, S.; Tacke, T.; Trauthwein, H. *Appl. Catal A: General* **2005**, *280*, 17-46.
- (18) (a) Bergbreiter, D. E. *Immobilized Catalysts Topics In Current Chemistry* **2004**, *242*, 113-176. (b) Heitbaum, M.; Glorius, F.; Escher, I. *Angew. Chem. Int. Ed.* **2006**, *45*, 4732-4762. (c) McMorn, P.; Hutchings, G. J. *Chem. Soc. Rev.* **2004**, *33*, 108-122. (d) Saluzzo, C.; Lemaire, M. *Adv. Synth. Catal.* **2002**, *344*, 915-928.
- (19) Tzschucke, C. C.; Markert, C.; Bannwarth, W.; Roller, S.; Hebel, A.; Haag, R. *Angew. Chem. Int. Ed.* **2002**, *41*, 3964-4000.
- (20) Ablan, C. D.; Hallett, J. P.; West, K. N.; Jones, R. S.; Eckert, C. A.; Liotta, C. L.; Jessop, P. G. *Chem. Commun.* **2003**, 2972-2973.

- (21) (a) Heldebrant, D. J.; Witt, H. N.; Walsh, S. M.; Ellis, T.; Rauscher, J.; Jessop, P. G. *Green Chem.* **2006**, *8*, 807-815. (b) Heldebrant, D. J.; Jessop, P. G. *J. Am. Chem. Soc.* **2003**, *125*, 5600-5601.
- (22) (a) Merrifield, R. B. *J. Am. Chem. Soc.* **1963**, 2149. (b) Merrifield, R. B. *Science* **1986**, 341.
- (23) Grubbs, R. H.; Kroll, L. C. *J. Am. Chem. Soc.* **1971**, 3062.
- (24) Dumont, W.; Poulin, J. C.; Dang, T. P.; Kagan, H. B. *J. Am. Chem. Soc.* **1973**, 8295-8299.
- (25) Takaishi, N.; Imai, H.; Bertelo, C. A.; Stille, J. K. *J. Am. Chem. Soc.* **1978**, *100*, 264-268.
- (26) (a) Masuda, T.; Stille, J. K. *J. Am. Chem. Soc.* **1978**, *100*, 268-272. (b) Deschenaux, R.; Stille, J. K. *J. Org. Chem.* **1985**, *50*, 2299-2302.
- (27) (a) Baker, G. L.; Fritschel, S. J.; Stille, J. K. *J. Org. Chem.* **1981**, *46*, 2960-2965. (b) Baker, G. L.; Fritschel, S. J.; Stille, J. R.; Stille, J. K. *J. Org. Chem.* **1981**, *46*, 2954-2960.
- (28) Achiwa, K. *Chem. Lett.* **1978**, 905-908.
- (29) Noyori, R. *Catalysis in Organic Synthesis*; Wiley: New York, **1994**.
- (30) (a) Akutagawa, S. *Appl. Catal A:General* **1995**, *128*, 171-207. (b) Noyori, R.; Takaya, H. *Acc. Chem. Res.* **1990**, *23*, 345-350.
- (31) Bayston, D. J.; Fraser, J. L.; Ashton, M. R.; Baxter, A. D.; Polywka, M. E. C.; Moses, E. *J. Org. Chem.* **1998**, *63*, 3137-3140.
- (32) Cai, D. W.; Payack, J. F.; Bender, D. R.; Hughes, D. L.; Verhoeven, T. R.; Reider, P. J. *J. Org. Chem.* **1994**, *59*, 7180-7181.

- (33) Genet, J. P.; Mallart, S.; Pinel, C.; Juge, S.; Laffitte, J. A. *Tetrahedron: Asymmetry* **1991**, *2*, 43-46.
- (34) (a) Kitamura, M.; Ohkuma, T.; Inoue, S.; Sayo, N.; Kumobayashi, H.; Akutagawa, S.; Ohta, T.; Takaya, H.; Noyori, R. *J. Am. Chem. Soc.* **1988**, *110*, 629-631. (b) Mashima, K.; Kusano, K. H.; Sato, N.; Matsumura, Y.; Nozaki, K.; Kumobayashi, H.; Sayo, N.; Hori, Y.; Ishizaki, T.; Akutagawa, S.; Takaya, H. *J. Org. Chem.* **1994**, *59*, 3064-3076. (c) Mashima, K. *J. Chem. Soc., Chem. Commun.* **1989**, 1208-10.
- (35) (a) Kitamura, M.; Ohkuma, T.; Takaya, H.; Noyori, R. *Tetrahedron Lett.* **1988**, *29*, 1555-1556. (b) Kitamura, M.; Tokunaga, M.; Noyori, R. *J. Am. Chem. Soc.* **1995**, *117*, 2931-2932. (c) Kitamura, M.; Tokunaga, M.; Ohkuma, T.; Noyori, R. *Tetrahedron Lett.* **1991**, *32*, 4163-4166. (d) Nishi, T.; Kitamura, M.; Ohkuma, T.; Noyori, R. *Tetrahedron Lett.* **1988**, *29*, 6327-6330. (e) Noyori, R.; Ohkuma, T.; Kitamura, M.; Takaya, H.; Sayo, N.; Kumobayashi, H.; Akutagawa, S. *J. Am. Chem. Soc.* **1987**, *109*, 5856-5858.
- (36) (a) Noyori, R.; Ikeda, T.; Ohkuma, T.; Widhalm, M.; Kitamura, M.; Takaya, H.; Akutagawa, S.; Sayo, N.; Saito, T.; Taketomi, T.; Kumobayashi, H. *J. Am. Chem. Soc.* **1989**, *111*, 9134-9135. (b) Noyori, R.; Tokunaga, M.; Kitamura, M. *Bull. Chem. Soc. Jpn.* **1995**, *68*, 36-55.
- (37) Chapuis, C.; Barthe, M.; Laumer, J. Y. D. *Helv. Chim. Acta* **2001**, *84*, 230-242.

- (38) (a) Tani, K.; Yamagata, T.; Akutagawa, S.; Kumobayashi, H.; Taketomi, T.; Takaya, H.; Miyashita, A.; Noyori, R.; Otsuka, S. *J. Am. Chem. Soc.* **1984**, *106*, 5208-5217. (b) Tani, K.; Yamagata, T.; Otsuka, S.; Akutagawa, S.; Kumobayashi, H.; Taketomi, T.; Takaya, H.; Miyashita, A.; Noyori, R. *J. Chem. Soc., Chem. Commun.* **1982**, 600-601. (c) Kragl, U.; Dwars, T. *Trends Biotechnol.* **2001**, *19*, 442-449. (d) Blaser, H. U.; Studer, M. *Chirality* **1999**, *11*, 459-464.
- (39) Cole-Hamilton, D. J. *Science* **2003**, *299*, 1702-1706.
- (40) Noyori, R.; Kitamura, M.; Ohkuma, T. *Proc. Natl. Acad. Sci. U. S. A.* **2004**, *101*, 5356-5362.
- (41) Noyori, R.; Ohkuma, T. *Angew. Chem. Int. Ed.* **2001**, *40*, 40-73.
- (42) (a) Kumobayashi, H.; Miura, T.; Sayo, N.; Saito, T.; Zhang, X. Y. *Synlett* **2001**, 1055-1064. (b) Ohkuma, T.; Koizumi, M.; Doucet, H.; Pham, T.; Kozawa, M.; Murata, K.; Katayama, E.; Yokozawa, T.; Ikariya, T.; Noyori, R. *J. Am. Chem. Soc.* **1998**, *120*, 13529-13530.
- (43) (a) O'Shea, P. D.; Chen, C. Y.; Chen, W. R.; Dagneau, P.; Frey, L. F.; Grabowski, E. J. J.; Marcantonio, K. M.; Reamer, R. A.; Tan, L. S.; Tillyer, R. D.; Roy, A.; Wang, X.; Zhao, D. L. *J. Org. Chem.* **2005**, *70*, 3021-3030. (b) Chen, C. Y. *Abstracts of Papers of the American Chemical Society* **2003**, *226*, U629-U629.
- (44) Ohkuma, T.; Takeno, H.; Honda, Y.; Noyori, R. *Adv. Synth. Catal.* **2001**, *343*, 369-375.

- (45) (a) ter Halle, R.; Colasson, B.; Schulz, E.; Spagnol, M.; Lemaire, M. *Tetrahedron Lett.* **2000**, *41*, 643-646. (b) Saluzzo, C.; Lamouille, T.; Le Guyader, F.; Lemaire, M. *Tetrahedron: Asymmetry* **2002**, *13*, 1141-1146.
- (46) (a) Saluzzo, C.; ter Halle, R.; Touchard, F.; Fache, F.; Schulz, E.; Lemaire, M. *J. Organomet. Chem.* **2000**, *603*, 30-39. (b) ter Halle, R.; Schulz, E.; Spagnol, M.; Lemaire, M. *Synlett* **2000**, 680-682.
- (47) (a) Fan, Q. H.; Ren, C. Y.; Yeung, C. H.; Hu, W. H.; Chan, A. S. C. *J. Am. Chem. Soc.* **1999**, *121*, 7407-7408. (b) Fan, Q. H.; Wang, R.; Chan, A. S. C. *Bioorg. Med. Chem. Lett.* **2002**, *12*, 1867-1871.
- (48) (a) Kitamura, M.; Yoshimura, M.; Tsukamoto, M.; Noyori, R. *Enantiomer* **1996**, *1*, 281-303. (b) Ohta, T.; Takaya, H.; Kitamura, M.; Nagai, K.; Noyori, R. *J. Org. Chem.* **1987**, *52*, 3174-3176.
- (49) Fan, Q. H.; Deng, G. J.; Lin, C. C.; Chan, A. S. C. *Tetrahedron: Asymmetry* **2001**, *12*, 1241-1247.
- (50) (a) Pu, L. *Chem. Eur. J.* **1999**, *5*, 2227-2232. (b) Yu, H. B.; Hu, Q. S.; Pu, L. *Tetrahedron Lett.* **2000**, *41*, 1681-1685.
- (51) (a) Pradellok, W.; Kotas, A.; Walczyk, K. W.; Jedlinski, Z., 1978; Vol. PL 87054. (b) Yu, H. B.; Hu, Q. S.; Pu, L. *J. Am. Chem. Soc.* **2000**, *122*, 6500-6501.

Chapter 2

Reusable Polymeric Asymmetric Hydrogenation Catalyst Made by Ring Opening Metathesis Polymerization *

Introduction

As discussed in Chapter 1, the heterogenization of homogeneous catalysts has become a central topic in the area of asymmetric catalysis, especially as the trend towards “green chemistry” processes have gained much attention.¹ The general concept is to combine the advantages of homogeneous catalysis such as high definition, excellent selectivities and activities, with the advantages of heterogeneous catalysis such as easy separation, improved handling and recycling.^{2,3} Although numerous strategies have been employed to generate heterogenized asymmetric catalysts, it still remains a challenge to develop heterogenized systems that demonstrate catalytic efficiencies as good as or better than their corresponding homogeneous analogs. Despite some successes, the majority of reported heterogenized systems display no or limited reusability (< 3 x) before a significant decrease in activity or selectivity is observed.^{4,5} Thus new strategies towards the development of practical heterogenized asymmetric catalysts that sustain a large number of reuses under

*A version of this chapter has been published. Ralph, C. K.; Akotsi, O. M.; Bergens, S. H. *Organometallics* **2004**, 23, 1484-1486. With the exception of the stoichiometric investigations of the alternating ROMP of **41** and COE all work presented in this chapter is that of C. K. Ralph.

conditions similar to those used for the homogeneous reaction, and at the same time, maintain the same, or better activities and enantioselectivities without catalyst leaching are needed.

Drawing on the successes and failures of the previously reported polymeric hydrogenation catalysts, key insights towards the development of a more efficient and reusable system can be made. For example, most polymeric hydrogenation catalysts are made using the following types of reactions: radical copolymerization of vinyl derivatives of arenes and phosphines,⁶ condensation reactions between acid derivatives and amines or alcohols,^{7,8} condensation polymerizations between diamines and diisocyanates,⁹ and Suzuki-type couplings.¹⁰ As the presence of a metal center can interfere with these reactions, they are often used to either polymerize a chiral phosphine ligand, or to graft it to a polymer support. The critical step then becomes metallating the resulting polymeric ligand to produce the active catalytic sites. This procedure has several disadvantages. For example, due to restricted access to some of the chelating ligands in the polymer matrix, the metallation step may not be quantitative. In other words, a majority of the polymerized ligand may not be metallated. Unfortunately, this point is often not addressed in the literature. For example, solid-state ³¹P NMR studies of the resulting metallated polymers are rare, despite the availability of this analysis technique. Therefore, in order to overcome the matrix diffusion problems and to ensure high catalyst loadings, the polymeric ligands are typically treated with an excess of the metallic species in a swelling solvent. Unfortunately, not only is this an unnecessary waste of the very

commodity which is to be recycled, the extra step often results in oxidation of the phosphines which further prevents complete metallation and can lead to catalyst poisoning.⁴ An alternative approach would be the direct incorporation of the active catalyst by polymerization of a suitable metal containing monomer (MCM).¹¹ This would then result in a higher density of catalytic sites in the polymer matrix and provide maximum knowledge of the actual catalytic species. Furthermore, since the MCM can be studied as a homogeneous catalyst before polymerization, a more accurate mechanistic correlation between the homogeneous and heterogeneous systems can be made. Despite the obvious advantages associated with MCM's, there are relatively few examples of the straightforward approach of using a metal-phosphine complex directly as monomer in the synthesis of a polymeric catalyst.¹²

Another disadvantage of the previous methods used to prepare polymeric hydrogenation catalysts is the lack of control over the polymerization process, which leads to ill-defined polymeric systems. Random distribution of active sites, poor site isolation, limited access to the active sites, and unfavorable interactions with the supports are often the consequence. These factors combine for poor catalyst performance for the heterogenized systems compared to the homogeneous counterparts. Hence, we believe that a regular, rigid, polymeric system with a high density of isolated, well-defined active centres will provide a highly efficient and reusable polymeric catalyst. With these goals in mind we focused on using ring-opening metathesis polymerization (ROMP) to prepare such a well-defined polymeric system.

ROMP, a variant of olefin metathesis, has become one of the most powerful methods for the preparation of advanced functionalized polymers.^{13,14} The reason for the tremendous growth of ROMP-type polymers is due to the development and commercial availability of the well-defined olefin metathesis catalysts **36-38** (Figure 2-1), which promote controlled, living polymerizations.

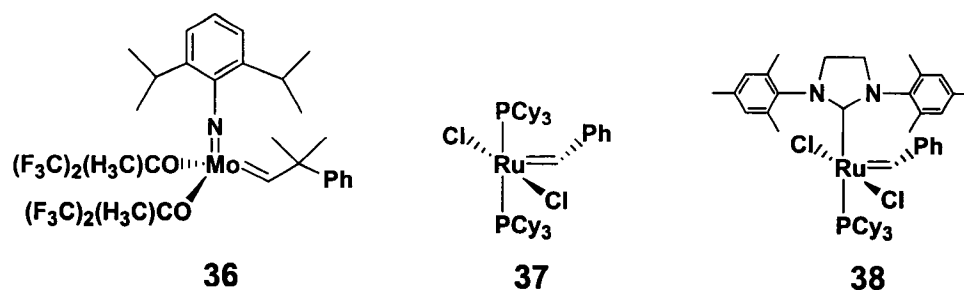


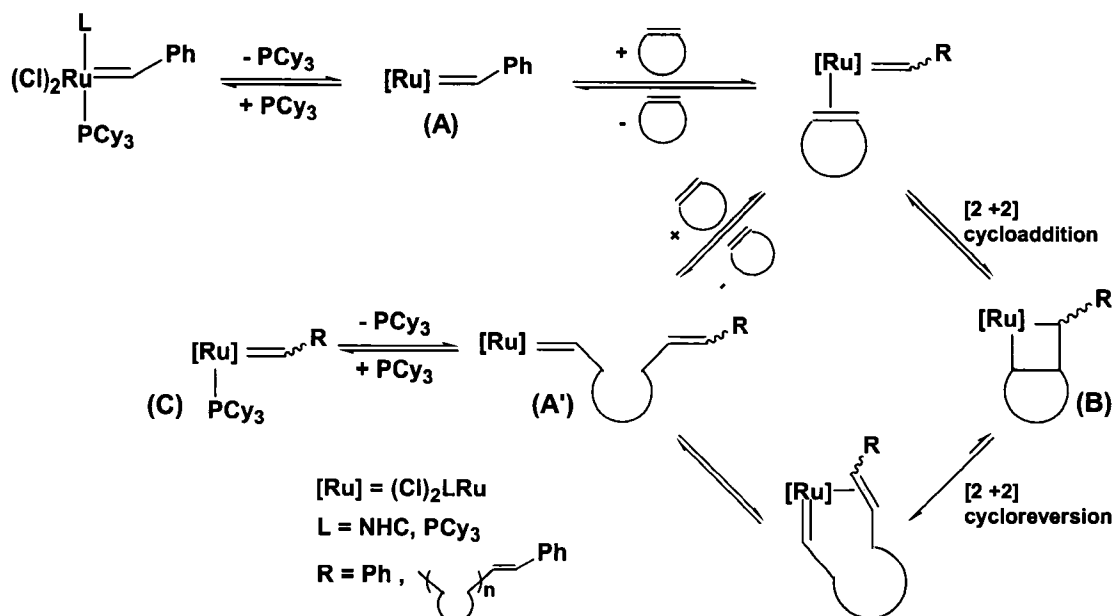
Figure 2-1. Commercially available catalysts for ROMP.

The molybdenum-based catalysts related to **36**, developed by Schrock et al, are known for their high activity and are often employed for the polymerization of sterically hindered and electron deficient monomers.¹⁵ However, uses of the “Schrock catalysts” may be limited by restricted functional group tolerance and sensitivity towards oxygen and moisture. These limitations were reduced with the development by Grubbs et al of the ruthenium-based catalyst (**37**; Cy = cyclohexyl), known as the “1st generation Grubbs catalyst”.¹⁶ Although **37** tolerates a wider range of protic and polar functional groups, it is less active than **36**. Further development by replacing one of the phosphine ligands in **37** by an *N*-heterocyclic carbene (NHC) ligand resulted in the “2nd generation Grubbs catalyst” such as **38** (NHC = 1,3-bis(2,4,6-trimethylphenyl)-4,5-dihydroimidazol-2-

ylidene), which exhibits activity comparable to or higher than **36** and remains tolerant of many functional groups.^{17,18} Thus, the ruthenium-based catalysts are more convenient to use and they allow for the direct incorporation of high degrees of functionality to afford novel polymers with well-defined structures.

The mechanism of olefin metathesis, known as the “Chauvin mechanism” involves the interconversion of olefins and metal alkylidenes via metallacyclobutane intermediates by a sequence of [2 + 2] cycloadditions and cycloreversions to generate new olefins and new alkylidenes (see Scheme 2-1).¹⁹ ROMP reactions are identical to this mechanism except for two important modifications. Specifically, since the reaction involves a cyclic olefin, the newly generated olefin remains attached to the active metal alkylidene as part of a growing polymer chain and the driving force for the reaction is release of ring strain from the cyclic olefin. As such, the most often employed monomers used for ROMP are based on norbornene derivatives since they possess sufficient ring strain to make the process irreversible. Further, a wide range of norbornene-type monomers are available either commercially or they can be synthesized by facile Diels-Alder reactions with cyclopentadiene.²⁰

Detailed mechanistic studies confirmed that ROMP reactions catalyzed by Grubbs catalysts also operate by the “Chauvin mechanism” as shown with a generic cyclic olefin in Scheme 2-1.^{21,22} The first, or the initiation step with Grubbs catalysts involves dissociation of one of the phosphines to generate the reactive 14-electron intermediate (**A**). This step is critical since **A** can either bind to an olefin to continue the catalytic cycle or it can rebind to the phosphine.



Scheme 2-1. Mechanism of Ring-Opening Metathesis Polymerization (ROMP).

Studies show that the rate of phosphine versus olefin coordination to **A** dictates the net activity of the catalyst. Such observations contributed to the discovery of the more active NHC-type catalysts which favor olefin coordination over rebinding of the phosphine.²¹ Once **A** enters the catalytic cycle it quickly undergoes a [2 + 2] cycloaddition to form the metallacyclobutane intermediate (**B**), followed by cycloreversion and olefin dissociation to generate a propagating metal alkylidene species (**A'**) with the attached polymer chain. **A'** can then react with another monomer unit to continue the catalytic cycle and promote polymer growth or it can rebind with free phosphines to generate the dormant species **C**, thereby removing it from the cycle. Typically, propagating species such as **A'** contain a bulky polymer chain that prevents phosphine coordination, thereby resulting in high propagation rates.²³ As well, the polymerization is defined as a

living process in the absence of chain transfer or termination steps and so the cycle continues until all monomer units are consumed.²⁴

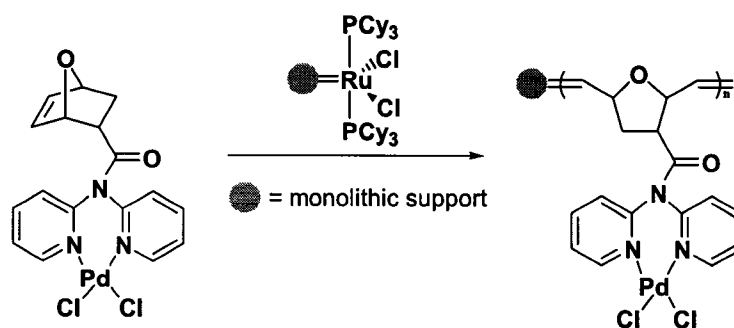
The living nature is an important feature of ROMP and it allows for the synthesis of reproducible well-defined polymers.²⁵ For example, since the propagating species remains attached at the end of the polymer chain even after complete consumption of the monomer, ROMP is an excellent method for preparing block copolymers.²⁶ Furthermore, molecular weights are controlled by adjusting the monomer/catalyst ratio or by chain termination, and narrow molecular weight distributions (polydispersities) are achieved by controlling the rates of initiation and propagation. Low polydispersities are obtained in cases where the initiation is faster than propagation.²⁵ As such, Grubbs et al have developed procedures whereby the rate of propagation is decreased without influencing the rate of initiation by simply adding excess phosphine (PCy_3 ; Scheme 2-1) to the polymerization process.²³ The authors rationalize these observations by suggesting that the excess phosphine competes with monomer units for \mathbf{A}' , thereby lowering the number of turnovers that occur before the propagating alkylidene species \mathbf{A}' is trapped to give the dormant species \mathbf{C} .

A related problem that is also encountered with ROMP reactions is the occurrence of secondary metathesis or “backbiting” that occurs when the active catalyst reacts with the olefin bonds in the growing polymer chain, thereby reducing the molecular weight and increasing the polydispersity. However, recent studies have shown that secondary metathesis reactions are minimized for the ROMP of norbornene monomers due to steric hindrance around the

olefins in the polymer chain.²⁷ Therefore, substituted norbornene monomers are especially suited for controlled living polymerizations. Combined with the benefits of high ring strain and availability, functionalized norbornene derivatives are the most preferred monomers for advanced functional polymer preparation for use in a wide range of potential applications.²⁰ Noteworthy examples include block copolymers,²⁸ bioactive,²⁹ electroactive,³⁰ liquid crystalline²⁶ and nonlinear optic polymers.³¹

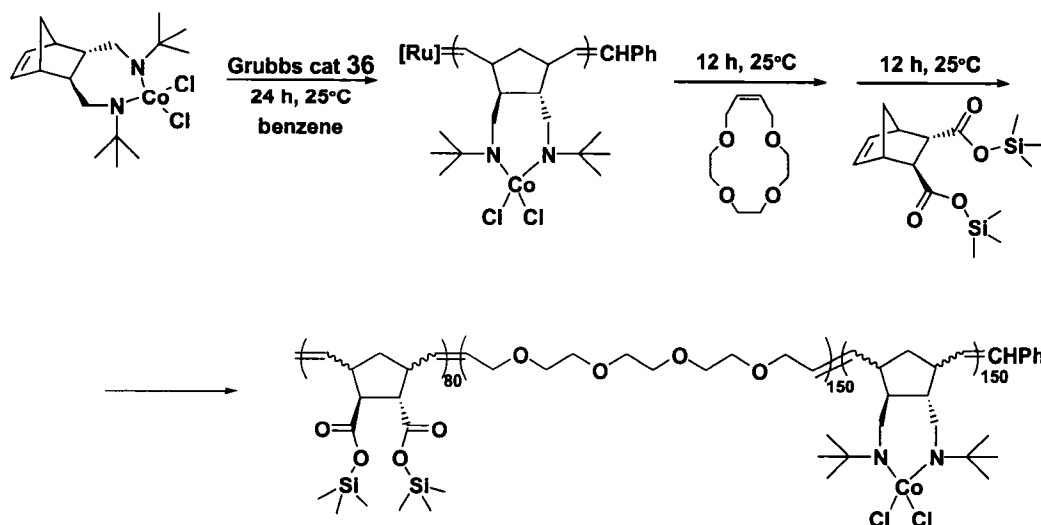
ROMP has also been used extensively to prepare a variety of norbornene-based polymers that were used as supports for polymer assisted organic synthesis,³² and, mostly by Buchmeiser *et al*, a smaller number of metal-based polymeric catalysts.³³ These include supported Pd-based systems for Heck and related reactions,³⁴⁻³⁶ and reusable Ru and Mo based metathesis catalysts grafted onto polymer supports,³⁷ and onto monolithic supports.³⁸⁻⁴⁰ As previously seen for other metal-based polymeric systems, the critical step is metallation of the polymeric ligand. In other words, the majority of metal-containing ROMP-type polymers also require a post-metallation step. However, there are a few reports that show ROMP can be carried out using certain metal complexes directly as monomers.^{33,41,42} For example, a Pd-based system used in the Heck C-C coupling reactions was prepared from a MCM as shown in Scheme 2-2. Here the researchers used a monolith-supported Grubbs catalyst to which the norbornene-based dipyridylamide-PdCl₂ complex was grafted to it by ROMP. The resulting immobilized catalyst was used in a model reaction between styrene and iodobenzene and was found to give high TON compared to a similar

supported system that was prepared by ROMP of the free ligand followed by metallation.^{35,43}



Scheme 2-2. Polymeric palladium catalyst prepared by ROMP.

In an elegant example, Kofinas et al. prepared an A/B/C organometallic triblock copolymer with potential application as a self-contained nanoscale battery (Scheme 2-3).⁴⁴ Using Grubbs catalyst **38** the triblock copolymer was synthesized in a systematic fashion where each block serves a different function. Specifically, the poly(organocobalt) block serves as the anode, the poly(ethylene oxide) block serves as the electrolyte, and finally the poly(norbornene-dicarboxylic acid) block capable of incorporating metal salts serves as the cathode. The key step in the synthesis of the triblock copolymer was the direct polymerization of the cobalt monomer. Other examples that show ROMP can be carried out using certain metal complexes directly include a variety of Sn, Pb, and Zn-based systems that were investigated for their thermal and electrical properties,⁴⁵ and an Fe-based system used for styrene polymerizations.⁴²



Scheme 2-3. Synthesis of A/B/C triblock copolymer.

The above examples show that the use of ROMP to prepare a wide range of functionalized polymers is well established. Therefore, it is surprising that such a well-controlled versatile technique has not been applied for the preparation of polymer catalysts for asymmetric hydrogenations, one of the most fundamental transformations in asymmetric catalysis. This chapter will discuss our efforts to prepare a well-defined polymer asymmetric hydrogenation catalyst by ROMP and the application of the polymer catalyst for reusable asymmetric hydrogenations. To the best of our knowledge, this is the first report that uses ROMP to prepare a polymerized asymmetric hydrogenation catalyst.⁴⁶

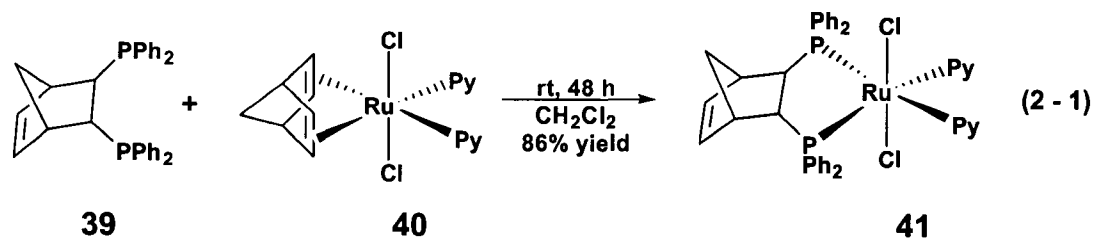
Results and Discussion

Synthesis of *trans*-RuCl₂(Py)₂((*R,R*)-Norphos) (41). Research in the Bergens' laboratories has focused on complexes of ruthenium(II) and chiral diphosphine ligands as catalyst systems for the asymmetric hydrogenation of prochiral olefins and ketones. A chiral diphosphine ligand that is commercially available and applicable to our studies is Norphos (**39**, 2,3-bis(diphenylphosphino)bicyclo-[2.2.1]hept-5-ene). The Norphos ligand is intrinsically reactive towards ROMP since it is based on the highly strained norbornene unit.⁴⁷ Furthermore, Norphos-based transition metal complexes have been used as catalyst precursors for a variety of asymmetric transformations,⁴⁸ and more specifically ruthenium-Norphos catalysts have been successfully applied to asymmetric hydrogenations of a variety of substrates.⁴⁹ Hence, we felt that synthesis of a well-defined polymeric catalyst by ROMP using a suitable ruthenium-Norphos complex was attainable.

A general and convenient synthetic route for the synthesis of ruthenium-diphosphine catalyst precursors, developed by Bergens et al, involves treatment of a chiral diphosphine ligand with the moderately air-stable ruthenium precursor *trans*-RuCl₂(NBD)Py₂ (**40**, NBD is norbornadiene, Py is pyridine) under mild conditions to give the corresponding *trans*-RuCl₂(diphosphine)Py₂ complex by displacement of the NBD ligand.^{50,51} The corresponding complex of **39** was prepared by reacting **40** with **39** overnight at room temperature in CH₂Cl₂ to

generate *trans*-RuCl₂(Py)₂((*R,R*)-Norphos) (**41**) in 85% yield (equation 2 - 1).

Crystals of **41** suitable for X-ray analysis were obtained by slow addition of



hexanes to a saturated solution of **41** in dichloromethane. The crystal structure is shown in Figure 2-2. The diphosphine ligand forms a five-membered ring with Ru in a λ -conformation that is characteristic of the (*R,R*)-Norphos ligand. The metal-ligand distances (Ru-P, Ru-N and Ru-Cl) and the cis disposition of the pyridine ligands are consistent with previously reported similar RuCl₂(diphosphine)Py₂ complexes.⁵² The bite angle, P1-Ru-P2, is 87.8°, very close to the 86.1° reported for the only other published Ru(II)-Norphos complex.⁵²

We chose **41** as monomer because it is easily prepared in pure form and it does not contain accessible donor atoms that may deactivate catalysts **2** or **3**. Specifically, one of the limitations of Grubbs catalysts is that ligating functional groups, such as phosphines, nitriles and amines, are known to deactivate the ruthenium-based catalyst.¹⁴ However, by virtue of using the MCM **41** the lone pairs from the phosphine and the pyridine ligands are protected from coordinating to the ruthenium core of the metathesis catalysts.⁴³ Another benefit is that *trans*-RuCl₂(diphosphine)Py₂ complexes are active catalyst precursors for a variety of hydrogenation reactions.⁵⁰ For example, they are active for

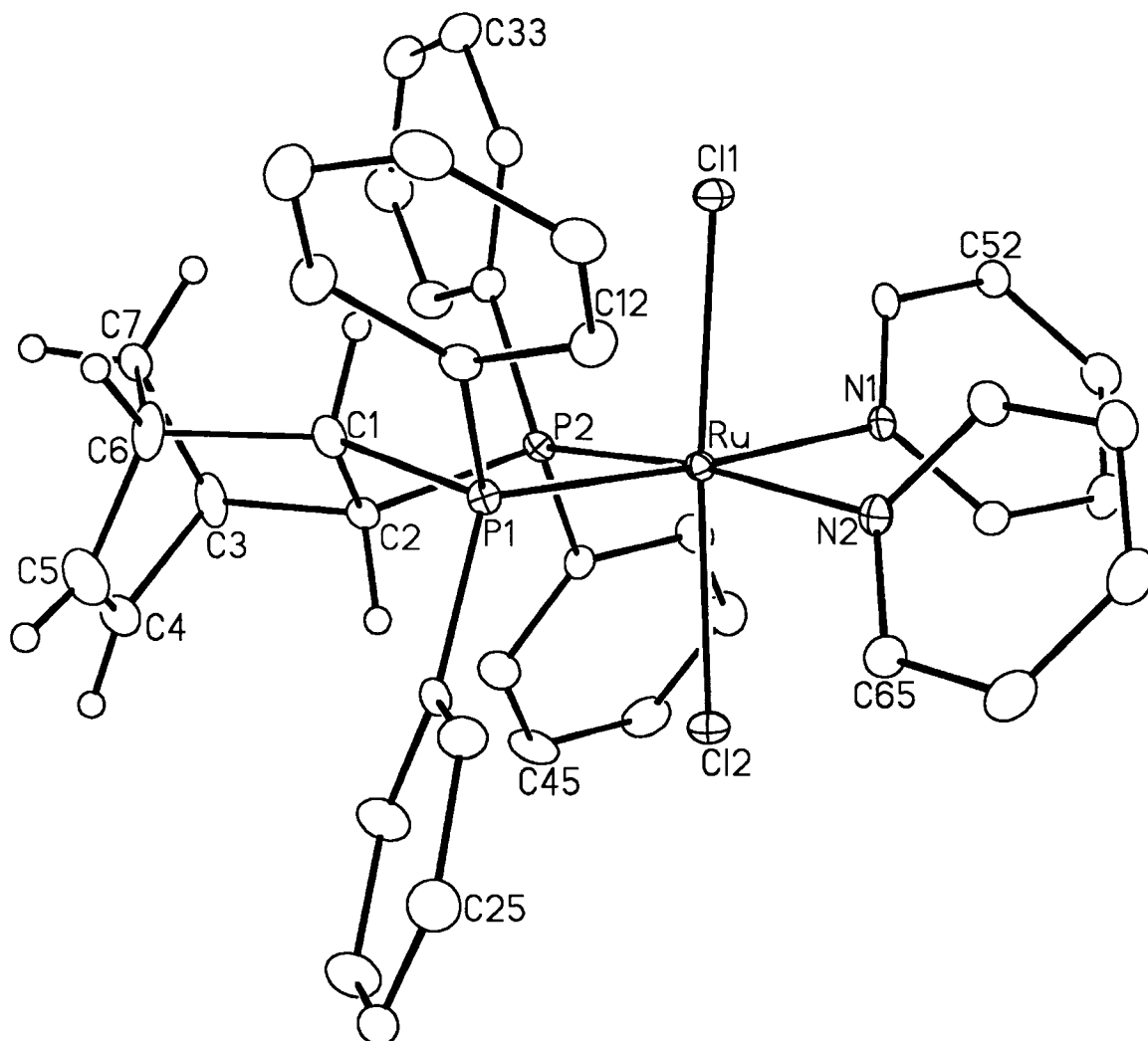
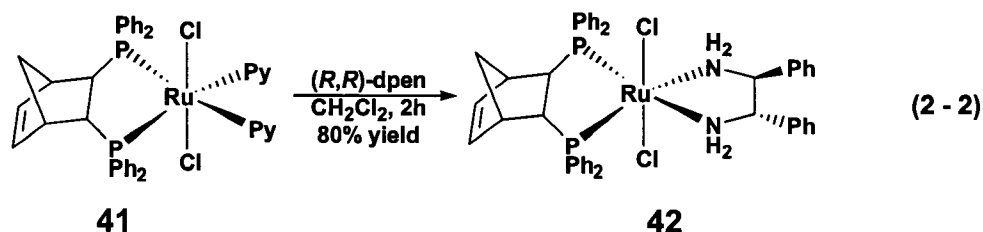


Figure 2-2. Perspective view of **41** showing the atom labeling scheme. Non-hydrogen atoms are represented by Gaussian ellipsoids at the 20% probability level. Hydrogen atoms are shown with arbitrarily small thermal parameters for the norbornene group, and are not shown for the phosphine phenyl and pyridine groups.

enantioselective hydrogenation of ketoesters and non-carboxylic olefins in the presence of small amounts of HBF_4 (aq.).⁵⁰ In another example, the Py ligands in **41** are readily displaced by (*R,R*)-dpen ((1*R*,2*R*)-1,2-diphenylethylene-diamine) to produce *trans*- $\text{RuCl}_2((R,R)\text{-Norphos})((R,R)\text{-dpen})$ (**42**) (equation 2 - 2),⁵⁰ an example of the well-known, enantioselective ketone hydrogenation catalyst precursors developed by Noyori *et al.*⁵³ Therefore a well-defined polymer with *trans*- $\text{RuCl}_2(\text{diphosphine})\text{Py}_2$ as active sites would make a versatile asymmetric hydrogenation platform.

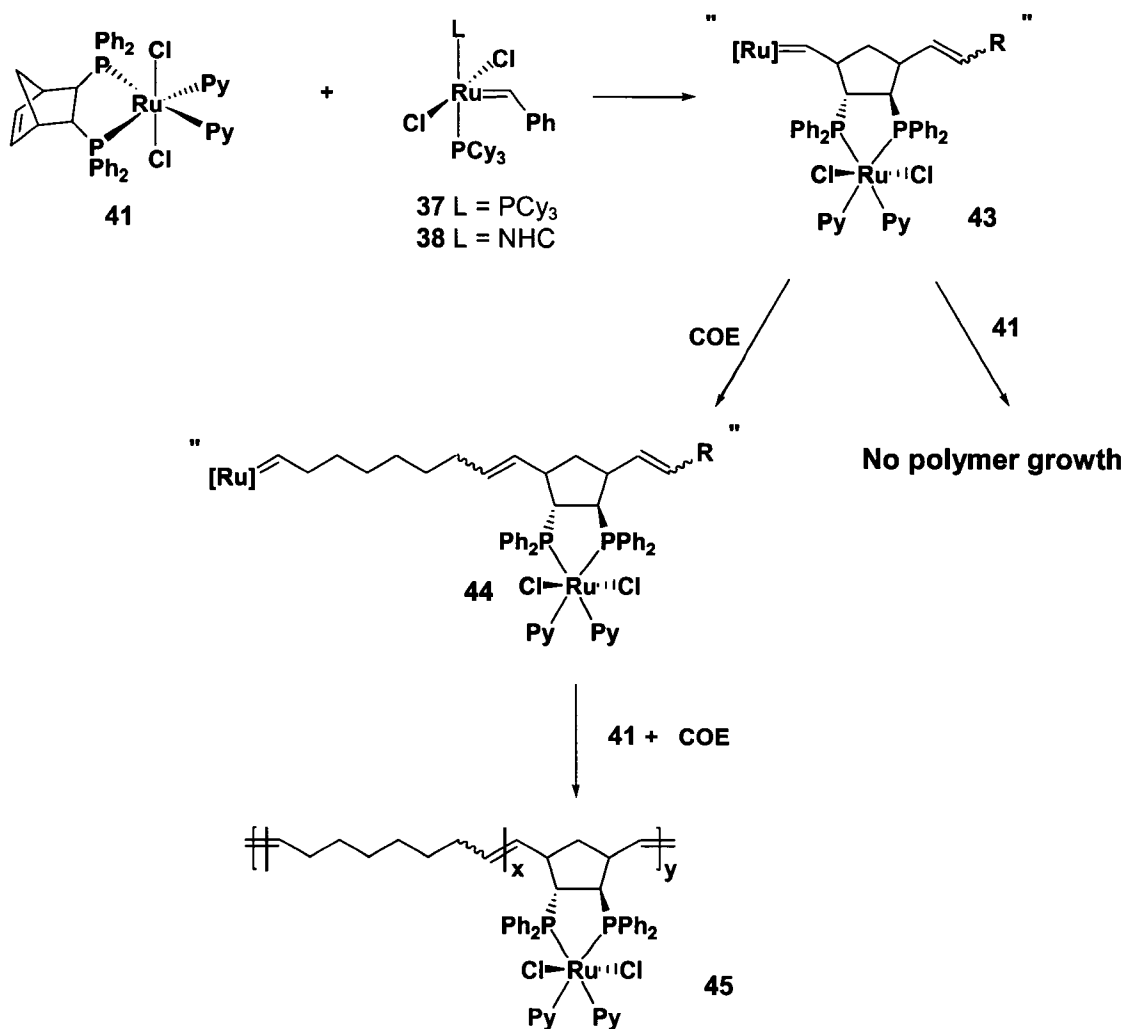


ROMP of monomer 41. The initial studies carried out in Bergens' laboratories on the ROMP of **41** using 5 mol % of Grubbs catalyst **2** or **3** failed to produce polymer after 24 h (22 °C, CH_2Cl_2). ^{31}P NMR analysis of the product mixture revealed that only a small trace of polymer had formed and that the majority of **41** remained unreacted. A stoichiometric reaction between **41** and **37** was carried out to determine if monomer **41** deactivated the metathesis catalyst **37**, thereby preventing its polymerization. This was not the case and after 30 min a mixture of **37**, **41**, PCy_3 and metathesis products was present. After three days all of **41** was consumed and apart from the complex mixture of metathesis products, free PCy_3 (50 %) and **37** (50 %) were also present. Therefore, **37** does

effect the ROMP of **41**, albeit slowly, suggesting there must be other factors inhibiting propagation of the polymer chain. Interestingly, the stoichiometric reaction between **41** and the highly active second generation Grubbs catalysts **38** was even slower resulting in only 33 % conversion after three days. Here, it was rationalized that the slower rate of polymerization was caused by the presence of the bulky mesityl groups in **38**. Hence, the lack of chain propagation for the ROMP of **41** was speculated to be a result of unfavorable steric interactions between the propagating alkylidenes and monomer **41**. Further investigation using molecular models show that severe steric crowding would exist between adjacent monomer units of **41**, explaining the lack of polymerization of **41** by ROMP.

Alternating ROMP of 41 and COE. To promote polymer growth we designed an alternating ROMP procedure using cyclooctene (COE) as a spacer monomer. A report of similar alternating reactions appeared in the literature while this work was in progress.⁵⁴ The reasoning was that COE is less crowded than **41**, but ring strain in the norbornyl group renders **41** intrinsically more reactive towards ROMP. It was envisioned that the polymerization would proceed in an alternating fashion involving two different propagating reactions, as described in Scheme 2-4. Specifically, reaction between **41** and **37** or **38** will generate bulky ruthenium-cyclopentylene chain-end species such as **43**. Monomer **41** is too bulky to react again with **43**, but less bulky COE can react to generate ruthenium-octylene chain-end species such as **44**. After COE has ring-

Scheme 2-4. Alternating ROMP of **41** and COE using catalysts **37** or **38**.



opened, the chain end becomes less sterically hindered and although it is now accessible to both monomers it preferentially reacts with **41** due to the higher ring strain. Alternating polymer growth would then proceed by reaction of **44** with **41**, then with COE, and so on, resulting in the alternating polymeric catalyst **45** (where x and y are integers representing the degree of alternation). As such, it was observed that when excess COE was added to a reaction mixture containing **41** and 5 mol % of **37**, the polymerization went to completion within three hours.

This was exciting since it confirmed that the metal-containing monomer **41** can be directly polymerized by an alternating ROMP mechanism, thereby avoiding the critical metallation step.

Another benefit of the alternating ROMP methodology is better control over the polymer's microstructural features such as site isolation, in which the active catalytic sites along the polymer chains are well-isolated from each other. Hence, for the alternating polymer **45** the catalytic ruthenium centers are well-isolated from each other by COE spacers. This approach is superior to previous methods whereby the polymeric catalysts are prepared by random processes that offer very little control over the distribution of the catalytic sites along the polymer chain. The issue of site isolation is very important since unfavorable interactions between adjacent active sites are believed to be one of the reasons for the limited activity and/or the deactivation of polymer catalysts prepared by such random processes.⁵⁵ Ideally, a sterically regular polymer, incorporating numerous well-isolated active centers throughout the polymer, would avoid adjacent site interactions. Although the alternating ROMP methodology provides excellent site isolation, a related issue that needs to be addressed deals with the regularity of the alternation achieved in the alternating ROMP of COE and **41**.

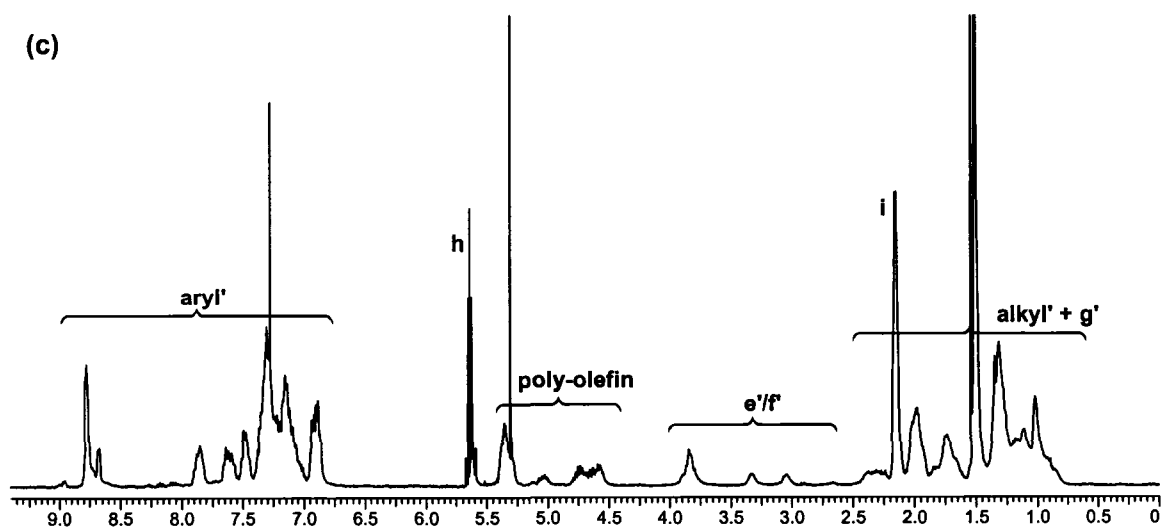
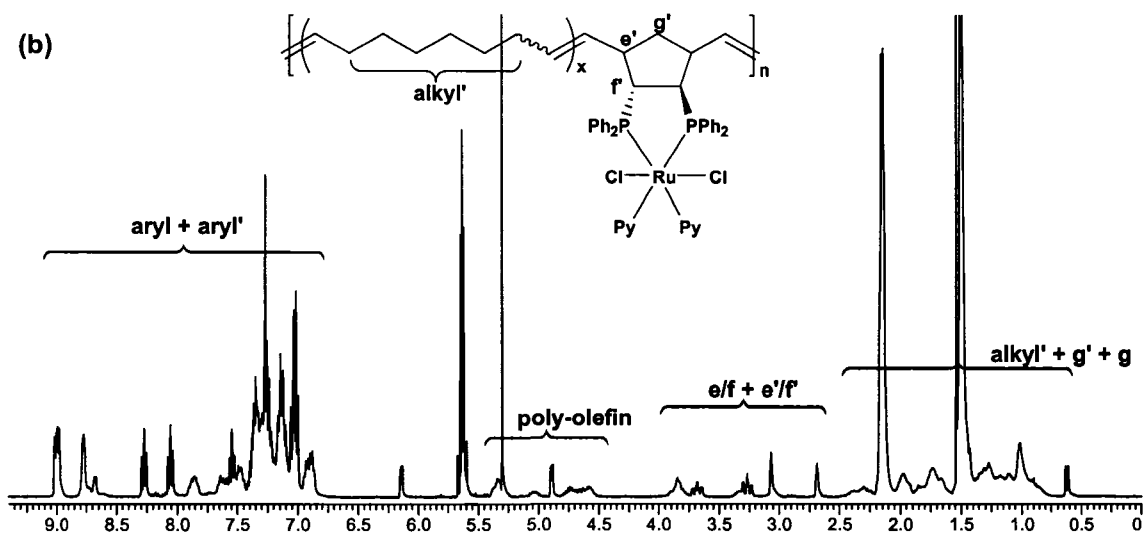
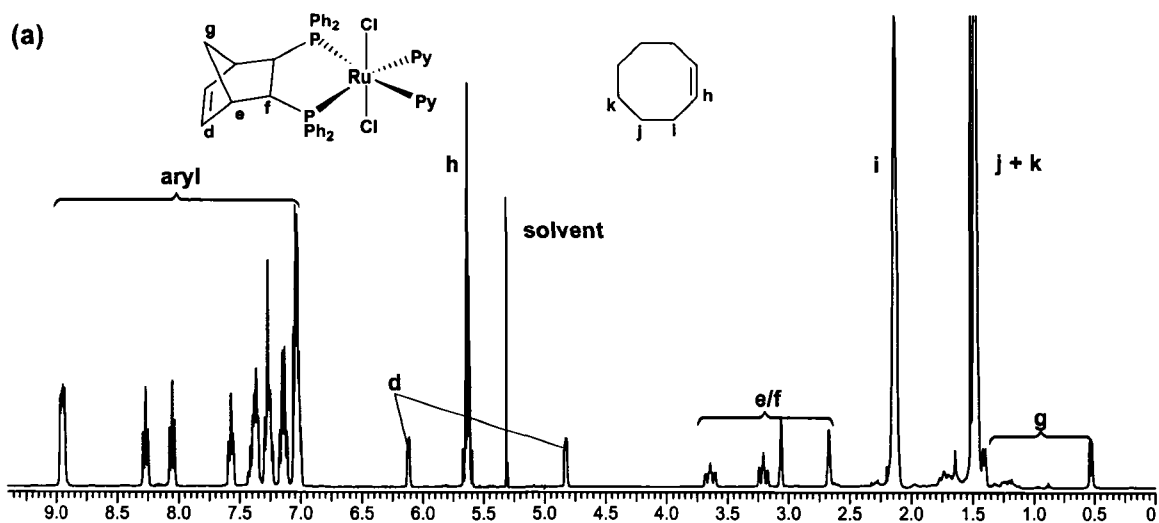
For a perfectly alternating copolymer structure, both monomers must be consumed equally and there must be no homopolymerization of either monomer. Homopolymerization would occur by the preferential consumption of one monomer over the consumption of the other monomer, thereby lowering the degree of alternation. In the alternating ROMP of COE and **41**, only the

homopolymerization of COE is possible since **41** does not polymerize in the absence of COE (*vide supra*). In the event of homopolymerization of COE a less precise alternating structure would be obtained in which the active catalytic sites would be separated by varying oligocyclooctene blocks. For the alternating polymer **45** this would occur when $x > y$ (Scheme 2-4). The presence of oligocyclooctene blocks would likely result in a more flexible polymer that would reduce the overall rigidity of the polymeric catalyst. Therefore, achieving a high degree of alternation is desirable since it would result in more control during synthesis of more complex catalyst polymer systems. In the few cases where ROMP has been used to prepare alternating polymers, it was essential to match the stoichiometry of both monomers in the reaction feed because any excess of one monomer resulted in its homopolymerization.⁵⁴

To maintain a high degree of alternation the polymerization was carried out with an equal molar mixture of **41** and COE using 5 mol % of ROMP catalyst **37**. The experiment was performed in an NMR tube and the extent of polymerization was monitored by ¹H and ³¹P NMR. Although the polymerization was slow, being only ~40 % complete after 24 h, this experiment confirmed that polymer growth occurred in a strictly alternating fashion rather than by random monomer consumption. Specifically, the rate of disappearance of each monomer was equal throughout the polymerization process and therefore no homopolymerization of COE occurred. For comparison, the homopolymerization of COE was carried out using a ratio of **37** to COE equal to 1:10 and the polymerization was complete in less than 30 min. The rate of

homopolymerization of COE was much faster than the rate of copolymerization of COE and **41**. This observation is further evidence that ROMP of an equal molar mixture of COE and **41** polymerized in a perfectly alternating fashion; otherwise COE would be consumed before monomer **41**. Unfortunately, despite achieving a perfectly alternating polymer structure, the rate of polymerization was too slow to be of practical use. Optimization studies revealed that by increasing the ratio of COE to **41** drastically increased the rate, and 4:1 (COE: **41**) polymerizations were 12 times faster than 1:1 polymerizations. As such, the polymers used in the catalytic reactions were prepared using excess COE and it was therefore necessary to investigate the degree of alternation achieved for non-equal molar mixtures of monomers.

Investigation of the degree of alternation for alternating polymers prepared with excess COE. The in situ monitoring of the alternating copolymerization of **41** with excess COE using metathesis catalyst **37** was carried out in a series of NMR tube experiments. The reagents were mixed at -20°C in an NMR tube that was quickly transferred to a pre-chilled (-20°C) probe. It was necessary to keep the NMR tube below -20°C to prevent the reaction from starting prematurely so that the initial monomer feed ratio could be determined. After recording the initial spectrum, the NMR tube was allowed to warm to room temperature and spectra were recorded in 10 min intervals until the reaction was complete. Selected ¹H NMR spectra recorded during the alternating polymerization experiment are shown in Figure 2-3. At -20°C (Figure 2-3a), the



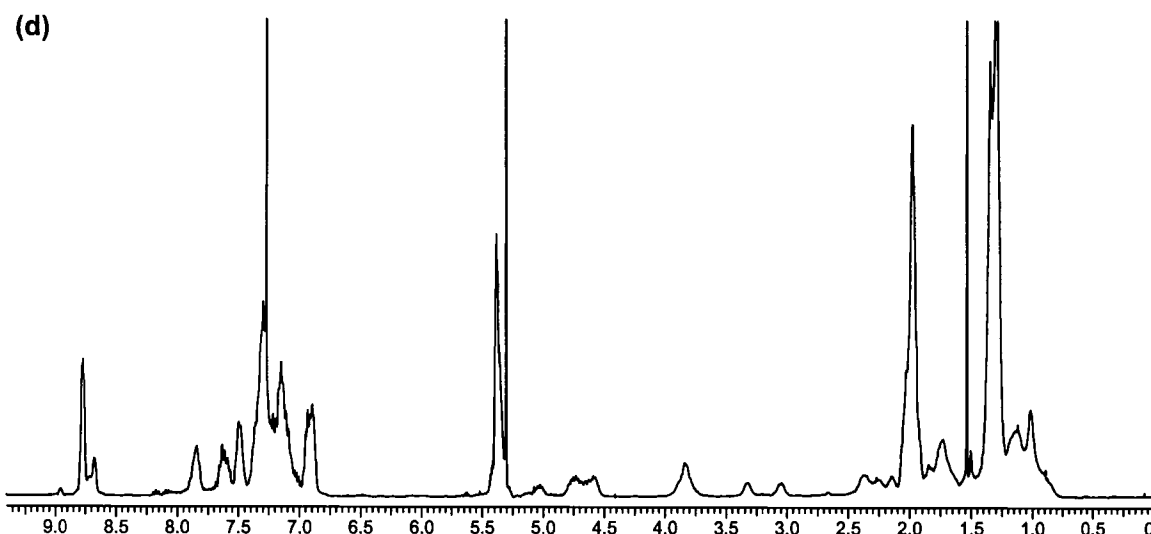


Figure 2-3. In situ ^1H NMR spectra of the alternating ROMP of **41** and COE (1:2.72) with 5 mol % of **37**; (a) recorded at start of reaction at -20°C . The probe was warmed to room temperature and the spectra were taken after (b) 55 min, (c) 135 min, and (d) 225 min from the start of the experiment.

polymerization had not started and an excess of 2.72 equivalents of COE was present as determined by integration of the olefinic resonances for **41** and COE. Upon warming, the polymerization started immediately and the sharp proton peaks of both monomers decreased as the broad polymer peaks increased during the polymerization.

For convenience, the resonances for the starting materials and the alternating polymer are labeled in the spectra shown in Figure 2-3a and Figure 2-3b. The aryl protons for **41** and the polymer aryl' protons appear between 6.8 – 9.0 ppm. The starting norbornene protons (**e/f**) and the polymer norbornene protons (**e'/f'**) appear between 2.5 – 4.0 ppm. The starting alkyl protons of both

monomers (**i,j,k**, and **g**) and the polymer alkyl protons (alkyl' + **g'**) are in the region between 0.5 – 2.4 ppm. Finally, the olefinic resonances for **41** and COE are labeled **d** and **h**, respectively, and the polymer olefin (poly-olefin) resonances appear as a broad set of peaks between 4.5 – 5.4 ppm (poly-olefin).

The degree of alternation could not be determined from the olefinic protons since they do not have distinct chemical shifts from the starting materials and homopolymer units of COE. The homopolymerization of COE results in a multiplet at 5.35 ppm, which overlaps with the multiplet from the alternating polymer. However, the extent of alternation was determined by ¹H NMR analysis since the consumption of both monomers could be monitored separately. The consumption of monomer **41** was followed by measuring the disappearance of the multiplet at 8.25 ppm since it does not overlap with the polymer aryl' signals. The consumption of **41** was also followed by ³¹P NMR which confirmed the accuracy of the results obtained from the ¹H NMR data. Likewise, COE consumption was followed by measuring the disappearance of the alkyl signal labeled **i** since it remains as a distinct signal throughout the polymerization process. Therefore, by integrating these peaks over the course of the polymerization the amount of each monomer consumed was easily measured. By plotting (Mole_{initial} – Mole_{time}) data for each monomer vs time, the degree of alternation throughout the polymerization was clearly visible as shown in Figure 2-4.

The plot reveals several key features of the polymerization sequence and the resulting polymer structure. Where the lines overlap a perfectly alternating

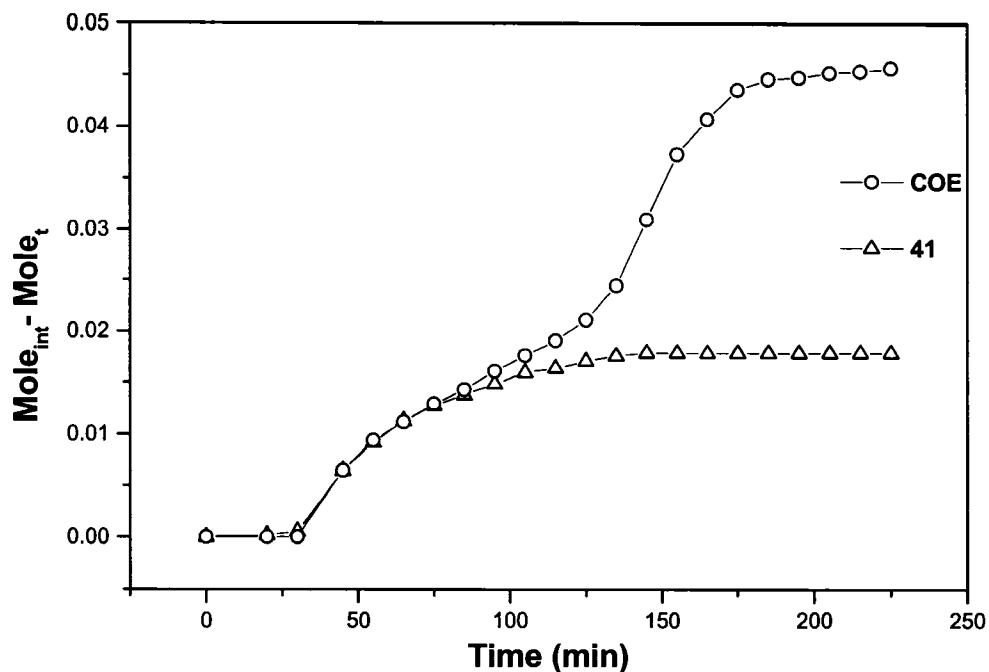


Figure 2-4. Plot of the consumption of COE and **41** vs time for the alternating ROMP of COE and **41** in a 2.72:1 ratio using **37** as catalyst.

structure is obtained and where the lines begin to separate the degree of alternation decreases. Hence, from this plot a more precise picture of the resulting polymer structure can be made. Specifically, the plot can be divided into three regions representing three different areas of polymer growth. In the first region (0 - 85 min), 80 % of **41** was consumed along with an equal amount of COE. In this region both monomers are consumed at the same rate suggesting that polymer growth occurs in a perfectly alternating fashion. It is noted that the first three data points were recorded at low temperatures while the sample was warmed to room temperature. However, even though the copolymerization

occurred at a slower rate this did not affect the degree of alternation and a perfectly alternating structure was obtained from the very onset of the polymerization. At around 85 min the lines begin to separate and from 85 -135 min (2nd region) the rate of consumption of COE becomes increasingly faster than the rate of consumption of **41**. In this region oligocyclooctene blocks are formed and therefore the remaining 20 % of **41** was polymerized with a lower degree of alternation. At 135 min, all of **41** has been consumed and only 50 % of COE remained (Figure 2-3c). In the third region (135 – 225 min), the remaining COE is polymerized to give a polycyclooctene unit at the end of the alternating structure. As expected the remaining COE polymerizes at a much faster rate since there is no competition with monomer **41**. This rate is now closer to the rate observed for the homopolymerization of COE (*vide supra*). Also, comparison of the spectra shown in Figure 2-3c and Figure 2-3d shows that the olefinic resonance for the polycyclooctene unit overlaps with the olefinic protons from the alternating polymer unit at 5.35 ppm. From the above analysis the resulting polymer structure from the alternating ROMP of **41** with excess COE (2.72 equiv) is made up of an area with perfect alternation, a smaller area that has a lower degree of alternation and finally the end of the polymer chain is capped with a polycyclooctene unit. As well, the above results suggest that the rate-determining step in the alternating ROMP of **41** with COE is the reaction between COE and the propagating alkylidene species such as **43** (Scheme 2-4). This rate is dependent on the concentration of COE.

These results confirm that even with excess COE a high degree of alternation is achieved in the ROMP of **41** and COE. More importantly, a perfectly alternating structure is obtained from the very onset of the polymerization and only at low concentrations of **41** does the degree of alternation decrease. Precisely, from the plot it was calculated that the degree of alternation decreased only after the ratio of COE to **41** became greater than 8.4:1. Therefore at monomer feed ratios less than 8.4 the ROMP of COE and **41** are governed by an alternating mechanism instead of random monomer addition. Achieving a high degree of alternation with such a large excess of either monomer is quite remarkable. To the best of my knowledge it is the only example of an alternating polymer prepared by ROMP where a high degree of alternation is achieved with a non-equal molar mixture of monomers.^{27,54} The findings in this experiment are very beneficial since it shows that we can prepare reproducible alternating polymers, with well-isolated active centers, and in practical time frames, while avoiding the tedious task of matching the stoichiometry of both monomers.

The alternating ROMP of **41** with excess COE was also followed in situ by ³¹P NMR spectroscopy and a representative sampling of the spectra is shown in Figure 2-5. In the top spectrum, polymerization has not started and the singlet peak at $\delta = 39.0$ ppm is due to **37** and the doublets at $\delta = 37.8$ and 36.7 ppm are due to **41**. The middle spectrum was taken during the polymerization and as the amount of **41** decreases new peaks representing the alternating polymer **45** appear in the range $\delta = 53 - 58$ ppm. The extent of polymerization of **41** was

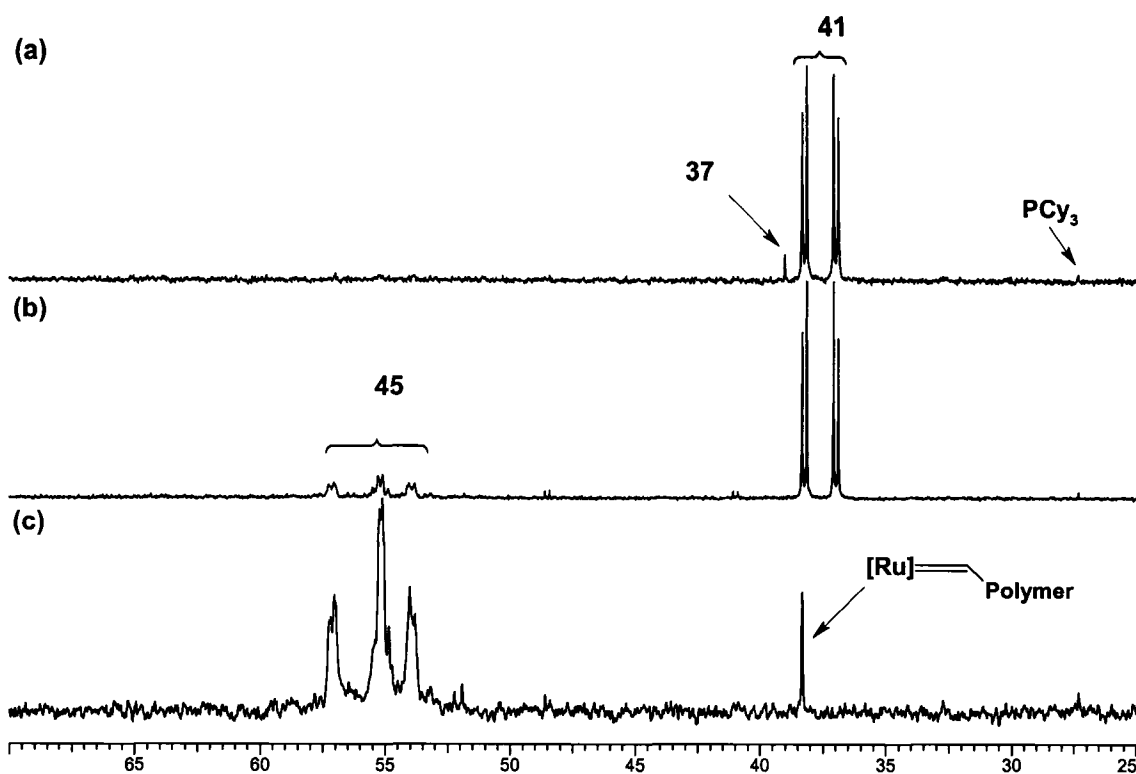


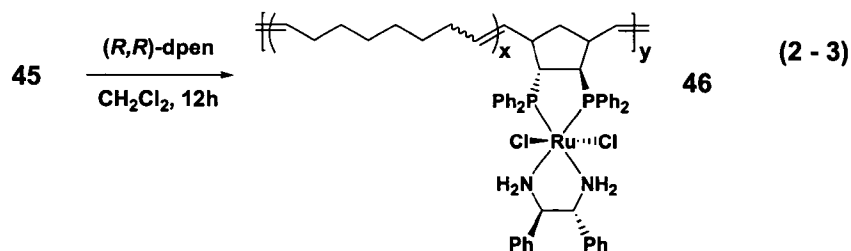
Figure 2-5. $^{31}\text{P}\{^1\text{H}\}$ NMR spectra (at 162 MHz in CDCl_3) of the alternating ROMP of **41** and COE with 5 mol % of **37**; (a) recorded at start of reaction at -20°C . The probe was warmed to room temperature and the spectra were taken (b) during the polymerization and (c) after **41** was completely consumed.

easily followed by integrating these peaks. The disappearance of the resonance for **37** is evidence that all of the metathesis catalyst has initiated. The bottom spectrum was taken after **41** was completely polymerized and only peaks for **45** and a singlet at $\delta = 38.3$ are observed. This singlet peak belongs to the newly generated propagating chain end species and that there is only one sharp singlet present is evidence of a highly uniform polymer structure. It is noted that the bottom spectrum is not from the same experiment as the top two spectra due to

better spectrum quality and so the increase in peak height of the metal alkylidene species is simply because they are from different experiments. As well, in all three spectra a small peak at $\delta = 27.4$ ppm is present, due to PCy_3 which dissociates from the metathesis catalyst. In the middle spectrum there are small unidentified peaks at $\delta = 41.0$ ppm and at $\delta = 48.5$ ppm which may represent propagating chain end species. However, further investigations are required in order to confirm the identity of these peaks. Nevertheless, the ^{31}P NMR of the alternating polymer **45** consists of multiple overlapping signals ($\delta = 58 - 53$ ppm) with two major species predominated over the others. Specifically, there are two doublets and an AB quartet, which are approximately in a 1:1 ratio. This peak pattern is observed from the start of the polymerization. It does not change once the excess COE is polymerized at the end of the polymer and it is the only peak pattern observed regardless of the polymer chain length. These observations show that in the alternating ROMP of COE and **41** a highly reproducible polymeric structure is obtained.

Generation of the polymeric catalyst *trans*-[RuCl₂((*R,R*)-Norphos)((*R,R*)-dpen)]_x[COE]_y (46**).** Interestingly, the (*R,R*)-dpen analogue of **41**, *trans*-RuCl₂((*R,R*)-Norphos)((*R,R*)-dpen) (**42**), was inactive towards alternating ROMP using **37** as catalyst. It is unclear why the dpen complex **42** did not polymerize, but strong donor ligands are known to deactivate Grubbs metathesis catalyst and it may be that the bidentate nature of dpen inhibits polymerization.¹⁴ However, this was a surmountable problem because the polymeric version of **42** was easily

obtained by reacting a dilute solution of the alternating polymer **45** with excess (*R,R*)-dpen for 12 h in CH₂Cl₂ to form the alternating polymer **46** (equation 2 - 3).



Complete displacement of the pyridine ligands for (*R,R*)-dpen was confirmed by ³¹P NMR (Figure 2-6). The singlet at $\delta = 51.9$ ppm represents the propagating chain end species for the dpen complex and **46** consist of multiple overlapping signals ($\delta = 63 - 53$ ppm) predominated by four major species in the relative ratio 4.1:4.1:1.0:0.8. COSY experiments indicate these sites result from *Z* and *E* olefin geometries in the polymer. As well, the chemical shifts and ratios of these peaks remain constant regardless of the polymer length.

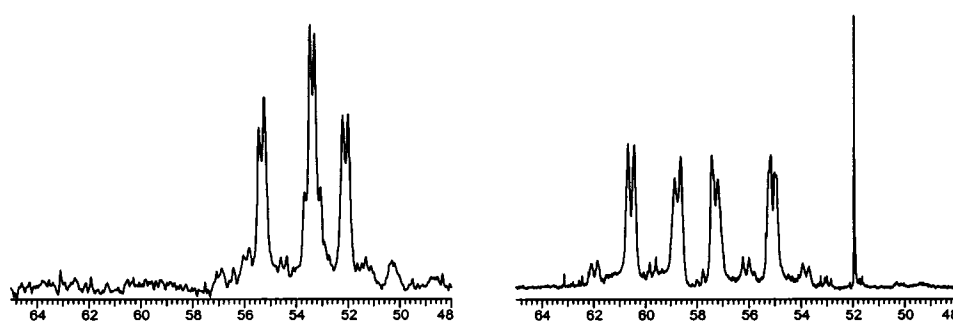


Figure 2-6. ³¹P NMR spectra (at 161.8 MHz in CD₂Cl₂) of the alternating polymer **45** before (left) and after (right) treatment with (*R,R*)-dpen to give **46**.

Preparation of a reusable alternating polymer catalyst. After demonstrating a new approach for the preparation of a well-defined polymer catalyst, the next step was to test its catalytic efficiency. For an immobilized catalyst to be effective, it is essential that it remain insoluble in the reaction media to facilitate easy separation and recovery of the catalyst from the product stream. Furthermore, the recovered catalyst must retain its activity and selectivity through multiple cycles which are at least as good as or better than those of the homogeneous analogue. Therefore, in our case, high molecular weight polymers that are insoluble in *iso*-propanol were required for use in hydrogenation. A benefit of the alternating ROMP methodology is that the polymer chain length can be easily increased by simply varying the monomer to catalyst ratio. However, the alternating ROMP of COE and **41** using catalyst **37** with loadings less than 1 mol % failed to effect the polymerizations, and polymers prepared with higher catalyst loadings were partially soluble in the reaction media. To address this issue we found that insoluble high molecular weight polymers could be obtained using the more active “2nd generation Grubbs catalyst” **38**.¹⁷ An issue with catalyst **38** is that the rate of initiation is low compared to **37** which results in less control over the polymerization process and this is discussed in more detail in Chapter 4.⁵⁶ For now, since we are concerned with the use of the polymer catalyst as a heterogeneous system and due to the solubility issue discussed above it was necessary to employ catalyst **38** in order to prepare insoluble long-chain polymers.

A typical reaction for the preparation of an insoluble long-chain polymer was carried out using a loading of **38:41:COE** equal to 1:3000:15000. As discussed previously, it was important to maintain less than 8.4 equivalents of COE to **41** to ensure a high degree of alternation. For the long-chain polymers, the reaction had to be monitored closely since during the polymerization the reaction mixture became quite viscous and the growing polymer chain often precipitated during the reaction. It was important to keep the polymer in solution since once it precipitated from solution it could not be re-dissolved. Therefore, to avoid losing the polymer catalyst, the reaction mixture had to be diluted with extra solvent once it became viscous. Unfortunately, diluting the reaction mixture also slowed down the polymerization which prevented the complete consumption of **41**. The extent of polymerization was monitored by NMR spectroscopy and after 24 h the COE was consumed, with 61 % of **41** incorporated into the polymer. That not all of **41** was incorporated into the polymer indicates that the steric bulk of the mesityl groups in catalyst **38** decreases the ratio of its reactivity towards **41** and COE. Therefore, a lower degree of alternation was likely achieved. However, based on the previous studies it was shown that initially a high degree of alternation is achieved at the start of the polymerization and only as the concentration of **41** decreases does the degree of alternation decrease. Since only 61 % of **41** was consumed it is speculated that it was polymerized with a high degree of alternation and the end of the polymer is simply capped with the polycyclooctene unit. The ^{31}P NMR spectrum of the resulting polymer from this polymerization showed the same chemical shift and a similar population

of isomers as seen in Figure 2-6 for the short chain polymer **45**. This is strong evidence of a similar polymer structure and so it is believed that a high degree of alternation was achieved.

Next, we took advantage of the living nature of these polymerizations and cross-linked the polymer by adding dicyclopentadiene (DCPD) to the reaction mixture and it was found that cross-linking further decreased the solubility of the polymer matrix.³⁵ As well, cross-linking with DCPD also imparts rigidity to the polymer matrix and reduces the chain mobility of the polycyclooctene ends, thereby restricting interactions between the polymer backbone and the catalytic sites.⁵⁷ Finally, a dilute solution of the cross-linked polymer was treated with excess (*R,R*)-dpen to generate the Noyori-type active sites within the cross-linked polymer. Exchange of the pyridine ligands was confirmed by ³¹P NMR, which consisted of the same peak pattern and relative ratios of isomers as shown for polymer **46** in the ³¹P NMR in Figure 2-6. Finally, in an effort to increase the surface area of the cross-linked polymer it was coated over BaSO₄ as described below.

Deposition of the polymer catalysts onto BaSO₄. A common difficulty encountered when immobilizing homogeneous catalysts is lower catalytic activity and stereoselectivity due to restrictions of the polymer matrix that block most of the active sites from the reactants. In other words, the active surface areas of the resulting heterogenized catalysts are low, and only those sites on the surface are involved in the catalytic process. This difficulty is particularly evident with

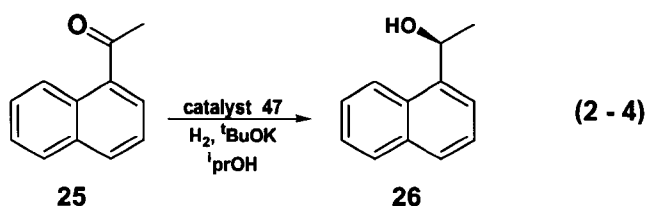
polymeric catalysts containing flexible polymer backbones that wrap around the catalysts. The common approaches used by researchers to increase the active surface area of heterogenized catalysts are as follows. Co-solvents are used during catalytic reactions that swell the polymer matrix thereby opening pathways to and from the active sites.^{58,59} Crosslinking agents are used to impart rigidity, and thereby prevent the polymer matrix from collapsing on the active sites. High surface area monolithic^{40,60} or silica systems,^{38,61} and nanoparticles³⁴ have been used to support either thin films of polymeric catalysts, or bonded monomeric catalysts. The approach adopted for this research was to use a simple, economic, inert, and high surface area support that does not require additional functionalization of the polymeric catalyst to attach it to the support. This was accomplished by depositing the catalyst framework as a thin film over BaSO₄ solid in a one-pot procedure. The BaSO₄ support acts as a filtration aid, and imparts mechanical stability towards rapidly stirred batch reactions in which the catalyst is reused. To the best of my knowledge BaSO₄ has not been used as polymer support prior to this work.

The cross-linked polymeric catalyst prepared above was supported as a uniform thin film over BaSO₄ by slow evaporation of a dilute solution of the polymer in CH₂Cl₂ with rapid stirring. The dilute solution of the alternating polymer was prepared by diluting the reaction mixture after the alternating polymerization and exchange of the pyridine ligands with (*R,R*)-dpen were complete. In previous experiments, it was observed that the polymer could not be re-dissolved if the reaction solvent was first removed under vacuum. A

primary concern in the use of polymer catalysts is that metal leaching is caused by the presence of un-polymerized or soluble low molecular weight oligomers of the catalyst monomer, which, in some cases, renders the reaction mechanism homogeneous.⁶² To remove any low molecular weight oligomers present from the polymerization the BaSO₄-supported catalyst was washed with methanol before use. The methanol washings did not contain any detectable (NMR) amounts of low molecular weight polymer, only un-polymerized **41** and unreacted (*R,R*)-dpen were present. The BaSO₄-supported polymer catalyst (**47**) was then tested as a heterogeneous hydrogenation catalyst.

Use of the BaSO₄-supported alternating polymer catalyst 47. Among the most significant advances in asymmetric catalysis is Noyori and coworkers development of the asymmetric hydrogenation of ketones using *trans*-RuCl₂(diphosphine)(diamine) plus base in alcohol as the catalyst system.⁶³ As discussed in Chapter 1, these systems have been used extensively for the rapid and productive asymmetric hydrogenation of a range of ketones such as alkyl-aryl, vinyl, and recently alkyl-alkyl ketones with high turnover numbers, frequencies, and enantiomeric excess.⁶⁴ As well, numerous industries have licensed this technology and several industrial processes have been developed.⁶⁵ Due to their high efficiency and industrial potential many researchers have attempted to immobilize this catalyst system with very limited success.^{3,5} For these reasons we chose this hydrogenation as the control reaction to test our polymeric catalyst.

Use of the supported polymer catalyst **47** for the asymmetric hydrogenation of 1'-acetonaphthone (**25**) was successful (equation 2 - 4). The hydrogenation of **25** to give 1-(naphthyl)ethanol (**26**) was used as the model reaction since it is most frequently used for evaluating immobilized Ru-diphosphine/diamine type catalysts.⁶⁶ The supported catalyst **47**, with a loading



of 9.99 mg (1.18×10^{-5} mol) of catalyst precursor **42** per gram of BaSO₄ support, was used in the repeated hydrogenation of **25** and the results are summarized in Figure 2-7. The hydrogenations were carried out in *iso*-propanol, under 4 atm of H₂ at room temperature with a substrate/catalyst (S/C) molar ratio of 500/1 and with 4 equivalents of KO^tBu per active site. These are standard reaction conditions used for the homogeneous reaction and therefore a direct correlation with the data obtained from the soluble catalyst can be made.⁶⁷

The first run was stopped after 2 h (Figure 2-7) and compared to a homogeneous run using **42** under identical conditions. The homogeneous catalyst gave 42 % conversion of hydrogenated product after 2 h, whereas the heterogeneous catalyst **47** gave 16 % conversion after 2 h. Thus, the rate (per active site) using the heterogeneous catalyst **47** was ~ 40 % the rate using the dissolved catalyst **42**, showing that mass transport losses were low using the polymer system. In contrast, the level of enantioselectivity observed for the

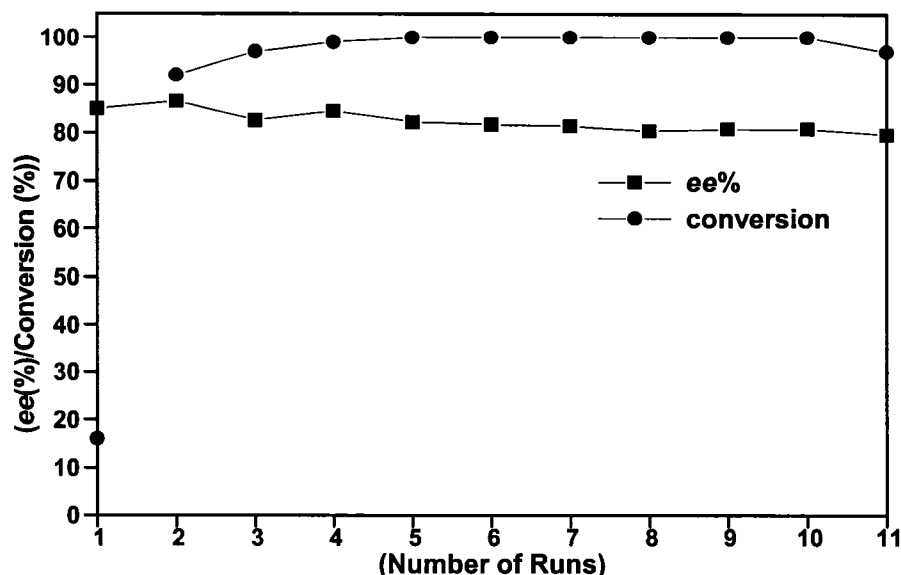


Figure 2-7. Conversion (%) and ee vs. runs for hydrogenation of 1'-acetonephthone catalyzed by **47** (S/C = 500/1, 4 equiv ^tBuOK, 4 atm H₂, 22°C, 15 h, 2-propanol).

heterogeneous catalyst **47** was substantially higher than the dissolved catalyst **42** (83 % vs 48 % (S)). The origin of this marked increase in selectivity is likely a result of the structural change in the Norphos ligand upon ring-opening. Specifically, the Norphos ligand goes from a highly strained norbornene unit to a more relaxed 5-membered ring system, which likely influences the spatial domains of the catalytic sites. However, further investigations are required to examine this effect as well as possible influences of the support or of polymer conformations on ee values. Despite a 35% increase in selectivity on going from the homogeneous system to the heterogeneous system for the hydrogenation of **25**, the level of selectivity obtained is not comparable as seen for other more

successful chiral diphosphine systems. For example, the hydrogenation of **25** with the homogeneous catalyst $[\text{RuCl}_2((R)\text{-BINAP})((R,R)\text{-dpen})]$ under identical conditions as above, afforded the chiral alcohol product **26** in 97 % ee.⁶⁷

The most significant result obtained from the use of the supported polymer catalyst **47** is the level of reusability achieved with this catalyst system. As shown in Figure 2-7, **47** was reused for 10 more runs after the first run without significant drops in enantiomeric excess (ee) or rate. Another benefit of this system is the ease of recovery of the catalyst and set-up of the recycling experiments. Specifically, between runs the reaction mixture was left undisturbed and the supported catalyst quickly settled and the clear product mixture was then easily removed by cannula filtration under a hydrogen atmosphere. For each run a fresh sample of substrate and base was introduced into the pressure reactor as a solution in *iso*-propanol. At the time of this research this was the highest number of reuses of a polymeric asymmetric hydrogenation catalyst that is not soluble in the reaction medium,⁸ and that does not require use of a swelling co-solvent.⁵⁸ Since this work we have prepared a polymer hydrogenation catalyst that surpasses this previous record and this is presented in Chapter 4.

Conclusion

In summary, this is the first report of an alternating ROMP methodology used to prepare a polymeric chiral hydrogenation catalyst. The newly developed alternating ROMP methodology provides key improvements to previous procedures used to prepare polymeric asymmetric hydrogenation catalysts. The procedure avoids the critical polymer metallation step and provides adequate site isolation of the catalytic sites. In addition the polymers prepared by the alternating ROMP methodology showed a high level of alternation despite having an excess of one monomer. We addressed the issue of low accessibility of the catalytic sites by depositing the polymer catalyst as thin films over an inert support such as BaSO₄ in order to increase the active surface area. The insoluble supported polymer catalyst **47** was much more selective than the homogeneous analogue **42** and was readily recovered and recycled for up to 10 times without loss of activity and enantioselectivity. Since norbornene groups are made by facile Diels-Alder reactions using cyclopentadiene, this methodology can, in principle, be readily adapted to other more successful phosphine ligands. The focus of the remaining work presented in this thesis is to prepare ROMP active versions of a more privileged ligand system (i.e. BINAP) and to use this new alternating ROMP technology to prepare the corresponding polymeric catalyst.

Experimental

General Procedures and Methods. All operations were carried out under a nitrogen atmosphere using standard Schlenk and glovebox techniques unless stated otherwise. Nitrogen gas (Praxair, 99.998 %) was passed through a drying train containing 3 Å molecular sieves and P₄O₁₀ before use. The solvents, n-hexane (K, Ph₂CO), methylene chloride (CaH₂), *iso*-propanol (Mg(O^{*i*}pr)₂), and methanol (MgOMe) were distilled under a dinitrogen atmosphere using standard drying agents. The diphosphine ligand, (*R,R*)-Norphos, and the 1,2-chiral diamine ligand, (*R,R*)-dpen, were used as received from Strem Chemical Co., Inc. The ROMP catalysts, (bis(tricyclohexyl-phosphine)benzylidene ruthenium (IV) dichloride) (**37**) and (tricyclohexylphosphine-[1,3-bis(2,4,6-trimethylphenyl)-4,5-dihydroimidazol-2-ylidene][benzylidene] ruthenium (IV) dichloride) (**38**) were used as received from Strem Chemicals Co., Inc. White reflectance BaSO₄ was obtained from Eastman Chemical Co., Inc. and washed thoroughly with CH₂Cl₂ and dried under vacuum before use. Unless stated otherwise, all other reagents were obtained from Aldrich Chemical Co., Inc. The synthon *trans*-RuCl₂(NBD)Py₂ (**40**) was synthesized according to literature procedure.^{50,51} The substrate 1'-acetonaphthone was distilled, washed with 0.1 M KOH_{aq}, and distilled again before use. (*S*)-(+)-1-(1'-naphthyl)ethanol (Aldrich) was used without further purification. The hydrogen gas was ultra high purity grade purchased from Praxair (99.99 %). The glass pressure reactor used for the

catalytic hydrogenations was silanized by reaction with chlorotrimethylsilane that was then removed by heating under vacuum.⁶⁸

All ^1H , ^{13}C , and $^{31}\text{P}\{^1\text{H}\}$ NMR spectra were measured with Varian Inova-400 or Inova-500 or Unity-500 spectrometers. ^1H , and ^{13}C NMR chemical shifts are reported in parts per million (δ) relative to TMS with the solvent as the internal reference. ^{31}P NMR chemical shifts are reported in parts per million (δ) relative to an 85% H_3PO_4 external reference. Gas chromatography was performed using a Hewlett Packard 5890 chromatograph equipped with a flame ionization detector, a 3392A integrator, and a Beta DexTM 120 fused silica capillary column (30m \times 0.25mm \times 0.25 μm thickness, Supelco) using 20.5 psi He as carrier gas. Microanalysis was performed at the University of Alberta Microanalysis Laboratory. Dr. Mike Ferguson performed the solid-state structure determination. Final atomic coordinates and displacement parameters for compound **41** can be obtained from the Structure Determination Laboratory, Department of Chemistry, University of Alberta under the files SHB 0301.

Synthesis of *trans*-RuCl₂(Py)₂((*R,R*)-Norphos) (41**).** Under a N₂ atmosphere, a 25 mL side-arm round bottom flask equipped with a stir bar was charged with (*R,R*)-Norphos (401 mg, 0.867 mmol) and *trans*-RuCl₂(NBD)Py₂ (**40**) (366 mg, 0.867 mmol). The solids were dissolved in freshly distilled dichloromethane (15 mL) and the resulting orange solution was stirred at room temperature for 12 h. The solvent was removed under high vacuum and the resulting orange solid was dissolved in minimum amount of dichloromethane

(~15 mL) and precipitated by the slow addition of hexanes (~10 mL) to afford orange needle shaped crystals of **41** in 86.1% yield (0.592 g): ^1H NMR (400 MHz, CD_2Cl_2): δ 0.59 (d, $J=8.42$ Hz, 1 H), 1.41 (d, $J=8.42$ Hz, 1 H), 2.68 (br. s, 1 H), 3.07 (br. s, 1 H), 3.14 - 3.22 (m, 1 H), 3.56 - 3.65 (m, 1 H), 4.84 (dd, $J=5.68$, 2.93 Hz, 1 H, olefin), 6.15 (dd, $J=5.68$, 2.93 Hz, 1 H, olefin), 6.96 - 7.15 (m, 12 H), 7.22 - 7.43 (m, 8 H), 7.59 - 7.64 (m, 2 H), 8.02 - 8.07 (m, 2 H), 8.23 - 8.28 (m, 2 H), 8.94 - 9.00 (m, 4 H); $^{31}\text{P}\{^1\text{H}\}$ NMR (162 MHz, CD_2Cl_2): δ 35.12 (d, $J_{\text{pp}} = 29$ Hz, 1P), 36.34 (d, $J_{\text{pp}} = 29$ Hz, 1P). $^{13}\text{C}\{^1\text{H}, ^{31}\text{P}\}$ NMR (101 MHz, CD_2Cl_2): δ 41.04, 43.55, 49.75, 50.40, 50.64, 123.81, 127.28, 127.36, 127.54, 127.95, 128.41, 128.44, 129.95, 132.47, 132.73, 134.68, 136.01, 136.03, 136.65, 137.23, 137.52, 137.76, 139.57, 155.55. Anal. Calcd for $\text{C}_{41}\text{H}_{38}\text{N}_2\text{P}_2\text{Cl}_2\text{Ru}$: C, 62.12; H, 4.83; N, 3.53. Found: C, 62.43; H, 4.65; N, 3.71.

Synthesis of *trans*- $\text{RuCl}_2((R,R)\text{-Norphos})((R,R)\text{-dpen})$ (42**).** Under a N_2 atmosphere, a 25 mL side-arm round bottom flask equipped with a stir bar was charged with **41** (120 mg, 0.151 mmol) and $(R,R)\text{-dpen}$ (32.1 mg, 0.151 mmol). The solids were dissolved in dichloromethane (5 mL) and the resulting orange solution was stirred at room temperature for 2 h. The solvent was removed under high vacuum and the yellow solid was dissolved in minimum amount of dichloromethane (~1.5 mL) and precipitated by the slow addition of hexanes (~5 mL) to afford a yellow solid of **42** in 80.5 % yield (0.103 g): ^1H NMR (400 MHz, CD_2Cl_2): δ 0.71 (d, $J=7.8$ Hz, 1 H), 1.55 (d, $J=7.8$ Hz, 1 H), 2.79 (br. s, 1 H), 2.95 (br t, $J=12.2$ Hz, 1 H), 3.11 (br. s, 1 H), 3.44 (br s, 2 H), 3.66 (br. s, 1 H), 4.47 -

4.53 (m, 4 H), 5.18 (d, $J=2.4$ Hz, 1 H), 6.23 (d, $J=2.4$ Hz, 1 H), 7.03 - 7.42 (m, 26 H), 7.96 (t, $J=8.31$ Hz, 2 H), 8.09 (t, $J=8.31$ Hz, 2 H); ^{31}P NMR (162 MHz, CD_2Cl_2): δ 44.57 (AB d, $J_{\text{pp}} = 33$ Hz, 1P), 36.34 (AB d, $J_{\text{pp}} = 33$ Hz, 1P). Anal. Calcd for $\text{C}_{45}\text{H}_{44}\text{N}_2\text{P}_2\text{Cl}_2\text{Ru}$: C, 63.83; H, 5.24; N, 3.31. Found: C, 63.40; H, 5.26; N, 3.29.

General procedures for the alternating ROMP of **41 and COE using **37** or **38**.** A 50 mL flask was charged with **41** (96.3 mg, 1.21×10^{-4} mol), dichloromethane (2.0 mL), and COE (63 μL , 4.85×10^{-4} mol). A separate flask was charged with the metathesis catalyst **37** (10.0 mg, 1.22×10^{-5} mol) and dissolved in dichloromethane (1 mL). A 0.50 μL aliquot of the catalyst solution (containing 5.0 mg **37**, 6.08×10^{-6} mol) was added to the polymerization reaction flask and the reaction mixture was stirred at room temperature overnight. The solvent was removed under vacuum at room temperature, and the resulting orange solid was further dried under vacuum for 1 h. ^1H NMR (498.1 MHz, CDCl_3): δ 2.45 - 0.8 (m), 3.96 - 3.0 (m), 4.8 - 4.5 (m), 5.41 - 5.0 (m), 9.0 - 6.8 (m). ^{13}C NMR (100.6 MHz, CD_2Cl_2): δ 155.2 - 155.0 (overlapping multiplet (om), py), 136.8 - 136.1 (om, ph), 134.4 - 131.7 (om, py), 131.5 - 126.7 (om, olefin + ph), 123.6 (s, py), 54.9 - 54.3 (om, ring CH), 51.2 - 50.6 (om, ring CH), 48.3 - 48.0 (om, ring CH_2), 42.7 (om, ring CH), 36.7 (om, ring CH), 33.0 - 25.8 (om, alkyl). ^{31}P NMR (201.6 MHz, CDCl_3): No unreacted **41** was present. Polymer consists of multiple overlapping signals δ 57 - 51. Two species predominated over the others: one, consist of two doublets (δ 52.24, $J = 35.3$ Hz; δ 54.7, $J =$

35.3 Hz), and the other, an AB quartet δ 53.1. These species were present in an approximately 1:1 ratio. Elemental analysis for a 4:1 (COE:1) polymer: Anal. Calcd for $C_{73}H_{94}Cl_2N_2P_2Ru$: C = 70.8; H = 7.72; N = 2.21. Found: C = 69.6; H = 7.84; N = 2.20.

Elemental analysis for a 20:1 (COE:1) polymer: Anal. Calcd for $C_{201}H_{318}Cl_2N_2P_2Ru$: C = 80.6; H = 10.7; N = 0.9. Calcd. %: C = 80.1; H = 11.0; N = 0.8.

Treatment of the alternating polymer with dpen to exchange the pyridine ligands. A NMR tube was charged with the alternating polymer (25 mg, containing approximately 3.15×10^{-5} mol of Ru) prepared above and (*R,R*)-dpen (20 mg, 9.45×10^{-5} mol). The tube was flushed with dinitrogen gas for 10 min, sealed with a septum and under a dinitrogen atmosphere $CDCl_3$ (1 mL) was added. The tube was shaken to ensure complete mixing and the orange reaction mixture was left overnight. ^{31}P NMR recorded the next day confirmed complete exchange of the pyridine ligands for (*R,R*)-dpen. There were no signals for coordinated Py ligands. 1H NMR (499.8 MHz, $CDCl_3$): δ 2.5 – 0.9 (m), 4.8 – 3.0 (m), 5.5 – 4.8 (m), 7.8 – 6.8 (m). ^{13}C NMR (100.6 MHz, CD_2Cl_2): δ 158.3 (s), 141.0 (s, ipso C on dpen), 136.8 -136.5 (om, ph), 133.7 - 132.6 (om, dpen ph), 132.0 - 127.2 (om, ph + olefin), 63.7 – 63.1 (om, dpen CH), 51.8 – 50.5 (om, ring CH), 48.9 – 48.4 (om, ring CH_2), 42.3 – 41.3 (om, ring CH), 36.0 - 35.3 (om, ring CH), 33.0 – 26.2 (om, alkyl). ^{31}P NMR (201.6 MHz, $CDCl_3$): multiple overlapping signals δ 63 – 53. The polymer signal set consisted mainly of 5

species in the amounts A, 40.7%; B, 10.2%; C, 40.7%; D, 8.0%; and E, 0.4%. A: 59.1 (d, J = 39 Hz), 57.6 (d, J = 39 Hz); B: 60.8 (d, J = 37 Hz), 56.6 (d, J = 39 Hz); C: 61.0 (d, J = 39 Hz), 55.5 (d, J = 40 Hz); D: 62.2 (d, J = 39 Hz), 53.7 (d, J = 39 Hz).

In situ monitoring by ^1H and ^{31}P NMR of the alternating ROMP of **41 and COE using metathesis catalyst **37**.** Compound **41** (14.2 mg, 0.0179 mmol) was weighed in air and transferred to a NMR tube. The tube was sealed with a septum, flushed with dinitrogen gas, and kept in a dry-ice acetonitrile bath at -40°C . Next, COE (9.32 μL , 0.0716 mmol) was added to the NMR tube using a syringe and CDCl_3 (0.3 mL) was then transferred slowly, down the walls of the NMR tube to give a orange solution. In the glovebox, **37** (1.3 mg, 0.00158 mmol) was weighed into a sample vial and the vial was sealed with a septum. Under an inert atmosphere CDCl_3 (0.5 mL) was added to the vial to dissolve the catalyst. An aliquot (0.28 mL, 0.736 mg, 0.000894 mmol) of the resulting purple solution was carefully transferred to the NMR tube, and finally CDCl_3 (0.22 mL) was added down the sides of the tube to ensure all reagents were in solution. The NMR tube was transferred to the pre-chilled NMR probe at -20°C and ^1H and ^{31}P NMR were recorded. The probe was warmed to room temperature and ^1H NMR spectra were taken every 10 min and ^{31}P NMR spectra were taken every 20 min, until the polymerization was complete.

Preparation of the heterogeneous polymeric catalyst [RuCl₂((*R,R*)-Norphos)((*R,R*)-dpen)]_x[COE]_y/BaSO₄ (47). Compound **41** (81.7 mg, 1.03 × 10⁻⁴ mol) was weighed in air and transferred to a 50 mL flask with a side arm. The flask was sealed with a septum, evacuated and back-filled with nitrogen several times. Dichloromethane (1.0 mL) was added, followed by the addition of COE (67 μL, 5.15 × 10⁻⁴ mol), to give a orange solution. A separate flask was charged with the metathesis catalyst **38** (5.5 mg, 6.4₈ × 10⁻⁶ mol) and dichloromethane (10 mL). 50 μL (containing 0.027₅ mg **38**, 3.2₃ × 10⁻⁸ mol) of the purple catalyst solution was added to the polymerization reaction flask via a syringe. The reaction mixture was stirred at room temperature and after 5 h the reaction mixture became very viscous. An additional 4 mL of dichloromethane was added to ensure the polymer remained in solution, and the mixture was stirred overnight. ¹H and ³¹P NMR spectra of an aliquot of the reaction mixture after 24 h, showed that 61 % of **41** (50 mg) and all the COE had polymerized. A solution of dicyclopentadiene (DCPD), (15.4 mg, 1.16 × 10⁻⁴ mol) in dichloromethane (1 mL) was transferred to the polymerization reaction, and the mixture was stirred for a further 4 h. Next, a solution of (*R,R*)-dpen (65.7 mg, 3.09 × 10⁻⁴ mol) in dichloromethane (1 mL), was added to the polymerization flask, and the reaction mixture was stirred overnight. The peaks in ¹H and ³¹P NMR spectra recorded at this stage were identical to the polymer prepared above (**41**/COE (1:4)) except for the presence of cross-linked DCPD peaks in the ¹H NMR spectrum at δ 2.2 (m), 3.0 - 2.7 (m), 6.0 – 5.6 (m). The homogeneous reaction mixture was diluted with dichloromethane (10 mL), and transferred onto

a slurry of BaSO₄ (5.00 g) and dichloromethane (20 mL). The yellow mixture was vigorously stirred for 10 min, and then the solvent was slowly removed under vacuum with stirring over ~ 1 h at room temperature. The solid was washed with methanol (3 x 50 mL) to remove any unreacted **41** and (*R,R*)-dpen, and then dried under vacuum at room temperature overnight to give **47** as a fine yellow powder. The catalyst loading on BaSO₄, based on 61 % polymerization of **41** (*vide supra*), was calculated at 1.18×10^{-5} mol of ruthenium per gram of BaSO₄ support or 9.99 mg of active (*R,R*)-Norphos/(*R,R*)-dpen catalyst per gram of support.

Procedure for the hydrogenation of 1'-acetonaphthone using heterogeneous catalyst 47. A silanized glass pressure reactor equipped with a magnetic stir bar was charged with the supported polymeric catalyst, **47** (1.00 g, containing 9.99 mg, (1.18×10^{-5}) mol) of ruthenium). The reactor was fitted with a rubber septum, flushed with nitrogen, and charged with 1'-acetonaphthone (1.00 g, 5.89×10^{-3} mol, 500 equiv) in dry, distilled *iso*-propanol (5 mL). A solution of *t*-C₄H₉OK (5.29 mg, 4.72×10^{-5} mol, 4 equiv) in 1 mL *iso*-propanol was then added to the reactor. Hydrogen gas was bubbled through the solution with stirring for 10 min, the septum was replaced with a hydrogen line, and the reactor was pressurized to 50 psi (gauge). The mixture was rapidly stirred at room temperature for the times specified in Table 2-1. The reactor was then depressurized, fitted with a septum, and kept under an atmosphere of hydrogen gas. The mixture was allowed to settle, and the solution was removed by inverse

filtration. After the solvent was removed on the rotovap an aliquot of the product mixture was analyzed by gas chromatography (GC) to determine yield and ee %. For catalyst reuse, the solid catalyst was left under an atmosphere of hydrogen gas at all times, and a fresh sample of substrate and base were added to the hydrogenation bomb as a solution in *iso*-propanol under a hydrogen atmosphere. The repeat runs were set up immediately after the previous run, without any down time between the runs.

Table 2-1. Enantioselective hydrogenation of 1'-acetonaphthone with **47**. ^[a]

<i>Run No.</i>	<i>Time (h)</i>	<i>ee (%)</i>	<i>Conv.(%)</i>
1	2 ^[b]	84.9	16
2	8.5 ^[b]	86.5	92
3	14	82.6	97
4	14.25	84.5	100
6	15	81.7	100
5	15	82.2	100
7	14.5	81.4	100
8	15	80.4	100
9	15.5	80.8	100
10	15.5	80.8	100
11	15.25	79.6	97

^[a]Reactions carried out in 1.0 M solution of 1'-acetonaphthone (2-propanol); H₂ = 50 psi; rt.; S/C/ ^tBuOK = 500/1/4. ^[b] Run was interrupted after 2 h and compared with homogenous run using **1** under the same conditions (42% yield, 48% ee). Based on 16% conversion in 2 h, 100% conversion will require 12.5 h. Run 2 gave 92% conversion after 8.5 h, all subsequent runs were 14-15 h.

Comparison of the initial TOF's between the heterogeneous catalyst 47 and the homogeneous catalyst 42. The procedure for the hydrogenation of 1'-acetonaphthone using the homogeneous catalyst *trans*-RuCl₂((*R,R*)-Norphos)((*R,R*)-dpen) **42** is as follows. The homogeneous catalyst **42** (9.81 mg, 1.16×10^{-5} mol) was weighed in air and transferred to the silanized glass pressure reactor equipped with a magnetic stirbar. The reactor was sealed with a septum, purged with hydrogen gas, and charged with 1'-acetonaphthone (0.985 g, 5.79×10^{-3} mol). Next, hydrogen purged *iso*-propanol (5 mL) and a solution of *t*-C₄H₉OK (5.19 mg, 4.63×10^{-5} mol) in 1 mL *iso*-propanol were added to the reactor using a gas tight syringe. The yellow reaction mixture was bubbled with hydrogen for 10 min. The reactor was connected to the hydrogen line, pressurized to 50 psi (gauge) and the reaction mixture was stirred at room temperature for 2 h. The solvent was removed on the rotovap and an aliquot of the product mixture analyzed by GC gave an initial TOF of 105 h⁻¹. The results were compared to run 1 from Table 2-1 for the hydrogenation of 1'-acetonaphthone using the heterogeneous catalyst **47**. The comparison shows that the rate (per active site) using the heterogeneous catalyst **47** was ~ 40 % of the rate using the homogeneous catalyst **42**.

Product work-up and determination of enantiomeric excess (ee). The products from a run were concentrated under reduced pressure, and an aliquot was passed through a Florisil plug using ethyl acetate (5 mL) as eluent to remove any contaminants. The ethyl acetate was removed under reduced pressure, and

the enantiomeric excess (*ee*) and % conversion were measured by chiral GC analysis carried out in house. The absolute configuration of the major product enantiomer was determined by comparison to an authentic sample of (*S*)-(+)-1-(1'-naphthyl)ethanol. The sample was injected as a dichloromethane solution with concentration = 2 mg/mL. Initial oven temperature: 150 °C for 45 min, increased at 1 °C/min to 170 °C; held at 170 °C for 10 min. The retention times were (*R*)-(+)-1-(1'-naphthyl)ethanol, $t_{R(R)} = 64.1$ min; (*S*)-(-)-1-(1'-naphthyl)ethanol, $t_{R(S)} = 62.2$ min; 1'-acetonaphthone, $t = 37.9$ min. The *ee* was measured 2x times for each run, and the measurements were confirmed against racemic 1-(1'-naphthyl)ethanol. There was 2.1% overlap of the peaks in the chromatograms of the racemic mixture taken every 4 chromatograms. This was normalized to give 0% *ee*, and the normalization factor applied to the *ee*'s summarized in Table 2-1.

Crystallographic analysis of *trans*-RuCl₂(Py)₂((*R,R*)-Norphos) (41**).**

Suitable crystal for the X-ray diffraction studies were obtained by slow addition of hexanes to a saturated solution of **41** in dichloromethane. At the first sign of a fluffy precipitate, the solution was filtered through a small plug of celite into a small round bottom flask with a side arm. Hexanes were added to the clear orange solution until small crystals could be seen on the sides of the flask. The flask was set aside overnight to allow for slow crystal growth and fine orange needle shaped crystals of **41** were collected by inverse filtration. The crystal system of **41**·CH₂Cl₂ was orthorhombic, and the space group P2₁2₁2₁ (No. 19).

Crystal data, details of data collection, and structure solution and refinement are displayed in Table 2-2. Selected bond distances and angles are displayed in Table 2-3 and Table 2-4.

Table 2-2. Crystallographic Experimental Details for 41•CH₂Cl₂.

A. Crystal Data

formula	C ₄₂ H ₄₀ Cl ₄ N ₂ P ₂ Ru
formula weight	877.57
crystal dimensions (mm)	0.24 × 0.12 × 0.06
crystal system	orthorhombic
space group	<i>P</i> 2 ₁ 2 ₁ 2 ₁ (No. 19)
unit cell parameters ^a	
<i>a</i> (Å)	9.5104 (11)
<i>b</i> (Å)	18.049 (2)
<i>c</i> (Å)	22.486 (3)
<i>V</i> (Å ³)	3859.8 (8)
<i>Z</i>	4
ρ_{calcd} (g cm ⁻³)	1.510
μ (mm ⁻¹)	0.800

B. Data Collection and Refinement Conditions

diffractometer	Bruker PLATFORM/SMART 1000 CCD ^b
radiation (λ [Å])	graphite-monochromated Mo K α (0.71073)
temperature (°C)	-80
scan type	ω scans (0.2°) (25 s exposures)
data collection 2θ limit (deg)	52.84
total data collected	22585 ($-11 \leq h \leq 11, -22 \leq k \leq 22, -28 \leq l \leq 22$)
independent reflections	7905 ($R_{\text{int}} = 0.0790$)
number of observed reflections (<i>NO</i>)	6559 [$F_o^2 \geq 2\sigma(F_o^2)$]
structure solution method	direct methods (<i>SHELXS-86</i> ^c)
refinement method	full-matrix least-squares on F^2 (<i>SHELXL-93</i> ^d)
absorption correction method	multi-scan (<i>SADABS</i>)
range of transmission factors	0.9536–0.8312
data/restraints/parameters	7905 [$F_o^2 \geq -3\sigma(F_o^2)$] / 0 / 459
Flack absolute structure parameter ^e	0.05(4)
goodness-of-fit (<i>S</i>) ^f	1.037 [$F_o^2 \geq -3\sigma(F_o^2)$]
final <i>R</i> indices ^g	
<i>R</i> ₁ [$F_o^2 \geq 2\sigma(F_o^2)$]	0.0506
<i>wR</i> ₂ [$F_o^2 \geq -3\sigma(F_o^2)$]	0.1099
largest difference peak and hole	0.930 and -0.761 e Å ⁻³

^aObtained from least-squares refinement of 4994 reflections with $4.51^\circ < 2\theta < 49.48^\circ$.

^bPrograms for diffractometer operation, data collection, data reduction and absorption correction were those supplied by Bruker.

^cSheldrick, G. M. *Acta Crystallogr.* **1990**, *A46*, 467–473.

^dSheldrick, G. M. *SHELXL-93*. Program for crystal structure determination. University of Göttingen, Germany, 1993. Refinement on F_o^2 for all reflections (all of these having $F_o^2 \geq -3\sigma(F_o^2)$). Weighted R -factors wR_2 and all goodnesses of fit S are based on F_o^2 ; conventional R -factors R_1 are based on F_o , with F_o set to zero for negative F_o^2 . The observed criterion of $F_o^2 > 2\sigma(F_o^2)$ is used only for calculating R_1 , and is not relevant to the choice of reflections for refinement. R -factors based on F_o^2 are statistically about twice as large as those based on F_o , and R -factors based on ALL data will be even larger.

^eFlack, H. D. *Acta Crystallogr.* **1983**, *A39*, 876–881; Flack, H. D.; Bernardinelli, G. *Acta Crystallogr.* **1999**, *A55*, 908–915; Flack, H. D.; Bernardinelli, G. *J. Appl. Cryst.* **2000**, *33*, 1143–1148. The Flack parameter will refine to a value near zero if the structure is in the correct configuration and will refine to a value near one for the inverted configuration.

$$fS = [\Sigma w(F_o^2 - F_c^2)^2 / (n - p)]^{1/2} \quad (n = \text{number of data}; p = \text{number of parameters varied}; w = [\sigma^2(F_o^2) + (0.0472P)^2]^{-1} \text{ where } P = [\text{Max}(F_o^2, 0) + 2F_c^2] / 3).$$

$$gR_1 = \Sigma ||F_o| - |F_c|| / \Sigma |F_o|; wR_2 = [\Sigma w(F_o^2 - F_c^2)^2 / \Sigma w(F_o^4)]^{1/2}.$$

Table 2-3. Selected Interatomic Distances (Å) for 41.

Atom1	Atom2	Distance	Atom1	Atom2	Distance
Ru	Cl1	2.4205(13)	P2	C31	1.838(6)
Ru	Cl2	2.4072(14)	P2	C41	1.844(5)
Ru	P1	2.3151(14)	N1	C51	1.352(7)
Ru	P2	2.3140(15)	C1	C2	1.559(7)
Ru	N1	2.146(4)	C1	C6	1.572(8)
Ru	N2	2.178(4)	C2	C3	1.578(8)
P1	C1	1.841(6)	C3	C4	1.508(8)
P1	C11	1.845(5)	C3	C7	1.568(10)
P1	C21	1.859(6)	C4	C5	1.248(9)
P2	C2	1.832(5)	C5	C6	1.407(10)
P2	C31	1.838(6)	C6	C7	1.571(10)
P2	C41	1.844(5)	C11	C12	1.376(7)
P2	C2	1.832(5)	C11	C16	1.371(8)

Table 2-4. Selected Interatomic Angles (deg) for 41.

Atom1	Atom2	Atom3	Angle
Cl1	Ru	Cl2	174.97(5)
Cl1	Ru	P1	89.34(5)
Cl1	Ru	P2	99.03(5)
Cl1	Ru	N1	87.17(12)
Cl1	Ru	N2	87.70(12)
P1	Ru	P2	87.74(5)
P1	Ru	N1	175.96(13)
P2	Ru	N2	172.98(13)
N1	Ru	N2	87.53(16)
Ru	P1	C1	102.86(17)
Ru	P1	C11	117.70(17)
Ru	P1	C21	120.33(18)
C1	P1	C11	104.8(3)
C1	P1	C21	109.7(3)
Ru	P2	C2	103.51(17)
Ru	P2	C31	128.23(18)
Ru	N1	C51	122.0(4)
Ru	N2	C65	122.6(4)

References

- (1) (a) Cornils, B.; Herrmann, W. A. *J. Catal.* **2003**, *23*, 31. (b) Dijkstra, H. P.; Van Klink, G. P. M.; Van Koten, G. *Acc. Chem. Res.* **2002**, *35*, 798-810. (c) Tumas, W.; Baker, R. T. *Science* **1999**, *284*, 1477-1479.
- (2) (a) Benaglia, M.; Puglisi, A.; Cozzi, F. *Chem. Rev.* **2003**, *103*, 3401-3429. (b) Clapham, B.; Reger, T. S.; Janda, K. D. *Tetrahedron* **2001**, *57*, 4637-4662. (c) Fan, Q. H.; Li, Y. M.; Chan, A. S. C. *Chem. Rev.* **2002**, *102*, 3385-3465. (d) Leadbeater, N. E. *Curr. Med. Chem.* **2002**, *9*, 2147-2171. (e) Leadbeater, N. E.; Marco, M. *Chem. Rev.* **2002**, *102*, 3217-3273.
- (3) Saluzzo, C.; Lemaire, M. *Adv. Synth. Catal.* **2002**, *344*, 915-928.
- (4) *Chiral Catalyst Immobilization and Recycling*; Wiley-VCH: (Eds.: D. E. De Vos, I. F. J. Vankelecom, P. A. Jacobs), **2000**.
- (5) Heitbaum, M.; Glorius, F.; Escher, I. *Angew. Chem. Int. Ed.* **2006**, *45*, 4732-4762.
- (6) (a) Bianchini, C.; Frediani, M.; Mantovani, G.; Vizza, F. *Organometallics* **2001**, *20*, 2660-2662. (b) Bianchini, C.; Frediani, M.; Vizza, F. *Chem. Commun.* **2001**, 479-480. (c) Deschenaux, R.; Stille, J. K. *J. Org. Chem.* **1985**, *50*, 2299-2302.
- (7) (a) Bayston, D. J.; Fraser, J. L.; Ashton, M. R.; Baxter, A. D.; Polywka, M. E. C.; Moses, E. *J. Org. Chem.* **1998**, *63*, 3137-3140. (b) Deng, G. J.; Fan, Q. H.; Chen, X. M.; Liu, D. S.; Chan, A. S. C. *Chem. Commun.* **2002**, 1570-1571.

- (8) Fan, Q. H.; Ren, C. Y.; Yeung, C. H.; Hu, W. H.; Chan, A. S. C. *J. Am. Chem. Soc.* **1999**, *121*, 7407-7408.
- (9) (a) Saluzzo, C.; Lamouille, T.; Herault, D.; Lemaire, M. *Bioorg. Med. Chem. Lett.* **2002**, *12*, 1841-1844. (b) Saluzzo, C.; ter Halle, R.; Touchard, F.; Fache, F.; Schulz, E.; Lemaire, M. *J. Organomet. Chem.* **2000**, *603*, 30-39. (c) ter Halle, R.; Colasson, B.; Schulz, E.; Spagnol, M.; Lemaire, M. *Tetrahedron Lett.* **2000**, *41*, 643-646. (d) ter Halle, R.; Schulz, E.; Spagnol, M.; Lemaire, M. *Synlett* **2000**, 680-682.
- (10) (a) Pu, L. *Chem. Rev.* **1998**, *98*, 2405-2494. (b) Pu, L. *Chem. Eur. J.* **1999**, *5*, 2227-2232. (c) Yu, H. B.; Hu, Q. S.; Pu, L. *J. Am. Chem. Soc.* **2000**, *122*, 6500-6501.
- (11) Mastrorilli, P.; Nobile, C. F. *Coord. Chem. Rev.* **2004**, *248*, 377-395.
- (12) Fan, Q. H.; Deng, G. J.; Lin, C. C.; Chan, A. S. C. *Tetrahedron: Asymmetry* **2001**, *12*, 1241-1247.
- (13) (a) Casey, C. P. *J. Chem. Educ.* **2006**, *83*, 192-195. (b) Ivin, K. J. M., J. C. *Olefin Metathesis and Metathesis Polymerization*; Academic Press: (Eds., 1997. (c) Furstner, A. *Angew. Chem. Int. Ed.* **2000**, *39*, 3013-3043. (d) Grubbs, R. H. *Tetrahedron* **2004**, *60*, 7117-7140.
- (14) Trnka, T. M.; Grubbs, R. H. *Acc. Chem. Res.* **2001**, *34*, 18-29.
- (15) (a) Schrock, R. R.; Hoveyda, A. H. *Angew. Chem. Int. Ed.* **2003**, *42*, 4592-4633. (b) Schrock, R. R. *Acc. Chem. Res.* **1990**, *23*, 158-165. (c) Schrock, R. R.; Murdzek, J. S.; Bazan, G. C.; Robbins, J.; Dimare, M.; Oregan, M. *J. Am. Chem. Soc.* **1990**, *112*, 3875-3886.

- (16) Schwab, P.; Grubbs, R. H.; Ziller, J. W. *J. Am. Chem. Soc.* **1996**, *118*, 100-110.
- (17) Bielawski, C. W.; Grubbs, R. H. *Angew. Chem. Int. Ed.* **2000**, *39*, 2903-2906.
- (18) (a) Frenzel, U.; Weskamp, T.; Kohl, F. J.; Schattenman, W. C.; Nuyken, O.; Herrmann, W. A. *J. Organomet. Chem.* **1999**, *586*, 263-265. (b) Scholl, M.; Ding, S.; Lee, C. W.; Grubbs, R. H. *Org. Lett.* **1999**, *1*, 953-956. (c) Herrmann, W. A. *Angew. Chem. Int. Ed.* **1999**, *38*, 262-262.
- (19) Herisson, J. L.; Chauvin, Y. *Makromol. Chem.* **1971**, *141*, 161.
- (20) Slugovc, C. *Macromol. Rapid Commun.* **2004**, *25*, 1283-1297.
- (21) Love, J. A.; Sanford, M. S.; Day, M. W.; Grubbs, R. H. *J. Am. Chem. Soc.* **2003**, *125*, 10103-10109.
- (22) (a) Sanford, M. S.; Love, J. A.; Grubbs, R. H. *J. Am. Chem. Soc.* **2001**, *123*, 6543-6554. (b) Sanford, M. S.; Ullman, M.; Grubbs, R. H. *J. Am. Chem. Soc.* **2001**, *123*, 749-750.
- (23) Bielawski, C. W.; Grubbs, R. H. *Macromolecules* **2001**, *34*, 8838-8840.
- (24) Szwarc, M. *Nature* **1956**, 1168-1169.
- (25) Bielawski, C. W.; Grubbs, R. H. *Prog. Polym. Sci.* **2007**, *32*, 1-29.
- (26) Maughon, B. R.; Weck, M.; Mohr, B.; Grubbs, R. H. *Macromolecules* **1997**, *30*, 257-265.
- (27) Choi, T. L.; Rutenberg, I. M.; Grubbs, R. H. *Angew. Chem. Int. Ed.* **2002**, *41*, 3839-3841.

- (28) (a) Slugovc, C.; Riegler, S.; Hayn, G.; Saf, R.; Stelzer, F. *Macromol. Rapid Commun.* **2003**, *24*, 435-439. (b) Bazzi, H. S.; Bouffard, J.; Sleiman, H. F. *Macromolecules* **2003**, *36*, 7899-7902.
- (29) (a) Leeuwenburgh, M. A.; van der Marel, G. A.; Overkleeft, H. S. *Curr. Opin. Chem. Biol.* **2003**, *7*, 757-765. (b) Iyer, S.; Rele, S.; Grasaa, G.; Nolan, S.; Chaikof, E. L. *Chem. Commun.* **2003**, 1518-1519.
- (30) (a) Rutenberg, I. M.; Scherman, O. A.; Grubbs, R. H.; Jiang, W. R.; Garfunkel, E.; Bao, Z. *J. Am. Chem. Soc.* **2004**, *126*, 4062-4063. (b) Akcelrud, L. *Prog. Polym. Sci.* **2003**, *28*, 875-962.
- (31) Sattigeri, J. A. S., C-W.; Hsu, C. C.; Yeh, F-F.; Liou, S.; Jin, B-Y.; Luh, T-H. *J. Am. Chem. Soc.* **1999**, 1607.
- (32) Barrett, A. G. M.; Hopkins, B. T.; Kobberling, J. *Chem. Rev.* **2002**, *102*, 3301-3323.
- (33) Buchmeiser, M. R. *Chem. Rev.* **2000**, *100*, 1565-1604.
- (34) (a) Buchmeiser, M. R. *Bioorganic & Medicinal Chemistry Letters* **2002**, *12*, 1837-1840. (b) Buchmeiser, M. R.; Kroll, R.; Wurst, K.; Schareina, T.; Kempe, R.; Eschbaumer, C.; Schubert, U. S. *Macromolecular Symposia* **2001**, *164*, 187-196. (c) Buchmeiser, M. R.; Sinner, F.; Mupa, M. *Macromolecular Symposia* **2001**, *163*, 25-34.
- (35) Buchmeiser, M. R.; Wurst, K. *J. Am. Chem. Soc.* **1999**, *121*, 11101-11107.
- (36) Pollino, J. M.; Weck, M. *Org. Lett.* **2002**, *4*, 753-756.
- (37) (a) Ahmed, M.; Barrett, A. G. M.; Braddock, D. C.; Cramp, S. M.; Procopiou, P. A. *Tetrahedron Lett.* **1999**, 8657-8662. (b) Hultsch, K. C.;

- Jernelius, J. A.; Hoveyda, A. H.; Schrock, R. R. *Angew. Chem. Int. Ed. Engl.* **2002**, *41*, 589. (c) Nguyen, S. T.; Grubbs, R. H. *J. Organomet. Chem.* **1995**, *497*, 195-200.
- (38) Krause, J. O.; Lubbad, S.; Nuyken, O.; Buchmeiser, M. R. *Adv. Synth. Catal.* **2003**, *345*, 996-1004.
- (39) (a) Krause, J. O.; Lubbad, S. H.; Nuyken, O.; Buchmeiser, M. R. *Macromol. Rapid Commun.* **2003**, *24*, 875-878. (b) Kroll, R. M.; Schuler, N.; Lubbad, S.; Buchmeiser, M. R. *Chem. Commun.* **2003**, 2742-2743.
- (40) Mayr, M.; Mayr, B.; Buchmeiser, M. R. *Angew. Chem. Int. Ed.* **2001**, *40*, 3839.
- (41) (a) Abd-El-Aziz, A.; Todd, E. K.; Okasha, R. M.; Afifi, T. H. *Macromol. Symp.* **2003**, *196*, 89-99. (b) Abd-El-Aziz, A. S.; Okasha, R. M.; Afifi, T. H.; Todd, E. K. *Macromol. Chem. Phys.* **2003**, *204*, 555-563.
- (42) Kroll, R.; Eschbaumer, C.; Schubert, U. S.; Buchmeiser, M. R.; Wurst, K. *Macromol. Chem. Phys.* **2001**, *202*, 645-653.
- (43) Buchmeiser, M. R.; Lubbad, S.; Mayr, M.; Wurst, K. *Inorg. Chim. Acta* **2003**, *345*, 145-153.
- (44) Bullock, S. E. K., P. *Macromolecules* **2004**, 1783-1786.
- (45) Cummins, C. C.; Beachy, M. D.; Schrock, R. R.; Vale, M. G.; Sankaran, V.; Cohen, R. E. *Chem. Mater.* **1991**, *3*, 1153-1163.
- (46) (a) Arstad, E.; Barrett, A. G. M.; Tedeschi, L. *Tetrahedron Lett.* **2003**, *44*, 2703-2707. (b) Nomura, K.; Ogura, H.; Imanishi, Y. *J. Mol. Catal. A* **2002**, *185*, 311-316.

- (47) Chan, Y. C. S., R. R.; Cohen, R. E. *J. Am. Chem. Soc.* **1992**, 7295-7296.
- (48) (a) Alexakis, A.; Burton, J.; Vastra, J.; Mangeney, P. *Tetrahedron: Asymmetry* **1997**, 8, 3987-3990. (b) Paneghetti, C.; Gavagnin, R.; Pinna, F.; Strukul, G. *Organometallics* **1999**, 18, 5057-5065. (c) Tararov, V. I.; Kadyrov, R.; Monsees, A.; Riermeier, T. H.; Borner, A. *Adv. Synth. Catal.* **2003**, 345, 239-245.
- (49) (a) Genet, J. P.; Mallart, S.; Pinel, C.; Juge, S.; Laffitte, J. A. *Tetrahedron: Asymmetry* **1991**, 2, 43-46. (b) Genet, J. P.; Pinel, C.; Mallart, S.; Juge, S.; Thorimbert, S.; Laffitte, J. A. *Tetrahedron: Asymmetry* **1991**, 2, 555-567.
- (50) Akotsi, O. M.; Metera, K.; Reid, R. D.; McDonald, R.; Bergens, S. H. *Chirality* **2000**, 12, 514-522.
- (51) Leong, C. G.; Akotsi, O. M.; Ferguson, M. J.; Bergens, S. H. *Chemical Communications* **2003**, 750-751.
- (52) Nishiyama, H.; Brunner, H.; Jones, P. G. *J. Organomet. Chem.* **1991**, 405, 247-255.
- (53) Noyori, R. *Angew. Chem. Int. Ed.* **2002**, 41, 2008-2022.
- (54) (a) AlSamak, B.; Carvill, A. G.; Hamilton, J. G.; Rooney, J. J.; Thompson, J. M. *Chem. Commun.* **1997**, 2057-2058. (b) Ilker, M. F.; Coughlin, E. B. *Macromolecules* **2002**, 35, 54-58.

- (55) (a) Song, C. E.; Lim, J. S.; Kim, S. C.; Lee, K. J.; Chi, D. Y. *Chem. Commun.* **2000**, 2415-2416. (b) Basso, A.; Bradley, M. *Tetrahedron Lett.* **2003**, *44*, 2699-2702.
- (56) Grubbs, R. H. *Angew. Chem. Int. Ed.* **2006**, *45*, 3760-3765.
- (57) Woodson, C. S., Grubbs, R. H. In *U.S. Patent 6,020,443*; Advanced Polymer Technologies, Inc.: U. S., 2000.
- (58) Ohkuma, T.; Takeno, H.; Honda, Y.; Noyori, R. *Adv. Synth. Catal.* **2001**, *343*, 369-375.
- (59) Rana, S.; White, P.; Bradley, M. *J. Comb. Chem.* **2001**, *3*, 9-15.
- (60) Buchmeiser, M. R. *Macromol. Rapid Commun.* **2001**, *22*, 1082-1094.
- (61) Mayr, M.; Buchmeiser, M. R.; Wurst, K. *Adv. Synth. Catal.* **2002**, *344*, 712-719.
- (62) Kohler K., H. R. G., Krauter J.G.E., Pietsch J. *Chem. Eur. J.* **2002**, 622.
- (63) (a) Noyori, R.; Koizumi, M.; Ishii, D.; Ohkuma, T. *Pure Appl. Chem.* **2001**, *73*, 227-232. (b) Noyori, R.; Ohkuma, T. *Angew. Chem. Int. Ed.* **2001**, *40*, 40-73.
- (64) (a) Noyori, R.; Ohkuma, T. *Pure Appl. Chem.* **1999**, *71*, 1493-1501. (b) Ohkuma, T. S., C. A.; Srinivasan, R.; Lin, Q.; Wei, Y.; Muniz, K.; Noyori, R. *J. Am. Chem. Soc.* **2005**, *127*, 8288-8289.
- (65) Blaser, H. U.; Pugin, B.; Spindler, F. *J. Mol. Catal. A* **2005**, *231*, 1-20.
- (66) Blaser, H. U.; Malan, C.; Pugin, B.; Spindler, F.; Steiner, H.; Studer, M. *Adv. Synth. Catal.* **2003**, *345*, 103-151.

- (67) Ohkuma, T.; Ooka, H.; Hashiguchi, S.; Ikariya, T.; Noyori, R. *J. Am. Chem. Soc.* **1995**, *117*, 2675-2676.
- (68) Ashby, M. T.; Halpern, J. *J. Am. Chem. Soc.* **1991**, *113*, 589-594.

Chapter 3

Synthesis of a ROMP active BINAP monomer.

Introduction

In Chapter 2 we demonstrated a new methodology to prepare a polymeric asymmetric hydrogenation catalyst using an alternating ring-opening metathesis polymerization (ROMP). We successfully recycled the prepared polymeric heterogeneous catalyst, *trans*-RuCl₂((*R,R*)-Norphos)((*R,R*)-dpen)]_x[COE]_y (**46**), for a record number of reuses.¹ The versatility of this new methodology encouraged us to apply it to other ligand systems that have a broader utility than has been established for Norphos. Although Norphos is an excellent chiral diphosphine substrate for ROMP, it has not displayed a combination of high activity and selectivity as seen for other more successful chiral diphosphine systems. Rather than attempting to increase the chiral efficiency of the Norphos-based polymers, and developing them for other asymmetric transformations, we chose to adapt the alternating ROMP methodology to a more successful ligand system: BINAP.

As discussed in Chapter 1, BINAP appears to be the most used and useful ligand, forming compounds with many transition metals that are active and highly enantioselective catalysts for a wide variety of reactions.^{2,3} In fact, as a result of its versatility and industrial potential, most recent methodologies aimed

at immobilizing homogeneous catalysts are developed with BINAP as the test ligand (see Chapter 1) and so in choosing BINAP a direct comparison of our alternating ROMP methodology to the literature methods can be made. Most reported methodologies require that BINAP be functionalized to allow for heterogenization of the catalysts. Likewise, to adapt our alternating ROMP methodology, the key step was to functionalize BINAP with a cyclic olefin susceptible to ROMP. Although there are no known examples whereby BINAP has been modified with a cyclic olefin, the vast literature precedent documenting numerous methods to functionalize BINAP encouraged us that functionalizing BINAP in this manner was attainable.⁴

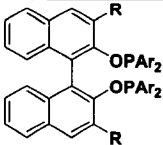
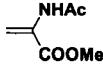
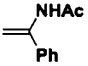
Previously, the BINAP framework was functionalized either to increase the catalyst activity and selectivity, or to facilitate separation of the catalyst from the reaction mixture. Both the phenyl groups and the naphthyl rings of BINAP have been modified. Even though our goal is to immobilize BINAP, it is worthwhile to mention that changes to the BINAP framework can influence its catalytic efficiency and this should be considered whenever modifications to BINAP are made. Typically, changes in the catalyst performance are observed for modifications made to the phenyl rings since they are directly bonded to the phosphorus atom. Modifying the phenyl substituents influences the electron density on the phosphorus atoms and the steric hindrance around these coordinating sites.⁵ Two well-known examples are the ToIBINAP and XyIBINAP derivatives, whereby the phenyl groups are substituted for $p\text{-CH}_3\text{C}_6\text{H}_4$ and $3,5\text{-(CH}_3)_2\text{C}_6\text{H}_3$, respectively. The increased steric bulk of the modified phenyl

substituents can result in a significant increase in enantioselectivity. For example, Noyori's *trans*-RuCl₂(diphosphine)(diamine) catalyst systems for the hydrogenation of aromatic ketones displayed >20% ee enhancements with XylBINAP.⁶ Also, a team at Takasago International Corporation have prepared various derivatives of BINAP and observed that electron-rich phenyl groups increase the catalyst activity.⁷

In terms of catalyst recycling, modifications to the binaphthyl skeleton are more often employed because of their accessibility. As well, modifications to the naphthyl rings are less likely to interfere with the catalyst selectivity since it is distal from the active catalytic sites. However, this is dependent on which position is functionalized on the naphthyl ring. For example, introduction of substituents at the 3,3'-positions can affect the steric bulk around the catalytic sites, and thereby influence the asymmetric induction of the catalysts. Zhang et al. prepared BINAP-phosphinite derivatives with various groups such as phenyl, methyl, etc. at the 3,3'-positions and used these new ligands to prepare rhodium-based catalysts. The substituted ligands showed a marked increase in selectivity for the asymmetric hydrogenation of dehydroamino acid derivatives and enamides as shown in Table 3-1.⁸

In principle, the positions on the naphthyl rings furthest from the active sites are least likely to modify the ligand properties. Therefore, the 5,5'- and the 6,6'-positions of the binaphthyl skeleton are considered to be privileged sites and modifications are most frequently made at these positions when dealing with heterogenization of BINAP. For this reason we also focused on functionalization

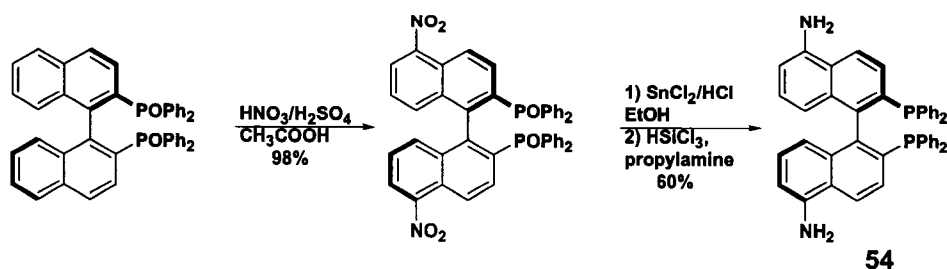
Table 3-1. Rh(I)-catalyzed asymmetric hydrogenation of functionalized olefins.

		
R=Me, Ar=Ph	95% ee	97% ee
R=Ph, Ar=Ph	99% ee	94% ee
R=3,5-Me ₂ C ₆ H ₄ , Ar=Ph	95% ee	89% ee
R=Ph, Ar=3,5-Me ₂ C ₆ H ₄	93% ee	90% ee
R=H, Ar=Ph	73% ee	28% ee

Reaction were done at 22°C under 3 atm H₂ for 12h in THF (S/C=100).

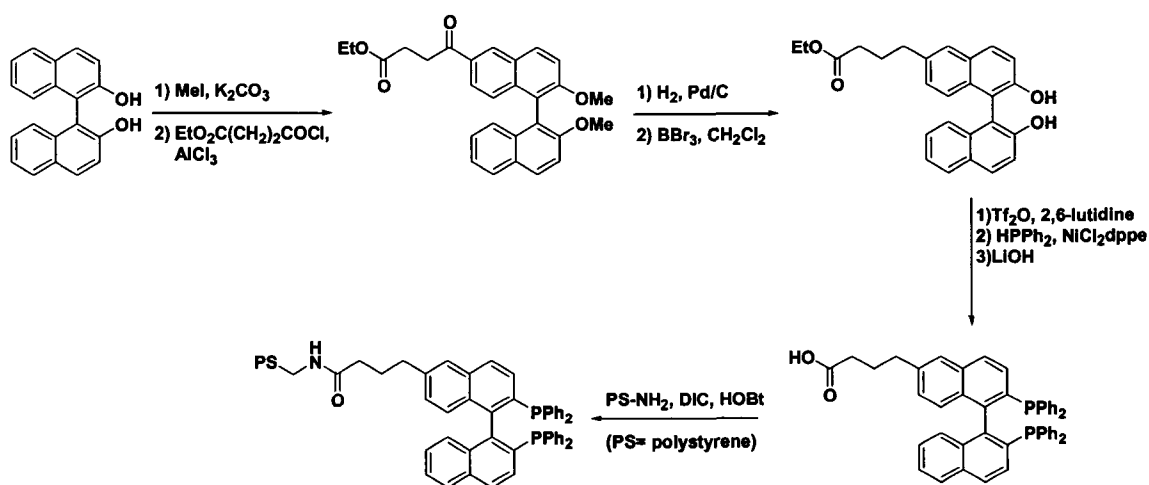
of the binaphthyl backbone at these positions. Conveniently, both sites are accessible by electrophilic substitutions and various synthetic methods have been employed to functionalize these sites.⁴ For example, BINAP can be functionalized at the 5,5'-positions by nitration⁹ and halogenation.¹⁰ The major advantage with functionalizing at the 5,5'-positions is optically active BINAP can be used directly as starting material and the stereochemistry is preserved throughout the synthetic sequence. Nitration was first carried out by Kumobayashi et al.⁹ in 1986 to give (*R*)-5,5'-diamino-BINAP (**54**) according to Scheme 3-1. As was shown in Chapter 1 (Scheme 1-12), **54** has been used to prepare soluble polymer¹¹ or dendrimer¹² supported catalysts to facilitate in catalyst recycling, although the number of recycles achieved with these systems were low. We also felt that **54** would be an ideal building block for the synthesis of our target molecule. Unfortunately, **54** is not commercially available and must be prepared in house. This Chapter will include an improved synthesis of **54**, along with a more complete characterization than in the literature.

Scheme 3-1. Synthesis of (*R*)-5,5'-diamino-BINAP.



Unlike the 5,5'-positions, the 6,6'-positions are not accessible by electrophilic substitution of BINAP. These positions are functionalized by electrophilic substitutions of BINOL precursors and the phosphine groups are introduced after functionalization of the binaphthyl moiety.¹³ Despite this indirect approach, the 6,6'-positions are more frequently studied for the immobilization of BINAP. For example, as was shown in Chapter 1, Bayston et al. used this approach for the selective Friedel-Crafts acylation of protected BINOL precursors (Scheme 3-2).¹⁴ After removal of the protecting groups using BBr_3 , the BINOL derivative was protected as the ditriflate and then phosphinated according to the

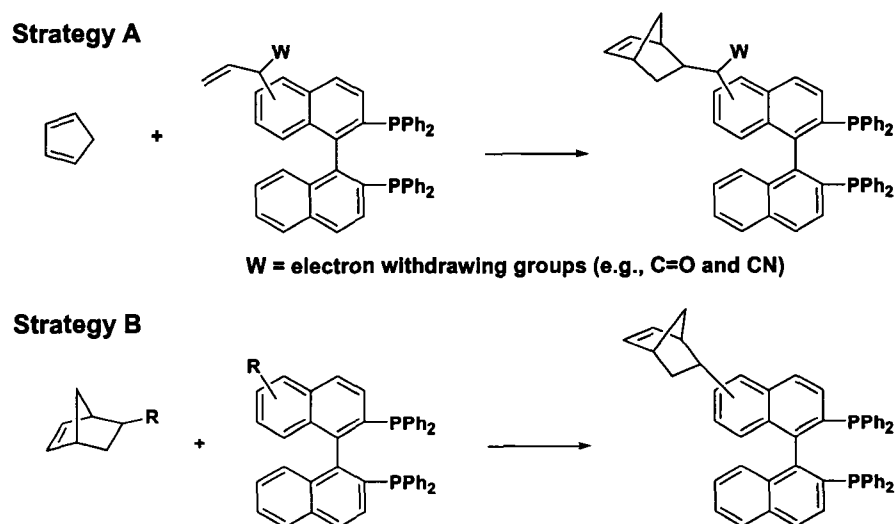
Scheme 3-2. Bayston's route for derivatizing BINAP.



procedure developed by Cai et al.¹⁵ The monofunctionalized BINAP derivative was attached to aminomethylated polystyrene using the standard peptide coupling reagents diisopropyl-carbodiimide (DIC) and hydroxybenzotriazole (HOBt) and the polymeric supported BINAP was used for the heterogeneous hydrogenation of olefins and β -keto esters. It is noted that this is the only example of commercially available supported BINAP.

Our ultimate objective was to prepare a ROMP-active BINAP monomer that can be used to make recyclable BINAP-based catalysts via the alternating ROMP methodology. The highly strained norbornene (bicyclo[2.2.1]heptene) group was the cyclic olefin of choice, since it displays excellent activity towards ROMP. Two strategies are proposed for the incorporation of norbornene groups onto the BINAP framework as shown in Scheme 3-3. Strategy A involves the

Scheme 3-3. Strategies for incorporating norbornene groups onto BINAP.

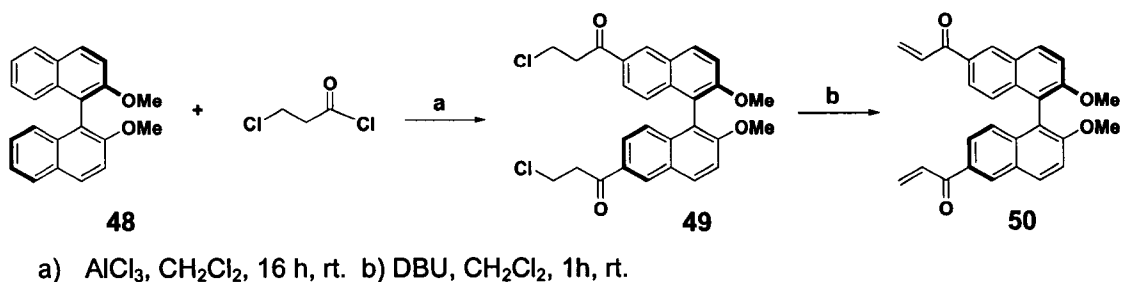


assembly of the norbornene functionality onto the binaphthyl backbone by the Diels-Alder reaction with cyclopentadiene and a suitably functionalized BINAP derivative. Strategy B involves direct attachment of a norbornene monomer to a suitably modified BINAP ligand. This Chapter discusses both strategies, along with the functionalization of BINAP at the 5,5'- and 6,6'-positions.

Results and Discussion

Our initial attempt was to incorporate dienophile groups on the binaphthyl backbone that could then be reacted with cyclopentadiene via Diels-Alder addition to give the norbornene unit. The functionalization route employed started from optically pure BINOL and the proposed synthetic sequence was conceptually similar to the procedure used by Bayston et al. to prepare their polymer-supported BINAP ligand (vide supra). The synthesis involved the functionalization of protected BINOL precursors at the 6,6'-positions to give (*R*)-6,6'-bis(acryloyl)-2,2'-bis(methoxy)-1,1'-binaphthyl (**50**), according to Scheme 3-4.

Scheme 3-4. Functionalization of BINAP at the 6,6'-positions.



Enantiomerically pure (*R*)-BINOL was protected as the methyl ether using standard literature procedures. This step was necessary in order to prevent racemization of the binaphthyl backbone, since BINOL does racemize under acidic and basic conditions.¹⁶ Friedel-Crafts acylation of **48** with 1 equiv. of 3-chloropropionyl chloride provided a mixture of products consisting of bis- and mono-acylated materials. However, separation of the product mixture by column chromatography was unsuccessful. Instead, the reaction was carried out with excess (2.5 equiv.) acid chloride to give only the bis-acylated product **49** in 65% yield. In retrospect the bis-acylated product is more desirable since the C₂-symmetry of the binaphthyl framework is maintained. ¹H NMR analysis revealed that acylation had occurred regioselectively at the 6,6'-positions of the binaphthyl skeleton. Slow addition of hexanes to a saturated solution of **49** in CH₂Cl₂ led to X-ray quality crystals. The solid-state structure of **49** was determined and is shown in Figure 3-1. X-ray analysis confirmed unambiguously that the 6,6'-positions were acylated.

Treatment of **49** with 1,8-diaza-bicyclo[5.4.0]undec-7-ene (DBU) afforded the α,β -unsaturated groups to give **50** in 80% yield. However, it was observed that **50** was unstable and if left for extended periods in solution an insoluble mass resulted. It was speculated that the presence of the acryloyl substituents on the conjugated binaphthyl backbone promotes polymerization of the bis-acryloyl product. The remaining steps were to involve the Diels-Alder reaction with cyclopentadiene to generate the norbornene units, followed by the phosphination step of the BINOL derivative (Scheme 3-5). The Diels-Alder reaction was

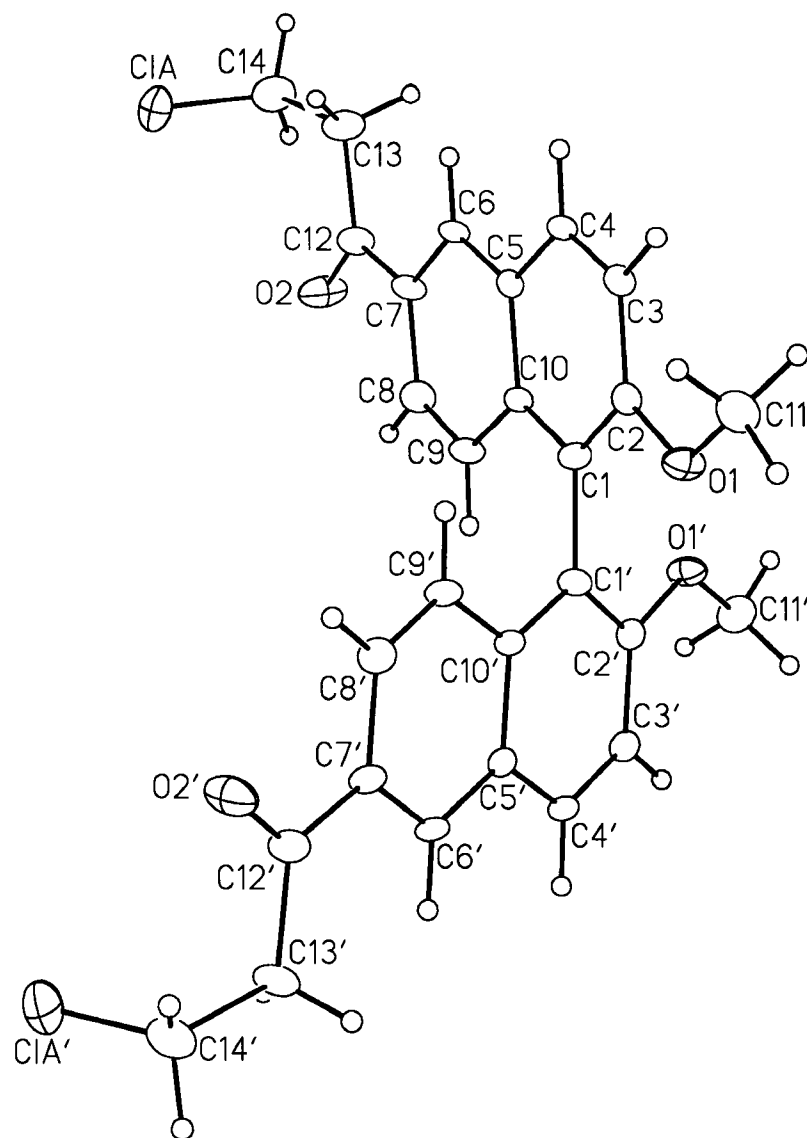
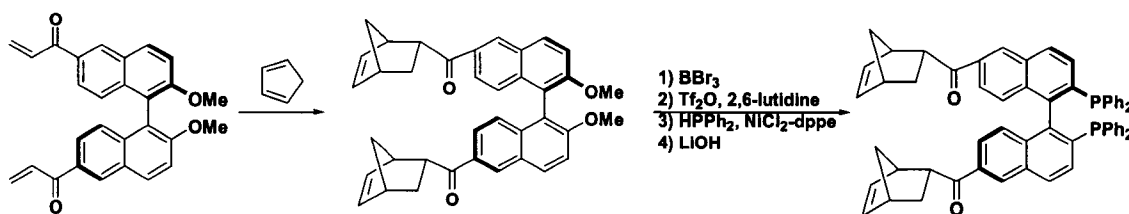


Figure 3-1. Perspective view of **49** showing the atom labeling scheme. The primed atoms are related to the unprimed ones by the 2-fold rotational axis located at $x, 0, 1/2$. Only one part of the disorder in the 3-chloropropionyl groups (about the C14 and C14' atoms) is shown for clarity. Non-hydrogen atoms are represented by Gaussian ellipsoids at the 20% probability level. Hydrogen atoms are shown with arbitrarily small thermal parameters.

Scheme 3-5. Attempted Diels-Alder reaction.

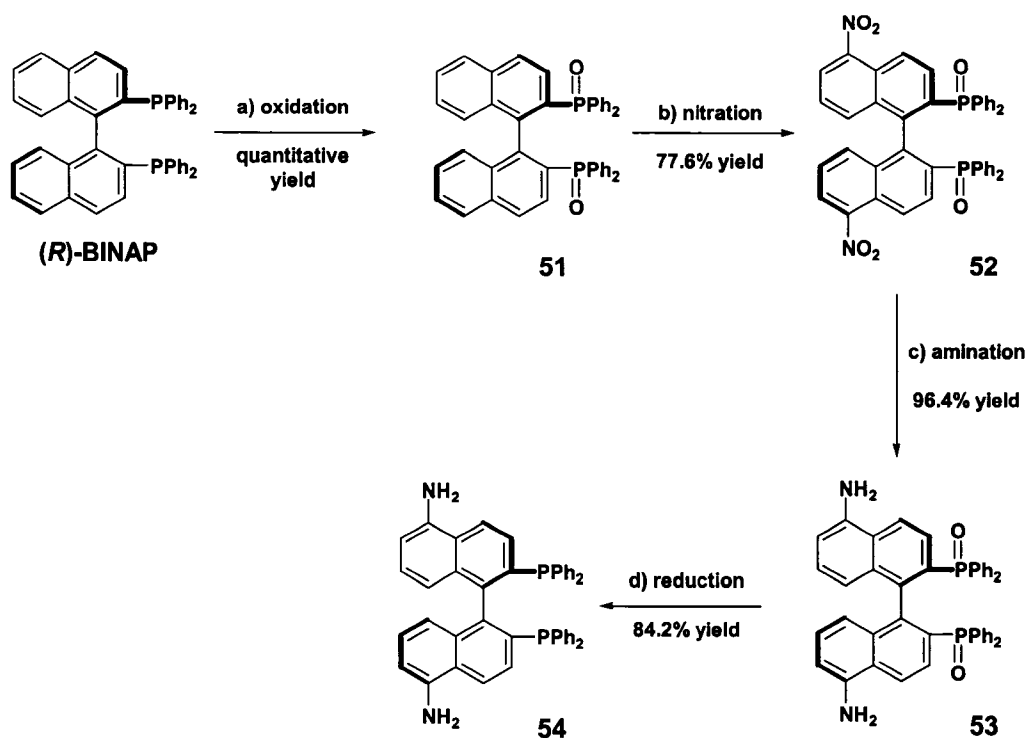


attempted several times under various conditions but failed to give the desired product. The reaction was sluggish and most often an insoluble solid precipitated from solution during the reaction. The incompatibility of the acryloyl groups on the binaphthyl backbone led us to discard this route.

One of the drawbacks to the above strategy is the number of steps required to functionalize BINAP, particularly the steps involved in the subsequent transformation of the BINOL derivative into the BINAP derivative. Even though the majority of examples involving the immobilization of BINAP are prepared by similar synthetic strategies, the lengthy functionalization sequence is a major deterrent from practical applications of these systems. Therefore, to avoid these drawbacks, we sought to functionalize enantiomerically pure BINAP directly. At the time of our work, the only method to functionalize BINAP directly at the privileged sites (*vide supra*) was by the nitration route shown previously in Scheme 3-1.⁹ However, the method described in the patent for the synthesis of 5,5'-diamino-BINAP gave low yields and several of the procedures, particularly involving product isolation, could not be duplicated in our hands. Inconsistencies in the original patent are likely why a broader application of this important BINAP monomer has not been observed. In any event, 5,5'-diamino-BINAP was

prepared according to Scheme 3-6 and an improved and reproducible synthesis of (*R*)-5,5'-diamino-BINAP (**54**) is described below.

Scheme 3-6. Nitration route to (*R*)-5,5'-diamino-BINAP (**54**).



a) 10% H₂O₂, toluene. b) HNO₃, (CH₃CO)₂O, H₂SO₄, 0°C. c) SnCl₂/HCl, EtOH, reflux 16h. d) Glass bomb, triethylamine, SiHCl₃, 120°C, 16h.

Improved synthesis of (*R*)-5,5'-diamino-BINAP (54**).** Commercially available (*R*)-BINAP was oxidized with 10% hydrogen peroxide to produce BINAP dioxide, BINAPO (**51**), in quantitative yield. The nitration of **51** was carried out using nitric acid and acetic anhydride as nitrating agent in the presence of a small amount of sulfuric acid as catalyst to produce (*R*)-5,5'-dinitro-BINAP dioxide (**52**). The procedure described in the patent for the isolation of

clean product was attempted several times but failed to give pure product. Unlike the patent method which used a hot THF/water mixture for purification, the present method gave **52** as a crystalline solid in 77% yield by recrystallization from a methylene chloride/hexanes solution. X-ray quality crystals of **52** were obtained by slow addition of hexanes to a saturated solution of **52** in methylene chloride. The crystal structure, shown in Figure 3-2, confirmed that nitration occurred regioselectively at the 5,5'-positions of the binaphthyl skeleton.

The nitro groups in **52** are selectively reduced using stannous chloride in concentrated hydrochloric acid as a reducing agent to form (*R*)-5,5'-diamino-BINAP dioxide (**53**). Again, the method for product isolation described in the patent could not be duplicated. Our method afforded **53** as a crystalline solid in 96% yield by recrystallization from THF. Finally, (*R*)-5,5'-diamino-BINAP (**54**) was obtained in 84% yield by reducing **53** with trichlorosilane as the reducing agent in the presence of triethylamine at 120°C for 16 h in a sealed pressure reactor. The crude product mixture was dissolved in hot toluene/methylene chloride solution and upon cooling, X-ray quality crystals of **54** were obtained. The solid-state structure is shown in Figure 3-3. With **54** in our toolbox the next step was to take advantage of the diamine functionality to prepare the desired ROMP active BINAP monomer.

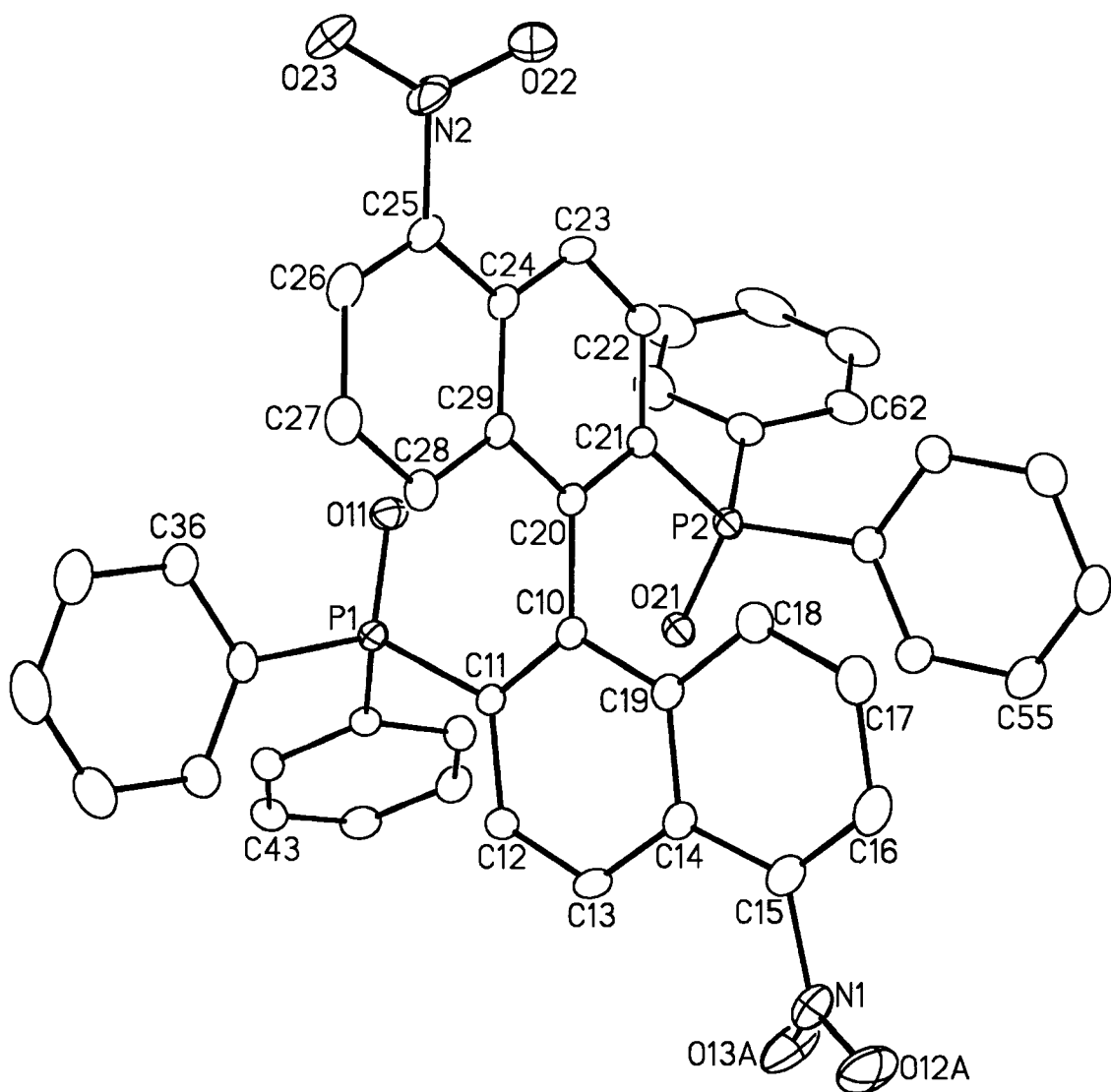


Figure 3-2. Perspective view of **52** showing the atom labeling scheme. Non-hydrogen atoms are represented by Gaussian ellipsoids at the 20% probability level. Hydrogen atoms are not shown. Only the major (80%) part of the disordered nitro group (O12A–N1–O13A) is shown.

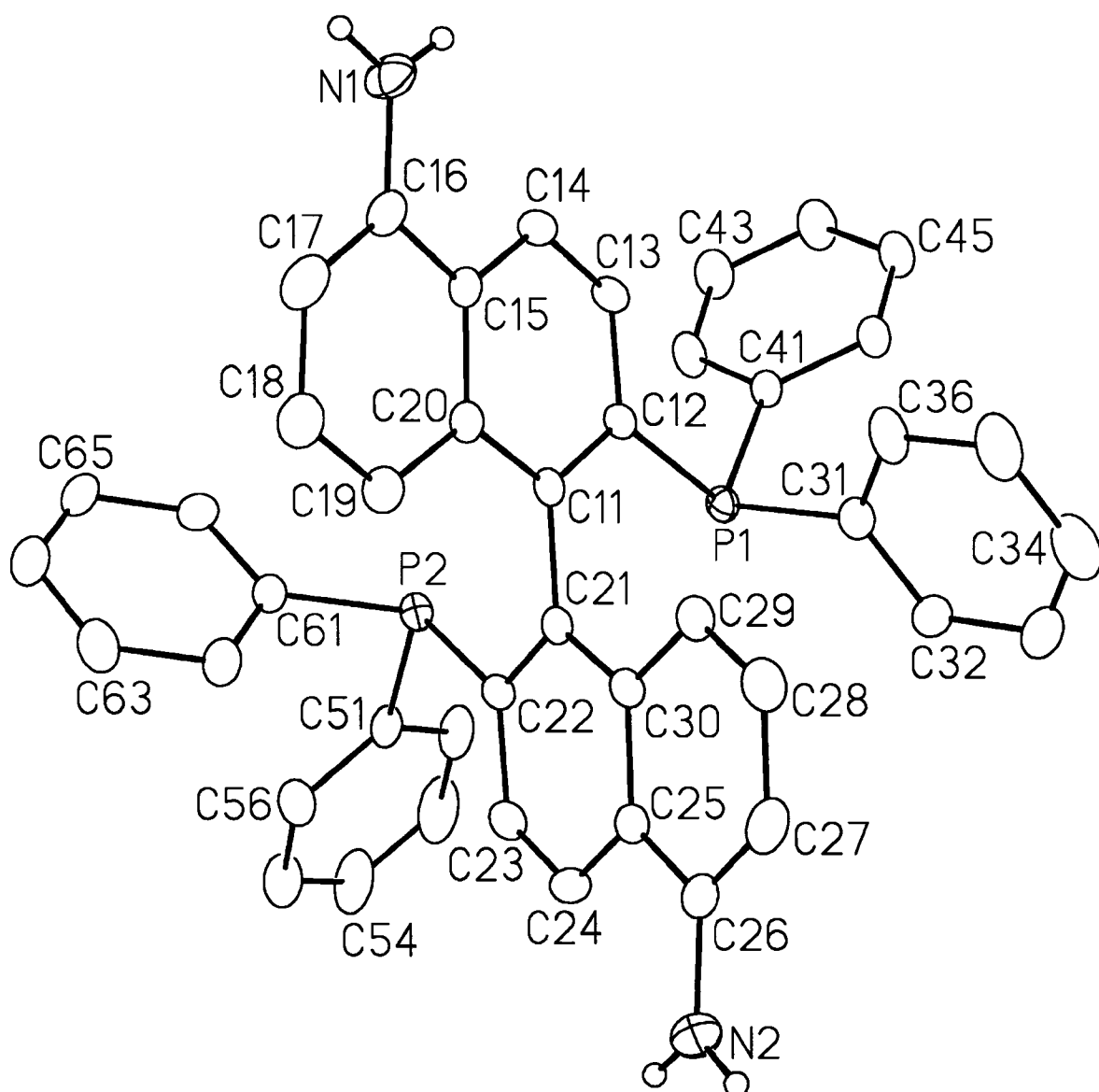
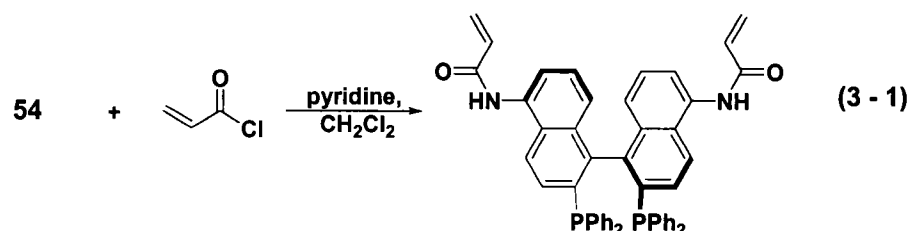


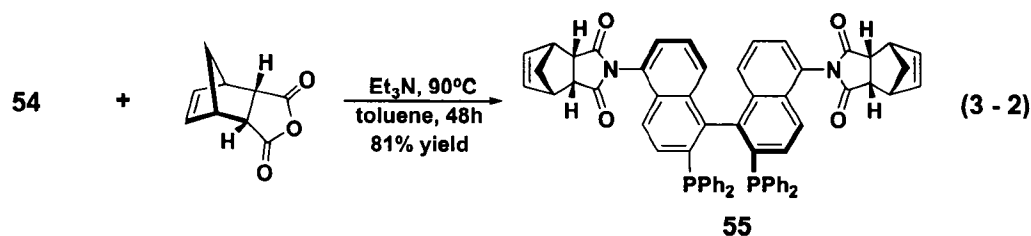
Figure 3-3. Perspective view of **54** showing the atom labeling scheme. Non-hydrogen atoms are represented by Gaussian ellipsoids at the 20% probability level. Hydrogen atoms attached to nitrogens are shown with arbitrarily small thermal parameters; all other hydrogens are not shown.

Amines are versatile functional groups that can react in a variety of ways, such as acylation and alkylation, and numerous derivatives of **54** have been prepared in this way.⁹ Our first attempt involved acylating **54** with acryloyl chloride to give the corresponding acrylamide as shown in equation 3 - 1. The



idea was to then assemble the norbornene groups by Diels-Alder reaction with cyclopentadiene, as described for strategy A. This acylation reaction failed completely and under the conditions employed an insoluble precipitate was always obtained. The reaction appears to promote polymerization, a result consistent with the behavior observed with **50**, whereby it was speculated that resonance between the acryloyl substituent and the conjugated binaphthyl backbone resulted in polymerization. This approach was abandoned and the direct attachment of a norbornene monomer to **54** (strategy B) for the generation of a ROMP active BINAP monomer proved to be more successful.

We prepared a ROMP-active version of BINAP in one step by condensation between **54** and cis-5-norbornene-endo-2,3-dicarboxylic anhydride to give (*R*)-5,5'-di(cis-5-norbornene-2,3-endo-dicarboximido)-2,2'-bis(diphenylphosphine)-1,1'-BINAP, or (*R*)-5,5'-dinorimido-BINAP (**55**) (equation 3 - 2). This reaction did not proceed smoothly and our initial attempts to react **54** with two equivalents of maleic anhydride in the presence of triethylamine at room



temperature failed. After refluxing overnight, both the ^1H and ^{31}P NMR spectrum indicated that a reaction had occurred, but it did not produce the expected product **55**. Rather, a mixture of unreacted starting materials, along with mono- and bis-substituted products was obtained. However, it was found that the condensation reaction went to completion in the presence of excess anhydride (12 equiv.) to give one major product. The excess anhydride could not be easily separated by chromatography or by recrystallization. Instead, washing the crude reaction mixture in toluene with aqueous base (1M NaOH) hydrolyzed only the unreacted anhydride to give maleic acid which was soluble in water. The organic product, which was believed to be **55**, did not hydrolyze under these conditions and was easily recovered from the organic phase in 81% yield.

Originally there was some uncertainty regarding the molecular formula and purity of the isolated product. Although both the elemental analysis and mass spectroscopy supported that the isolated product was indeed **55**, the NMR data suggested that a mixture of products was present. Specifically, the ^{31}P NMR spectra of **55** (Figure 3-4) consisted of a multiplet and this was not expected since the ^{31}P NMR spectra of C_2 -symmetric compounds, such as (*R*)-BINAP and (*R*)-5,5'-diamino-BINAP (**5**), consist of a sharp singlet peak due to the chemical equivalence of phosphines. The multiplet signal for **55** was unexpected

since it was thought that by functionalizing at the same position on the binaphthyl framework, the C_2 -symmetry of BINAP should be preserved. NMR spectroscopy studies revealed that **55** formed as a mixture of three NMR-distinct, diastereomeric atropisomers that differ by the relative rotameric orientations of the norimido groups about the naphthyl-N bonds. The origin and behavior of the diastereomers, along with an interpretation of the NMR spectra are presented in the following section.

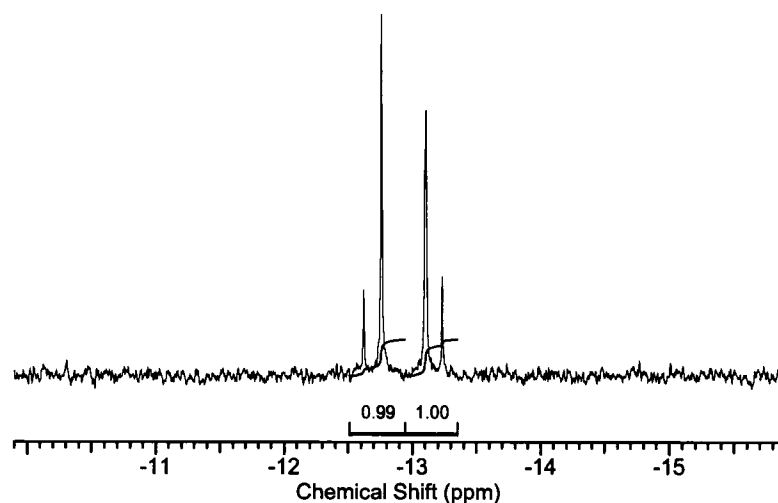


Figure 3-4. ^{31}P NMR (162MHz, CDCl_3 ,) of **55**.

Atropisomers as a result of restricted rotation about the naphthyl-N bond. Inspection of molecular models of **55** revealed two new chiral axes along the naphthyl-N bonds and restricted rotation of the norimido groups about these axes give rise to a mixture of diastereomeric atropisomers. Atropisomers are stereoisomers resulting from hindered rotation about single bonds where the steric strain barrier to rotation is high enough to allow for the isolation of the conformers.¹⁷ As such, three limiting non-planar conformations giving rise to three diastereomeric atropisomers were postulated based on the molecular

model study (Figure 3-5). In the extreme case, the norimido and naphthyl ring planes lie perpendicular to each other with the ethylene bridge on the norimido groups projected towards the 4,4'- or 6,6'-positions of the binaphthyl backbone. In this manner the three possible conformations consist of two C_2 dissymmetric diastereomers, and a non- C_2 dissymmetric diastereomer. The C_2 dissymmetric diastereomers are depicted in Figure 3-5a and Figure 3-5c. In each case both norimido groups have the same spatial orientation and based on the absolute configuration are denoted as (R,R,R) and (S,R,S) , respectively. Both the (R,R,R) and (S,R,S) diastereomers maintain the C_2 axis that renders the ^{31}P nuclei chemically equivalent and are therefore expected to show a singlet. The non- C_2 dissymmetric or meso diastereomer (Figure 3-5b), consist of a NMR equivalent pair where the norimido groups have the opposite spatial orientation and are

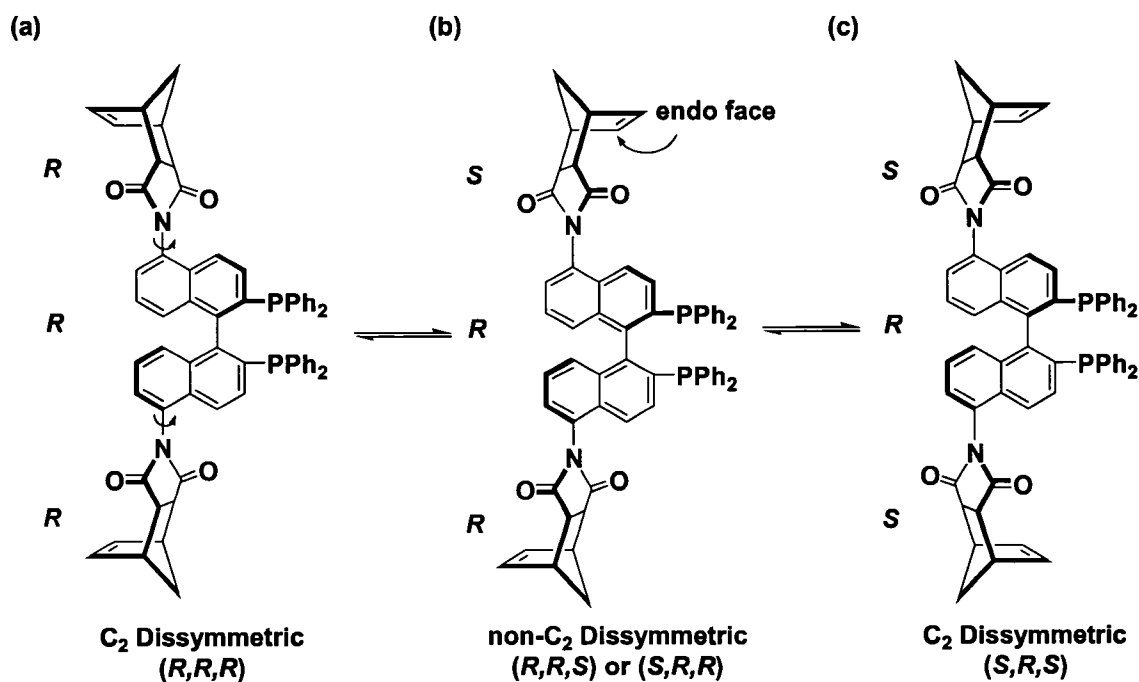
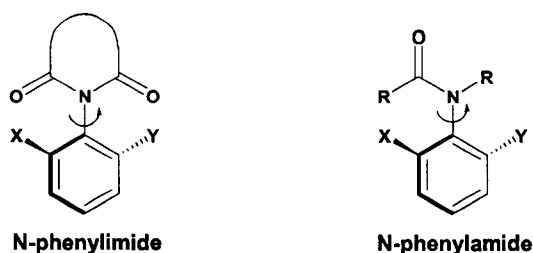


Figure 3-5. Three diastereomeric atropisomers of **55**.

denoted as (*R,R,S*) or (*S,R,R*). The non- C_2 dissymmetric diastereomer does not have a C_2 axis and therefore the ^{31}P nuclei are chemically non-equivalent and are expected to show two doublets. The restriction of free rotation of the norimido groups about the naphthyl-N bonds dictates whether the molecule retains or loses its C_2 symmetry, resulting in a mixture of rotational isomers that can be observed separately by ^{31}P NMR. This concept is well-known, and axially chiral compounds derived from appropriately substituted amides and imides have long been recognized.^{18,19}

Optically active compounds which possess axial chirality based on restricted rotation around a C-N bond are often referred to as non-biaryl atropisomers.²⁰ Such non-biaryl atropisomers have been utilized for asymmetric reactions,^{21,22} molecular recognition,²³ enzyme mimics,²⁴ and for the preparation of functionalized polymers.²⁵ The origin of the rotational barrier in N-aryl-amides and -imides is attributed to the resonance interaction between the nitrogen lone pair, the polarized carbonyl group and the aromatic ring. By assuming sp^2 hybridization the aryl-N bonds adopt partial double bond character and a significant barrier to rotation around the sp^2 - sp^2 aryl-N bond. These molecules are not coplanar, but instead twist to relieve unfavorable steric interactions between the *ortho*-aryl substituent and the imide or amide group. As shown in Figure 3-6, variation in the twist angle and the barrier to rotation are controlled by the size of the *ortho* substituent.²² Replacement of the *ortho*-hydrogen with a bulky substituent increases both the aryl-N torsion angle and the barrier to rotation through planarity. Curran et al. prepared a series of N-arylmaleimides

Figure 3-6. Effect of *ortho* substituents on twist angle.

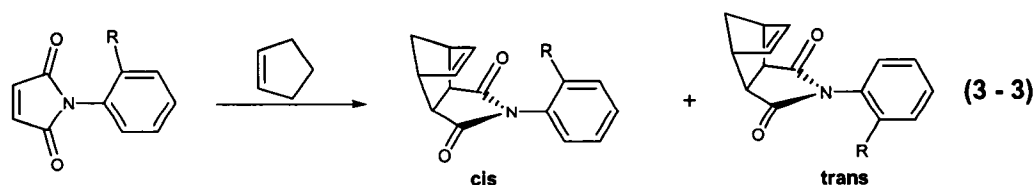


X, Y = H; low barrier to rotation, small twist angle (~30°)

X, Y = alkyl, OR; high barrier to rotation, large twist angle (~90°)

X = H, Y = tert-alkyl; high barrier to rotation, large twist angle (~90°)

bearing *ortho*-substituted aryl groups and found them to react diastereoselectively, favoring a single atropisomer.²⁶ For example, the Diels-Alder reactions with cyclopentadiene were shown to react selectively from the face unshielded by the substituents (equation 3 - 3). The cycloaddition products were isolated as mixtures from the *ortho*-ethyl (4.6/1) and *ortho*-isopropyl (6.1/1) systems and these mixtures underwent rapid equilibration by aryl-N bond rotation (as measured by NMR). In contrast, the Diels-Alder reaction with the *ortho*-^tbutyl system gave only the single trans isomer and it did not equilibrate even after heating at 140°C for 7 days. These results show the relationship between stereoselectivity and rotation barrier as a function of the *ortho* substituent. In our



R	trans	cis	Equilibration
Et	4.6	1	1.1/1
ⁱ Pr	6.1	1	1.4/1
^t Bu	only trans	-	no 2 nd product

case, the ortho substituent can be considered as the 4,4'-position of the naphthyl rings and the presence of multiple singals in the ^{31}P NMR of **55** suggest that the barrier to rotation of the norimido groups about the naphthyl-N bonds is restricted enough to prevent rapid interconversion of the three possible diastereomeric atropisomer on the NMR timescale.

In NMR spectroscopy the dynamic process of interconversion between conformers, as a result of intramolecular rotation about a single bond, is referred to as a chemical exchange phenomenon.²⁷ In the limit of slow exchange (lower temperatures), distinct resonances are observed for all conformers. In the fast exchange limit (high temperatures), rotation becomes faster and the lines in the spectrum broaden, coalesce, and finally sharpen into a single peak. In our case, we expected similar behavior for **55** because of the restricted rotation of the norimido groups about the naphthyl-N bonds. Specifically, if the rotation were rapid on the NMR timescale, the ^{31}P NMR spectra should consist of a singlet. Whereas if the rotation were slow, three distinct signals corresponding to the mixture of diastereomeric atropisomers should be seen. As shown in Figure 3-4 the ^{31}P NMR spectra of **55** consisted of a multiplet, which is believed to be a mixture of the frozen atropisomers, suggesting that at room temperature we are in the limit of slow exchange. In fact, by recording at a higher field, resonances for all three atropisomers is observed in the ^{31}P NMR spectra of **55** (Figure 3-7). At a higher field the redundancies of overlapping peaks are removed and three distinct sets of signals become visible. Two sharp singlets at -13.88 ppm and -14.12 ppm, representing each of the C_2 dissymmetric diastereomers, (*R, R, R*)

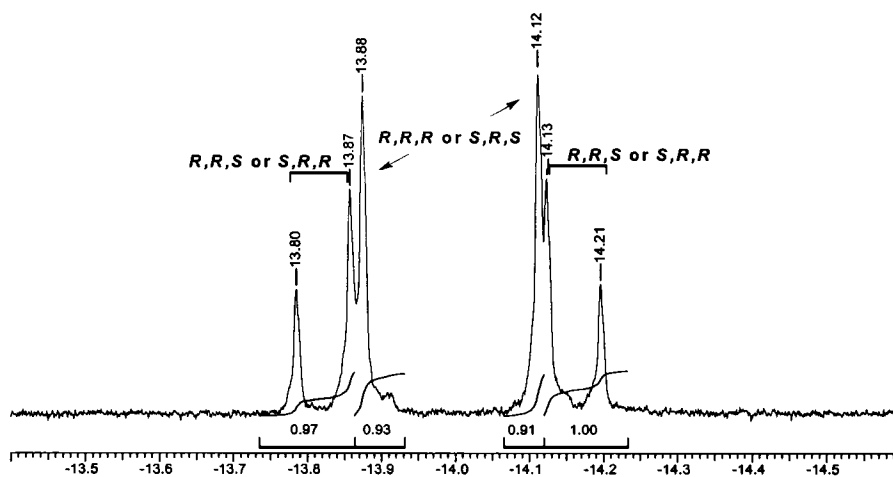


Figure 3-7. ^{31}P NMR of **55** (202MHz, CD_2Cl_2): δ -14.12 (s), -13.88 (s), -14.17 (d, $J_{\text{pp}} = 14.65$ Hz, 1P), -13.83 (d, $J_{\text{pp}} = 14.65$ Hz, 1P).

and (S, R, S), and two doublets at -14.17 ppm ($J_{\text{pp}} = 14.65$ Hz) and -13.83 ppm ($J_{\text{pp}} = 14.65$ Hz), representing the non- C_2 dissymmetric diastereomer, (R, R, S) or (S, R, R), are observed. The non- C_2 dissymmetric diastereomer actually consists of two possible arrangements but these are the same compound and therefore only one set of doublets are observed. The roughly equal integration of the C_2 dissymmetric and non- C_2 dissymmetric atropisomers suggests that at room temperature **55** exists as an equilibrated mixture, and there is a high barrier to rotation preventing rapid interconversion of the atropisomers.

Further proof that **55** forms a mixture of three diastereomeric atropisomers was obtained in a $^{31}\text{P} - ^{31}\text{P}$ COSY NMR experiment of a ruthenium complex of **55** (Figure 3-8). Treatment of **55** with *trans*-(NBD) RuCl_2Py_2 (**40**), in CH_2Cl_2 affords an orange crystalline powder, ((R)-5,5'-dinorimido-BINAP) RuCl_2Py_2 (**57**). The experimental procedure is discussed in the Chapter 4 and for now only the COSY NMR spectra is discussed. The ^{31}P NMR spectrum of **57** was

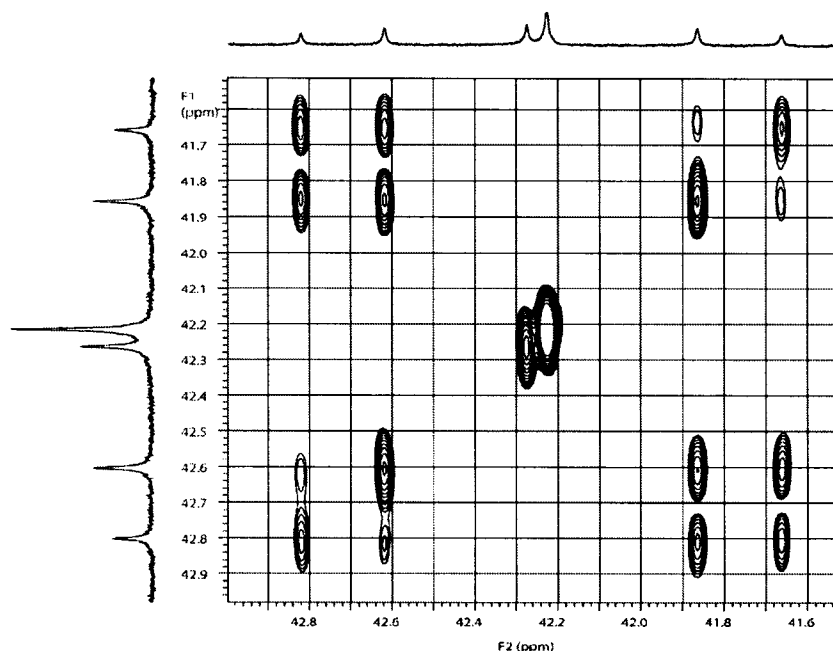


Figure 3-8. $^{31}\text{P} - ^{31}\text{P}$ COSY of (**57**).

also a multiplet consisting of two singlets representing the C_2 dissymmetric diastereomers, and two doublets representing the non- C_2 dissymmetric diastereomer. The COSY NMR experiment clearly shows that there is no correlation between the three sets of signals, confirming that three distinguishable chemical species are present. ^{31}P nuclei decoupling experiments performed on **57** also confirmed the presence of three different chemical species. Specifically, the doublet of doublet collapsed when irradiated with no change in the two singlets, and when either of the singlet peaks were irradiated the other singlet and the doublet of doublet peaks were not affected. For clarity only the interconversion process of the diastereomeric atropisomers of the free ligand **55** is discussed in this Chapter. The behavior of the rotational barrier for the metal complex **57** is discussed in Chapter 4.

To overcome the barrier to rotation in **55** and thereby promote rapid interconversion of the atropisomers, the temperature was increased. However, quite an interesting result occurred, namely, when a solution of **55** in toluene was heated to 90°C a white solid precipitated from solution. The ^{31}P NMR of the isolated solid (**56**) in CDCl_3 was taken at room temperature immediately after the sample was prepared and the spectra in Figure 3-9a consisted of a sharp singlet peak instead of the multiplet signal seen for **55**. Interestingly, this sharp singlet peak started to change at room temperature and new peaks resembling the multiplet signal for **55** appeared (Figure 3-9b). After 2 h (Figure 3-9c) it had totally converted back to the original multiplet with the same ratio of atropisomers as seen in Figure 3-4 for **55**. Clearly **56** must be one of the C_2 -dissymmetric diastereomeric atropisomers of **55** and the only difference between them is in the spatial orientation of the norimido groups. This was also supported by elemental analysis since **56** and **55** were found to have the same elemental composition. The isolation of a single C_2 -dissymmetric diastereomer is explained by considering that as the temperature is raised there is enough thermal energy to overcome the barrier to rotation about the naphthyl-N bonds and the diastereomeric atropisomers are able to interconvert more freely. As it turns out, the solubilities of the diastereomers are different since **56** is precipitated from toluene upon heating and remains insoluble in toluene at lower temperatures, whereas **55** is readily dissolved in toluene. It is envisioned that upon heating the population of the mixture of diastereomers changes whereby one of the C_2 dissymmetric diastereomers becomes more populated and falls out of solution

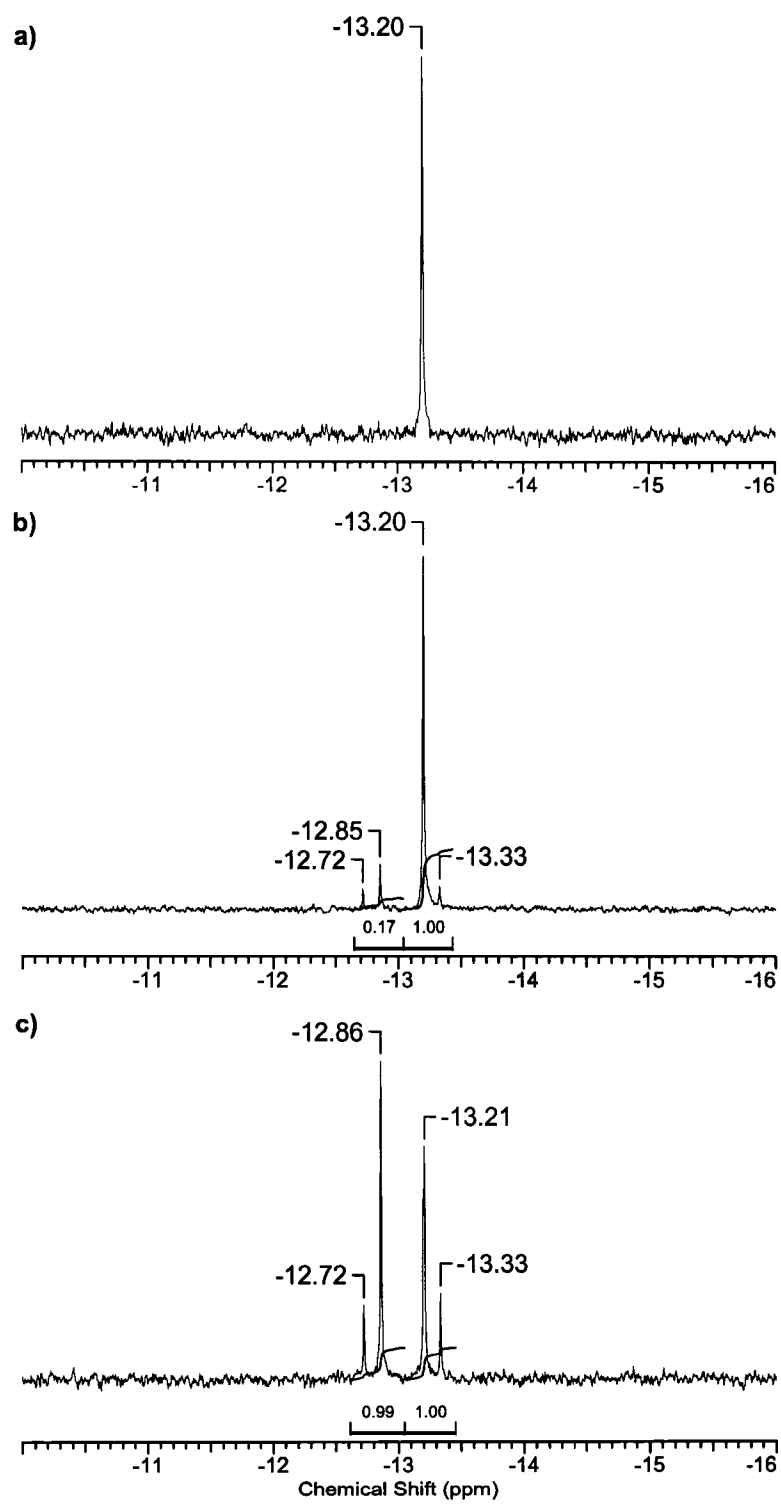


Figure 3-9. ^{31}P NMR (162 MHz, CDCl_3), of **56** at room temperature a) 0 min b) after 10-15 min c) after 2 h.

since it is less soluble in toluene. Essentially, equilibrium between the different populations of diastereomeric atropisomers is established more quickly at the higher temperature. Since **56** precipitates from solution, this drives the interconversion process forward in order to maintain equilibrium. With prolonged heating **56** is obtained in 87% yield from 90°C solutions of **55** in toluene. In solution **56** must be kept at low temperature to prevent interconversion. Allowing the solution to warm to room temperature results in the equilibration of **56** to **55** within in 2 h, and this is believed to be the thermodynamic product. By contrast, cooling a sample of **55** does not interconvert to give **56** but it remains as a mixture of atropisomers.

Interconversion of the diastereomeric atropisomers was also visible in the ^1H NMR spectra as shown in Figure 3-10. The ^1H NMR spectra in Figure 3-10a is of the isolated C_2 -dissymmetric atropisomers **56**, and it was recorded at -20°C to prevent interconversion. The sample is warmed to room temperature to allow the interconversion process to take place and from Figure 3-10b a set of new peaks appear. The final equilibrated mixture gave the identical spectra as seen for **55** (Figure 3-10c). Initially it may be expected that there should be three different sets of peaks since there are three diastereomers, as confirmed by the ^{31}P NMR experiment. Instead two sets of peaks which have identical patterns are observed. Basically the number of peaks has doubled and from a correlation experiment these are two distinguishable sets of peaks.

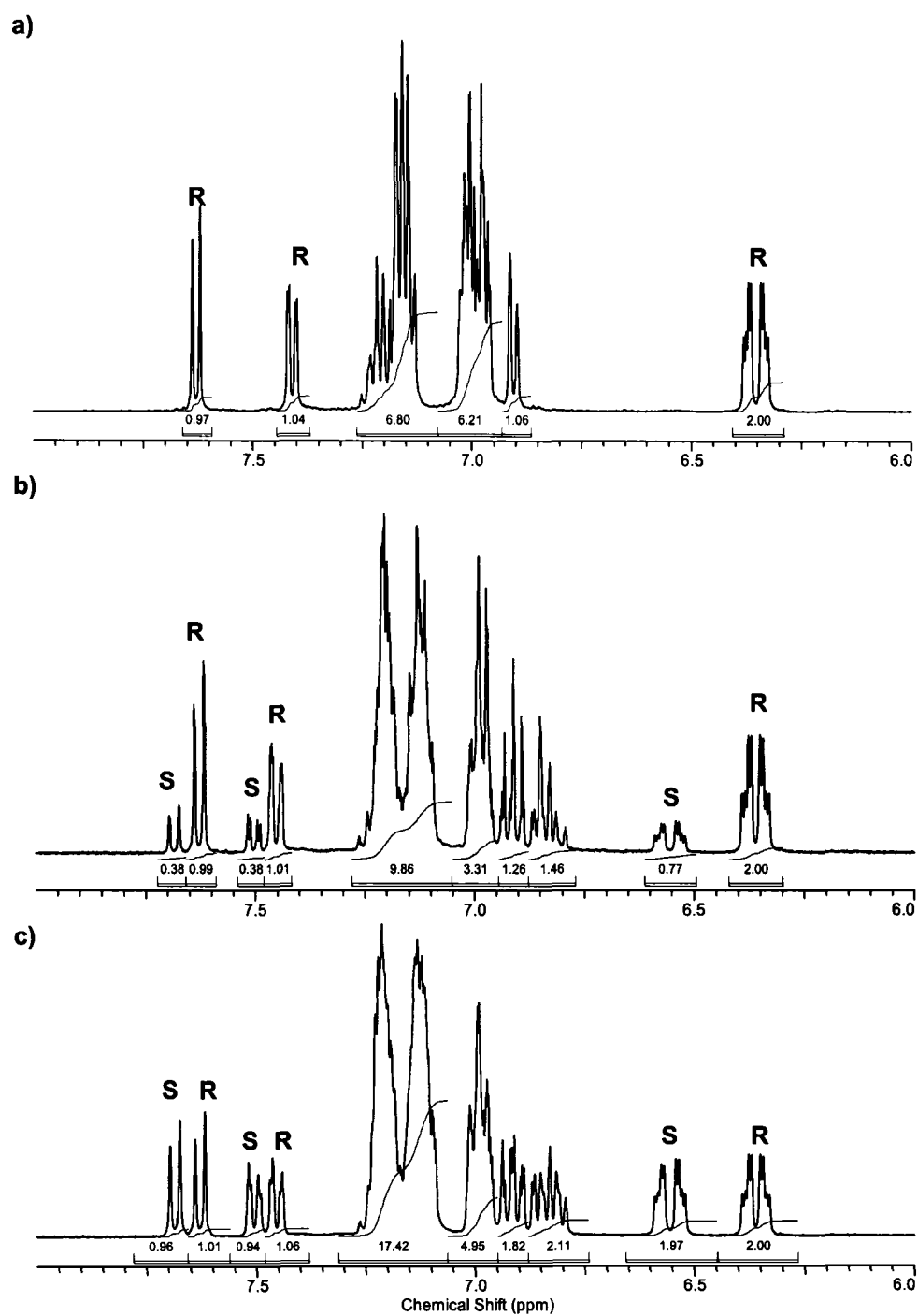


Figure 3-10. ^1H NMR (400MHz, CD_2Cl_2) of **56** a) at -20°C b) at room temperature 10 min c) of **55** at room temperature.

A simple explanation for this anomaly is given by considering that the three diastereomeric atropisomers are a result of new chiral axes due to the restriction of rotation of the norimido groups about the naphthyl-N bond and that the axial chirality of the binaphthyl framework does not change. Therefore if we dissect the ligand through the 1,1'-bond of the binaphthyl framework the two halves are related by the relative orientation of the norimido groups about the naphthyl rings. When the norimido groups have the same orientation the two halves are identical and this is either one of the C_2 dissymmetric diastereomers (R, R, R or S, R, S). When the norimido groups have the opposite orientation the two halves are not identical and this is now the non- C_2 dissymmetric diastereomer (R, R, S). As such, the non- C_2 dissymmetric diastereomer is expected to give rise to twice as many signals as a C_2 dissymmetric diastereomer, and this is exactly what is observed in the ^1H NMR spectra. We know from the ^{31}P NMR that **56** is a C_2 dissymmetric diastereomer and therefore the set of signals in the spectra in Figure 3-10a represents either the (R, R, R) or the (S, R, S) diastereomer. For the sake of clarity, we can arbitrarily assigned this as the (R, R, R) or **R** set, and the new set of signals that appear upon warming has a result of interconversion of the diastereomers (Figure 3-10b) can be assigned as the (S, R, S) or **S** set. Since the non- C_2 dissymmetric diastereomer is a combination of both the C_2 dissymmetric diastereomer, with one side as (S) and the other being (R), the ^1H NMR signals will simply overlap with the **R** and **S** sets of signals. Hence in Figure 3-10c the mixture of all three diastereomeric atropisomers of **55** are present but because of overlap only two

distinct sets are not observed. Similar overlapping of peaks was also observed in the ^{13}C NMR spectra of **55** and **56**, where the number of peaks has doubled for **55**. Due to the complexity of the ^1H NMR and the overlapping peaks the interconversion process was better studied by ^{31}P NMR.

The interconversion phenomenon of **55** was observed by variable temperature ^{31}P NMR studies and the temperature dependent spectra are shown in Figure 3-11. It proved difficult to observe this behavior since most deuterated solvents were unsuitable due to a combination of solubility problems and low boiling points. Often the solvent that displayed sufficient solubilities (i.e., C_6D_6 , CD_2Cl_2 , CDCl_3) were limited because of low boiling points or those that had higher boiling points (i.e., toluene- D_8 , $\text{DMSO-}\text{D}_6$) the ligand was either insoluble or would fall out of solution upon heating. Nitrobenzene- D_5 was found to be the solvent of choice. As the temperature is raised the multiplet signals move closer and coalescence occurs at 150°C (temperature limit of the NMR spectrometer). The interconversion process was reversible and when cooled to room temperature the broad single peak converts back to the original multiplet representing the equilibrated mixture of the three diastereomeric atropisomers. The high coalescence temperature is indicative of a substantial barrier to rotation of the norimido groups about the naphthyl-N bond, and similar barriers to rotation for N-aryl imides have been reported.¹⁹ Further investigations are being carried out in Bergens laboratory on the variable temperature NMR experiments to determine the rate of interconversion and the activation energy for rotation of the norimido groups about the naphthyl-N bonds.

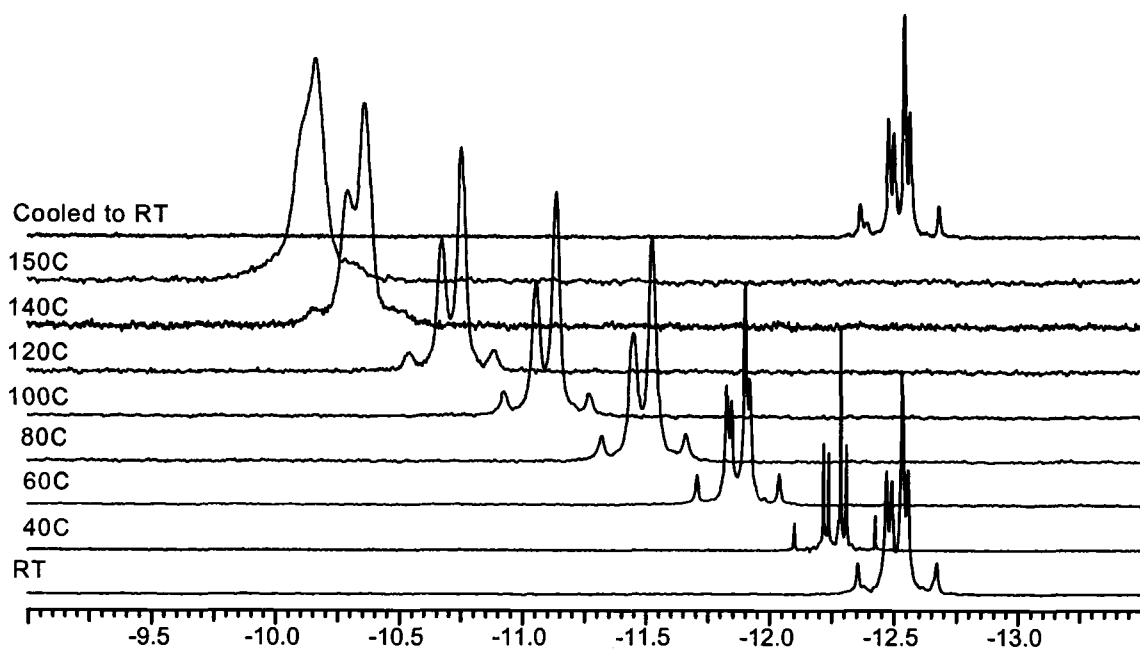


Figure 3-11. Variable Temperature ^{31}P NMR of **55** (400MHz, $\text{C}_6\text{D}_5\text{NO}_2$).

Conclusion

The work described in this Chapter presents the first example of a ROMP active BINAP monomer, (*R*)-5,5'-dinorimido-BINAP **55**, whereby the binaphthyl backbone of BINAP was functionalized with highly ROMP active norbornene units. The newly modified ligand **55** formed as a mixture of three NMR-distinct, diastereomeric atropisomers that differed by their relative rotameric orientations of the norimido groups about the naphthyl-N bonds. Two of these diastereomeric atropisomers, (*R,R,R*)- and (*S,R,S*)-, were C_2 -dissymmetric; while the other, (*R,R,S*)-, was not. Interestingly, the ligand **55** precipitated from 90°C solutions of toluene as only one C_2 -dissymmetric diastereotopic atropisomer in 87% yield. This

single atropisomer underwent interconversion after 2 h at 22°C in CD₂Cl₂ into the mixture of diastereomeric atropisomers in the same ratio as that from the preparation reaction. Variable temperature NMR experiments confirmed a substantial barrier to rotation about the naphthyl-N bonds, which prevents rapid interconversion of the diastereomeric atropisomers. The rigid nature of the naphthyl-N bond may have further implications on the polymerization of monomers of **55** and on the resulting polymer structure and this will be discussed in the next Chapter. With the ROMP active BINAP ligand **55** on hand the focus of the remaining work in this thesis deals with preparing immobilized BINAP based catalysts by the alternating ROMP methodology and testing them as reusable heterogeneous catalysts for various asymmetric hydrogenations.

Experimental

General Procedures and Materials. The solvents hexanes (K, Ph₂CO), methylene chloride (CaH₂), tetrahydrofuran (K, Ph₂CO), diethyl ether (K, Ph₂CO), toluene (K, Ph₂CO), triethylamine (CaH₂) and methanol (MgOMe) were distilled from drying agents under dinitrogen gas. Dinitrogen gas (Praxair, 99.998%) was passed through a drying train containing 3 Å molecular sieves and P₂O₅ before use. Unless stated otherwise, all operations were performed under an inert atmosphere of dinitrogen gas. All common reagents and solvents were obtained from Sigma-Aldrich Co. and used without purification unless stated otherwise.

Cis-5-Norbornene-2,3-endo-dicarboxylic anhydride (97%) was purchased from Aldrich, and purified by recrystallization from hot toluene and hexanes to yield a white crystalline product.

^1H , ^{13}C , and ^{31}P NMR spectra were recorded using Varian Inova (400 or 500 MHz) spectrometers. ^1H and ^{13}C NMR chemical shifts are reported in parts per million (δ) relative to TMS with the solvent as the internal reference. ^{31}P NMR chemical shifts are reported in parts per million (δ) relative to an 85 % H_3PO_4 external reference. NMR peak assignments were made using COSY and ^{13}C - ^1H HMQC and HMBC 2D NMR experiments. ESI mass spectra were obtained on a Micromass ZabSpec Hybrid Sector-TOF spectrometer. C/H/N elemental analyses were carried out at the University of Alberta Microanalysis Laboratory. Optical rotations were measured with a Perkin-Elmer 241 polarimeter at 589 nm (sodium D line) using 10 cm cells. Specific rotations $[\alpha]_D$ are reported in grams per 100 mL. Melting points were measured with Gallenkamp capillary melting point apparatus and are uncorrected. Drs. Robert McDonald and Mike J. Ferguson performed all solid-state structure determinations. Final atomic coordinates and displacement parameters for compounds **49**, **52**, and **54** can be obtained from the Structure Determination Laboratory, Department of Chemistry, University of Alberta under the files SHB 0207, SHB 0402 and SHB 0405 respectively.

Synthesis of (*R*)-2,2'-Dimethoxy-1,1'-binaphthalene (48). A nitrogen purged 3-neck flask was charged with (*R*)-binaphthol (1.10 g, 3.84 mmol) and

anhydrous acetone (100 mL). To the stirred solution were added anhydrous K_2CO_3 (1.06 g, 7.68 mmol) and iodomethane (1.09 g, 7.68 mmol). The mixture was refluxed under nitrogen atmosphere for 20 h. Volatiles were removed under reduced pressure and the residue was dissolved in CH_2Cl_2 (200 mL) and H_2O (150 mL). The layers were separated and the aqueous layer was extracted with CH_2Cl_2 (3 x 50 mL). The combined organic layers were dried over Na_2CO_3 , filtered, and solvent was removed under reduced pressure to leave a pale yellow solid. The solid was purified by washing with MeOH (3 x 50 mL) and dried under reduced pressure to afford **48** as a white crystalline solid in 97% yield (1.18 g). NMR data correspond to those previously reported.¹⁴

(R)-6,6'-bis(3-chloropropionyl)-2,2'-bis(methoxy)-1,1'-binaphthyl (49).

A nitrogen purged 3-neck flask, charged with solid $AlCl_3$ (1.06 g, 7.94 mmol) and **48** (0.999 g, 3.18 mmol) was placed in an ice-water bath. The solids were dissolved in CH_2Cl_2 (100 mL) and the red solution was stirred for 10 min. A solution of 3-chloropropionyl (1.01 g, 7.94 mmol) in CH_2Cl_2 (25 mL) was added dropwise over 1 h. The resulting orange solution was warmed to room temperature and stirred for 16 h. In air, the reaction mixture was poured carefully onto crushed ice (100 g) and the mixture was stirred until all of the ice had melted. The layers were separated and the aqueous layer was extracted with CH_2Cl_2 (3 x 50 mL). The combined organic layers were dried over Na_2SO_4 , filtered, and concentrated under reduced pressure. The resulting beige solid was recrystallized from CH_2Cl_2 /hexanes to afford white crystals of **49** in 65% yield

(1.02 g): mp 134-136°C; ^1H NMR (600 MHz, CDCl_3): δ 3.53 (t, J = 6.6 Hz, 4H), 3.79 (s, 6H), 3.94 (t, J = 6.6 Hz, 4H), 7.10 (d, J = 9.6 Hz, 2H), 7.52 (d, J = 9.0 Hz, 2H), 7.74 (dd, J = 9.6, 2.4 Hz, 2H), 8.12 (d, J = 9.0 Hz, 2H), 8.50 (s, 2H); ^{13}C NMR (101 MHz, CDCl_3): δ 39.02, 41.25, 56.60, 114.53, 118.78, 124.33, 125.58, 127.98, 130.52, 131.79, 131.86, 136.49, 157.34, 196.34. HRMS (EI). Calcd for $\text{C}_{28}\text{H}_{24}\text{Cl}_2\text{O}_4$: 494.1052. Found: 494.1049. Anal Calcd. for $\text{C}_{28}\text{H}_{24}\text{Cl}_2\text{O}_4$: C, 67.89; H, 4.88. Found: C, 67.74; H, 4.84.

Synthesis of (*R*)-6,6'-bis(acryloyl)-2,2'-bis(methoxy)-1,1'-binaphthyl (50). A solution of **49** (1.82 g, 3.67 mmol) in CH_2Cl_2 (120 mL) was treated with DBU (1.19 g, 7.71 mmol) at room temperature for 1 h. The reaction mixture was carefully quenched with HCl solution (0.12 N, 100 mL). The layers were separated and the aqueous layer was extracted with CH_2Cl_2 (3 x 50 mL). The combined organic layers were washed with brine (3 x 50 mL), dried over MgSO_4 , filtered, and concentrated under reduced pressure to afford a yellow solid. Further purification was carried out by flash column chromatography (silica gel, diethyl ether-chloroform, 50%) to afford a slightly yellow solid of **50** in 80% yield (1.24 g): ^1H NMR (400 MHz, CDCl_3): δ 3.79 (s, 6H), 5.91 (dd, J = 10.8, 1.6 Hz, 2H), 6.46 (dd, J = 17.2, 1.6 Hz, 2H), 7.12 (d, J = 8.8 Hz, 2H), 7.28 (dd, J = 17.2, 10.8 Hz, 2H), 7.51 (d, J = 9.2 Hz, 2H), 7.77 (dd, J = 9.2, 2.0 Hz, 2H), 8.11 (d, J = 9.2, 2H), 8.51 (d, J = 2.0 Hz, 2H); ^{13}C NMR (101 MHz, CDCl_3): δ 56.65, 114.38, 118.81, 125.08, 125.54, 127.96, 129.58, 130.94, 131.67, 132.31, 132.54, 136.20,

157.08, 190.29. HRMS (EI). Calcd for $C_{28}H_{22}O_4$: 422.1518. Found: 422.1506.

Anal Calcd. for $C_{28}H_{22}O_4$: C, 79.60; H, 5.25. Found: C, 78.96; H, 5.43.

Synthesis of (*R*)-BINAP Dioxide (51). Commercially available (*R*)-BINAP (0.855 g, 1.37 mmol) was dissolved in toluene (200 mL, undistilled) and oxidized by adding a solution of 10% H_2O_2 (90 mL). The reaction mixture was stirred for 60 min and then washed with a solution of saturated $Na_2S_2O_3$ (3 x 50 mL) until the excess H_2O_2 was neutralized. This was followed by washing with H_2O (3 x 50 mL) and saturated NaCl solution (3 x 50 mL). The organic layer was dried over Na_2SO_4 , filtered, and concentrated under reduced pressure to afford a white powder of **51** in 97.4% yield (0.874 g). Further purification was unnecessary: 1H NMR (600 MHz, $CDCl_3$): δ 6.81 (d, $J=3.66$ Hz, 4 H), 7.23 - 7.27 (m, 8 H), 7.34 - 7.46 (m, 12 H), 7.68 - 7.72 (m, 4 H), 7.82 (d, $J=8.06$ Hz, 2 H), 7.85 (dd, $J=8.42, 2.20$ Hz, 2 H); ^{13}C NMR (101 MHz, $CDCl_3$): δ 125.86, 127.15, 127.20, 127.34, 127.74, 127.85, 128.05, 128.15, 129.09, 130.92, 131.12, 132.06, 132.54, 133.05, 133.40, 134.03, 134.56, 143.00; ^{31}P NMR (162 MHz, $CDCl_3$): δ 29.27. HRMS (EI). Calcd for $C_{44}H_{32}P_2O_2$: 654.1877. Found: 654.1872. Anal. Calcd for $C_{44}H_{32}O_2P_2$: C, 80.72; H, 4.93. Found: C, 80.55; H, 4.93.

Synthesis of (*R*)-5,5'-Dinitro-BINAP Dioxide (52). Under a N_2 atmosphere, a 100 mL side-arm round bottom flask was charged with 20 mL of freshly distilled acetic anhydride. The flask was chilled in a salt (NaCl) ice bath, and 3 mL of 69% nitric acid was added dropwise with stirring over a period of 1

hour. A small amount of sulfuric acid (0.3 mL) was added to the reaction mixture. Compound **51** (2.27 g, 3.46 mmol) was added to the colorless reaction mixture, followed by stirring at 0°C, for 2 hours. The resulting yellow reaction mixture was quenched by slow addition into 200 mL of a 10% sodium hydroxide aqueous solution. A yellow precipitate immediately crashed out of solution and the mixture was left in the ice-water bath for 1 hr. The yellow precipitate was collected by filtration, washed with H₂O (3 x 10 mL), and dried under reduced pressure. The yellow solid was dissolved in minimum amount of dichloromethane (~15 mL) and precipitated by the slow addition of hexanes (~10 mL) to afford orange crystals of **52** in 76.5% yield (1.97 g): ¹H NMR (600 MHz, CDCl₃): δ 6.83 (t, *J*=8.42, 8.42 Hz, 2 H), 7.05 (d, *J*=8.79 Hz, 2 H), 7.27 - 7.46 (m, 16 H), 7.68 (s, 6 H), 8.09 (d, *J*=6.96 Hz, 2 H), 8.63 (d, *J*=8.79 Hz, 2 H); ¹³C NMR (101 MHz, CDCl₃): δ 122.86, 124.23, 125.03, 126.06, 128.28, 128.50, 131.48, 131.59, 131.71, 131.87, 131.90, 131.97, 132.47, 132.82, 133.35, 133.98, 142.43, 146.73; ³¹P NMR (162 MHz, CDCl₃): δ 28.72. Anal. Calcd for C₄₄H₃₀N₂O₆P₂: C, 70.97; H, 4.06; N, 3.76. Found: C, 70.46; H, 4.19; N, 3.89.

Synthesis of (*R*)-5,5'-Diamino-BINAP Dioxide (53**).** A 100 mL flask was charged with anhydrous ethanol (20 mL) and **52** (0.595 g, 0.799 mmol), followed by the dropwise addition of 12.1N hydrochloric acid (50 mL) over a period of 1 hour. A solution of SnCl₂•2H₂O (10.8 g, 47.9 mmol) in anhydrous ethanol (12 mL) was then added dropwise to the reaction mixture. The resultant yellow reaction mixture was refluxed for 17 hours and upon cooling to room temperature

a yellow precipitate crashed out of solution. The reaction mixture was concentrated under reduced pressure by 75% to ensure all of the hydrochloride salt had precipitated from solution. The precipitate was isolated by filtration and quickly washed with ice cold H₂O (10 mL). The precipitate was dissolved in ethanol (50 mL), and the solution was neutralized with 10% sodium hydroxide (10 mL). The resultant brown reaction mixture was concentrated under reduced pressure to near dryness. The concentrate was extracted with CH₂Cl₂, filtered and concentrated under reduced pressure to afford a brown solid. The solid was recrystallized from THF (5 mL) to yield brown crystalline solid of **53** in 96.4% yield (0.527 g): ¹H NMR (400 MHz, CDCl₃): δ 4.15 (br s, 4H), 6.28 - 6.30 (m, 2 H), 6.59 - 6.64 (m, 4 H), 7.21 - 7.27 (m, 9 H), 7.34 - 7.46 (m, 9 H), 7.67 - 7.72 (m, 4 H), 7.81 (d, *J*=8.79, 2 H); ¹³C NMR (101 MHz, CDCl₃): δ 111.47, 118.99, 120.45, 124.51, 126.40, 127.30, 127.95, 128.19, 128.90, 131.05, 131.20, 132.31, 132.75, 133.27, 134.54, 134.96, 142.06, 144.00; ³¹P NMR (162 MHz, CDCl₃): δ 29.55. HRMS (EI). Calcd for C₄₄H₃₄P₂N₂O₂: 684.2095. Found: 684.2091.

Synthesis of (*R*)-5,5'-Diamino-BINAP (54**).** A high pressure reactor flask was charged with a solution of **53** (1.05 g, 1.53 mmol) in distilled toluene (18 mL). The reactor was placed in an ice-water bath. Distilled triethylamine (4.27 mL, 30.6 mmol) and trichlorosilane (3.09 mL, 30.6 mmol) were added, and the reactor was sealed. The reaction mixture was warmed to room temperature and then heated at 120°C for 16 h. The reactor was cooled to room temperature, and the reaction mixture was treated with 10% deoxygenated aqueous NaOH (150 mL).

The reaction mixture was stirred at room temperature under N₂ atmosphere overnight. The layers were separated and the aqueous layer was back-extracted with deoxygenated toluene (3 x 75 mL). The combined organic layers were washed with deoxygenated water (3 x 50 mL). The organic layer was dried over Na₂SO₄, filtered, and concentrated under reduced pressure. The remaining brown solid was recrystallized from hot toluene and CH₂Cl₂ to afford brown cube shaped crystals of **54** in 84.2% yield (0.842 g): ¹H NMR (400 MHz, CDCl₃): δ 4.13 (s, 4 H), 6.38 (d, *J*=8.30 Hz, 2 H), 6.68 (d, *J*=7.08 Hz, 2 H), 6.78 (t, *J*=7.82 Hz, 2 H), 7.08 - 7.28 (m, 20 H), 7.40 (d, *J*=8.79, 2 H), 7.86 - 7.89 (d, *J*=8.79 Hz, 2 H); ³¹P NMR (162 MHz, CDCl₃): δ -14.92. Anal. Calcd for C₄₄H₃₄N₂P₂ + C₇H₈: C, 82.24; H, 5.68; N, 3.76. Found: C, 82.15; H, 5.68; N, 3.98.

Synthesis of ((*R*)-5,5'-N-di(*cis*-5-norbornene-2,3-dicarboximido)-2,2'-bis(diphenylphosphino)-1,1'-binaphthyl), (*R*)-5,5'-Dinorimido-BINAP (55**).** A heavy glass walled Schlenk flask was charged with (**54**) (0.144 g, 2.21 x 10⁻⁴ mol). The flask was evacuated and back-filled (3 x) with dinitrogen and then sealed with a rubber septum. 5 mL of deoxygenated toluene were added to the flask using a gas-tight syringe to form an orange mixture, with the ligand only partially dissolved. A large excess (12 eq) of *cis*-5-norbornene-endo-2,3-dicarboxylic anhydride (0.4355 g, 2.65 x 10⁻³ mol) was quickly weighed in air and transferred to a 25 mL round bottom flask equipped with a side arm. The flask was evacuated and back-filled (3 x) with dinitrogen and 5 mL of deoxygenated toluene were added to the flask using a gas-tight syringe to form a clear colorless

solution. The solution was transferred by cannula to the high-pressure reactor flask using 5 mL of toluene wash. Next, freshly distilled (from CaH₂) triethylamine (0.268 g, 2.65 x 10⁻³ mol) was transferred to the high-pressure reaction flask using a gas-tight syringe. The high-pressure reactor flask was sealed with a teflon high vacuum valve and the reaction mixture was heated at 90°C with stirring for 48 h. All solutes dissolved above 70°C resulting in a clear orange solution. The reactor was then cooled to room temperature and reaction mixture was transferred via a cannula to a dinitrogen-purged round bottom flask (200 mL) with a side arm using toluene wash (3 x 5 mL). The combined toluene fractions were then treated with 1M deoxygenated aqueous NaOH (100 mL) to hydrolyze the excess unreacted anhydride. The flask was gently swirled for 20 min to ensure complete mixing and then left to settle. The layers were separated and the aqueous layer was back-extracted with deoxygenated toluene (4 x 20 mL). The combined organic layers were washed with deoxygenated water (3 x 20 mL), dried over anhydrous Na₂SO₄, and cannula filtered using toluene wash (3 x 10 mL) into a round bottom flask (250 mL). The volatiles were quickly removed under reduced pressure on a rotary evaporator. The remaining orange solid was dissolved in minimum amount of dichloromethane (~5 mL) and precipitated by the slow addition of hexanes (~25 mL) to yield an orange crystalline powder of **55** in 81% yield (0.169 g). The NMR data represents the mixture of all three diastereomeric atropisomers: ¹H NMR (400 MHz, CD₂Cl₂): δ 1.68 (d, *J* = 8.79 Hz, 1H, CH₂ bridge), 1.72 (d, *J* = 8.79 Hz, 1H, CH₂ bridge), 1.82 (d, *J* = 8.79 Hz, 1H, CH₂ bridge), 1.87 (d, *J* = 8.79 Hz, 1H, CH₂ bridge), 3.52 -

3.62 (m, 8 H, CH norbornyl ring), 6.34 (ABX dd, $J = 5.68, 2.74\text{Hz}$, 1H, CH olefin), 6.38 (ABX dd, $J = 5.58, 2.83\text{Hz}$, 1H, CH olefin), 6.53 (ABX dd, $J = 5.58, 2.83\text{Hz}$, 1H, CH olefin), 6.58 (ABX dd, $J = 5.68, 2.74\text{Hz}$, 1H, CH olefin), 6.79 - 6.87 (m, 2H, naphthyl), 6.89 - 6.94 (m, 2H, naphthyl), 6.96 - 7.01 (m, 5H, ph + naphthyl), 7.09 - 7.26 (m, 17H, ph + naphthyl), 7.45 (dd, $J=8.79, 2.38\text{ Hz}$, 1H, naphthyl), 7.50 (dd, $J=8.79, 2.38\text{ Hz}$, 1H, naphthyl), 7.63 (d, $J=8.79\text{ Hz}$, 1H, naphthyl), 7.69 (d, $J=8.79\text{ Hz}$, 1H, naphthyl). $^{13}\text{C}\{^1\text{H}\}$ NMR (101 MHz, CD_2Cl_2): δ 45.71 (s, 2 CH), 46.00 (s, 2 CH), 46.39 (s, 2 CH), 47.46 (s, 2 CH), 52.71 (s, 2 CH_2 , bridge), 122.73 (s, 1 CH, naphthyl ring (nap)), 123.47 (s, 1 CH, nap), 125.78 (s, 1 CH, nap), 125.86 (s, 1 CH, nap), 127.22 (s, 1 CH, nap), 127.66 (s, 1 CH, nap), 128.30 (br. s., 2 CH, nap), 128.62 - 128.70 (m, 8 CH, ph), 129.05 - 129.12 (m, 4 CH, ph), 129.49 (br. s., 2 C, N-C-C_{fused}), 129.82 - 129.98 (m, 2 C. N-C-C_{fused}), 131.66 (s, 1 CH, nap), 131.85 (s, 1 CH, nap), 133.19 - 133.38 (m, 4 CH, ph), 134.23 (br. s., 2 C, C-C-P), 134.50 - 134.78 (m, 4 CH, ph), 135.09 (s, 1 CH, olefin), 135.15 (s, 1 CH, olefin), 136.04 (s, 1 CH, olefin), 136.26 (s, 1 CH, olefin), 136.71 (br. s., 2 C, C_{fused}-C-C), 137.42 (s, 2 C, C_{ispo-ph}), 137.53 (s, 2 C, C_{ispo-ph}), 145.03 - 145.56 (m, 2 C, C_{ispo-naphthyl}), 177.22 (s, 1 C, C=O), 177.42 (s, 1 C, C=O), 177.46 (s, 1 C, C=O), 177.68 (s, 1 C, C=O). $^{31}\text{P}\{^1\text{H}\}$ NMR (161.9 MHz, CD_2Cl_2): δ -14.10 - -14.52 (m). $^{31}\text{P}\{^1\text{H}\}$ NMR (202.3 MHz, CD_2Cl_2): δ -14.17 (d, $J = 14.65\text{ Hz}$, 1P), -13.83 (d, $J = 14.65\text{ Hz}$, 1P), -13.88 (s, 2 P), -14.12 (s, 2 P). ESI+ (M + H): 945.3013, Calc. 945.3011 for $\text{C}_{62}\text{H}_{47}\text{N}_2\text{O}_4\text{P}_2$ (-0.2 ppm, -0.2 mDa). Anal. Calcd for $\text{C}_{62}\text{H}_{46}\text{O}_4\text{N}_2\text{P}_2$: C, 78.80; H, 4.91; N, 2.96. Found: C, 78.73; H, 4.99; N, 2.90.

Isolation of a C₂ dissymmetric diastereomer (56) from the mixture of diastereomeric atropisomers of 55. A nitrogen purged high pressure flask was charged with **55** (0.514 g) and 15 mL of deoxygenated toluene. The flask was sealed with a teflon high vacuum valve and the orange solution was warmed 90°C. Almost immediately a white precipitate could be seen falling out of solution once the temperature reached 90°C. After continued heating for 12 h the sides of the flask was covered with the white precipitate and the flask was cooled to room temperature. The remaining solid was isolated by cannula filtration, washed with cold toluene (2 x 5 mL), hexanes (2 x 5 mL), and dried under high vacuum overnight to yield a white powder of **56** in 87% yield (0.445 g). NMR experiments were performed at low temperature to prevent interconversion of the diastereomeric atropisomers. ¹H NMR (400.1 MHz, -20°C, CD₂Cl₂): δ 1.65 (d, J = 8.8Hz, 2H, CH₂ bridge), 1.78 (d, J = 9.2Hz, 2H, CH₂ bridge), 3.51 (br d, J = 13.2Hz, 4H, CH bridgehead), 3.61–3.56 (m, 4H, CH norbornyl ring), 6.32 (dd, J = 5.6, 2.8Hz, 2H, CH olefin), 6.36 (dd, J = 5.6, 2.8Hz, 2H, CH olefin), 6.90 (d, J = 8.0Hz, 2H, naphthyl), 7.01-6.94 (m, 12H, ph + naphthyl), 7.22-7.11 (m, 12H, ph + naphthyl), 7.39 (d, J = 8.8Hz, 2H, naphthyl), 7.62 (d, J = 8.8Hz, 2H, naphthyl). ³¹P [¹H] NMR (161.9 MHz, -60°C, CD₂Cl₂): δ -16.0. ¹³C{³¹P} APT NMR (100 MHz, -60°C, CD₂Cl₂): C/CH₂; δ 177.82 (s, C=O), 177.70 (s, C=O), 144.94 (s, ipso C, C_{Naphthyl}-P), 136.24 (s, ipso C, C_{phenyl}-P), 136.16 (s, ipso C, C_{phenyl}-P), 135.74 (s, C_{fused}-C-C-P), 133.24 (s, C-C-P), 129.01 (s, N-C-C_{fused}), 128.49 (s, N-C-C_{fused}), 52.29 (s, CH₂). CH/CH₃; δ 134.55 (s, C olefin), 134.50 (s, C olefin), 133.35 (s, 2C, C_{ortho-ph}), 132.54 (s, 2C, C_{ortho-ph}), 131.85 (s, C_{naphthyl}), 128.74 (s,

$C_{\text{para-Ph}}$), 128.49 (s, $C_{\text{para-Ph}}$), 128.17 (s, 2C, $C_{\text{meta-ph}}$), 128.00 (s, 2C, $C_{\text{meta-ph}}$), 127.83 (s, C_{naphthyl}), 127.05 (s, C_{naphthyl}), 125.61 (s, C_{naphthyl}), 122.08 (s, C_{naphthyl}), 45.80 (s, 2C, $C_{\text{norbornyl}}$), 45.50 (s, 2C, $C_{\text{norbornyl}}$). MS (ES^+) m/z 945 ($M^+ + 1$). Anal. Calcd for $\text{C}_{62}\text{H}_{46}\text{O}_4\text{N}_2\text{P}_2$: C, 78.8; H, 4.91; N, 2.96. Found: C, 78.70; H, 5.21; N, 3.10.

Crystallographic analysis of (*R*)-6,6'-bis(3-chloropropionyl)-2,2'-bis(methoxy)-1,1'-binaphthyl (49). Suitable crystal for X-ray diffraction study were obtained by slow addition of hexanes to a saturated solution of **49** in dichloromethane. The crystal system was orthorhombic, and the space group $\text{C}222_1$ (No. 20), which was consistent with an enantiomerically pure compound. Crystal data, details of data collection, and structure solution and refinement are displayed in Table 3-2. Selected bond distances and angles are displayed in Table 3-3 and Table 3-4.

Crystallographic analysis of (*R*)-5,5'-Dinitro-BINAP Dioxide (52). Suitable crystals for X-ray diffraction study were obtained by slow addition of hexanes to a saturated solution of **52** in dichloromethane. The crystal system was orthorhombic, and the space group $\text{P}2_12_12_1$ (No. 19), which was consistent with an enantiomerically pure compound. Crystal data, details of data collection, and structure solution and refinement are displayed in Table 3-5. Selected bond distances and angles are displayed in Table 3-6 and Table 3-7.

Crystallographic analysis of (*R*)-5,5'-Diamino-BINAP (54). Suitable crystal for the X-ray diffraction studies were obtained by dissolving **54** in hot toluene and CH₂Cl₂. The CH₂Cl₂ was removed from the solution by evaporating on a steam bath under a stream of nitrogen gas. The solution was placed in the freezer and brown cube shaped crystals of **54** were obtained. The crystal system was orthorhombic, and the space group P2₁2₁2₁ (No. 19), which was consistent with an enantiomerically pure compound. Crystal data, details of data collection, and structure solution and refinement are displayed in Table 3-8. Selected bond distances and angles are displayed in Table 3-9 and Table 3-10.

Table 3-2. Crystallographic Experimental Details for 49.**A. Crystal Data**

formula	C ₂₈ H ₂₄ Cl ₂ O ₄
formula weight	495.37
crystal dimensions (mm)	0.28 × 0.22 × 0.08
crystal system	orthorhombic
space group	C222 ₁ (No. 20)
unit cell parameters ^a	
<i>a</i> (Å)	11.001 (5)
<i>b</i> (Å)	11.682 (5)
<i>c</i> (Å)	19.543 (8)
<i>V</i> (Å ³)	2511.5 (19)
<i>Z</i>	4
ρ_{calcd} (g cm ⁻³)	1.310
μ (mm ⁻¹)	0.290

B. Data Collection and Refinement Conditions

diffractometer	Bruker PLATFORM/SMART 1000 CCD ^b
radiation (λ [Å])	graphite-monochromated Mo K α (0.71073)
temperature (°C)	-80
scan type	ω scans (0.2°) (25 s exposures)
data collection 2θ limit (deg)	50.00
total data collected	6109 ($-11 \leq h \leq 13, -13 \leq k \leq 13, -23 \leq l \leq 23$)
independent reflections	2214 ($R_{\text{int}} = 0.1471$)
number of observed reflections (<i>NO</i>)	1081 [$F_o^2 \geq 2\sigma(F_o^2)$]
structure solution method	direct methods (<i>SIR97</i> ^c)
refinement method	full-matrix least-squares on F^2 (<i>SHELXL-93</i> ^d)
absorption correction method	empirical (<i>SADABS</i>)
range of transmission factors	0.9771–0.9231
data/restraints/parameters	2214 [$F_o^2 \geq -3\sigma(F_o^2)$] / 0 / 163
Flack absolute structure parameter ^e	0.0(3)
goodness-of-fit (S) ^f	0.898 [$F_o^2 \geq -3\sigma(F_o^2)$]
final <i>R</i> indices ^g	
<i>R</i> ₁ [$F_o^2 \geq 2\sigma(F_o^2)$]	0.0732
<i>wR</i> ₂ [$F_o^2 \geq -3\sigma(F_o^2)$]	0.1996
largest difference peak and hole	0.235 and -0.256 e Å ⁻³

Crystallographic Experimental Details (continued)

^aObtained from least-squares refinement of 1046 reflections with $5.09^\circ < 2\theta < 39.67^\circ$.

^bPrograms for diffractometer operation, data collection, data reduction and absorption correction were those supplied by Bruker.

^cAltomare, A.; Burla, M. C.; Camalli, M.; Cascarano, G. L.; Giacovazzo, C.; Guagliardi, A.; Moliterni, A. G. G.; Polidori, G.; Spagna, R. *J. Appl. Cryst.* **1999**, *32*, 115–119.

^dSheldrick, G. M. *SHELXL-93*. Program for crystal structure determination. University of Göttingen, Germany, 1993. Refinement on F_o^2 for all reflections (all of these having $F_o^2 \geq -3\sigma(F_o^2)$). Weighted R -factors wR_2 and all goodnesses of fit S are based on F_o^2 ; conventional R -factors R_1 are based on F_o , with F_o set to zero for negative F_o^2 . The observed criterion of $F_o^2 > 2\sigma(F_o^2)$ is used only for calculating R_1 , and is not relevant to the choice of reflections for refinement. R -factors based on F_o^2 are statistically about twice as large as those based on F_o , and R -factors based on ALL data will be even larger.

^eFlack, H. D. *Acta Crystallogr.* **1983**, *A39*, 876–881; Flack, H. D.; Bernardinelli, G. *Acta Crystallogr.* **1999**, *A55*, 908–915; Flack, H. D.; Bernardinelli, G. *J. Appl. Cryst.* **2000**, *33*, 1143–1148. The Flack parameter will refine to a value near zero if the structure is in the correct configuration and will refine to a value near one for the inverted configuration. In this case the relatively large standard uncertainty indicates that the structural data alone should not be used to confirm absolute stereochemistry, but should be used in conjunction with the established stereochemistry of the precursor compounds.

$$fS = [\sum w(F_o^2 - F_c^2)^2 / (n - p)]^{1/2} \quad (n = \text{number of data}; p = \text{number of parameters varied}; w = [\sigma^2(F_o^2) + (0.0876P)^2]^{-1} \text{ where } P = [\text{Max}(F_o^2, 0) + 2F_c^2] / 3).$$

$$gR_1 = \sum ||F_o| - |F_c|| / \sum |F_o|; wR_2 = [\sum w(F_o^2 - F_c^2)^2 / \sum w(F_o^4)]^{1/2}.$$

Table 3-3. Selected Interatomic Distances (Å) for 49.

Atom1	Atom2	Distance	Atom1	Atom2	Distance
CIA	C14	1.650(10)	C4	C5	1.373(8)
CIB	C14	1.647(8)	C5	C6	1.422(8)
O1	C2	1.367(6)	C5	C10	1.441(7)
O1	C11	1.417(8)	C6	C7	1.389(8)
O2	C12	1.222(8)	C7	C8	1.418(8)
C1	C1'	1.525(11) [†]	C7	C12	1.449(8)
C1	C2	1.363(8)	C8	C9	1.334(8)
C1	C10	1.407(7)	C9	C10	1.418(8)
C2	C3	1.408(8)	C12	C13	1.532(9)
C3	C4	1.369(8)	C13	C14	1.536(9)

Table 3-4. Selected Interatomic Angles (deg) for 49.

Atom1	Atom2	Atom3	Angle	Atom1	Atom2	Atom3	Angle
C2	O1	C11	120.5(5)	C6	C7	C12	124.2(5)
C1'	C1	C2	120.7(5) [†]	C8	C7	C12	118.3(6)
C1'	C1	C10	119.3(6) [†]	C7	C8	C9	122.8(6)
C2	C1	C10	120.0(5)	C8	C9	C10	121.6(5)
O1	C2	C1	115.7(5)	C1	C10	C5	118.9(5)
O1	C2	C3	123.0(5)	C1	C10	C9	123.4(5)
C1	C2	C3	121.2(5)	C5	C10	C9	117.6(5)
C2	C3	C4	118.9(5)	O2	C12	C7	121.4(6)
C3	C4	C5	122.5(5)	O2	C12	C13	119.9(6)
C4	C5	C6	122.7(5)	C7	C12	C13	118.8(6)
C4	C5	C10	118.4(5)	C12	C13	C14	112.0(6)
C6	C5	C10	118.9(5)	CIA	C14	C13	111.2(6)
C5	C6	C7	121.5(5)	CIB	C14	C13	116.9(6)
C6	C7	C8	117.6(5)				

[†]Primed atoms related to unprimed ones by the 2-fold rotational axis at $x, 0, 1/2$.

Table 3-5. Crystallographic Experimental Details for 52.**A. Crystal Data**

formula	C ₄₄ H ₃₀ N ₂ O ₆ P ₂
formula weight	744.64
crystal dimensions (mm)	0.44 × 0.25 × 0.22
crystal system	orthorhombic
space group	<i>P</i> 2 ₁ 2 ₁ 2 ₁ (No. 19)
unit cell parameters ^a	
<i>a</i> (Å)	10.5379 (8)
<i>b</i> (Å)	16.7409 (13)
<i>c</i> (Å)	20.9809 (17)
<i>V</i> (Å ³)	3701.3 (5)
<i>Z</i>	4
ρ_{calcd} (g cm ⁻³)	1.336
μ (mm ⁻¹)	0.171

B. Data Collection and Refinement Conditions

diffractometer	Bruker PLATFORM/SMART 1000 CCD ^b
radiation (λ [Å])	graphite-monochromated Mo K α (0.71073)
temperature (°C)	-80
scan type	ω scans (0.3°) (20 s exposures)
data collection 2θ limit (deg)	52.78
total data collected	28352 ($-13 \leq h \leq 13, -20 \leq k \leq 20, -26 \leq l \leq 26$)
independent reflections	7551 ($R_{\text{int}} = 0.0364$)
number of observed reflections (<i>NO</i>)	6769 [$F_0^2 \geq 2\sigma(F_0^2)$]
structure solution method	direct methods (<i>SHELXS-86</i> ^c)
refinement method	full-matrix least-squares on F^2 (<i>SHELXL-93</i> ^d)
absorption correction method	multi-scan (<i>SADABS</i>)
range of transmission factors	0.9634–0.9287
data/restraints/parameters	7551 [$F_0^2 \geq -3\sigma(F_0^2)$] / 0 / 495
Flack absolute structure parameter ^e	-0.10(7)
goodness-of-fit (S) ^f	1.046 [$F_0^2 \geq -3\sigma(F_0^2)$]
final <i>R</i> indices ^g	
<i>R</i> ₁ [$F_0^2 \geq 2\sigma(F_0^2)$]	0.0381
<i>wR</i> ₂ [$F_0^2 \geq -3\sigma(F_0^2)$]	0.0949
largest difference peak and hole	0.343 and -0.211 e Å ⁻³

Crystallographic Experimental Details (continued)

^aObtained from least-squares refinement of 6635 reflections with $4.32^\circ < 2\theta < 52.20^\circ$.

^bPrograms for diffractometer operation, data collection, data reduction and absorption correction were those supplied by Bruker.

^cSheldrick, G. M. *Acta Crystallogr.* **1990**, *A46*, 467–473.

^dSheldrick, G. M. *SHELXL-93*. Program for crystal structure determination. University of Göttingen, Germany, 1993. Refinement on F_o^2 for all reflections (all of these having $F_o^2 \geq -3\sigma(F_o^2)$). Weighted R -factors wR_2 and all goodnesses of fit S are based on F_o^2 ; conventional R -factors R_1 are based on F_o , with F_o set to zero for negative F_o^2 . The observed criterion of $F_o^2 > 2\sigma(F_o^2)$ is used only for calculating R_1 , and is not relevant to the choice of reflections for refinement. R -factors based on F_o^2 are statistically about twice as large as those based on F_o , and R -factors based on ALL data will be even larger.

^eFlack, H. D. *Acta Crystallogr.* **1983**, *A39*, 876–881; Flack, H. D.; Bernardinelli, G. *Acta Crystallogr.* **1999**, *A55*, 908–915; Flack, H. D.; Bernardinelli, G. *J. Appl. Cryst.* **2000**, *33*, 1143–1148. The Flack parameter will refine to a value near zero if the structure is in the correct configuration and will refine to a value near one for the inverted configuration.

$fS = [\sum w(F_o^2 - F_c^2)^2 / (n - p)]^{1/2}$ (n = number of data; p = number of parameters varied; $w = [\sigma^2(F_o^2) + (0.0501P)^2 + 0.7244P]^{-1}$ where $P = [\text{Max}(F_o^2, 0) + 2F_c^2] / 3$).

$gR_1 = \sum ||F_o| - |F_c|| / \sum |F_o|$; $wR_2 = [\sum w(F_o^2 - F_c^2)^2 / \sum w(F_o^4)]^{1/2}$.

Table 3-6. Selected Interatomic Distances (Å) for 52.

Atom1	Atom2	Distance	Atom1	Atom2	Distance
P1	O11	1.4783(16)	C16	C17	1.394(4)
P1	C11	1.826(2)	C17	C18	1.363(3)
P1	C31	1.812(2)	C18	C19	1.421(3)
O12A	N1	1.190(3)	C31	C32	1.396(4)
O13A	N1	1.242(3)	C31	C36	1.380(4)
N1	C15	1.473(3)	C32	C33	1.382(4)
C10	C11	1.375(3)	C33	C34	1.373(5)
C10	C19	1.442(3)	C34	C35	1.370(5)
C10	C20	1.495(3)	C35	C36	1.384(4)
C11	C12	1.414(3)	C41	C42	1.394(3)
C12	C13	1.366(3)	C41	C46	1.398(3)
C13	C14	1.400(3)	C42	C43	1.387(3)
C14	C15	1.429(3)	C43	C44	1.369(4)
C14	C19	1.424(3)	C44	C45	1.373(4)
C15	C16	1.348(4)	C45	C46	1.385(3)

Table 3-7. Selected Interatomic Angles (deg) for 52.

Atom1	Atom2	Atom3	Angle	Atom1	Atom2	Atom3	Angle
O11	P1	C11	113.79(9)	N1	C15	C14	119.8(2)
O11	P1	C31	112.15(11)	N1	C15	C16	116.4(2)
C11	P1	C31	103.75(10)	C14	C15	C16	123.8(2)
C31	P1	C41	107.97(10)	C15	C16	C17	119.6(2)
O12A	N1	O13A	122.3(3)	C16	C17	C18	120.3(2)
O12A	N1	C15	119.0(3)	C17	C18	C19	120.8(2)
O13A	N1	C15	118.3(2)	C10	C19	C14	119.03(18)
C11	C10	C19	119.75(18)	C10	C19	C18	120.88(19)
C11	C10	C20	123.38(17)	C14	C19	C18	120.08(18)
C19	C10	C20	116.83(17)	P1	C31	C32	123.45(19)
P1	C11	C10	122.74(15)	P1	C31	C36	117.3(2)
P1	C11	C12	117.78(15)	C32	C31	C36	119.2(2)
C10	C11	C12	119.49(18)	C31	C32	C33	119.6(3)
C11	C12	C13	121.94(19)	C32	C33	C34	120.5(3)
C12	C13	C14	120.2(2)	C33	C34	C35	120.2(3)
C13	C14	C15	125.3(2)	C34	C35	C36	120.0(3)
C13	C14	C19	119.42(18)	C31	C36	C35	120.5(3)
C15	C14	C19	115.3(2)				

Table 3-8. Crystallographic Experimental Details for 54.**A. Crystal Data**

formula	C ₅₁ H ₄₂ N ₂ P ₂
formula weight	744.81
crystal dimensions (mm)	0.58 × 0.39 × 0.28
crystal system	orthorhombic
space group	<i>P</i> 2 ₁ 2 ₁ 2 ₁ (No. 19)
unit cell parameters ^a	
<i>a</i> (Å)	10.5353 (8)
<i>b</i> (Å)	10.9527 (8)
<i>c</i> (Å)	34.510 (2)
<i>V</i> (Å ³)	3982.1 (5)
<i>Z</i>	4
ρ_{calcd} (g cm ⁻³)	1.242
μ (mm ⁻¹)	0.148

B. Data Collection and Refinement Conditions

diffractometer	Bruker PLATFORM/SMART 1000 CCD ^b
radiation (λ [Å])	graphite-monochromated Mo K α (0.71073)
temperature (°C)	-80
scan type	ω scans (0.4°) (10 s exposures)
data collection 2θ limit (deg)	52.82
total data collected	27555 (-13 ≤ <i>h</i> ≤ 13, -13 ≤ <i>k</i> ≤ 13, -43 ≤ <i>l</i> ≤ 43)
independent reflections	8145 (<i>R</i> _{int} = 0.0476)
number of observed reflections (<i>NO</i>)	6362 [<i>F</i> _o ² ≥ 2 σ (<i>F</i> _o ²)]
structure solution method	direct methods (<i>SHELXS-86</i> ^c)
refinement method	full-matrix least-squares on <i>F</i> ² (<i>SHELXL-93</i> ^d)
absorption correction method	multi-scan (<i>SADABS</i>)
range of transmission factors	0.9598–0.9191
data/restraints/parameters	8145 [<i>F</i> _o ² ≥ -3 σ (<i>F</i> _o ²)] / 0 / 497
Flack absolute structure parameter ^e	0.05(9)
goodness-of-fit (<i>S</i>) ^f	1.034 [<i>F</i> _o ² ≥ -3 σ (<i>F</i> _o ²)]
final <i>R</i> indices ^g	
<i>R</i> ₁ [<i>F</i> _o ² ≥ 2 σ (<i>F</i> _o ²)]	0.0508
<i>wR</i> ₂ [<i>F</i> _o ² ≥ -3 σ (<i>F</i> _o ²)]	0.1221
largest difference peak and hole	0.260 and -0.166 e Å ⁻³

Crystallographic Experimental Details (continued)

^aObtained from least-squares refinement of 7719 reflections with $4.40^\circ < 2\theta < 51.40^\circ$.

^bPrograms for diffractometer operation, data collection, data reduction and absorption correction were those supplied by Bruker.

^cSheldrick, G. M. *Acta Crystallogr.* **1990**, *A46*, 467–473.

^dSheldrick, G. M. *SHELXL-93*. Program for crystal structure determination. University of Göttingen, Germany, 1993.

^eFlack, H. D. *Acta Crystallogr.* **1983**, *A39*, 876–881; Flack, H. D.; Bernardinelli, G. *Acta Crystallogr.* **1999**, *A55*, 908–915; Flack, H. D.; Bernardinelli, G. *J. Appl. Cryst.* **2000**, *33*, 1143–1148. The Flack parameter will refine to a value near zero if the structure is in the correct configuration and will refine to a value near one for the inverted configuration.

$$fS = [\Sigma w(F_o^2 - F_c^2)^2 / (n - p)]^{1/2} \quad (n = \text{number of data}; p = \text{number of parameters varied}; w = [\sigma^2(F_o^2) + (0.0582P)^2 + 0.7551P]^{-1} \text{ where } P = [\text{Max}(F_o^2, 0) + 2F_c^2] / 3).$$

$$gR_1 = \Sigma ||F_o| - |F_c|| / \Sigma |F_o|; wR_2 = [\Sigma w(F_o^2 - F_c^2)^2 / \Sigma w(F_o^4)]^{1/2}.$$

Table 3-9. Selected Interatomic Distances (Å) for 54.

Atom1	Atom2	Distance	Atom1	Atom2	Distance
P1	C12	1.846(2)	C27	C28	1.393(5)
P1	C31	1.835(3)	C28	C29	1.357(5)
P1	C41	1.829(3)	C29	C30	1.410(4)
P2	C22	1.838(3)	C31	C32	1.390(4)
P2	C51	1.837(3)	C31	C36	1.383(4)
P2	C61	1.834(3)	C32	C33	1.413(6)
N1	C16	1.382(4)	C33	C34	1.379(7)
N2	C26	1.389(4)	C34	C35	1.359(7)
C11	C12	1.380(3)	C35	C36	1.370(5)
C11	C20	1.439(4)	C41	C42	1.386(4)
C11	C21	1.493(4)	C41	C46	1.390(3)
C12	C13	1.410(4)	C42	C43	1.374(4)
C13	C14	1.368(4)	C43	C44	1.385(4)
C14	C15	1.398(4)	C44	C45	1.357(4)
C15	C16	1.445(4)	C45	C46	1.384(4)
C15	C20	1.421(4)	C51	C52	1.384(4)
C16	C17	1.369(4)	C51	C56	1.387(4)
C17	C18	1.391(5)	C52	C53	1.389(5)
C18	C19	1.359(4)	C53	C54	1.371(6)
C19	C20	1.414(4)	C54	C55	1.353(6)
C21	C22	1.390(4)	C55	C56	1.387(4)
C21	C30	1.435(4)	C61	C62	1.391(4)
C22	C23	1.421(4)	C61	C66	1.378(4)
C23	C24	1.363(4)	C62	C63	1.395(4)
C24	C25	1.409(4)	C63	C64	1.366(5)
C25	C26	1.435(4)	C64	C65	1.367(6)
C25	C30	1.420(4)	C65	C66	1.388(5)
C26	C27	1.376(5)			

Table 3-10. Selected Interatomic Angles (deg) for 54.

Atom1	Atom2	Atom3	Angle	Atom1	Atom2	Atom3	Angle
C12	P1	C31	100.08(13)	C25	C26	C27	118.9(3)
C12	P1	C41	101.08(12)	C26	C27	C28	120.8(3)
C31	P1	C41	101.41(11)	C27	C28	C29	121.6(3)
C22	P2	C51	102.32(13)	C28	C29	C30	120.1(3)
C22	P2	C61	101.77(13)	C21	C30	C25	119.1(2)
C51	P2	C61	100.06(11)	C21	C30	C29	121.8(3)
C12	C11	C20	119.9(2)	C25	C30	C29	119.1(3)
C12	C11	C21	120.9(2)	P1	C31	C32	117.6(3)
C20	C11	C21	119.1(2)	P1	C31	C36	123.5(2)
P1	C12	C11	118.34(19)	C32	C31	C36	118.9(3)
P1	C12	C13	122.25(19)	C31	C32	C33	118.8(4)
C11	C12	C13	119.4(2)	C32	C33	C34	119.7(4)
C12	C13	C14	121.2(3)	C33	C34	C35	121.4(4)
C13	C14	C15	121.3(3)	C34	C35	C36	118.9(4)
C14	C15	C16	122.1(3)	C31	C36	C35	122.3(4)
C14	C15	C20	118.5(2)	P1	C41	C42	118.0(2)
C16	C15	C20	119.4(2)	P1	C41	C46	124.6(2)
N1	C16	C15	120.1(3)	C42	C41	C46	117.4(3)
N1	C16	C17	121.6(3)	C41	C42	C43	121.7(3)
C15	C16	C17	118.3(3)	C42	C43	C44	119.5(3)
C16	C17	C18	121.3(3)	C43	C44	C45	120.0(3)
C17	C18	C19	121.9(3)	C44	C45	C46	120.3(3)
C18	C19	C20	119.5(3)	C41	C46	C45	121.0(3)
C11	C20	C15	119.4(2)	P2	C51	C52	116.8(2)
C11	C20	C19	121.5(2)	P2	C51	C56	124.3(2)
C15	C20	C19	119.2(2)	C52	C51	C56	118.9(3)
C11	C21	C22	120.7(2)	C51	C52	C53	119.9(4)
C11	C21	C30	118.5(2)	C52	C53	C54	120.2(4)
C22	C21	C30	120.8(2)	C53	C54	C55	120.5(4)
P2	C22	C21	119.0(2)	C54	C55	C56	120.2(4)
P2	C22	C23	122.4(2)	C51	C56	C55	120.3(3)
C21	C22	C23	118.7(3)	P2	C61	C62	124.3(2)
C22	C23	C24	121.0(3)	P2	C61	C66	117.1(3)
C23	C24	C25	121.8(3)	C62	C61	C66	118.6(3)
C24	C25	C26	122.1(3)	C61	C62	C63	120.5(3)
C24	C25	C30	118.6(3)	C62	C63	C64	119.2(4)
C26	C25	C30	119.3(3)	C63	C64	C65	121.3(3)
N2	C26	C25	120.3(3)	C64	C65	C66	119.3(4)
N2	C26	C27	120.7(3)	C61	C66	C65	121.0(4)

References

- (1) Ralph, C. K.; Akotsi, O. M.; Bergens, S. H. *Organometallics* **2004**, *23*, 1484-1486.
- (2) Akutagawa, S. *Appl. Catal A:General* **1995**, *128*, 171-207.
- (3) (a) Noyori, R. *Angew. Chem. Int. Ed.* **2002**, *41*, 2008-2022. (b) Noyori, R. *Acta Chem. Scand.* **1996**, *50*, 380-390.
- (4) Berthod, M.; Mignani, G.; Woodward, G.; Lemaire, M. *Chem. Rev.* **2005**, *105*, 1801-1836.
- (5) Mashima, K. M., Y. I.; Kusano, K. H.; Kumobayashi, H.; Sayo, N.; Hori, Y.; Ishizaki, T.; Akutagawa, S.; Takaya, H. *Chem. Commun.* **1991**, 609.
- (6) (a) Doucet, H.; Ohkuma, T.; Murata, K.; Yokozawa, T.; Kozawa, M.; Katayama, E.; England, A. F.; Ikariya, T.; Noyori, R. *Angew. Chem. Int. Ed.* **1998**, *37*, 1703-1707. (b) Noyori, R.; Koizumi, M.; Ishii, D.; Ohkuma, T. *Pure Appl. Chem.* **2001**, *73*, 227-232. (c) Ohkuma, T.; Koizumi, M.; Doucet, H.; Pham, T.; Kozawa, M.; Murata, K.; Katayama, E.; Yokozawa, T.; Ikariya, T.; Noyori, R. *J. Am. Chem. Soc.* **1998**, *120*, 13529-13530.
- (7) Mashima, K.; Kusano, K. H.; Sato, N.; Matsumura, Y.; Nozaki, K.; Kumobayashi, H.; Sayo, N.; Hori, Y.; Ishizaki, T.; Akutagawa, S.; Takaya, H. *J. Org. Chem.* **1994**, *59*, 3064-3076.
- (8) Zhang, X., Patent WO 02/4091 (**2002**).
- (9) Okano, T.; Kumobayashi, H.; Akutagawa, S.; Kiji, J.; Konishi, H.; Fukuyama, K.; Shimano, Y., US Patent 4 705 895 (**1987**).

- (10) Berthod, M.; Saluzzo, C.; Mignami, G.; Lemaire, M. *Tetrahedron: Asymmetry* **2004**, *15*, 639.
- (11) (a) Fan, Q. H.; Deng, G. J.; Chen, X. M.; Xie, W. C.; Jiang, D. Z.; Liu, D. S.; Chan, A. S. C. *J. Mol. Catal. A* **2000**, *159*, 37-43. (b) Fan, Q. H.; Ren, C. Y.; Yeung, C. H.; Hu, W. H.; Chan, A. S. C. *J. Am. Chem. Soc.* **1999**, *121*, 7407-7408.
- (12) Fan, Q. H.; Chen, Y. M.; Chen, X. M.; Jiang, D. Z.; Xi, F.; Chan, A. S. C. *Chem. Commun.* **2000**, 789-790.
- (13) Chen, Y.; Yekta, S.; Yudin, A. K. *Chem. Rev.* **2003**, *103*, 3155-3211.
- (14) Bayston, D. J.; Fraser, J. L.; Ashton, M. R.; Baxter, A. D.; Polywka, M. E. C.; Moses, E. *J. Org. Chem.* **1998**, *63*, 3137-3140.
- (15) Cai, D. W.; Payack, J. F.; Bender, D. R.; Hughes, D. L.; Verhoeven, T. R.; Reider, P. J. *J. Org. Chem.* **1994**, *59*, 7180-7181.
- (16) (a) Kyba, E. P.; Gokel, G. W.; Jong, F. d.; Koga, K.; Sousa, L.; Seigel, M. G.; Kaplan, L.; Sogah, G. D. Y.; Cram, D. J. *J. Org. Chem.* **1977**, *42*, 4173-4184. (b) Yudin, A. K.; Martyn, L. P.; Pandiaraju, S.; Zheng, J.; Lough, A. *Organic Letters* **2000**, *2*, 41-44.
- (17) Bringmann, G.; Mortimer, A. J. P.; Keller, P. A.; Gresser, M. J.; Garner, J.; Breuning, M. *Angew. Chem. Int. Ed.* **2005**, *44*, 5384-5427.
- (18) (a) Adams, R.; Sundholm, N. K. *J. Am. Chem. Soc.* **1948**, *70*, 2667-2673. (b) Kishikawa, K.; Yoshizaki, K.; Kohmoto, S.; Yamamoto, M.; Yamaguchi, K.; Yamada, K. *J. Chem. Soc., Perkin Trans. 1* **1997**, 1233-1239. (c) Oki, M. *Topics in Stereochemistry*: (Eds.: Allinger, N. L., Eliel, E., Wilen, S.

- H.), 1986. (d) Stewart, W. E.; Siddall, T. H. *Chem. Rev.* **1970**, *70*, 517-&.
- (e) Yamada, S. *Reviews on Heteroatom Chemistry* **1999**, *19*, 203-236.
- (19) Verma, S. M.; Singh, N. B. *Aust. J. Chem.* **1976**, *29*, 295-300.
- (20) Clayden, J. *Angew. Chem. Int. Ed. Engl.* **1997**, *36*, 949-951.
- (21) (a) Ates, A.; Curran, D. P. *J. Am. Chem. Soc.* **2001**, *123*, 5130-5131. ()
Clayden, J. *Chem. Commun.* **2004**, 127-135. (b) Clayden, J.; Vassiliou, N. *Organic & Biomolecular Chemistry* **2006**, *4*, 2667-2678. (c) Kitagawa, O.; Momose, S.; Fushimi, Y.; Taguchi, T. *Tetrahedron Lett.* **1999**, *40*, 8827-8831.
- (22) Curran, D. P.; Qi, H. Y.; Geib, S. J.; Demello, N. C. *J. Am. Chem. Soc.* **1994**, *116*, 3131-3132.
- (23) (a) Shimizu, K. D.; Dewey, T. M.; Rebek, J. *J. Am. Chem. Soc.* **1994**, *116*, 5145-5149. (b) Rebek, J. *Angew. Chem. Int. Ed. Engl.* **1990**, *29*, 245-255.
- (24) (a) Clayden, J.; Lund, A.; Vallverdu, L. S.; Helliwell, M. *Nature* **2004**, *431*, 966-971. (b) Ohno, A.; Kunitomo, J.; Kawai, Y.; Kawamoto, T.; Tomishima, M.; Yoneda, F. *J. Org. Chem.* **1996**, *61*, 9344-9355.
- (25) (a) Vlad-Bubulac, T.; Hamciuc, C.; Petreus, O.; Bruma, M. *Polymers for Advanced Technologies* **2006**, *17*, 647-652. (b) Yu, D.; Gharavi, A.; Yu, L. P. *J. Am. Chem. Soc.* **1995**, *117*, 11680-11686. (c) Hoyt, A. E.; Ricco, A. J.; Yang, H. C.; Crooks, R. M. *J. Am. Chem. Soc.* **1995**, *117*, 8672-8673.
- (26) Curran, D. P.; Geib, S.; DeMello, N. *Tetrahedron* **1999**, *55*, 5681-5704.
- (27) Bain, A. D. *Prog. Nucl. Magn. Reson. Spectrosc.* **2003**, *43*, 63-103.

Chapter 4

A Highly Reusable Catalyst for Enantioselective Ketone Hydrogenation. Catalyst-Organic Frameworks by Alternating ROMP Assembly*

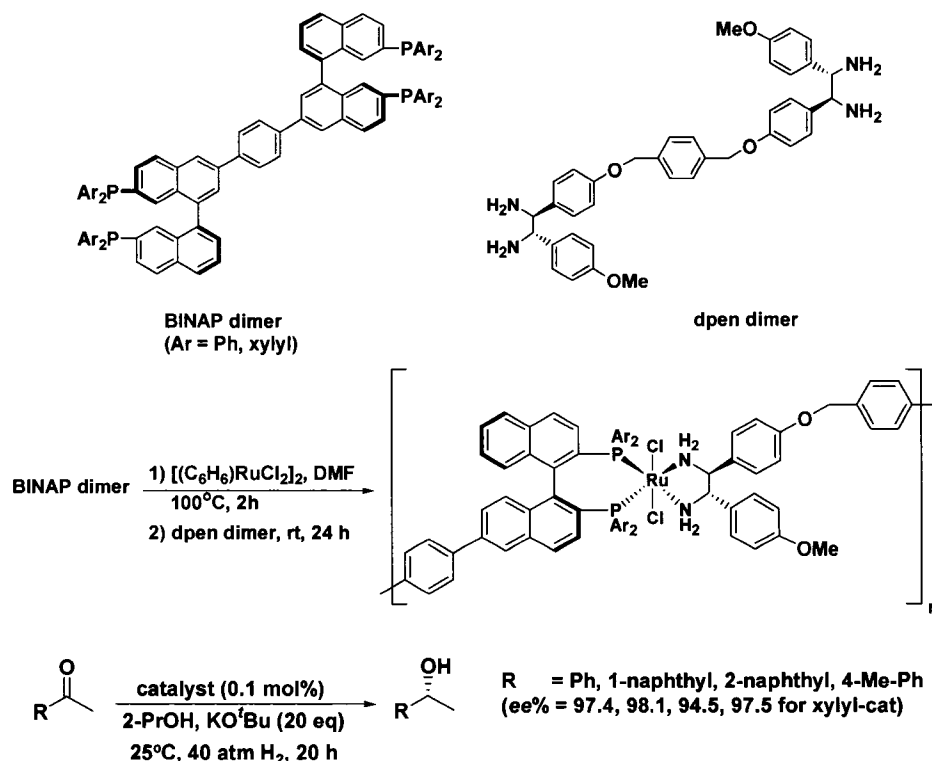
Introduction

As outlined in the previous Chapters, the immobilization of highly enantioselective catalysts provides a convenient approach to recovery and recycling of expensive chiral catalysts, as well as the minimization of product contamination caused by metal leaching. Among the numerous techniques developed, a new strategy for homogeneous catalyst immobilization, that is, a “self-assembly” approach, has attracted a great deal of interest in the last five years.^{1,2} In this approach, insoluble metal-organic frameworks (MOFs) are prepared by an in situ self-assembly of chiral multitopic ligands and metal ions, both acting as linkers and nodes, respectively. The main benefits of this approach is that the resulting MOFs are usually highly ordered, porous structures with a high density of catalytically active sites. In some cases, MOF's have shown excellent activity and selectivity for asymmetric hydrogenations. As an example, Ding and co-workers recently immobilized Noyori's catalyst by reacting bridged BINAP ligands with $[\text{Ru}(\text{C}_6\text{H}_6)\text{Cl}_2]_2$ in DMF at 100°C, followed by

*A version of this Chapter has been published. Corbin K. Ralph and Steven H. Bergens. “A Highly Reusable Catalyst for Enantioselective Ketone Hydrogenation. Catalyst-Organic Frameworks by Alternating ROMP Assembly” *Organometallics* 2007, 26, 1571-1574.

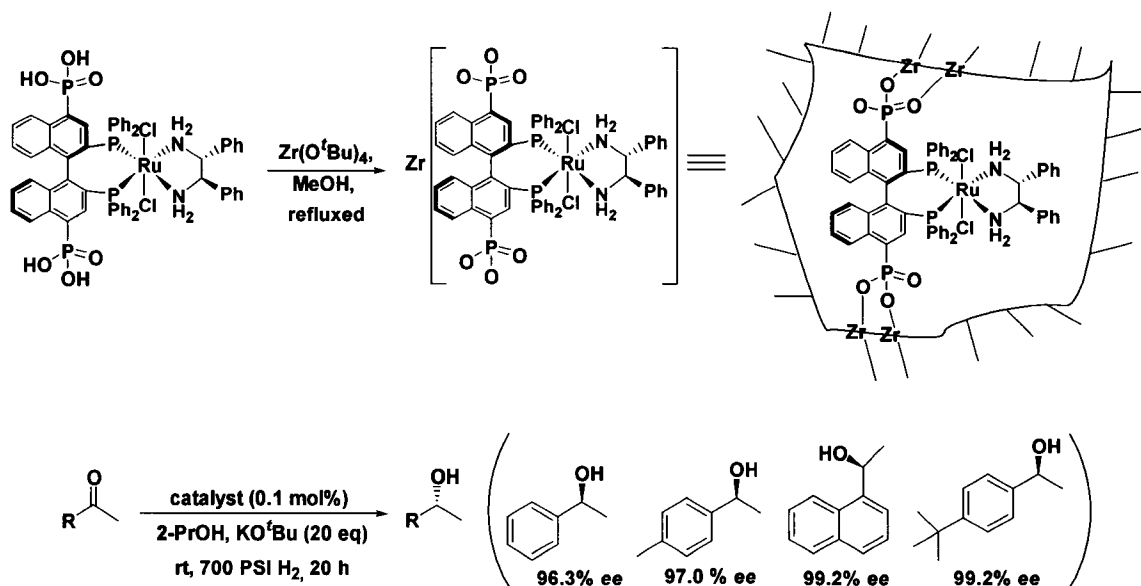
treatment with a bridged dpn ligand at room temperature (Scheme 4-1).³ The self-supported catalysts were used for the asymmetric hydrogenation of a series of aromatic ketones to yield the corresponding secondary alcohols with excellent enantioselectivities (94.5 – 98.1% ee) and TOF's ~ 500 h⁻¹. More importantly, the immobilized catalyst could be recovered by filtration and was reused six times for the asymmetric hydrogenation of acetophenone without significant loss of enantioselectivity or activity and without detectable metal leaching.

Scheme 4-1. Self-supported Noyori's catalyst for asymmetric hydrogenation.



Lin et al. also immobilized Noyori's catalyst by self-assembly of a phosphonic acid-substituted Ru-BINAP-dpen derivative with zirconium *tert*-butoxide, to afford highly porous Zr phosphonate solids (Scheme 4-2).⁴ The

Scheme 4-2. Metal-organic catalyst for asymmetric hydrogenation of ketones.



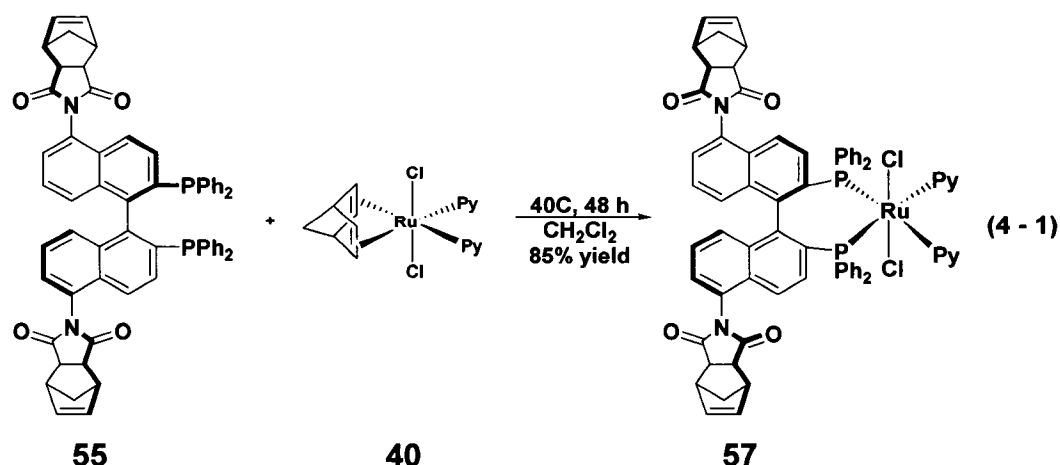
immobilized catalyst was also used for the asymmetric hydrogenation of aromatic ketones with TOF $\sim 700\text{ h}^{-1}$ and high enantioselectivities (96.3 - 99.2% ee). In this case, the immobilized catalyst was recovered by centrifugation/filtration and recycled six times without loss in activity and enantioselectivity. The MOF prepared by Lin et al. differs from those prepared by Ding's group. In the former case, the active metal centers are located on the backbone of the polymer, whereas in Lin's case the active metal was present as pendant groups on the Zr-linked backbone. These examples are among the most recent advances in heterogenized BINAP-based hydrogenation catalysts and demonstrate the concept that robust, sterically regular systems with a high density of catalytically active sites are key design features to achieve highly efficient and reusable immobilized catalysts. The level of reusability achieved with these MOFs, however, is still quite low. Hence, it remains a significant challenge in this field to

develop practical heterogenized catalysts that sustain a large number of reuses with constant activity and enantioselectivity, and without detectable metal leaching. The work highlighted in this Chapter focuses on the synthesis of catalyst-organic frameworks by the newly developed alternating ROMP methodology, with *trans*-RuCl₂((R)-5,5'-dinorimido-BINAP)(Py)₂ (**57**) as the MCM, and the subsequent use of the immobilized catalysts for asymmetric hydrogenations of aromatic ketones.

Results and Discussion

Section A: Preparation of metal containing monomers for ROMP.

Synthesis of *trans*-RuCl₂((*R*)-5,5'-dinorimido-BINAP)(Py)₂ (57**).** The purpose of incorporating norbornyl functionalities at the 5,5'-positions to give (*R*)-5,5'-dinorimido-BINAP (**55**), was to adapt our alternating ROMP methodology to a more versatile ligand system than Norphos, and to a system that is not intrinsically active towards ROMP thereby expanding the scope of this methodology. With the newly functionalized BINAP ligand **55** on hand, the next step was to prepare active hydrogenation catalysts that can then be polymerized to give the corresponding polymeric catalysts. The catalyst monomer *trans*-RuCl₂((*R*)-5,5'-dinorimido-BINAP)(Py)₂ (**57**) was prepared by replacing the norbornadiene (NBD) ligand in the compound *trans*-RuCl₂(NBD)Py₂ (**40**, NBD is norbornadiene, Py is pyridine) with **55** (equation 4 - 1).⁵ The reaction was carried out at 40°C in CH₂Cl₂ over 48 h and **57** was obtained in 85% yield.



It was surprising that the metallation of **55** required such a long reaction time given that (*R*)-BINAP reacts with **40** over 12 h at room temperature in CH₂Cl₂ to generate *trans*-RuCl₂((*R*)-BINAP)Py₂ in high yield.⁵ The norimido substituents therefore must have an influence on the coordinating ability of **55** even though they are not in close proximity to the phosphorus atoms. As discussed in Chapter 3, the norimido groups likely donate electrons into the binaphthyl π-system causing the arene-nitrogen bonds to adopt multiple bond character, thereby limiting rotation of the norimido groups to give rise to three NMR distinguishable diastereomeric atropisomers. Although this matter was not investigated further, it is likely that the π-conjugation between the norimido groups and the binaphthyl framework induces a preference for a conformation of the free ligand that hinders coordination to the metal center. For example, π-conjugation from the norimido groups may decrease the C₁-C_{1'} bond length and favor a dihedral angle between the naphthyl rings closer to zero, thereby restricting the bite angle of the coordinating phosphorus atoms. In a comparative study between several diphosphine ligands Genet et al. showed that the dihedral angle is geometrically related to the bite angle and a smaller dihedral angle corresponds to a smaller bite angle.⁶ In any event the decreased coordinating ability of **55** was overcome, and **57** was obtained in high yield as an orange crystalline solid. Like **55**, **57** exist as a mixture of three diastereomeric atropisomers. Crystals of **57** suitable for structure determination by X-ray diffraction could not be obtained, but **57** was characterized by solution NMR spectroscopy and elemental analysis.

One of the goals of this work was to functionalize BINAP in a manner that would not disrupt the integrity of the catalyst center. This was a primary concern since it was imperative to maintain the high level of reactivity and selectivity associated with BINAP. As well, maintaining the integrity of the catalyst center should allow for direct correlation of the literature results obtained using BINAP-based catalysts with those obtained using the new ligand **55**. The ^{31}P NMR signals (in CD_2Cl_2) for BINAP and the free ligand **55** are both ~ -14 ppm. The signals for the corresponding metal complexes, *trans*- $\text{RuCl}_2((R)\text{-BINAP})\text{Py}_2$ and **57** are both ~ 42 ppm. These similarities in chemical shifts suggest that the electronic environment around the phosphorus atoms in **55** and **57** are similar to the parent BINAP compounds. Therefore, it is believed that the catalytic properties of **57** should be similar to the corresponding catalyst prepared with BINAP. Although it appears that the electronic environment of the metal center of **57** was not significantly influenced by the norimido substituents, it may not hold that the metal center has no effect on the rate of interconversion of the diastereomeric atropisomers of **57**. The focus of the next section is to examine the influence that the metal center may have on the interconversion process.

Influence of the metal center on the interconversion process. As shown in Figure 4-1 the ^{31}P NMR signals for **57** are similar to the pattern observed for compound **55**, which, as described in Chapter 3, exists as a mixture of three diastereomeric atropisomers. That is, the ^{31}P NMR of **55** consist of two singlets representing the C_2 -dissymmetric atropisomers, (*R,R,R* and *S,R,S*), and

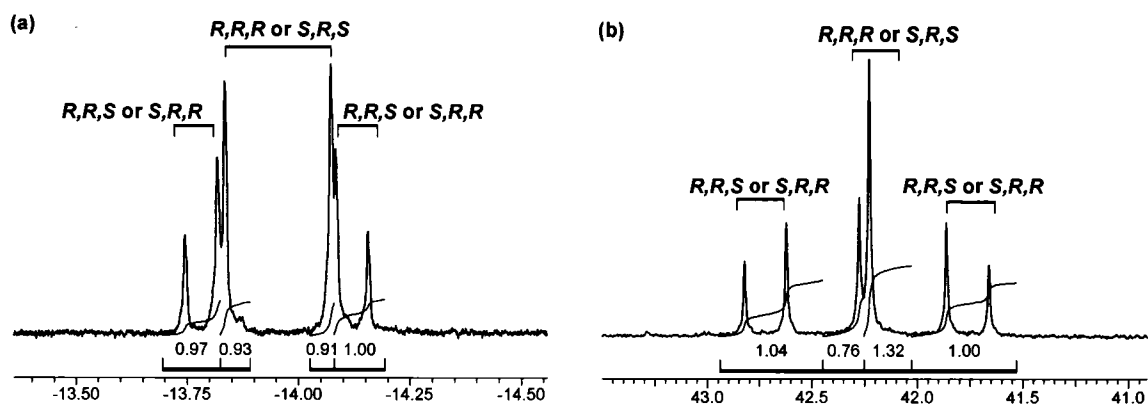


Figure 4-1. ^{31}P NMR spectra (at room temperature in CD_2Cl_2) of (a) **55** recorded at 202 MHz and (b) **57** recorded at 161.8 MHz.

two doublets representing the non-dissymmetric atropisomers, (R,R,S or S,R,R). These are NMR equivalent, and therefore only one set of doublets are observed. The origin of the diastereomeric atropisomers is determined by the relative orientation of the norimido groups, and exchange between the three diastereomeric atropisomers as a result of rotation of the norimido groups about the arene-nitrogen bond is defined as the interconversion process.

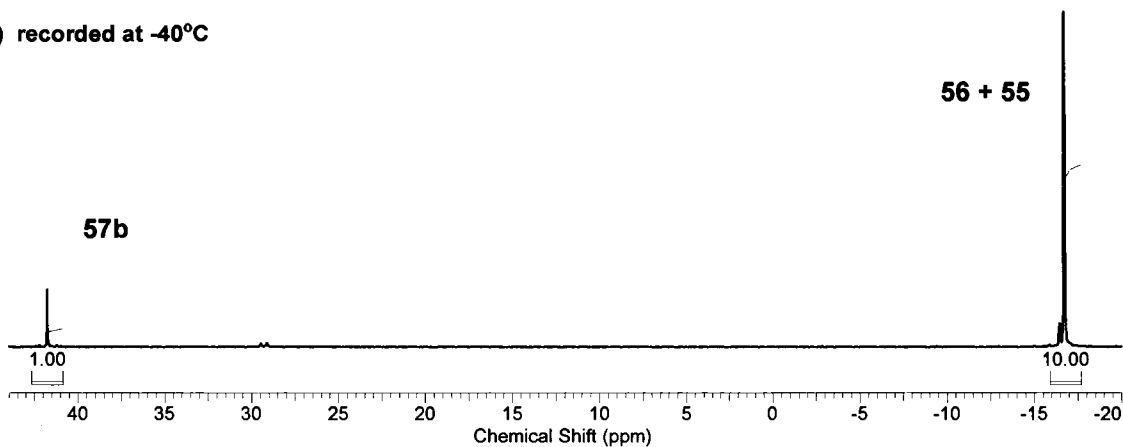
As explained in Chapter 3, it was necessary to record the ^{31}P NMR of **55** at a higher field so that the signals for all three of the diastereomeric atropisomers are separated. This was not the case for the metal complex **57**, and all three diastereomeric atropisomers are present in the spectra taken at a lower field. Interestingly, the relative ratios of the diastereomeric atropisomers of **57** are similar to that of **55**. Specifically, from the integration there is no change in the ratio of the C_2 -dissymmetric atropisomers to non-dissymmetric atropisomers between compounds **55** and **57**. The ratio of the C_2 -dissymmetric

atropisomers is 1.0:1.0 for ligand **55**, whereas in the metal complex **57** it is 0.76:1.3. The cause for this slight difference in population of the C₂-dissymmetric atropisomers is unknown.

To examine the possible influence that ruthenium has on the interconversion between the diastereomeric atropisomers, attempts were made to prepare a single atropisomer of **57** by reacting **56**, the C₂-dissymmetric atropisomer of the ligand precipitated from toluene at 90°C (as described in Chapter 3), with the ruthenium precursor **40**. The reaction was carried out at -20°C in an attempt to minimize the interconversion process of the free ligand **55**. The sharp singlet at 41.8 ppm in the ³¹P NMR spectra displayed in Figure 4-2a represents **57b**, a C₂-dissymmetric atropisomer of **57**. From the integration 10% of the metal complex **57b** had formed after 24 h. Unfortunately, the metallation reaction was too slow at -20°C, resulting in only 15% of **57b** after seven days (Figure 4-2b). More significantly, minor peaks are seen near the peaks for **56** and **57b**, evidence that the interconversion process has occurred even at -20°C. As a result, a single diastereomeric form of **57** could not be prepared by this method and it was beyond the scope of this work to develop a method for that purpose.

Despite the inability to prepare a single diastereomeric form of **57**, several key observations from this low temperature metallation experiment do show that the Ru metal center does have an influence on the interconversion process. For example, the minor peaks for **57** are not observed after the first 24 h at -20°C (Figure 4-2a), but only in the spectra taken after seven days (Figure 4-2b).

(a) recorded at -40°C



(b) recorded at -40°C

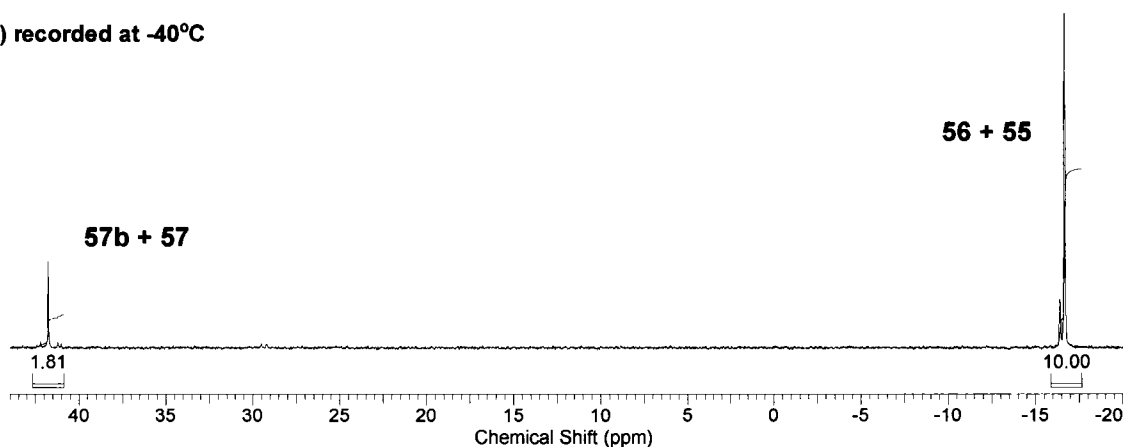


Figure 4-2. ^{31}P NMR (at 161.8 MHz in CD_2Cl_2) of the metallation of **56** (a) after 24 h (b) after 7 days.

Whereas the minor peaks for **55** are clearly present after the first 24 h at -20°C . This suggests that the interconversion process occurs faster for the free ligand **55** than for the ruthenium complex **57**. Furthermore, it is unclear whether the interconversion process has occurred for the metal complex since it is possible that the minor peaks observed in Figure 4-2b for **57** may have resulted from the reaction of the small amount of **55**, with **40**, and not from the interconversion of **57b**. As well, it is unknown if the reaction between **55** and **40** is faster than the

reaction between **56** and **40**. Finally, in a separate experiment whereby **57** was warmed to 40°C there was no line broadening in the ^{31}P NMR, which would be expected upon interconversions of the diastereomers. Based on the above observations, it is believed that the ruthenium metal center does have a small effect on the rotational behavior of the norimido groups, resulting in a slower exchange between the diastereomeric atropisomers.

A much more drastic change in the interconversion process was observed when **55** was coordinated to rhodium. With rhodium as the metal center the interconversion process occurred at a much faster rate at room temperature. $[\text{Rh}(\text{NBD})((R)\text{-}5,5'\text{-dinorimido-BINAP})]\text{BF}_4$ (**59**) was easily prepared by reacting **55** with $[\text{Rh}(\text{NBD})_2]\text{BF}_4$ (**58**) over 12 h at room temperature in CH_2Cl_2 . The ^{31}P NMR spectra of **59** recorded at room temperature and at -40°C are displayed in Figure 4-3. Due to coupling from the rhodium center, which has a nuclear spin = $\frac{1}{2}$, the resulting signals for **59** are doubled.

The ^{31}P NMR of **59** at room temperature (Figure 4-3a) is a doublet, rather than the multiple signals that are observed for **57** in Figure 4-1b. The doublet at room temperature corresponds to **59** being C_2 -dissymmetric, and this implies that exchange between the diastereomeric atropisomers is occurring faster than the relaxation time so that on the NMR time scale all three of the diastereomeric atropisomers become equivalent. Upon cooling **59** to -40°C (Figure 4-3b) the rate of exchange between the diastereomeric atropisomers is decreased, and as a result all three diastereomeric atropisomers become visible. The peak pattern for **59** at -40°C (Figure 4-3b) closely resembles the pattern for **57** taken at room

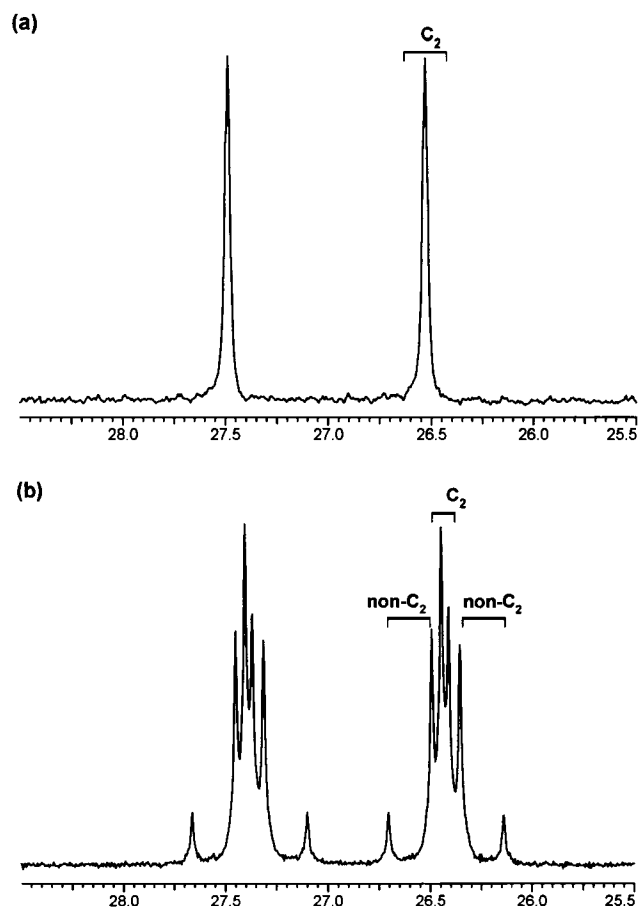


Figure 4-3. ^{31}P NMR (at 161.8 MHz in CD_2Cl_2) of **59** (a) at RT and (b) at -40°C .

temperature (for comparison see Figure 4-1b). As was observed with the free ligand **55** (see Chapter 3), this process was completely reversible and upon warming to room temperature the rate of interconversion increases, and the multiple signals in Figure 4-3b convert back to the doublet pattern observed in Figure 4-3a. The interconversion process is temperature dependent and the difference in behavior between **57** and **59** shows that **59** has a lower energy barrier to rotation of the norimido groups than **57**. Compound **57** more closely resembles the free ligand, having a higher energy barrier and requiring high

temperatures before rapid exchange of the diastereomeric atropisomers is observed.

From the above studies it is evident that the ability of the norimido groups to rotate about the arene-nitrogen bond, which results in the diastereomeric atropisomers, can be dictated by changing the electron density of the metal center. This phenomenon can be explained by considering the electronic changes that occur upon coordination to a metal center and the influence that the metal center may have on the π -conjugation between the norimido groups and the binaphthyl framework. Coordination of a phosphine ligand to a transition metal involves σ -donation from the ligand to the metal and π -backbonding from the metal to the ligand.⁶ The rate of rotation about the arene-nitrogen bonds will depend, in part, on the amount of π -donation from the norimido groups to the naphthylene units. As a result of π -conjugation in the binaphthyl framework, it is believed that the amount of π -donation from the metal to the ligand is influenced by the amount of π -donation from the norimido groups to the binaphthyl framework, and vice versa. Our results show that the d^6 moiety $\text{Ru(II)(Cl)}_2(\text{Py})_2$ of **57**, is a poorer π -donor than the d^8 moiety $[\text{Rh(I)(NBD)}]^+$ of **59**.⁷ The binaphthyl aromatic π -conjugated system in **57** thereby has less electron density than **59**, and as a result the arene-nitrogen bond in **57** has more double bond character than **59**. As such, the increase in double bond character along the arene-nitrogen bond restricts the rotation of the norimido groups, and thereby a decrease in the rate of interconversion between the diastereomeric atropisomers of **57** is observed. Conversely, the interconversion process is faster with rhodium

as the metal center because the norimido groups are able to rotate more freely about the arene-nitrogen bond.

It is unknown what effect the mixture of diastereomeric atropisomers may have on the polymerization of these types of monomers, and on the structure of the resulting polymeric catalyst. As well, it is possible that the rotational behavior of the norimido groups may have an effect on the catalytic properties of the resultant polymeric catalysts. Therefore the ability to dictate the rotational behavior by changing the electron density of the metal center and the temperature may allow for better control of both the polymerization process and the polymer structure, and this should be studied in more detail.

Synthesis of the *trans*-RuCl₂((*R*)-5,5'-dinorimido-BINAP)((*R,R*)-dpen) (60). An added feature of the RuCl₂(diphosphine)Py₂ catalysts is that the pyridine ligands are readily displaced by chiral diamine ligands to generate the well-known RuCl₂(diphosphine)(diamine) catalysts for hydrogenation of ketones developed by Noyori and co-workers.⁸ Reaction of **57** with (*R,R*)-dpen over 2 h at room temperature in CH₂Cl₂ generated *trans*-RuCl₂((*R*)-5,5'-dinorimido-BINAP)((*R,R*)-dpen) (**60**). It is interesting that the ³¹P NMR of **60** is very similar to that of **57** suggesting that the dpen ligand does not change the rotational behavior of the norimido ligands (Figure 4-4). Although catalyst **60** is easily obtained from **57**, our earlier work has shown that such dpen complexes do not easily undergo ROMP. Therefore ROMP was studied using **57** as the monomer to prepare the polymeric catalyst.

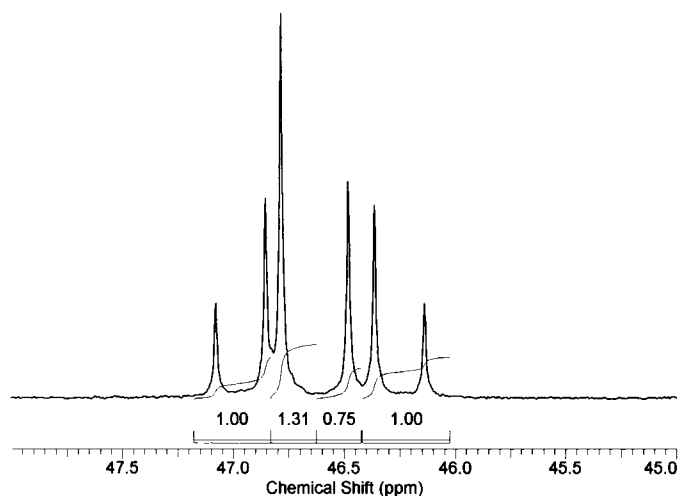


Figure 4-4. ^{31}P NMR spectra (at 161.8 MHz in CD_2Cl_2) of **60**.

Section B: Immobilization of the homogeneous catalyst 57 by the alternating ROMP methodology.

Control of polymer growth by judicial choice between Grubbs metathesis catalysts. The initial studies on the alternating ROMP methodology to prepare a reusable polymeric catalyst, involved the alternating polymerization of *trans*- $\text{RuCl}_2((R,R)\text{-Norphos})(\text{Py})_2$ (**41**) and COE, with either *trans*- $\text{RuCl}_2(=\text{CHPh})(\text{PCy}_3)_2$ (**37**; Cy = cyclohexyl) or $\text{RuCl}_2(=\text{CHPh})(\text{PCy}_3)(\text{NHC})$ (**38**; NHC = 1,3-bis(2,4,6-trimethylphenyl)-4,5-dihydroimidazol-2-ylidene), as the olefin metathesis catalysts developed by Grubbs et al.⁹ Although this original work was groundbreaking in developing a new method for preparing polymeric catalysts, improvements were needed in order to optimize the alternating polymerization process to make it more efficient. For example, the highly reusable Norphos-based polymeric catalyst, $\text{RuCl}_2((R,R)\text{-Norphos})((R,R)\text{-dpen})_x[\text{COE}]_y$ (**46**), was

prepared using **38** as the metathesis catalyst, and only 61% of the catalyst monomer *trans*-RuCl₂((*R,R*)-Norphos)(Py)₂ (**41**) was consumed during the polymerization. As well, the preparation of the reusable catalyst **46** involved an additional step whereby dicyclopentadiene was added to the reaction mixture as a crosslinking agent. It was found that crosslinking the Norphos-polymer with dicyclopentadiene decreased the solubility of the polymeric matrix, making it robust enough to withstand repeated use.

From unpublished results carried out in this laboratory it was shown that better control over the alternating ROMP was achieved using the less active 1st generation Grubbs catalyst **37**, than using the more active 2nd generation Grubbs catalyst **38**. This better control is illustrated by separate experiments involving the alternating polymerization of **41**:COE:**37** or **38** in 20:80:1 ratio. During the reaction with catalyst **37**, it was observed by ³¹P NMR spectroscopy that a peak representing free PCy₃ was present in equal intensity as **37**, whereas for the experiment involving catalyst **38** only a trace amount of free PCy₃ was present. Since initiation of Grubbs catalysts involves dissociation of PCy₃,¹⁰ the difference in intensity of the signals for PCy₃ in the ³¹P NMR of the reaction mixtures suggests that the initiation is faster for catalyst **37** than for **38**. Hence, the rate of propagation is slower than the rate of initiation for catalyst **37** and the reverse is true for catalyst **38**, and only traces of **38** are active during the alternating ROMP. It is known that faster initiation catalysts result in narrower molecular weight distributions of ROMP products, and it is therefore expected that for our polymerization process catalyst **37** should produce an alternating polymer with a

narrower molecular weight distribution.¹¹ In addition, the in situ NMR studies shown in Chapter 2 showed that a high degree of alternation was achieved when catalyst **37** was employed.

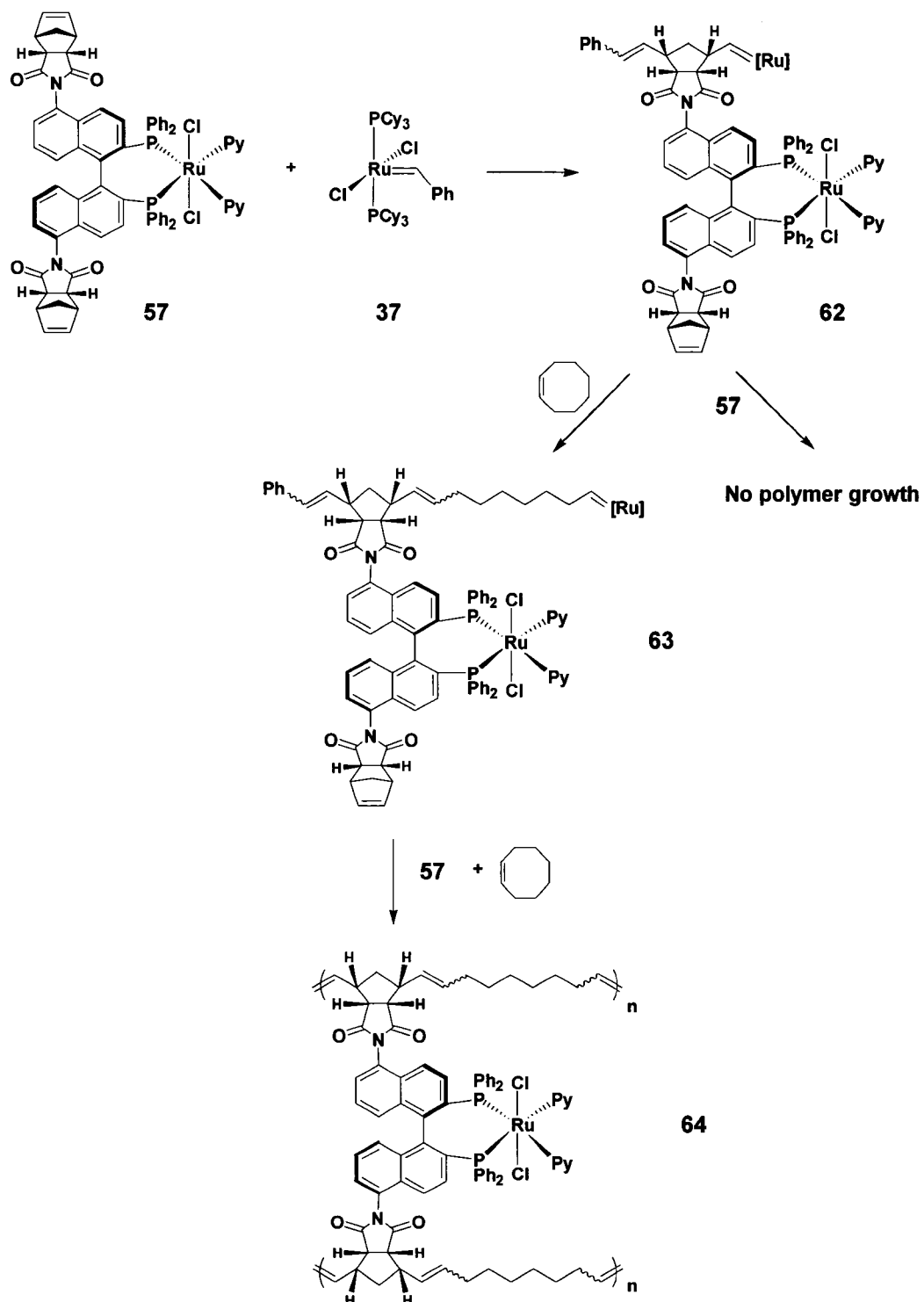
Further, it was also observed that the alternating polymerization went to completion when catalyst **37** was employed, whereas when catalyst **38** was used, there was a considerable amount of unreacted **41** left in solution after all the COE was consumed. This suggests that the balance between reactivity towards COE and the metal monomer **41**, favored consumption of COE. As a result, the addition of extra COE during the polymerization was required in order for **41** to be consumed. It was speculated that the steric bulk of the mesityl groups in catalyst **38** decreased the ratio of its reactivity towards **41** and COE. As well, it was likely that not all of **38** had quantitatively formed to generate the propagating catalyst since only a small trace of free PCy₃ was observed in the ³¹P NMR. The differences in the rate of consumption of the monomers and the rates of initiation between Grubbs metathesis catalysts suggest that a higher degree of alternation and better control over the polymerization process is achieved when catalyst **37** is employed. Therefore, 1st generation Grubbs catalyst **37** is the catalyst of choice for the alternating ROMP of **57** and COE.

Alternating ROMP assembly of *trans*-RuCl₂((*R*)-5,5'-dinorimido-BINAP)(Py)₂ (57**) and COE.** Inspections of molecular models showed that the olefins are crowded in **57** and that the steric crowding between the propagating alkylidene and another monomer of **57** would prevent polymer growth by ROMP.

In fact, attempts were made to polymerize **57** by adding 5 mol % of **37** in CH₂Cl₂ at room temperature and leaving the reaction mixture for 24 h. As predicted, ³¹P NMR analysis of the mixture showed no signs of polymer formation. Therefore it was necessary to employ the newly developed alternating ROMP methodology to polymerize **57**. Addition of COE (4 equiv.) as spacer monomer to the reaction mixture of **57** and **37**, showed alternating polymerization occurred, but it was slow at room temperature. Heating the mixture at 45°C for 40 h, however, resulted in complete polymerization of both monomers.

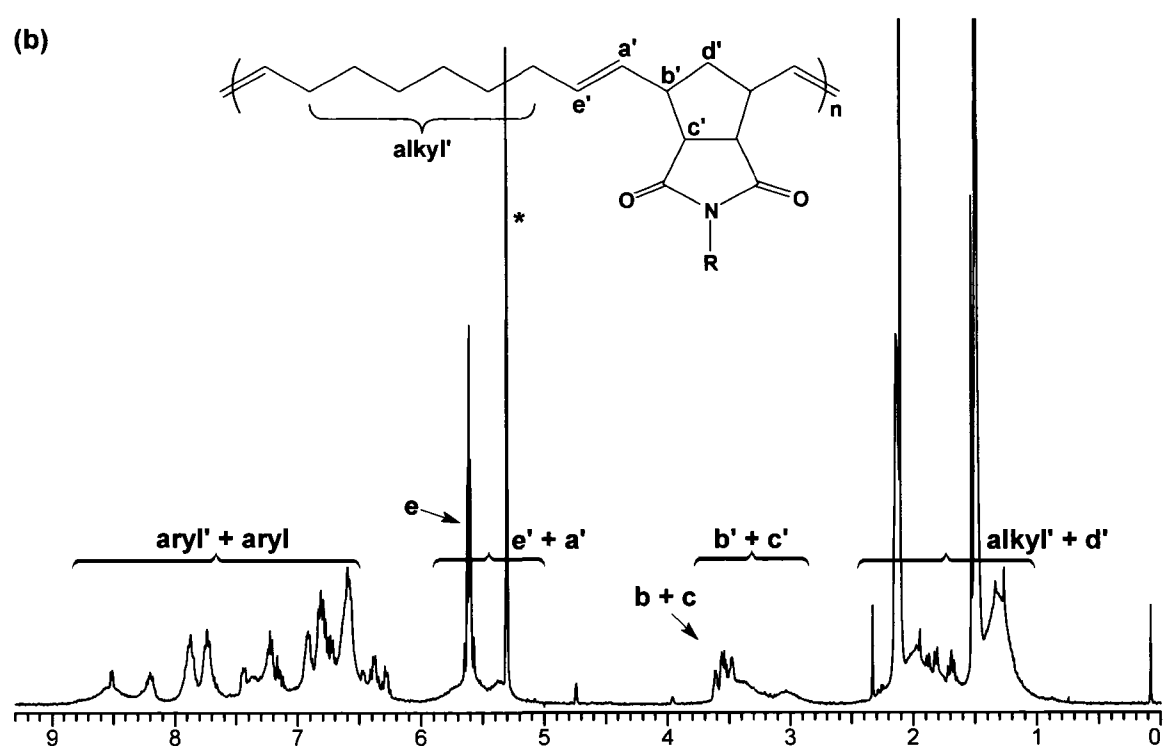
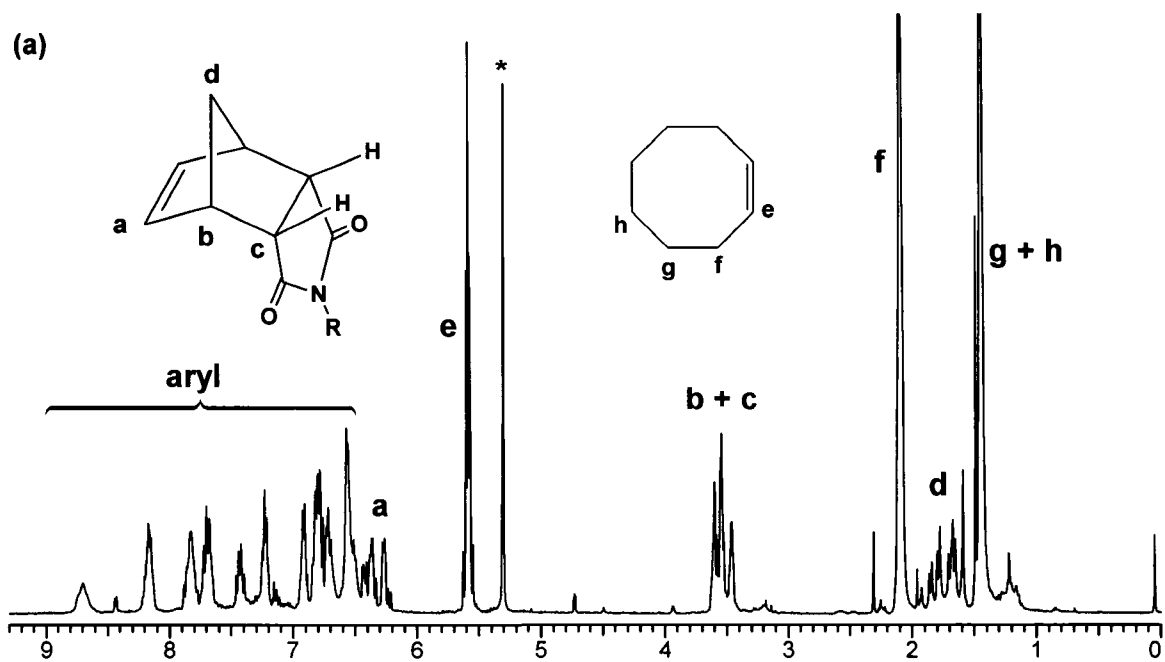
It was envisioned that the polymerization proceeded in an alternating fashion as described in Scheme 4-3. The principles are that the strained norbornyl groups in **57** are intrinsically more reactive towards metathesis than COE, and **57** thereby reacts with **37** first to form a corresponding Ru-alkylidene species such as **62**. The propagating alkylidene **62** is too crowded to react with another molecule of **57**, but it is not too crowded to react with COE to generate **63**, with the corresponding Ru-alkylidene on the end of a C₈ spacer. Since **57** is intrinsically more reactive towards ROMP than COE, the alternating polymer growth proceeds by reaction of **63** with **57**, then with COE, and so on. A detailed investigation of the alternating polymerization process is given below as evidence that this system reacts via such a sequence of steps. Furthermore, since there are two norbornyl groups per molecule in monomer **57**, the alternating ROMP process results in a cross-linked alternating polymeric framework such as **64**. The nature of this framework is discussed in more detail below.

Scheme 4-3. Alternating ROMP assembly of **57** and COE.



NMR investigations on the alternating ROMP of **57 and COE.** The nature of the alternating copolymerization between COE and **57** using metathesis catalyst **37** was monitored by a series of in situ NMR experiments using the loading **37:57:COE** equal to 1:20:72. The reagents were mixed in a NMR tube at -10°C that was quickly transferred to the pre-chilled (0°C) probe. The ¹H and ³¹P NMR spectra were recorded at different times during the polymerization and they are displayed in Figure 4-5 and Figure 4-6, respectively. At 0°C (Figure 4-5a), the small polymer peaks at ~3.2 ppm show that the polymerization has begun, but polymerization is proceeding very slowly. The rate of polymer growth was increased to practical levels by heating the NMR tube at 45°C. Although a general trend in the relative reactivities of each monomer was observable, it was not possible to determine the exact rate of polymerization of each monomer because the product polymer peaks were typically broad and they overlapped with those of the starting materials.

Analysis of the ¹H NMR spectra displayed in Figure 4-5 reveals some key characteristic features of the polymerization sequence as the sharp proton peaks of both monomers decrease and the broad polymer peaks increase during the polymerization. The olefinic resonances for **57** and COE are labeled **a** and **e** respectively and the polymer olefin signals are labeled **e' + a'**. As the polymerization proceeds the olefin protons **a** in **57** convert into the polymer olefin region between 5.15 – 5.95 ppm when **57** is consumed. The olefin protons **e** in COE overlap with the polymer olefin region and these also convert into this region when COE is consumed. Therefore the integration for the polymer olefin



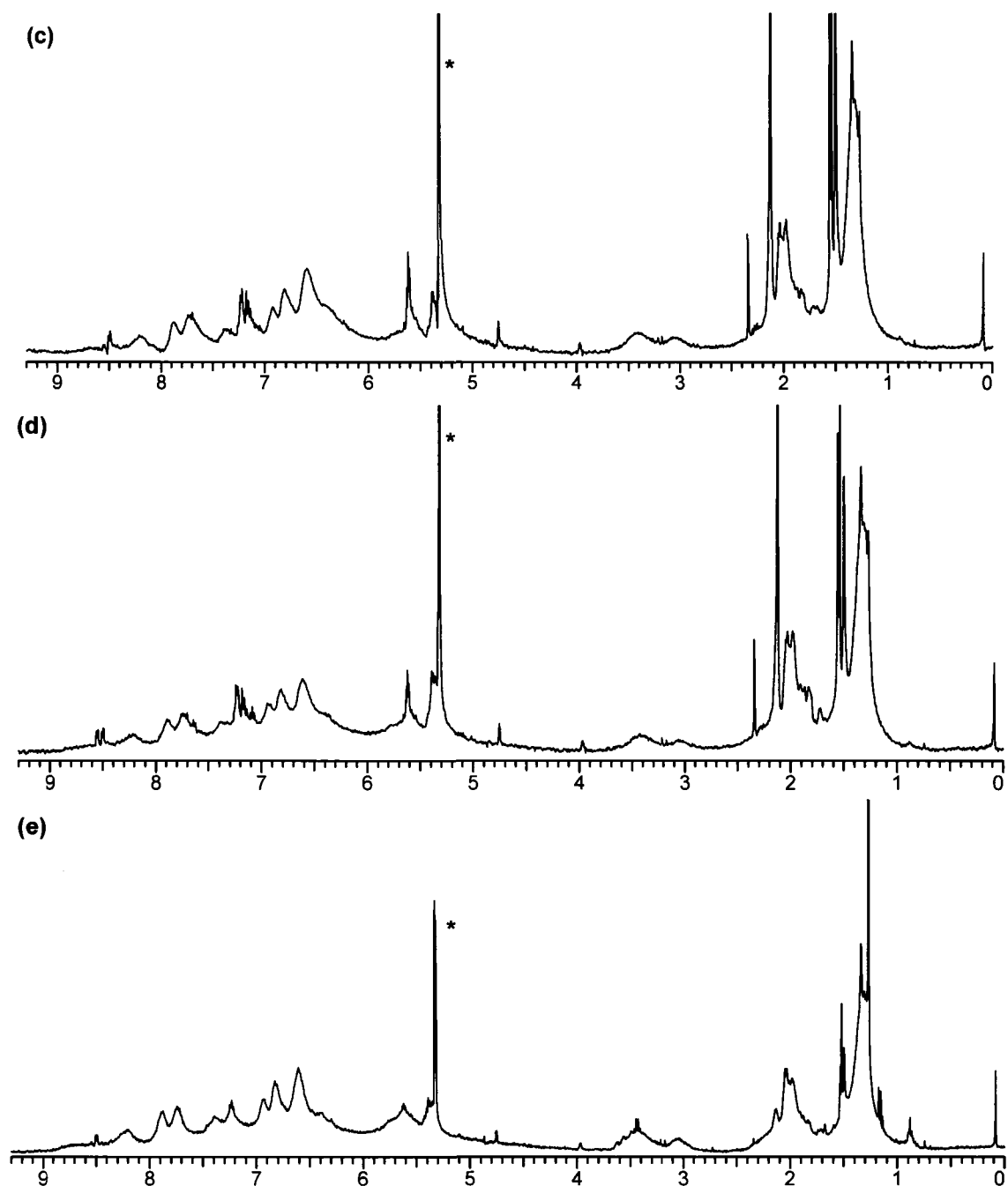


Figure 4-5. Comparison of ^1H NMR spectra (at 399.8 MHz in CD_2Cl_2) of the alternating ROMP of **57** and COE (1:4) with catalyst **37** (5 mol%); (a) recorded at start of reaction at 0°C , (b) recorded after 4 h at 45°C , (c) after 25 h at 45°C , (d) after 35 h at 45°C , (e) after 48 h at 45°C . (* is solvent peak).

region should only increase by the same amount that **a** decreases since the olefin signals **e** remain in this region. In this case an increase of four protons was expected when **57** was completely polymerized. Unfortunately this change could not be measured because the polymer aryl + starting aryl region (aryl' + aryl) overlap with the olefin signals **a** between 6.2 – 8.8 ppm. As a result, the integration cannot be accurate for this region and the consumption of **57** cannot be measured. Also of note is that the norbornene protons (**b** + **c**) are buried under the broad polymer norbornene signals (**b'** + **c'**) between 2.75 – 3.70 ppm, and as a result the total integrated area does not change during the polymerization. Finally, the alkyl protons of both monomers overlap with the polymer alkyl protons (alkyl' + **d'**) between 0.95 – 2.40 ppm, and again this integrated area does not change during the polymerization. Nevertheless, the following observations can be made despite the overlap of the resonances from the copolymer and the starting monomers in the NMR spectrums.

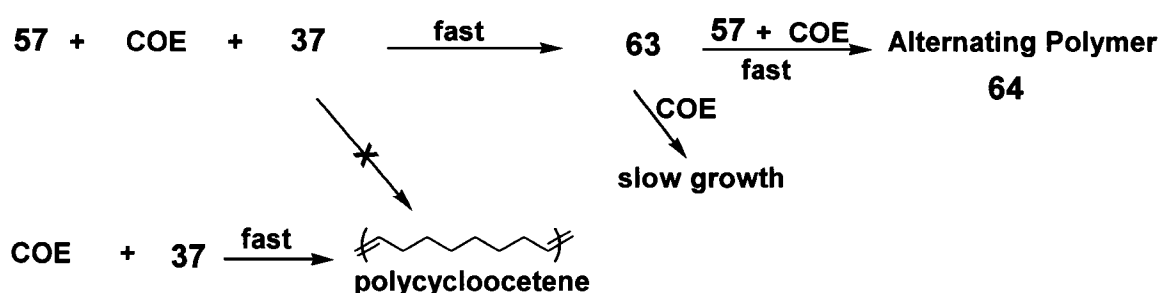
After 4 h the olefin signals for both monomers (**a** and **e**) have decreased confirming that both are reacting and signals for the growing polymeric framework are observed in the regions labeled in Figure 4-5b. Note that **57** reacts very slowly in the absence of COE and the fact that both are now reacting confirms that the polymeric framework grows in an alternating fashion. Figure 4-5c shows that after 25 h, monomer **57** has been fully polymerized, and while the proton signals for **57** (**a**, **b** and **c**) have disappeared some un-polymerized COE still remains. That un-polymerized COE remains after all of **57** has been polymerized shows that the ratio of alternation of COE: **57** in the alternating

copolymer is less than 1.8:1. Specifically, the initial ratio of COE: **57** was 3.6:1 and since **57** consists of two norbornyl units, the ratio of COE:norbornyl is actually 1.8:1. Thus polymer growth proceeds with a high degree of alternation which must be less than 1.8:1. Furthermore, although the product NMR peaks were broad and they overlapped with those of the starting materials peaks, a peak height analysis of the spectrum recorded after 4 h indicated that roughly 75% of **57** had reacted with COE to form the polymer. The ratio of reacted norbornyl groups in **57** to the amount of COE consumed at this point was ~ 1:1. This is consistent with the results obtained from Chapter 2, where it was also shown that a high degree of alternation is achieved for these alternating ROMP processes (see Figure 2-4 in Chapter 2).

As can be seen in Figure 4-5d and e, the remaining COE eventually polymerized (~20h) after the polymerization of **57** was complete, illustrating that the polymerization does not terminate once all of **57** is consumed. Interestingly, the polymerization of the remaining COE was very slow. Considering that **57** does not undergo ROMP in the absence of COE, but COE does in the absence of **57**, the roughly equal decrease in both norbornyl groups in **57** and COE is strong evidence of an alternating-, rather than a block ROMP process. As well, the rate of initiation of **57** using the metathesis catalyst **37** must be faster than the rate of propagation under these conditions or it would be expected that all of COE would be consumed before **57** since COE readily polymerizes with catalyst **37** (Scheme 4-4).¹² The reason why COE is not polymerized before **57** is attributed to the higher reactivity of the highly strained norbornyl units towards

the ROMP catalyst **37**. That the initial ratio of COE to norbornyl groups in **57** was 1.8:1, and that free COE remained after **57** was consumed, shows that the ratio of COE to norbornyl groups in the ROMP product was less than 1.8:1, a result consistent with the peak height analysis (vide supra) that indicated the ratio was ~ 1:1.

Scheme 4-4. Rate of Polymer Growth.



The above analysis is good evidence that ROMP of **57** and COE proceeds in an alternating fashion as described in Scheme 4-3. The alternating polymer growth is dually controlled by the sterics associated with the propagating alkylidenes, **62** and **63**, and the differences in intrinsic activities of the monomers towards ROMP. The stereochemistry of the norimido groups likely also influences the reactivity of **57** towards ROMP. Specifically, by having the norimido groups arranged in an endo fashion, rather than exo, the steric constraints preventing polymer growth are even more pronounced since the metal alkylidenes in **62** and **63** will be in closer proximity to the binaphthyl rings.¹³ Having this level of sophistication associated with the polymer growth results in a high degree of alternation.

The polymerization progress was also followed by ^{31}P NMR spectroscopy as shown in Figure 4-6. During the polymerization there was no change in chemical shift between **57** and the copolymer; instead the sharp phosphine peaks belonging to **57** decreased as the broad polymer peaks increased. After 4 h (Figure 4-6b), it was estimated by integrating the remaining sharp phosphine peaks separately from the broad polymer region that ~55% of **57** had been

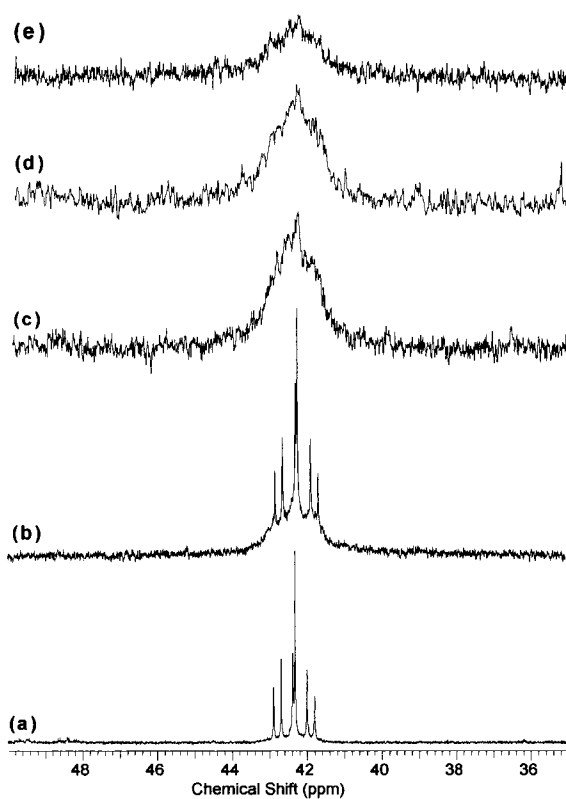
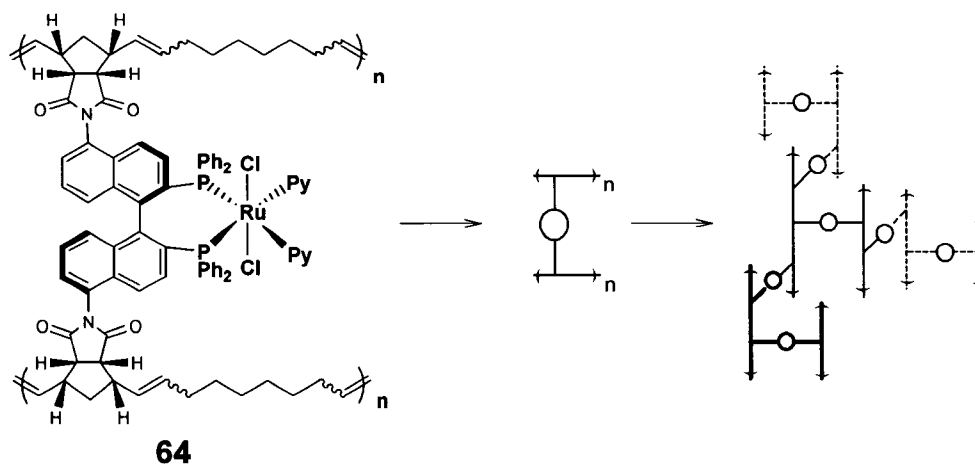


Figure 4-6. Comparison of the ^{31}P NMR spectra (at 161.8 MHz in CD_2Cl_2) of the alternating ROMP of **57** and COE (1:4) with catalyst **37** (5 mol%); (a) recorded at start of reaction at 0°C , (b) recorded after 4 h at 45°C , (c) after 25 h at 45°C , (d) after 35 h at 45°C , (e) after 48 h at 45°C .

polymerized and after 25 h (Figure 4-6c), **57** was completely polymerized, a result consistent with the ^1H NMR analysis. The chemical shift for the alternating polymer framework is similar to the homogeneous monomer **57**, suggesting that the electronic environment of the ruthenium catalyst center has not significantly changed during the alternating ROMP. This is a desirable aspect on both the design of the catalyst monomer and on the immobilization methodology since, as was discussed in Chapter 2, changes around the metal center of diphosphine-type catalysts can alter the catalyst performance in terms of selectivity and reactivity.¹⁴ Also of note is that the broad polymer peak for the polymer framework has the same shape as the sharp multiplet seen in **57** suggesting that there is no change in the population of the diastereomeric atropisomers.

Nature of the extended, three-dimensional alternating catalyst-organic framework. As previously mentioned, monomer **57** was designed to have two norimido units per monomer that are available to undergo the alternating ROMP with COE to form a cross-linked polymer as shown in Scheme 4-5. There is no reason to believe that this polymerization would proceed in a fashion that gives a linear ladder-like polymer. Instead, it is likely that the resulting polymer would resemble a highly self cross-linked, extended three-dimensional lattice-type scaffold with the active catalysts suspended between the lattice backbones. Scheme 4-5 shows a representation of the catalyst-organic framework with the catalyst complex as cross-linking units.

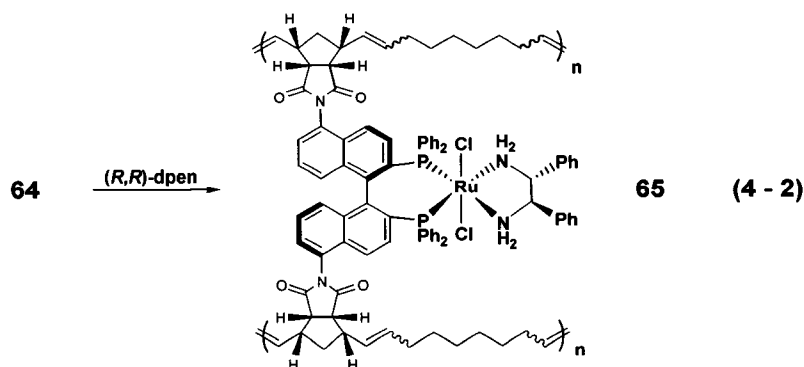
Scheme 4-5. Schematic representation of the extended, three-dimensional catalyst-organic framework **64**.



There are several potential advantages to having a catalyst-organic framework over a linear polymer. For example, the cross-linking framework imparts a degree of rigidity to the system making it more durable and less soluble than the previous linear Norphos-based polymer **46**. As well, the catalyst framework should provide excellent active-site isolation, preventing unfavorable interactions between adjacent catalytic sites. Also, leaching of the monomer units should be minimized since each unit is held by four covalent bonds within the macroscopic framework. Based upon the preceding analysis, the ratio of COE to norbornyl groups in the framework is near 1:1 (at least less than 1.8:1) when **57** is consumed, so the framework has a uniform, dense distribution of catalytic sites allowing for higher catalyst utilization. This system thereby shares characteristics with the metal-organic frameworks.^{6,1,15} One major difference being that metal-ligand covalent bonds are not part of the framework prepared by the alternating ROMP assembly of COE and **57**. Compared to linear type polymers, the

framework may allow for better mass transport of the substrates to and from the catalytic centers since the framework is less likely to wrap around the active sites and it may possess a porous quality. Apart from the advantages listed above for a polymeric framework, the self cross-linking nature of monomer **57** avoids the additional step of adding a cross-linking agent once the polymeric catalyst has been prepared.

Preparation of Noyori's catalyst within the polymeric framework and supported on BaSO₄. The polymerization of the (*R,R*)-dpen analogue of **57**, *trans*-RuCl₂((*R*)-5,5'-dinorimido-BINAP)((*R,R*)-dpen) (**60**), was not attempted using metathesis catalyst **37** for reason previously stated in Chapter 2. Instead, the polymeric version of **60** was obtained by reacting a dilute solution of the alternating polymer **64** with excess (*R,R*)-dpen to form the alternating polymer framework [RuCl₂((*R*)-5,5'-dinorimido-BINAP)((*R,R*)-dpen)]_x[COE]_y (**65**) (where *x* and *y* are integers determined by initial ratios of reagents) (equation 4 - 2). It was necessary to maintain a dilute reaction mixture; otherwise once the polymer framework came out of solution it could not be re-dissolved.



^{31}P NMR spectroscopy confirmed that after 12 h the pyridine ligands were completely exchanged for (*R,R*)-dpen, and the change in chemical shift is consistent with the change observed for the homogeneous analogs of **57** and **60** (Figure 4-7). Next, the alternating catalyst framework **65** was supported as a thin

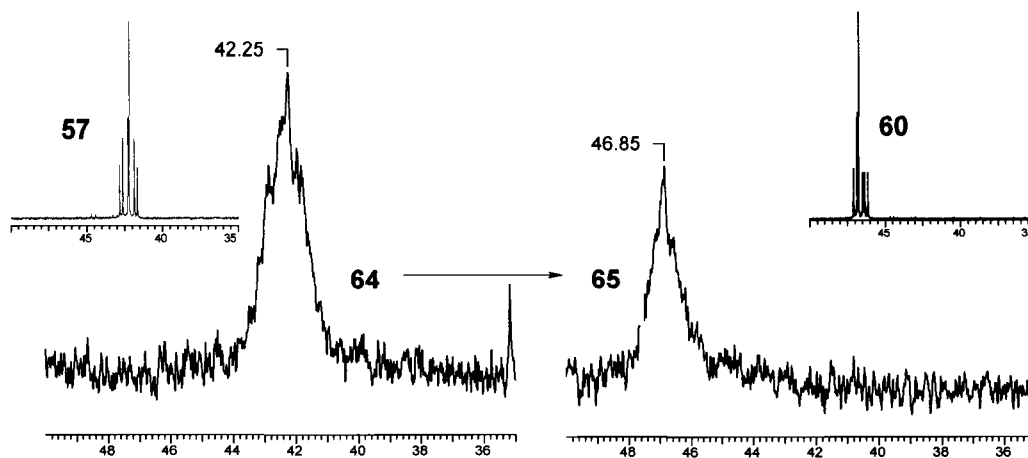


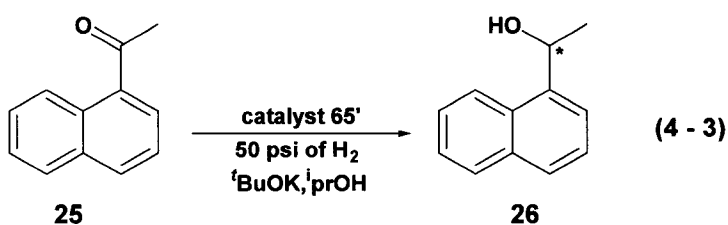
Figure 4-7. ^{31}P NMR spectra (161.8 MHz in CD_2Cl_2) of the alternating polymer framework **64** before (left) and after (right) treatment with (*R,R*)-dpen resulting in **65**. The insets depict the homogeneous analogs, **57** and **60**, respectively.

film over BaSO_4 to provide mechanical stability to the system, to act as a filtration aid, and to improve mass transport. To remove any soluble low molecular weight oligomers present from the polymerization of **57** and other impurities that could act as a poison, the BaSO_4 -supported catalyst was washed with methanol. The methanol washings did not contain any detectable (NMR) amounts of catalyst monomer, confirming the results from the previous NMR studies that showed that the consumption of monomer **57** was complete. Hence, no low-molecular weight

oligomers were formed during the polymerization and therefore the alternating polymerization of COE and **57** formed a high-molecular weight polymer framework (vide supra). The BaSO₄-supported catalyst-organic framework was tested as a heterogeneous hydrogenation catalyst as described in the next section.

Section C: Preliminary investigations of the supported alternating catalyst-organic framework towards asymmetric hydrogenations.

Initial hydrogenations. The asymmetric hydrogenation of 1'-acetonaphthone (**25**) was used to investigate the activity of the heterogeneous catalyst [RuCl₂((*R*)-5,5'-dinorimido-BINAP)((*R,R*)-dpen)]_x[COE]_y/BaSO₄ (**65'**), and its potential for recycling (equation 4 - 3).



The supported catalyst **65'**, with a loading of 8.48 mg (6.38 x 10⁻⁶ mol) of catalyst precursor **60** per gram of BaSO₄ support, was used in the repeated hydrogenation of **25** in a glass pressure vessel under the conditions described in Table 4-1. The initial conditions chosen were similar to the conditions used for the repeat hydrogenation of **25** using polymeric catalyst **46**.¹⁶ The first run was

done at room temperature, and gave 0% conversion. Run 2, using the same catalyst at 60°C, however, gave 100% yield in 91% ee. This dramatic increase in activity may have resulted from the use of the higher temperature, that generated the active dihydride catalyst, Ru(H)₂((*R*)-5,5'-dinorimido-BINAP)((*R,R*)-dpen). Based on the above assumption, run 3 was done at a lower temperature, but the catalyst was found to be less active. Since the catalyst was activated by heating at 60°C (run 2), the drop in activity observed when the temperature was lowered to 40°C (run 3), was likely a result of decreased swelling of the polymer framework. In other words, at higher temperatures the polymer matrix swells more, promoting access to and from the active sites. Between each run, the catalyst was isolated by simple filtration under a H₂ atmosphere, and the reaction vessel was recharged with fresh substrate and ^tBuOK as a solution in 2-propanol.

Table 4-1. Heterogeneous hydrogenation of 1'-acetonaphthone using **65'**.^[a]

Recycling Runs	Time (h)	Temperature (°C)	ee (%) ^c	Yield (%) ^c
1	2	RT	0	0
2	16	60	91	100
3	18	40	90	56
4	20	60	81	84
5	21	60	79	100
6 ^b	19	60	82	96
7 ^b	24	60	81	92

^[a] The hydrogenation was carried out in 1.0 M solution of 1'-acetonaphthone in 2-propanol under the following conditions: Sub./Cat./Base = 500/1/4; H₂ = 50 psi. ^[b] Sub./Cat./Base = 500/1/10. ^[c] Yield % and ee % were determined by chiral GC analysis.

Noyori reported that the hydrogenation of **25** using the homogeneous catalyst [RuCl₂((*R*)-BINAP)((*R,R*)-dpen)], affords the chiral product **26** with 97%

ee at 25°C.^{17,18} The ee obtained with catalyst **65'** was slightly less at 91% (run 2) and this was likely a result of the higher reaction temperature used for run 2. Run 4 was carried out at 60°C, which increased the yield from run 3 (at 40°C), but the enantioselectivity dropped to 81 %. That the ee dropped between runs 3 and 4, even though the reactions were carried out under the same conditions, shows that the catalyst underwent a deteriorative transformation. It has been shown for hydrogenations using ruthenium catalysts that Si-OH groups on the surface of glass reaction vessels have a detrimental effect on catalyst activity.¹⁹ In fact, Noyori recommends use of stainless steel pressure vessels for these hydrogenations carried out with high substrate loadings.^{20,21} Although our pressure vessel was initially silanized with chlorotrimethylsilane (TMSCl),¹⁹ repeated exposure to ^tBuOK in 2-propanol likely removed these groups. Since it is not practical to remove the solid catalyst and retreat the glass vessel between each run, this problem was avoided by using a stainless steel pressure vessel. The remaining runs (5-7) carried out with this sample of catalyst were done at 60°C. The catalyst continued to lose activity after run 5 and it was decided to not proceed any further with this sample of catalyst **65'**. A fresh batch of **65'** was used for the next experiment.

In an effort to increase the enantioselectivity by avoiding use of the high temperatures, we investigated the use of a swelling co-solvent (THF) at lower temperatures. A 1:1 mixture of THF:2-propanol was used as the solvent system at 40°C. As shown in Table 4-2, there was an increase in activity going from runs 1 to 3 that then quickly decreased in runs 4 and 5. The initial increase in

activity likely resulted from swelling of the polymer framework by THF. The subsequent decrease likely resulted from leaching of the catalyst, since the polymer framework appeared to be more soluble in the THF:2-propanol mixture. So although it was possible to increase the activity of the catalyst by using THF, it also proved detrimental to the durability of the polymer catalyst. As expected, the enantioselectivity increased to 95% at lower temperatures, levels now comparable to the homogeneous case. Furthermore, the *ee* did not decrease during repeated runs as it had done when the reaction was carried out in the glass pressure vessel.

Table 4-2. Hydrogenation of **25** using **65'** with a swelling co-solvent.^[a]

Recycling Runs	Time (h)	<i>ee</i> (%) ^c	Yield (%) ^c
1	22	93	33
2	22	95	72
3	42	95	100
4	21	95	54
5 ^b	23	95	47

^[a]The hydrogenation was carried out in 1.0 M solution of 1'-acetonaphthone in a 1:1 2-propanol:THF mixture under the following conditions: Sub./Cat./Base = 1000/1/20; H₂ = 10 bar; reaction temperature = 40°C. ^[b]Used only 2-propanol. ^[c]Yield % and *ee* % were determined by chiral GC analysis.

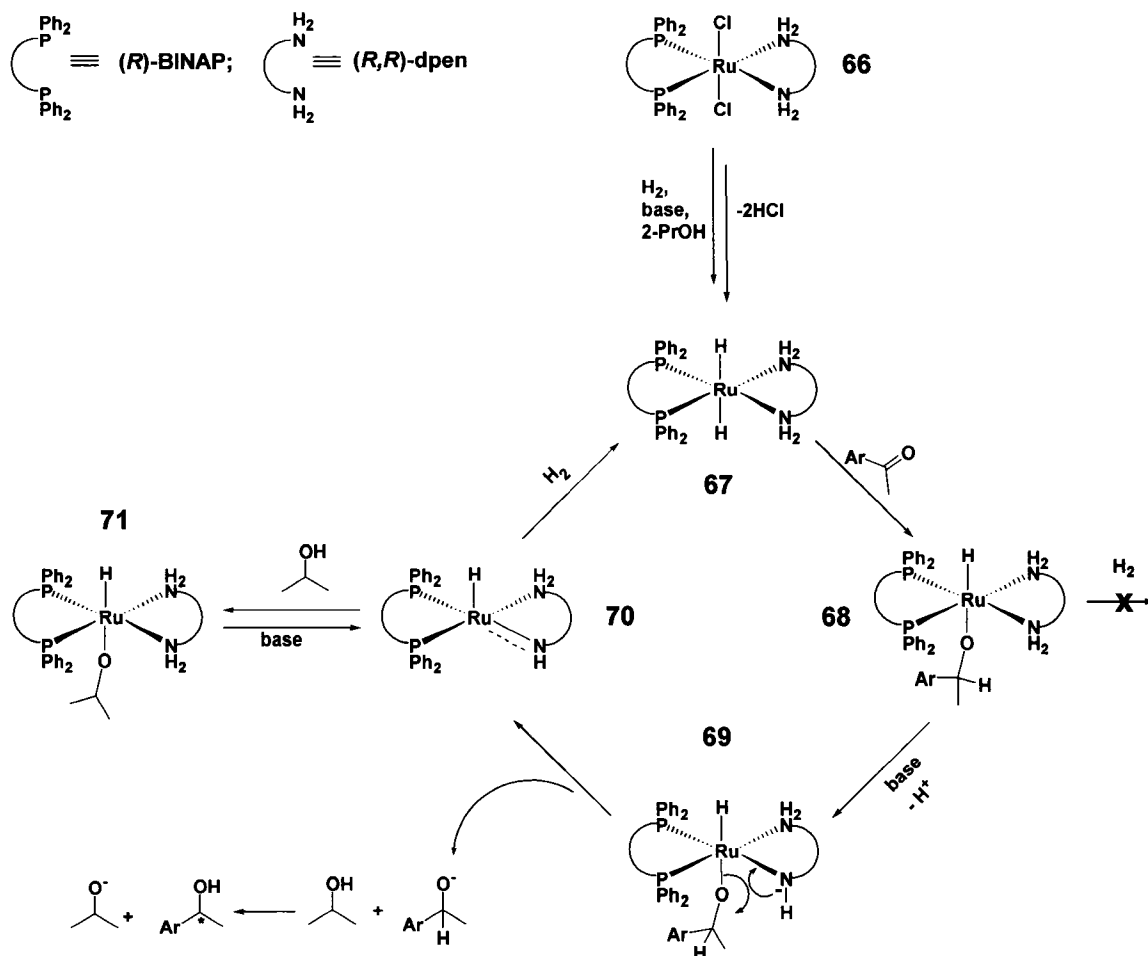
Optimized reaction conditions. The preliminary results from above were promising since they showed that the supported catalyst framework **65'** was catalytically active and it did show potential towards catalyst recycling. But the levels of activity, selectivity and reusability were not adequate. From these studies the behavior of the catalyst-organic framework was better understood,

which led to the following conditions to maximize the catalyst efficiency. The use of a co-solvent was to be avoided, as well as high temperatures, since both conditions caused the catalyst activity to deteriorate. The reactions must be carried out in a stainless steel pressure vessel to prevent the loss of selectivity. As well, during the set-up and take down of each run it is necessary to keep the system under a positive flow of H₂ gas to prevent catalyst deactivation, since the catalytically active Ru-hydride species decompose on exposure to air.²² All reagents used (2-propanol, ^tBuOK and ketone) were thoroughly purified, repeatedly if necessary, before use and were saturated with H₂ gas before addition to the reaction mixture. Apart from the measures taken to exclude air from entering the system, it was also believed that proper storage of the supported active catalyst between runs was essential in order to maintain the highest level of catalyst activity possible. To this effect efforts were taken to ensure that the catalyst framework always remained in a solution of 2-propanol between runs. This procedure likely ensured the reusability of the catalyst for two reasons. First, by keeping the catalyst framework always in 2-propanol assured that the polymer matrix did not collapse as a result of desolvation. This is particularly important since the activity of the catalyst framework has been shown to be directly related to the amount of swelling. In other words there is an initiation period, whereby the polymer framework must swell before a high level of activity is achieved and therefore it was believed that activity would be lost if the polymer dried out. Further, repetitive swelling and contracting of polymer-supported systems promotes degradation of the polymers. Secondly, it was

speculated that by keeping the catalyst framework in 2-propanol between runs protected the active catalyst by the formation of a stable solvento intermediate.²³ In fact, recent detailed mechanistic studies carried out in the Bergens lab on the hydrogenation of ketones using the *trans*-RuCl₂-(diphosphine)(diamine) plus base in alcohol solvents as the catalyst systems, established for the first time that 2-propanol reacts with the active catalyst to generate a stable 2-propoxide intermediate.²⁴ Specifically, by preparing the catalytic intermediates proposed for these hydrogenations in pure form at low temperature (-80°C) and reacting these separately to study their catalytic activities, they found that the stable 2-propoxide compound, *trans*-[Ru((*R*)-BINAP)(H)(2-PrO)((*R,R*)-dpen)] (**71**) formed during the reaction.

The proposed mechanism based on this work is shown in Scheme 4-6. First, there is an initial incubation period whereby the catalyst precursor **66** is converted into the active dihydride compound *trans*-[Ru((*R*)-BINAP)(H)₂((*R,R*)-dpen)] (**67**) with the aid of a base and a hydride source, H₂ and 2-PrOH. Compound **67** reacts with ketone to form the stable aryl-alkoxide intermediate, *trans*-Ru((*R*)-BINAP)(H)(aryl-alkoxide)((*R,R*)-dpen) (**68**), which does not react further in the presence of H₂, but in the presence of base generates **69** by deprotonation of an NH₂ group. This is followed by an intramolecular elimination of the aryl-alkoxide ligand to generate the amide *trans*-[Ru((*R*)-BINAP)(H)((*R,R*)-NH(CH(Ph))₂NH₂)] (**70**). Subsequently, the aryl-alkoxide is protonated by 2-propanol to give the chiral alcohol product and 2-propoxide. Compound **70** then reacts with H₂ to generate **67** thereby completing the catalytic cycle.

Scheme 4-6. Proposed mechanism for *trans*-RuCl₂-(diphosphine)(diamine).



Interestingly, it was discovered that **70** reacts with 2-propanol to form the stable 2-propoxide intermediate **71** that does not react with H₂. It was speculated that the stability of **71** was a result of intra-, or intermolecular H-bonding between the 2-propoxide ligand and an N-H group or 2-propanol, respectively. In the presence of base, **71** reacts to generate **70** through a base-assisted elimination of 2-propoxide. From these studies it was proposed that the addition of base favored formation of the amide compound **70** and subsequently increased the

reaction rate. In the absence of base and in a solution of 2-propanol, the formation of the stable intermediate **71** is favored. These mechanistic studies were very pertinent to developing the procedure of storing the catalyst framework in 2-propanol between runs.

The ability to store the catalyst framework in such a manner is beneficial to the handling of our heterogeneous catalyst system. Specifically, it gives robustness to the heterogenized catalyst by removing time constraints on the lifetime of the catalyst activity. In a separate experiment it was found that the catalyst framework could be stored for weeks at a time as the stable alkoxide intermediate. As well, a catalyst recycling study was done in which base was not added after the first couple runs in which the catalyst was activated. It was found that without added base the catalyst had little activity. Therefore added base was not just required for the initial incubation of the catalyst precursor to generate the active dihydride catalyst, but also to maintain catalyst activity. Also, the concentration of the base solution was increased, since it has been shown that the rate of the reaction increases at higher base concentrations.²¹

Section D: Reusability and versatility of the supported catalyst-organic framework.

Recycling. One of the main objectives for the immobilization of catalysts is the potential of recycling expensive homogeneous catalysts. Therefore, it is

essential to evaluate the reusability of our immobilized catalyst system. Using the above optimized conditions the reusability of the catalyst framework **65'** was tested in the repeated hydrogenation of 1'-acetonaphthone. Recently, the criterion for the turnover number (TON) of an enantioselective catalytic reaction before it can be applied to industrial small-scale production has been identified as ≥ 1000 .²⁵ Therefore, 1000:1 was chosen as the ratio of substrate to catalyst for each run, and the hydrogenation was carried out in 2-propanol, under 10 atm H₂, in the presence of 20 equiv KO^tBu per active site. These conditions are indigenous to the homogenous reaction.⁸

Figure 4-8 shows a graph plotting % yield and % ee vs number of recycles obtained for the hydrogenation of 1'-acetonaphthone reusing a single sample of the catalyst framework **65'**. The catalyst framework was reused for a remarkable 25 times, with the catalyst operating for 25 days, without loss in catalytic activity or selectivity. To the best of my knowledge this is the highest number of recycles achieved with an immobilized homogeneous asymmetric hydrogenation catalyst. The majority of reported heterogenized chiral hydrogenation catalysts operate at less than practical TON's/run (i.e. < 1000), and suffer from detrimental losses in activity by the third reuse. The only previous heterogenized hydrogenation catalyst system that sustained more than 10 reuses at practical TON's/run without loss in activity or ee were the Ru(BINAP)-type complexes attached to magnetic nanoparticles prepared by Lin *et al.*²⁶ These catalysts sustained 14 reuses at TON/run = 1000 under 48 atm H₂ for the hydrogenation of 1'-acetonaphthone. The catalyst-organic framework prepared here by alternating

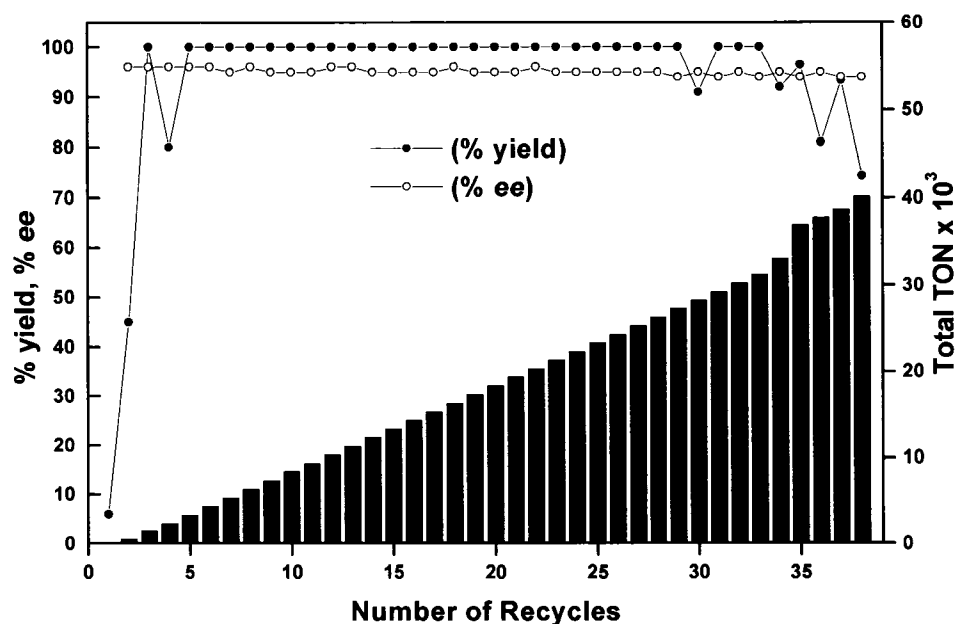


Figure 4-8. Plot of yield (%) and ee vs. the number of recycles for the hydrogenation of **25** catalyzed by **65'**. The superimposed bar graph represents the accumulated turnover number during the experiment.

ROMP assembly sustained at least 25 reuses under mild pressures. A thorough discussion of the recycling experiment is given below, and the details for each run are shown in Table 4-3.

Runs 1 through 4 were used to condition the catalyst framework and to optimize the reaction temperature and time. Run 1 was carried out at room temperature for 23 h and resulted in 6% yield. Run 2 was carried out at room temperature and resulted in 45% yield after 66 h. The increase in activity that occurred during these conditioning runs likely resulted from swelling of the catalyst framework and formation of the active catalyst from the ruthenium-

Table 4-3. Recycling of catalyst framework **65'** for hydrogenation of **25**^[a]

Recycling Runs	Substrate/Catalyst	Time (h)	ee (%) ^c	Conversion (%) ^c
1 ^b	1000	23	nd	6
2 ^b	1000	66.5	96	45
3	1000	21	96	100
4	1000	21	96	80
5	1000	21	96	100
6	1000	21	96	100
7	1000	21	95	100
8	1000	27	96	100
9	1000	19	95	100
10	1000	21	95	100
11	1000	21	95	100
12	1000	21	96	100
13	1000	21	96	100
14	1000	21	95	100
15	1000	21	95	100
16	1000	21	95	100
17	1000	21	95	100
18	1000	21	96	100
19	1000	21	95	100
20	1000	21	95	100
21	1000	73 ^d	95	100
22	1000	21	96	100
23	1000	21	95	100
24	1000	21	95	100
25	1000	21	95	100
26	1000	21	95	100
27	1000	21	95	100
28	1000	21	95	100
29	1000	21	94	100
30	1000	21	95	91
31	1000	45	94	100
32	1000	50	95	100
33	1000	45	94	100
34	2000	45	95	92
35	4000	141.5	94	96.4
36	1000	21	95	81
37	1000	40	94	93.4
38	2000	43.5	94	74.3

^[a] The hydrogenation was carried out in 1.0 M solution of 1'-acetonaphthone in 2-propanol under the following conditions: Sub./Cat./Base = 1000/1/20; H₂ = 10 atm; reaction temperature = 40°C except for runs 1 and 2 (see footnotes). ^[b] done at room temperature ^[c] Yield and ee were determined by chiral GC analysis. ^[d]After 21 h the solid catalyst was stored under H₂ in 2-PrOH for 52 h before the next run.

chloride precursor. This confirms that the catalyst framework does require an initiation period for the generation of the active catalyst and that 2-propanol solvent is sufficient to swell the catalyst framework. As run 3 (40°C, 21 h) gave 100% yield, and run 4 (35°C, 21 h) gave 80%, the subsequent runs were carried out at 40°C. The catalyst was reused until run 30 before a decrease in activity was observed. It was noted that during run 29 there was a change in stirbar pitch, and run 30 provided 91% yield without a change in *ee*. That there was no change in the enantioselectivity suggests that the active catalytic sites remained intact, and there was some event that occurred during run 29 that diminished the activity of the catalyst. In any event, runs 31 through 33 were carried out for 45 h with 100% yield, and with 95% *ee*, suggesting no further decrease in catalyst activity occurred after run 29.

After proving that the catalyst framework could be recycled for an extraordinary number of times, attention was shifted to push the limits of the catalyst loading despite the loss in net activity that occurred at run 29. Run 34 was carried out with 2000 equiv. of ketone, also for 45 h, and with 92% yield, which is comparable to the previous runs. Run 35 was carried out with 4000 equiv. of ketone and the catalyst activity had decreased by ~35% from the previous run. After run 35 the catalyst continued to lose activity, and it was decided to not proceed further. It is likely that the catalyst framework was more soluble at higher substrate concentrations, thereby causing catalyst deterioration as a result of increased catalyst leaching into the organic mixture. The total

turnover number (TON) achieved in 38 consecutive runs, with only 8.48 mg of active catalyst per run, was > 40,000.

Upon opening the steel reactor, it was surprising to find that only 25% of the supported catalyst framework **65'** remained in solution at the bottom of the reactor. 75% of the catalyst had splashed up on the sides and lid of the reactor, away from the reaction mixture (Figure 4-9). As well, the stir bar was worn flat from over 50 days of continued use. The system was calibrated at the beginning of the experiment for the starting shape of the stir bar, and it was found then that the reaction mixture stirred evenly, with no splashing, at a rate of ~500 rpm. Therefore, the change in shape of the stir bar may have resulted in splashing of the reaction mixture, decreasing the number of catalytic active sites in solution.

That the majority of the solid catalyst had accumulated on the sides and the lid of the vessel, away from the reaction media, was remarkable, and it implies that the catalyst activity is much higher than what was originally thought. In fact, as will be described in the next section the TOF for runs 5 through 29 was ~750 h⁻¹, a rate that is already comparable to the homogeneous hydrogenation.⁸ Given that the decrease in activity observed in the later runs (30-33) was a result of actual catalyst loss instead of deterioration of the catalyst, and that there was no drop in the enantioselectivity supports this conclusion. Runs 34 and 35, with a S/C = 2000 and 4000, were more likely done with only ~25% of the supported catalyst in use. Therefore, the catalyst activity is very high despite losing actual catalyst during the reaction and it is reasonable to assume that runs 34 and 35 were done at a much higher loading of S/C = 6000 and 12000, respectively.

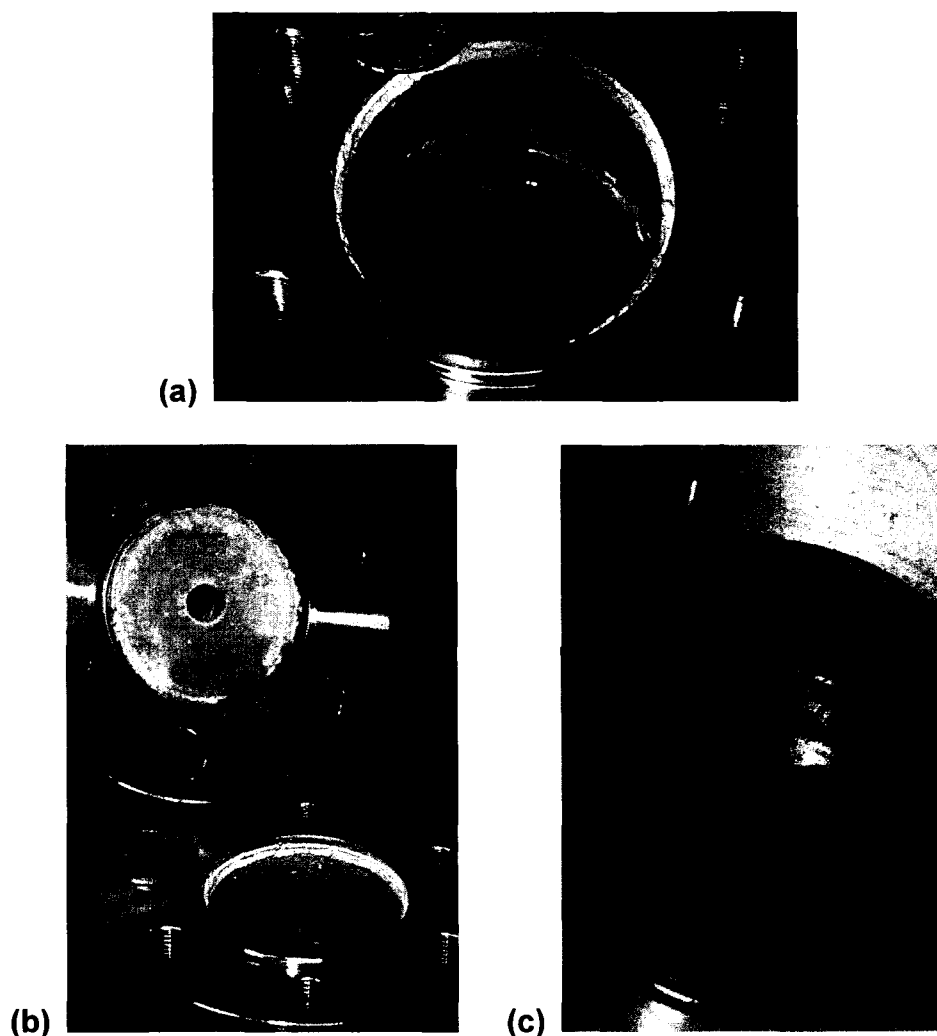


Figure 4-9. Pictures of the stainless steel hydrogenation bomb after the recycling experiment. (a) The solid catalyst was coated around the bomb walls away from the reaction solution, (b) and on the bomb lid. (c) Supported catalyst remaining after reaction mixture was removed.

Hence, despite the already unprecedented level of reusability achieved with the supported catalyst-organic framework, it is believed that this immobilized catalyst system has not attained its maximum potential in terms of activity and reusability.

Specifically, with an improved design on the hydrogenation system so that all of the supported catalyst framework would be in use during the reaction, with no loss of catalyst as a result of mechanical issues, a higher level of activity and reusability could be attained.

Rate of reaction for runs 5 through 29. The pressure drop in the sealed bomb corresponded to the amount of hydrogen consumed by each hydrogenation, and the rate of hydrogenation using the catalyst framework **65'** was estimated by using the ideal gas law. The recycling experiment shown in Figure 4-8 was carried out in a closed pressure reactor. As a result, it was possible to monitor the extent of the reaction by observing the drop in gauge pressure which corresponded to the amount of hydrogen gas consumed for the hydrogenation of **25**. Specifically, one mole of ketone hydrogenated equals one mole of hydrogen gas consumed, and the amount of hydrogen gas consumed was calculated by using the ideal gas law, $PV = nRT$. The validity of using the ideal gas law to monitor the extent of the reaction was verified by calculating the volume of the closed system and comparing the calculated value to the measured value. It was observed that upon completion for each run carried out with 6.38 mmol of ketone, the pressure dropped from 10 atm to 8 atm (measured at an ambient temperature of 296 K), resulting in a change in pressure, $\Delta P = 2$ atm. The change in number of moles, $\Delta n =$ the number moles of ketone consumed = 6.38 mmol. Using the ideal gas law the system volume, V_{system} , was calculated as follows:

$$\begin{aligned}
 V_{\text{gas}} &= \Delta nRT/\Delta P \\
 &= [(0.00638 \text{ mol})(0.08206 \text{ L}\cdot\text{atm}\cdot\text{K}^{-1}\cdot\text{mol}^{-1})(296 \text{ K})]/2 \text{ atm} \\
 &= 77.4_8 \text{ mL} \\
 V_{\text{system}} &= V_{\text{solvent}} + V_{\text{substrate}} + V_{\text{gas}} \\
 &= (6.4 \text{ mL} + 0.97 \text{ mL} + 77.48 \text{ mL}) \\
 &= 84.8_5 \text{ mL}
 \end{aligned}$$

The calculated V_{system} was in very close agreement with the measured volume of the closed system, which was determined to be 84.9 mL, and therefore establishes the validity of the method.

During the hydrogenation runs 5-29 the pressure dropped to ~9 atm after the first hour at 40°C. Using this pressure drop as an indicator, the turnover frequency (TOF) during the first hour of runs 5 through 29 was ~750 h⁻¹ at 75% conversion (see experimental for calculations). It is noted that this is an approximation of the rate of reaction due to the fact that the entire system was not at 40°C, since only a portion of the steel pressurized vessel was immersed in the 40°C oil bath. In any event this rate is comparable with the homogeneous hydrogenation catalyst, [RuCl₂((*R*)-BINAP)((*R,R*)-dpen) (**73**), showing that mass transport did not significantly slow the framework catalyst.⁸ Furthermore, the rate achieved with our immobilized catalyst framework exceeds that of other systems that have also immobilized Noyori's catalyst, **73**. For example, the polystyrene-anchored version of **73**, resulted in a TOF of 390 h⁻¹ in the first hour for the

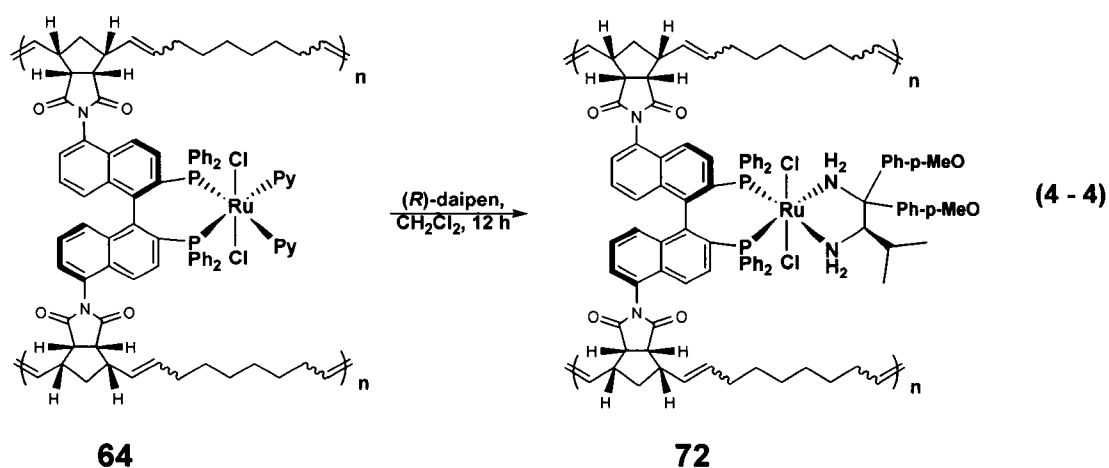
asymmetric hydrogenation of 1'-acetonaphthone carried out at 25°C, 8 atm, and with the aid of a co-solvent.²⁷ Similarly, Lin *et al* immobilized functionalized derivatives of **73** by self-assembly with one equivalent of soluble Zr(O^tBu)₄ to give chiral, porous zirconium phosphonates.⁴ The corresponding metal-organic catalyst gave a TOF ~700 h⁻¹ at 70% conversion for the asymmetric hydrogenation of 1'-acetonaphthone carried out at 25°C, and a much higher pressure of 48 atm.

Ruthenium leaching from the catalyst framework. Another critical factor in examining the durability of an immobilized catalytic system deals with the extent of metal leaching. Metal leaching is a primary concern for heterogenized catalytic systems, since it is imperative that the desired products are not contaminated with traces of toxic metal from the catalyst. Although reduced metal leaching is a goal of heterogenized systems, it is seldom addressed in evaluating the overall performance of the heterogenized catalytic systems.²⁸ Probably one of the reasons for this is because of the lack of a reliable, standard literature procedure for determining the amount of metal leaching in organic mixtures. This is somewhat surprising since many of the pharmaceutical companies that were contacted dealt with metal contamination on a regular basis and most had a team of specialist to address this issue. It may be that access to specialized equipment for determining metal content at such low levels was limited, and therefore the extent of metal leaching for most heterogenized systems were not investigated. In a few examples the extent of

metal leaching was addressed using an Inductively Coupled Plasma (ICP) spectrometer.⁴ We found that the literature standards or procedures using ICP were insufficient in dealing with this issue and they could not be reproduced for our case. One of the problems encountered was that the ICP instrument, to which we had access, was limited to only aqueous mixtures. Therefore, in consultation with several companies and specialists the following procedure was used to determine the amount of metal content in our organic mixtures.

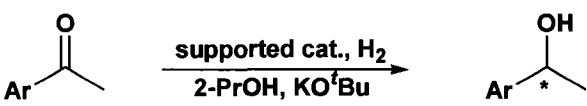
First, the oil products from the recycling experiment were combusted in a controlled manner using the sulfated ashing procedure.²⁹ Control experiments revealed that an insoluble ruthenium mirror can result from the sulfated ash procedure, so the residue was further treated with 4M KOH saturated in $K_2S_2O_8$ to dissolve any ruthenium content.³⁰ Next, this was diluted with 1% HNO_3 (aq) (25 mL) and ICP analysis was carried out on the resulting aqueous solutions. The reliability of this procedure was confirmed by preparing controlled samples and testing for ruthenium content. The inductively coupled plasma (ICP) spectroscopic analysis of the organic products from a representative sampling of the recycling runs (1, 3, 8, 14, 19, 23, 27, 29, and 30) determined that the Ru content was near or less than 4 ppb (detection limit) for each sample measured. At the start of the hydrogenation reaction the system was charged with 0.64 mg of Ru, and using 4 ppb as the upper limit, this implies that < 0.016% of Ru leached into the organic product during each run, confirming the heterogeneous nature of the catalyst system.

Versatility of the alternating catalyst-organic framework. As previously discussed, changes to the auxiliaries in the Noyori-type Ru-diphosphine/diamine catalyst can have an effect on the catalyst activity and selectivity.⁸ In this way, the (*R*)-daipen system was prepared by simply treating a dilute solution of the alternating polymer **64** with an excess of (*R*)-daipen to give $[\text{RuCl}_2((R)\text{-5,5'-dinorimido-BINAP})((R)\text{-daipen})]_x[\text{COE}]_y$ (**72**) (equation 4 - 4). ³¹P NMR confirmed that after 12 h the pyridine ligands were completely exchanged and the alternating catalyst framework **72** was deposited onto BaSO₄ following standard procedures. As shown in Table 4-4, the supported catalyst **72**/BaSO₄ (**72'**) was used to catalyze the hydrogenation of a series of aromatic ketones to



afford their corresponding secondary alcohols with high ee's and complete conversions. For comparison, the results obtained with the dpn-type supported catalyst **65'** are also given and as can be seen, switching the diamine ligands did have an effect on the catalyst selectivity. For example, 2'-methylacetophenone was hydrogenated using 0.1 mol % of **72'** or **65'** to afford 2-methylphenylethanol with complete conversions and 97% or 89% ee, respectively.

Table 4-4. Asymmetric hydrogenation of aromatic ketones^[a]



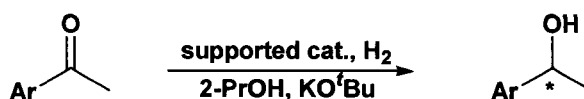
Ar	Catalyst 72' ee (%)	Catalyst 65' ee (%)
1-naphthyl	97	95
2'-Me-Ph	97	89
4'- ^t Bu-Ph	90	91

^[a]All reactions were carried out at 40°C under 10 atm pressure of H₂ at a substrate concentration of 1.0 M with substrate/KO^tBu/catalyst = 1000/20/1 for 21 h. ee (%) values were determined by GC on a Supelco β-Dex 120 Column and all conversions were >99% as determined by the integrations of GC peaks.

Having demonstrated the flexible nature of the catalyst-organic framework by simply changing the chiral diamine ligands, it was of interest to examine the effect, if any, of the solid support on catalyst selectivity. The premise for this idea was based on the approach used for traditional heterogeneous catalysts whereby the metal surface is made chiral by the addition of a suitable modifier.³¹ For example, Raney nickel modified with tartaric acid has been used for the asymmetric hydrogenation of functionalized ketones with ee's up to 98.6%.³² In our case, since a solid support was used already to increase surface area and to provide mechanical stability, we felt that a chiral solid support may have an added effect on catalyst selectivity. In this way, the dpen-type catalyst framework **65** was supported as a thin film over the chiral solid support Barium-L-tartrate and used for the hydrogenation of a series of aromatic ketones. The results are shown in Table 4-5 along with the results obtained using catalyst **65** supported on BaSO₄. In all three substrates tested there was a noticeable

change, albeit a small one, in selectivity between the different supported systems, indicating that the solid support does play a role in catalyst performance. These preliminary results were encouraging and further studies are needed to fully investigate and to exploit this feature.

Table 4-5. Ba-(L)-tartrate supported catalyst for asymmetric hydrogenations^[a]



<i>Ar</i>	65/ <i>Ba(L)</i> tartrate ee (%)	65/ <i>BaSO</i> ₄ ee (%)
2'-Me-Ph	92	89
4'- ^t Bu-Ph	94	91
acetophenone	82	78

^[a]All of the reactions were carried out under the experimental conditions described in Table 4-4.

Conclusion

The work presented in this Chapter further illustrates the versatility of the alternating ROMP methodology. Here, the novel ROMP-active BINAP monomer **55** prepared in Chapter 2 was used to prepare MCM's **57** and **59**. Detailed NMR studies provided a better understanding on the rotational behavior of the norimido groups in the MCM's and insight into ways to control the interconversion process of the diastereomeric atropisomers. Using Grubbs catalyst **37**, extended, three-dimensional catalyst-organic frameworks were prepared by the

alternating ROMP assembly of **57** and COE with the catalyst complex as a high-loading, cross-linking monomer. The catalyst-organic frameworks were converted to contain Noyori-type active sites and recycled for asymmetric hydrogenation for up to 25 times at low catalyst loadings without loss in enantioselectivity or activity and without detectable metal leaching. To the best of my knowledge this is the highest level of reusability ever demonstrated for an immobilized asymmetric hydrogenation catalyst. As well, the catalyst organic-frameworks showed excellent versatility and a series of ketones were hydrogenated with ee's typically over 90%; they were representatives of those from the homogeneous hydrogenations.⁸ Thus, confirming that the microscopic environment around the chiral active sites in the catalyst-organic framework resembled that of the homogeneous precatalysts. Further investigations are needed to determine the precise structure of the catalyst-organic frameworks.

Experimental

General Procedures and Materials. ¹H, ¹³C, and ³¹P, NMR spectra were recorded using Varian Inova (400 or 500 MHz) spectrometers. ¹H, and ¹³C NMR chemical shifts are reported in parts per million (δ) relative to TMS with the solvent as the internal reference. ³¹P NMR chemical shifts are reported in parts per million (δ) relative to an 85 % H₃PO₄ external reference. ESI mass spectra were obtained on a Micromass ZabSpec Hybrid Sector-TOF spectrometer. Gas

chromatography analysis were carried out using a Hewlett Packard 5890 chromatograph equipped with a flame ionization detector, a 3392A integrator, and a Supelco Beta DexTM 120 fused silica capillary column (30m x 0.25mm x 0.25 μ m, injector: 220°C, detector: 220°C, carrier gas: He 20 psi). C/H/N elemental analyses were carried out at the University of Alberta Microanalysis Laboratory. ICP-MS analysis of Ru leaching was measured with a Perkin Elmer Elan6000 quadrupole inductively coupled plasma mass spectrometer at the EAS Laboratory at the University of Alberta.

Unless stated otherwise, all operations were performed under an inert atmosphere using standard Schlenk and glovebox techniques. Dinitrogen gas (Praxair, 99.998%) was passed through a drying train containing 3Å molecular sieves and P₂O₅ before use. The hydrogen gas was ultra high purity grade purchased from Praxair. All solvents were dried and distilled under a dinitrogen atmosphere using standard drying agents. All common reagents and solvents were obtained from Sigma-Aldrich Co. and used without purification unless stated otherwise. All substrates were purchased from Aldrich, and purified by distillation, then washed with 0.1 M KOH_{aq}, and distilled a second time before use. (S)-(+)-1-(1'-naphthyl)ethanol and (S)-(-)-1-phenylethanol were purchased from Aldrich and used without further purification. The ROMP catalyst (bis(tricyclohexylphosphine)benzylidene ruthenium (IV) dichloride) (**37**), and the diamine ligands (*R,R*)-dpen ((1*R*,2*R*)-1,2-diphenylethylene-diamine), and (*R*)-daipen ((2*R*)-(-)-1,1-bis(4-methoxyphenyl)-3-methyl-1,2-butanediamine) were obtained from Strem Chemicals, Inc. and used without purification. (*R*)-5,5'-

diamino-BINAP (**57**) was prepared following the procedure described in Chapter 3.³³ The synthon *trans*-RuCl₂(NBD)Py₂ (**40**) was synthesized according to literature procedure.⁵ BaSO₄ (white reflectance) was obtained from Eastman Chemical Co., Inc. and washed thoroughly with CH₂Cl₂ and dried under vacuum before use.

1. Synthesis of *trans*-RuCl₂((*R*)-5,5'-dinorimido-BINAP)(Py)₂ (57**).** (*R*)-5,5'-dinorimido-BINAP (**55**) (149 mg, 1.58 x 10⁻⁴ mol) and *trans*-RuCl₂(NBD)Py₂ (**40**) (66.7 mg, 1.58 x 10⁻⁴ mol) were placed in a 20 mL Schlenk flask equipped with a stir bar. The flask was evacuated and back-filled three times with dinitrogen gas, and then 8 mL of deoxygenated dichloromethane was added using a gas tight syringe. The solids completely dissolved resulting in a clear orange solution. The flask was sealed with a teflon high vacuum valve and the solution was heated at 40°C with stirring for 48 h. After cooling to room temperature, the orange solution was transferred by cannula to a dinitrogen-purged round bottom flask (50 mL) equipped with a side arm using dichloromethane wash (2 x 5 mL), and the volatiles were removed under high vacuum. The remaining orange solid was purified by preparing a concentrated dichloromethane solution (5 mL) followed by drop wise addition of hexanes (20 mL) to yield a fine yellow powder. The powder was isolated by cannula filtration and washed sequentially with hexanes (3 mL) and ether (2 x 3 mL) resulting in 83% yield (0.158 g) of product. Although the ³¹P NMR indicates pure product, the ¹H NMR shows there is ~3% excess of unreacted **40** present. This 3%

excess of **40** does not affect the next polymerization step, and it is easily washed away after the polymer is prepared. Therefore the mixture of 97% of **57** and 3% of **40** was used without further purification. ^1H NMR (400 MHz, CD_2Cl_2): δ 1.71 (m, 2 H), 1.82 (d, $J = 8.79$ Hz, 1 H), 1.89 (d, $J = 8.50$ Hz, 1 H), 3.49 - 3.65 (m, 8 H), 6.25 - 6.41 (m, 4 H, olefin), 6.46 - 6.63 (m, 9 H), 6.72 - 6.95 (m, 11 H), 7.21 - 7.25 (m, 4 H), 7.44 - 7.49 (m, 4 H), 7.68 - 7.77 (m, 4 H), 7.83 - 7.93 (m, 4 H), 8.18 - 8.26 (m, 4 H). ^{31}P NMR (162 MHz, CD_2Cl_2): δ 42.24 (dd, $J=154.83$, 32.68 Hz, 2 P), 42.22 (s, 2 P), 42.27 (s, 2 P). ^{13}C NMR (101 MHz, CD_2Cl_2): δ 45.65 (s, 1 C), 45.74 (s, 1 C), 45.86 (s, 1 C), 46.00 (s, 1 C), 46.20 (s, 1 C), 46.45 (s, 1 C), 47.30 (s, 1 C), 47.38 (s, 1 C), 52.66 (s, 2 C), 120.85 - 121.06 (m), 121.87 - 122.01 (m), 126.16 - 126.92 (m), 127.67 - 128.78 (m), 128.97 - 129.09 (m), 129.35 - 129.67 (m), 130.31 - 130.58 (m), 133.95 - 134.24 (m), 134.74 - 134.79 (m), 135.06 - 135.38 (m), 135.86 (s), 136.10 - 136.80 (m), 136.85 (s), 138.59 - 139.18 (m), 141.38 - 142.14 (m), 176.96 (s, 1 C), 176.99 (s, 1 C), 177.23 (s, 1 C), 177.28 (s, 1 C), 177.55 (s, 1 C), 177.70 (s, 1 C).

Repeated recrystallization (3 x) of **5** from CH_2Cl_2 /hexanes resulted in pure product with no trace of **6** present, and elemental analysis was done accordingly. Anal. Calcd for $\text{C}_{72}\text{H}_{56}\text{Cl}_2\text{O}_4\text{N}_4\text{P}_2\text{Ru}$: C, 67.82; H, 4.43; N, 4.39. Found: C, 67.49; H, 4.59; N, 4.19.

2. Alternating ROMP assembly of an extended, three-dimensional catalyst-organic framework, supported as a thin film over BaSO₄.

(a) **Alternating ROMP of 57 and COE.** A 20 mL dinitrogen purged Schlenk flask was charged with **57** (50.9 mg, 3.99×10^{-5} mol), dichloromethane (5.0 mL), and COE (20.8 μ L, 1.60×10^{-4} mol) resulting in an orange solution. The metathesis catalyst **37**, *trans*-RuCl₂(=CHPh)(PCy₃)₂ (Cy is cyclohexyl), (1.64 mg, 2.00×10^{-6} mol) was weighed in a glovebox and transferred to a vial fitted with a septum. This solid was dissolved in dichloromethane (2 mL) under dinitrogen atmosphere resulting in a purple solution that was transferred to the Schlenk flask via cannula using dichloromethane wash (3 x 1 mL). The reaction flask was sealed, and the reaction mixture was stirred at 45°C in oil bath. The extent of polymerization was monitored by ¹H and ³¹P NMR by periodically cooling the reaction mixture to room temperature and removing an aliquot, after which the reaction mixture was placed back in the oil bath. Both the ¹H and ³¹P NMR spectra showed that both monomers, COE and **57**, were completely consumed and the polymerization was complete after 48 h yielding the alternating polymer **64**. The spectra obtained are similar to those shown in Figures 2 (e) and 3 (e). **64** was kept in solution and treated with (*R,R*)-dpen as described below to give **65**. ¹H NMR (400 MHz, CD₂Cl₂): δ 0.95 – 2.40 (br m), 2.80 – 3.70 (br m), 5.15 – 5.95 (br m), 6.20 – 8.80 (br m). ³¹P NMR (162 MHz, CD₂Cl₂): δ 40.5 – 44.0 (br m). ¹³C NMR (101 MHz, CD₂Cl₂): δ 179.8 – 172.1 (br m), 140.5 – 119.7 (br m), 35.6 – 25.8 (br m).

^1H and ^{31}P NMR investigation on the alternating ROMP of **57 and COE with metathesis catalyst **37**.** Compound **57** (10.2 mg, 8.00×10^{-6} mol) was weighed in air and transferred to a NMR tube. The NMR tube was sealed with a septum and flushed with dinitrogen gas. The NMR tube was then placed in a salt ice bath at -10°C . Next, COE (4.2 μL , 3.2×10^{-5} mol) was transferred to the NMR tube using a syringe and CD_2Cl_2 (0.47 mL) was then transferred slowly, down the walls into the NMR tube using a gas tight syringe resulting in an orange solution. **37** (1.0 mg, 1.22×10^{-6} mol) was weighed in a glovebox and charged into a vial fitted with a septum. This solid was dissolved in CD_2Cl_2 (1 mL) under dinitrogen atmosphere resulting in a purple solution. An aliquot (0.33 mL) of this purple solution was transferred to the NMR tube using a gas tight syringe. The NMR tube was wrapped firmly with paraffin film and ^1H and ^{31}P NMR were recorded at 0°C . The tube was then heated at 45°C and the polymerization was followed by NMR until polymerization was complete. Spectra obtained for the different stages of the polymerization are shown in Figure 4-5 and Figure 4-6.

(b) General procedure for displacement of the pyridine ligands with 1,2-diamine ligands, (*R,R*)-dpen or (*R*)-daipen, to generate the corresponding diphosphine/diamine-Ru hydrogenation catalysts, **65 and **72**, respectively.** A dinitrogen purged vial was charged with (*R,R*)-dpen (25.4 mg, 1.20×10^{-4} mol) and dichloromethane (1 mL) resulting in a clear solution. This was cannula transferred to the Schlenk flask containing the alternating polymer **64** prepared above and the mixture was stirred at room temperature for

12 h. An aliquot was taken and both ^1H and ^{31}P NMR (Figure 4-7) confirmed complete exchange of the pyridine ligands for (*R,R*)-dpen resulting in the alternating polymer framework **65**. ^1H NMR (400 MHz, CD_2Cl_2): δ 1.00 – 2.30 (br m), 2.70 – 3.70 (br m), 5.20 – 5.90 (br m), 6.10 – 8.45 (br m). ^{31}P NMR (162 MHz, CD_2Cl_2): δ 45.4 – 48.3 (br m). ^{13}C NMR (101 MHz, CD_2Cl_2): δ 178.1 - 172.0 (br m), 136.3 – 127.2 (br m), 32.9 – 25.8 (br m).

Similar procedure was carried out for exchange with (*R*)-daipen to generate **72**. ^1H NMR (400 MHz, CD_2Cl_2): δ 1.10 – 1.60 (br m), 1.60 – 2.3 (br m), 2.95 – 3.95 (br m), 5.20 – 5.90 (br m), 6.30 – 8.50 (br m). ^{31}P NMR (162 MHz, CD_2Cl_2): δ 43.9 – 48.5 (br m).

(c) Deposition of the alternating catalyst-organic frameworks, 65 and 72, onto BaSO_4 . 20 g of BaSO_4 was weighed in air and placed in a fritted Buchner filter (grade D). The BaSO_4 was washed with dichloromethane (3 x 50 mL), followed by a diethyl ether wash, and then dried under high vacuum overnight. 5.00 g of the clean BaSO_4 was charged into a round bottom flask (200 mL) equipped with a side arm and a magnetic stir bar. After the flask was evacuated and back-filled (3 x) with dinitrogen, the homogeneous reaction mixture of the polymers were transferred by cannula using dichloromethane wash (2 x 10 mL) onto the BaSO_4 resulting in a yellow slurry. The yellow slurry was stirred rapidly while the volatiles were slowly removed under high vacuum over 1 h. Care was taken to ensure even distribution of the polymer film over the solid support. Specifically, the evaporation was interrupted periodically, and the

supported catalyst which had splashed upon the sides of the flask was knocked down into the reaction mixture using the stir bar. The evaporation process was continued until all solvents were removed. The resulting homogeneous yellow powder was washed with methanol (3 x 30 mL), isolated by inverse cannula filtration and further dried under high vacuum for 24 h.

Catalyst Loading. The alternating catalyst-organic framework **65** was deposited onto BaSO₄ to result in 6.38×10^{-6} mol of ruthenium content per gram of support or 8.48 mg of active (*R*)-5,5'-dinorimido-BINAP/(*R,R*)-dpen catalyst per gram of support.

The alternating catalyst-organic framework **72** was deposited onto BaSO₄ to result in 8.26×10^{-6} mol of ruthenium content per gram of support or 11.8 mg of active (*R*)-5,5'-dinorimido-BINAP/(*R*)-daipen catalyst per gram of support.

General procedure for purification of commercial aryl-ketones. 4'-tert-butylacetophenone, 2'-methylacetophenone, acetophenone, and 1'-acetonaphthone were purified thoroughly before subjecting to hydrogenation. The substrates were distilled under vacuum yielding a light yellow viscous liquid. This was dissolved in diethyl ether (100 ml) and placed in a separatory funnel where it was washed with 0.1 M KOH_{aq} (3 x 50 mL). The collected organic layer was dried over Na₂SO₄, gravity filtered, and concentrated under reduced pressure to remove the volatiles. The concentrate was redistilled under vacuum yielding pure ketones as a colorless viscous liquid.

3. General procedure for heterogeneous asymmetric hydrogenation of aromatic ketones using the alternating catalyst-organic framework and catalyst recycling. A high pressure stainless steel bomb equipped with a magnetic stir bar was charged with the supported-polymeric catalyst, (1.00 g, containing 8.48 mg (6.38×10^{-6} mol) of **60**). The bomb was assembled and sealed under a positive flow of hydrogen gas and the system was purged by three cycles of pressurizing to 10 atm with hydrogen gas. The top inlet valve on the bomb was fitted with a septum and the system remained under a positive flow of H₂ during set-up. A base solution was prepared in a Schlenk flask (50 mL) by dissolving freshly sublimed potassium *tert*-butoxide (0.143 g, 1.28×10^{-2} mol) in anhydrous iso-propanol (20 mL). The base solution, iso-propanol, and 1'-acetonaphthone were bubbled with H₂ for 30 min before use. Next, the high pressure stainless steel bomb was charged with hydrogen saturated iso-propanol (4.4 mL), 1'-acetonaphthone (1.086 g, 6.38×10^{-3} mol, 1000 equiv), and an aliquot (2 mL) of the t-C₄H₉OK solution (14.3 mg, 1.28×10^{-4} mol, 20 equiv) using a gas tight syringe. The bomb was pressurized to 10 atm and then sealed so that the reaction was done in a closed system. Once complete the pressure reactor was cooled to room temperature, depressurized, and kept under an atmosphere of hydrogen. The reaction mixture was allowed to settle and the solution was removed by inverse filtration. An aliquot was analyzed on GC to determine yield and ee%.

For catalyst reuse, the solid catalyst was used directly without any treatment or downtime between runs. Care was taken to ensure the active, solid

catalyst remained in iso-propanol, and was kept under a hydrogen atmosphere at all times. For catalyst reuse, the solid catalyst was used directly without any treatment or downtime between runs. Immediately after the contents from the previous run were removed fresh samples of substrate, base solution and iso-propanol were added to the reactor through the inlet tube via a gas tight syringe. The bomb was pressurized to 10 atm and the hydrogenation reaction repeated. The reaction mixture was stirred at the temperatures and times specified in Table 4-3. The extent and rate of hydrogenation was accurately predicted by measuring the change in hydrogen pressure on the pressure gauge and using the ideal gas law to predict % completion (see below).

Calculation of the initial TOF of the hydrogenation for runs 5-29. It was observed that during the recycling hydrogenation experiment shown in Table 4-3, the pressure dropped to ~9 atm after the first hour at 40°C for runs 5-29. The experiments were carried out in a closed pressure vessel with a total volume, V_{system} , of 84.9 mL. The reaction mixture contained 6.38 mmol (0.97 mL) of ketone dissolved in 6.4 mL of solvent. As described above the system was pressurized to 10 atm at 23°C. Hence, using the ideal gas law the initial amount of hydrogen gas, n_{gas} , was determined as follows:

$$V_{\text{system}} = V_{\text{solvent}} + V_{\text{ketone}} + V_{\text{gas}}$$

$$\begin{aligned} V_{\text{gas}} &= V_{\text{Total}} - (V_{\text{solvent}} + V_{\text{ketone}}) \\ &= 77.5_3 \text{ mL.} \end{aligned}$$

$$\begin{aligned}
 \text{Therefore, } n_{\text{gas}} &= PV_{\text{gas}}/RT \\
 &= [(10 \text{ atm})(0.07753 \text{ L})]/[(0.08206 \text{ L}\cdot\text{atm}\cdot\text{K}^{-1}\cdot\text{mol}^{-1})(296 \text{ K})] \\
 &= 0.0319_2 \text{ mol.}
 \end{aligned}$$

At the start of the hydrogenations the system contains 31.9 mmol of hydrogen gas. The vessel was then heated at 40°C, and after the first hour the pressure dropped to 9 atm. The amount of gas consumed during the first hour of the reaction was calculated by first determining the amount of gas remaining at 9 atm at 40°C, and then subtracting it from the original amount of gas present in the closed system.

$$\begin{aligned}
 n_{\text{gas at 9 atm}} &= PV_{\text{gas}}/RT \\
 &= [(9 \text{ atm})(0.07753)]/[(0.08206 \text{ L}\cdot\text{atm}\cdot\text{K}^{-1}\cdot\text{mol}^{-1})(313 \text{ K})] \\
 &= 0.0271_7 \text{ mol.}
 \end{aligned}$$

$$\begin{aligned}
 n_{\text{gas consumed}} &= n_{\text{gas}} - n_{\text{gas at 9 atm}} \\
 &= (0.03192 - 0.02717) \text{ mol} \\
 &= 0.00475_2 \text{ mol.}
 \end{aligned}$$

This suggests that 4.75 mmol of ketone was hydrogenated in the first hour, since one mole of hydrogen gas consumed equals one mole of ketone hydrogenated. Therefore, the % conversion = $(0.00475/0.00638) \text{ mol} \times 100\% = 74.5\%$, corresponding to an initial TOF = 745 h^{-1} .

4. Product work-up and determination of enantiomeric excess (ee).

The products from the catalytic hydrogenations were concentrated under reduced pressure and an aliquot was flushed through a Florisil plug using ethyl acetate (5 mL) as an eluent to remove any catalyst residues. The solvent was removed under reduced pressure, and the ee % and yield were determined by chiral GC analysis. The sample was injected as a dichloromethane solution with concentration = 1 mg/mL. The retention times and GC conditions for the products and the starting materials are as follows. ¹H NMR spectra recorded are identical to the authentic samples.

1-naphthyl-ethanol: Column was held at 150°C for 45 min, increased to 170°C programmed at 1°C/min then kept at 170°C for 10 min. The retention times were (*R*)-(+)-1-(1'-naphthyl)ethanol, $t_R(R)$ = 64.1 min; (*S*)-(-)-1-(1'-naphthyl)ethanol, $t_R(S)$ = 62.2 min; 1'-acetonephthone, t = 37.9 min. The absolute configuration of the major product enantiomer was (*S*) as determined by comparison to an authentic sample of (*S*)-(+)-1-(1'-naphthyl)ethanol.

phenylethanol: Column was heated from 70°C to 120°C programmed at 1°C/min then kept at 120°C for 10 min. The retention times were (*R*)-(+)-1-phenylethanol, $t_R(R)$ = 41.7 min; (*S*)-(-)-1-phenylethanol, $t_R(S)$ = 43.2 min; acetophenone, t = 28.3 min. The absolute configuration of the major product enantiomer was (*S*) as determined by comparison to an authentic sample of (*R*)-(+)-1-phenylethanol.

4-tertbutylphenyl-ethanol: Column was held at 130°C for 40 min, increased to 140°C programmed at 1°C/min then kept at 140°C for 10 min. The retention times were, $t_1 = 39.6$ min (minor enantiomer); $t_2 = 40.9$ min (major enantiomer); 4-tertbutylacetophenone, $t = 32.6$ min. The retention times were confirmed by preparing racemic 4-tertbutylphenyl-ethanol as described below. Absolute configuration was not determined.

2-methylphenyl-ethanol: Column was heated from 70°C to 140°C programmed at 1°C/min then kept at 140°C for 10 min. The retention times were, $t_1 = 54.7$ min (minor enantiomer); $t_2 = 58.6$ min (major enantiomer); 2-methylacetophenone, $t = 33.3$ min. The retention times were confirmed by preparing racemic 2-methylphenyl-ethanol as described below. Absolute configuration was not determined.

A typical procedure for preparing racemic products. A 25 mL flask was charged with 4'-tert-butylacetophenone (0.84 g, 4.8 mmol), sodium borohydride (0.19 g, 5.0 mmol), and ethanol (15 mL). The reaction mixture was stirred overnight, and then quenched with HCl (0.1 M). The reaction mixture was diluted with CH₂Cl₂, and the organic phase was separated and dried over MgSO₄. Solvent was removed under reduced pressure to yield α -(4-tertbutylphenyl)ethanol as a white powder (>90% yield). ¹H NMR (300 MHz, CDCl₃): δ 7.35 (m, 4H), 4.89 (q, $J = 6.48$ Hz, 1H), 1.71 (br, 1H), 1.51 (d, $J =$

6.48Hz, 3H), 1.33 (s, 9H). GC conditions described above: t_1 = 39.6 min; t_2 = 40.9 min.

α -(2-methylphenyl)ethanol: ^1H NMR (300 MHz, CDCl_3): δ 7.52 (m, 1H), 7.20 (m, 3H), 5.14 (q, J = 6.48Hz, 1H), 2.36 (s, 3H), 1.48 (d, J = 6.48Hz, 3H). GC conditions described above: t_1 = 54.7 min; t_2 = 58.6 min.

5. Determination of Ru Leaching by Inductively Coupled Plasma Mass Spectrometry (ICP-MS). A representative sampling of the hydrogenation runs (1, 3, 8, 14, 19, 23, 27, 29, and 30) from the recycling experiment were used to determine any metal leaching from the solid catalyst. The sample was first prepared by standard Sulfated Ashing procedures²⁹ and the metal content was determined by ICP-MS. A control sample was prepared and tested for ruthenium content to confirm the validity of the procedure.

After the hydrogenation reaction (with 6.38×10^{-6} mol, 0.645 mg of Ru metal loading) the collected filtrate, containing the hydrogenation product was concentrated under reduced pressure. An aliquot was dissolved in CH_2Cl_2 (5 mL) and flushed through a celite plug to remove any insoluble residue. The collected filtrate was evaporated to dryness and the resulting viscous oil was transferred to a porcelain crucible. The crucible was gently heated using an open flame to destroy the organics and when the fumes ceased to evolve the contents in the crucible were charred for 5 min. The crucible is then cooled and wetted with a few drops of concentrated sulfuric acid. The sample is heated until all the white dense sulfur trioxide fumes cease to evolve and then heated red hot

until all the carbon has been oxidized. The crucible was filled with a saturated solution of potassium persulfate ($K_2S_2O_8$, Certified Regent, Fisher Scientific Company) in 4.0 M KOH and left overnight to ensure all Ru content present is dissolved.³⁰ The solution was then diluted with 1% HNO_3 (aq) (25 mL) and ICP analysis was carried out on the resulting solution. The Ru content was determined to be near or less than 4 ppb (detection limit) for each sample measured. Using 4 ppb as the upper limit, this implies that < 0.00016 equivalents of Ru leached into the organic product during each run, confirming the heterogeneous nature of the catalyst system.

References

- (1) (a) Dai, L. X. *Angew. Chem. Int. Ed.* **2004**, *43*, 5726-5729. (b) Ding, K. L.; Wang, Z.; Wang, X. W.; Liang, Y. X.; Wang, X. S. *Chem. Eur. J.* **2006**, *12*, 5188-5197. (c) Lin, W. B. *J. Solid State Chem.* **2005**, *178*, 2486-2490.
- (2) (a) Ding, K. L. *Pure Appl. Chem.* **2006**, *78*, 293-301. (b) Ngo, H. K.; Lin, W. B. *Topics in Catalysis* **2005**, *34*, 85-92.
- (3) Liang, Y. X.; Jing, Q.; Li, X.; Shi, L.; Ding, K. L. *J. Am. Chem. Soc.* **2005**, *127*, 7694-7695.
- (4) Hu, A. G.; Ngo, H. L.; Lin, W. B. *J. Am. Chem. Soc.* **2003**, *125*, 11490-11491.
- (5) (a) Akotsi, O. M.; Metera, K.; Reid, R. D.; McDonald, R.; Bergens, S. H. *Chirality* **2000**, *12*, 514-522. (b) Leong, C. G.; Akotsi, O. M.; Ferguson, M. J.; Bergens, S. H. *Chem. Commun.* **2003**, 750-751.
- (6) Jeulin, S.; de Paule, S. D.; Ratovelomanana-Vidal, V.; Genet, J. P.; Champion, N.; Dellis, P. *Proc. Natl. Acad. Sci. U. S. A.* **2004**, *101*, 5799-5804.
- (7) Curnow, O. J.; Hughes, R. P.; Mairs, E. N.; Rheingold, A. L. *Organometallics* **1993**, *12*, 3102-3108.
- (8) Noyori, R.; Ohkuma, T. *Angew. Chem. Int. Ed.* **2001**, *40*, 40-73.
- (9) (a) Scholl, M.; Trnka, T. M.; Morgan, J. P.; Grubbs, R. H. *Tetrahedron Lett.* **1999**, *40*, 2247-2250. (b) Schwab, P.; France, M. B.; Ziller, J. W.; Grubbs,

- R. H. *Angew. Chem. Int. Ed. Engl.* **1995**, *34*, 2039-2041. (c) Schwab, P.; Grubbs, R. H.; Ziller, J. W. *J. Am. Chem. Soc.* **1996**, *118*, 100-110.
- (10) (a) Sanford, M. S.; Love, J. A.; Grubbs, R. H. *J. Am. Chem. Soc.* **2001**, *123*, 6543-6554. (b) Sanford, M. S.; Ulman, M.; Grubbs, R. H. *J. Am. Chem. Soc.* **2001**, *123*, 749-750.
- (11) (a) Ulman, M., California Institute of Technology, PhD Thesis, 2000. (b) Schwab, P. G., R.H; Ziller, J. W. *J. Am. Chem. Soc.* **1996**, *118*, 100-110
- (12) Ilker, M. F.; Coughlin, E. B. *Macromolecules* **2002**, *35*, 54-58.
- (13) (a) Nishihara, Y.; Inoue, Y.; Nakayama, Y.; Shiono, T.; Takagi, K. *Macromolecules* **2006**, *39*, 7458-7460. (b) Rule, J. D.; Moore, J. S. *Macromolecules* **2002**, *35*, 7878-7882.
- (14) Berthod, M.; Mignani, G.; Woodward, G.; Lemaire, M. *Chem. Rev.* **2005**, *105*, 1801-1836.
- (15) Seo, J. S.; Whang, D.; Lee, H.; Jun, S. I.; Oh, J.; Jeon, Y. J.; Kim, K. *Nature* **2000**, *404*, 982-986.
- (16) Ralph, C. K.; Akotsi, O. M.; Bergens, S. H. *Organometallics* **2004**, *23*, 1484-1486.
- (17) Ohkuma, T.; Ooka, H.; Hashiguchi, S.; Ikariya, T.; Noyori, R. *J. Am. Chem. Soc.* **1995**, *117*, 2675-2676.
- (18) Doucet, H.; Ohkuma, T.; Murata, K.; Yokozawa, T.; Kozawa, M.; Katayama, E.; England, A. F.; Ikariya, T.; Noyori, R. *Angew. Chem. Int. Ed.* **1998**, *37*, 1703-1707.
- (19) Ashby, M. T.; Halpern, J. *J. Am. Chem. Soc.* **1991**, *113*, 589-594.

- (20) Noyori, R. *Angew. Chem. Int. Ed.* **2002**, *41*, 2008-2022.
- (21) Sandoval, C. A.; Ohkuma, T.; Muniz, K.; Noyori, R. *J. Am. Chem. Soc.* **2003**, *125*, 13490-13503.
- (22) Hamilton, R. J.; Leong, C. G.; Bigam, G.; Miskolzie, M.; Bergens, S. H. *J. Am. Chem. Soc.* **2005**, *127*, 4152-4153.
- (23) Abdur-Rashid, K.; Clapham, S. E.; Hadzovic, A.; Harvey, J. N.; Lough, A. J.; Morris, R. H. *J. Am. Chem. Soc.* **2002**, *124*, 15104-15118.
- (24) Hamilton, R. J.; Bergens, S. H. *J. Am. Chem. Soc.* **2006**, *128*, 13700-13701.
- (25) Blaser, H. U.; Pugin, B.; Spindler, F. *J. Mol. Catal. A* **2005**, *231*, 1-20.
- (26) Hu, A. G.; Yee, G. T.; Lin, W. B. *J. Am. Chem. Soc.* **2005**, *127*, 12486-12487.
- (27) Ohkuma, T.; Takeno, H.; Honda, Y.; Noyori, R. *Adv. Synth. Catal.* **2001**, *343*, 369-375.
- (28) Heitbaum, M.; Glorius, F.; Escher, I. *Angew. Chem. Int. Ed.* **2006**, *45*, 4732-4762.
- (29) Gaines, P., 2002.
- (30) Wiel, V. D. *Chem. Weekblad* **1952**, *48*, 597.
- (31) Studer, M.; Blaser, H. U.; Exner, C. *Adv. Synth. Catal.* **2003**, *345*, 45-65.
- (32) Blaser, H. U.; Malan, C.; Pugin, B.; Spindler, F.; Steiner, H.; Studer, M. *Adv. Synth. Catal.* **2003**, *345*, 103-151.
- (33) Okano, T. K., H.; Akutagawa, S.; Kiji, J.; Konishi, H.; Fukuyama, K.; Shimano, Y. U. S., **1987**.

Chapter 5

Concluding Remarks

Although homogeneous asymmetric catalysis is a powerful tool for the production of optically active compounds,¹ the high costs of the catalysts as well as product contamination caused by metal leaching has hindered its practical application.² In attempts to address these problems, many homogeneous chiral catalysts have been immobilized to provide a catalyst that can be quantitatively recovered from the product stream and reused with constant catalyst efficiencies.³ However, the majority of these attempts have failed, and resulted in immobilized catalysts that are less reactive and selective than their homogeneous counterparts. Further, few reported systems have shown more than three reuses without a significant loss in activity and selectivity. The ideal immobilized homogeneous enantioselective catalyst is one that can be recovered by simple procedures such as filtration, with no product contamination caused by metal leaching and can be recycled for a high number of reuses, with activities and enantioselectivities as good as or better than the homogeneous counterparts. Further, the immobilization technique should have a general applicability or adaptability to other homogeneous catalysts. The research presented in this thesis represents a significant advance towards achieving these goals.

Alternating ROMP methodology. This work involved the development of a new methodology to prepare polymeric asymmetric hydrogenation catalysts. Here, an alternating ROMP methodology was devised using the hydrogenation catalyst precursor *trans*-RuCl₂(Py)₂((*R,R*)-Norphos) (**41**) and COE as monomers and using the functional group tolerant Grubbs catalyst, *trans*-RuCl₂(=CHPh)(PCy₃)₂ (**37**) or *trans*-RuCl₂(=CHPh)(PCy₃)(NHC) (**38**) as initiators. The resulting alternating copolymer was cross-linked using dicyclopentadiene to impart rigidity to the polymer matrix, the pyridine ligands were easily replaced with (*R,R*)-dpen to generate the Noyori-type active sites, and the polymer was deposited on BaSO₄. Use of the relatively inert BaSO₄ as support reduced mass transport losses, provided a filtration aid, and improved mechanical stability toward rapidly stirred batch hydrogenations. To the best of our knowledge BaSO₄ has not been used as a polymer support prior to this work. The resulting supported polymeric catalyst [RuCl₂((*R,R*)-Norphos)((*R,R*)-dpen)]_x[COE]_y/BaSO₄ (**47**), sustained 10 reuses without detrimental loss in activity or enantioselectivity for the asymmetric hydrogenation of 1'-acetonaphthone (TON/run = 500, 83% ee, rate = 40% of the rate of the homogeneous catalyst). At the time of this work, this was the highest number of reuses reported for any insoluble polymeric asymmetric hydrogenation catalyst. In addition, the ee using the polymerized catalyst **47** was substantially higher than that observed for the parent Ru-Norphos-dpen homogenous catalyst which gave 48% ee for the hydrogenation of 1'-acetonaphthone under identical conditions. This is significant, since most

immobilized catalysts often suffer from reduced enantioselectivities in comparison with their homogenous counterparts.

The alternating ROMP methodology offered a number of advantages over previous methods used to prepare polymeric asymmetric hydrogenation catalysts. Mainly, this was a more straightforward approach, which allowed for the direct incorporation of the catalyst precursor by the polymerization of its metal-containing monomer, thereby avoiding the critical polymer metallation step associated with previous procedures. This resulted in a high catalyst loading with no vacant coordination sites that could potentially interfere with the catalyst performance, as well as providing maximum knowledge of the catalytic sites. In addition, the detailed NMR studies confirmed that the polymerization proceeded with a high degree of alternation, and therefore prevented the localization of catalytic sites in the polymer matrix. The alternating ROMP immobilization strategy offered a reproducible, well-controlled synthesis of polymeric catalysts with a high density of evenly distributed, well-isolated and defined active sites. Due to these salient features and the success that was achieved with the first polymeric asymmetric hydrogenation catalysts prepared by ROMP (*vide supra*) another goal of this work was to show the general applicability and adaptability of this methodology to other homogeneous catalysts.

ROMP active BINAP monomer. In this work, BINAP was chosen as the preligand since it is arguably one of the most influential and successful chiral ligands for asymmetric catalysis.⁴ A ROMP-active version of BINAP was prepared in one step by condensation between (*R*)-5,5'-diamino-BINAP (**54**) with

cis-5-norbornene-endo-2,3-dicarboxylic anhydride to afford (*R*)-5,5'-dinorimido-BINAP (**55**) in 81% yield. Multinuclear NMR studies revealed that **55** formed as a mixture of two C₂-dissymmetric diastereomers, (*R,R,R*)- and (*S,R,S*), and a non-C₂ dissymmetric diastereomer, (*R,R,S*)- or (*S,R,R*). The origin of the three NMR-distinct, diastereomeric atropisomers was their relative rotameric orientations of the norimido groups about the arene-nitrogen bonds. Despite the mixture of isomers, the catalyst monomer ((*R*)-5,5'-dinorimido-BINAP)RuCl₂Py₂ (**57**) was easily prepared by replacing the norbornadiene (NBD) ligand in the compound *trans*-RuCl₂(Py)₂(NBD) (**40**) with **55**. As was the case for **55**, monomer **57** formed as a mixture of three diastereomeric atropisomers, two with a C₂-axis of rotation and one without, these being in a ratio similar to that of the free ligand **55**. Interestingly, it was shown that exchange or interconversion of the diastereomeric atropisomers was influenced by the electron density of the metal center. Future investigations of these compounds should focus on determining the rates of interconversion and the activation energy barrier to rotation. It would also be interesting to develop procedures to control the interconversion process and to study its effect on the resulting polymerization process and polymer structure.

Highly reusable catalyst-organic frameworks. In this work, the newly developed alternating ROMP immobilization technique was employed to prepare the polymeric catalyst based on monomer **57**. By design, the alternating ROMP between COE and both norbornyl groups in **57** was carried out to result in assembly of an extended, three-dimensional catalyst-organic framework with the

catalyst complex as cross-linking units. The resulting framework exhibited a high density of well-isolated active center and the self-cross-linking nature imparted a high degree of rigidity to the framework, making it chemically and mechanically stable. The pyridine ligands at the Ru centers of the framework were replaced in 100% yield by reaction with either (*R,R*)-dpen or (*R*)-daipen to result in catalyst-organic frameworks $\text{RuCl}_2((R)\text{-5,5'-dinorimido-BINAP})((R,R)\text{-dpen})_x[\text{COE}]_y$ (**65**) and $[\text{RuCl}_2((R)\text{-5,5'-dinorimido-BINAP})((R)\text{-daipen})]_x[\text{COE}]_y$ (**66**), respectively. These frameworks were deposited on BaSO_4 as before and used for the asymmetric hydrogenation of a series aromatic ketones with activities and enantioselectivities comparable to those obtained using the homogeneous counterparts. More importantly, the supported catalyst **65** was recycled 25 times for the asymmetric hydrogenation of 1'-acetonephthone at low catalyst loadings (0.1 mol %) without loss in enantioselectivity or activity. Between runs the catalyst was easily separated by filtration and analysis of a representative sampling of the runs confirmed that no detectable Ru leached into the organic phase (<4 ppb). Including other experiments, one batch of the supported catalyst was used for 52 days of continued use.

In addition to the extraordinary level of reusability achieved with the catalyst-organic frameworks, this technology also displayed a modular nature which requires further investigation. For example, preliminary results have shown that by replacing BaSO_4 with an insoluble chiral support such as Ba-(L)-tartrate is a simple method to enhance the *ee* of the polymerized catalyst. Further, the framework may have conformations in which macroscopic pockets

and channels are formed in the extended structure.⁵ In principle, controlling the shape and size of these pockets and channels will control the space within which the active catalyst resides and may lead to substrate shape and size selectivity. Modifications of the chiral environment around the catalyst could be achieved by simply incorporating chiral spacer monomers in the polymerization process.

Future directions. As was shown in Chapter 1, BINAP-ruthenium catalysts have a broad application and have been used for the enantioselective hydrogenation of a wide range of functionalized olefins and ketones.⁶ In addition to hydrogenations, BINAP has also proven effective for a wide range of other asymmetric transformations such as hydrosilylation, hydroboration, hydroformylation, hydrocyanation, allylic alkylation and the asymmetric Heck reaction.⁷ Thus, efforts to broaden the scope of the immobilized BINAP frameworks for application to a variety of substrates and other transformations are underway. In addition, it has been shown that the alternating ROMP methodology is adaptable and therefore, in principle, extension of this technology to other ligands that are applied on a regular basis in industry is achievable.⁸

As was demonstrated in this work, the alternating ROMP methodology provides a superior way to prepare well-ordered, highly efficient and reusable polymeric asymmetric hydrogenation catalysts and coupled with the adaptability of this technology it is hoped that this work will contribute to the development of more environmentally sound and cost-effective applications of asymmetric catalysis.

References

- (1) (a) Farina, V.; Reeves, J. T.; Senanayake, C. H.; Song, J. H. *J. Chem. Rev.* **2006**, *106*, 2734-2793. (b) Knowles, W. S.; Noyori, R.; Sharpless, K. B. *Angew. Chem. Int. Ed. Engl.* **2002**, 1998-2022. (c) Trost, B. M. *Proc. Natl. Acad. Sci. U. S. A.* **2004**, *101*, 5348-5355.
- (2) Cole-Hamilton, D. J. *Science* **2003**, *299*, 1702-1706.
- (3) (a) *Chiral Catalyst Immobilization and Recycling*; Wiley-VCH: (Eds.: D. E. De Vos, I. F. J. Vankelecom, P. A. Jacobs), **2000**. (b) Heitbaum, M.; Glorius, F.; Escher, I. *Angew. Chem. Int. Ed.* **2006**, *45*, 4732-4762.
- (4) Berthod, M.; Mignani, G.; Woodward, G.; Lemaire, M. *Chem. Rev.* **2005**, *105*, 1801-1836.
- (5) (a) Song, C. E. *Annu. Rep. Prog. Chem., Sect. C, Phys. Chem.* **2005**, *101*, 143. (b) Song, C. E. *European Journal of Inorganic Chemistry* **2006**, 2927-2935.
- (6) Noyori, R.; Takaya, H. *Acc. Chem. Res.* **1990**, *23*, 345-350.
- (7) (a) Kumobayashi, H.; Miura, T.; Sayo, N.; Saito, T.; Zhang, X. Y. *Synlett* **2001**, 1055-1064. (b) Akutagawa, S. *Appl. Catal A:General* **1995**, *128*, 171-207.
- (8) (a) Blaser, H. U.; Malan, C.; Pugin, B.; Spindler, F.; Steiner, H.; Studer, M. *Adv. Synth. Catal.* **2003**, *345*, 103-151. (b) Yoon, T. P.; Jacobsen, E. N. *Science* **2003**, *299*, 1691-1693.